# SEISMIC DESIGN OF UNREINFORCED MASONRY STRUCTURES

by

Gregory Mark Klopp B.E.(Hons.)

A thesis submitted to the Faculty of Engineering at The University of Adelaide for the Degree of Doctor of Philosophy.

Department of Civil and Environmental Engineering,
The University of Adelaide.

January, 1996.

# CONTENTS

# LIST OF FIGURES

# LIST OF TABLES

# ABSTRACT

Unreinforced masonry buildings have generally performed poorly in earthquakes. This thesis reports on a study into the behaviour and design of unreinforced masonry buildings when subjected to forces induced into the structure from earthquake ground motion.

The study involved the monitoring of ambient vibrations in a number of unreinforced masonry buildings in Adelaide to identify their dynamic properties for use in later analyses of the building's response to earthquake induced forces. The dynamic properties of the buildings, specifically the natural period, were then compared to estimates of the dynamic properties given by formulae included in various earthquake design codes. The suitability of these formulae for use in the design of unreinforced masonry buildings for earthquake induced forces was then examined.

Shaking table tests were then conducted on fifteen unreinforced masonry wall specimens to determine the stiffness of the walls when subjected to dynamic excitation. The tests were conducted to examine the variability of the stiffness of the walls with variation in the excitation frequency, compressive stress level, and size of panel. The test results form the panels were then used in conjunction with a finite element model of the wall specimens to determine a Young's Modulus for unreinforced masonry walls for use in dynamic analyses.

The results from the first two parts of the study were then used in the modelling of the buildings from the ambient vibration tests. The Young's Modulus values determined from the results of the shaking table tests were used as the basis for the Young's Modulus of the brickwork elements in the models of the buildings. Modal analyses were undertaken of the building models and the results compared to the results of the ambient vibration tests. The building models were then used in response spectrum analyses in accordance with The Australian Standard "Minimum

design loads on structures - Part 4 : Earthquake Loads", AS1170.4-1993 to determine the predicted response of the buildings to the Australian design magnitude earthquake. Examined responses were the wall stresses, floor to wall connection forces, base shears, and storey shears. These results were compared to the predicted response of the buildings to the Australian design magnitude earthquake determined from equivalent static force analyses.

The results of the two types of analyses for predicting the response of a structure to earthquake excitation were then used as the basis of suggested modifications to the AS1170.4 equivalent static force design procedures for use with unreinforced masonry buildings.

# DECLARATION

This thesis contains no material which has been accepted for the award of any other degree or diploma in any university or other tertiary institution and, to the best of my knowledge and belief, contains no material previously published or written by another person, except where due reference is made in the text.

I give consent to this copy of my thesis, when deposited in the University Library, being made available for loan and photocopying.

Gregory Mark Klopp.

# ACKNOWLEDGMENTS

The author wishes to acknowledge the assistance, guidance and encouragement given by his supervisor, Dr. Michael Griffith, throughout this project. The work was made possible through his dedicated interest in the project and guidance during the preparation of the manuscript.

The author also wishes to acknowledge the late Dr. George Sved for his ideas and suggestions throughout the project. His experience in finite element modelling, in particular of unreinforced masonry, contributed greatly to the success of this part of the research.

The experimental work conducted as part of this research was undertaken with assistance and guidance from Mr. Bruce Lucas and Mr. Stan Woithe from the Instrumentation Laboratory, Mr. Colin Haese and his staff in the Engineering Workshops, and Mr. Werner Eidam and his staff in the Structure's Laboratory of the Department of Civil and Environmental Engineering and the author gratefully acknowledges their contribution to the project.

This project was funded by the Australian Research Council.

# 1. INTRODUCTION

Earthquakes are one of the most devastating of all natural disasters. Striking without warning, they kill and injure people, destroy buildings, and disrupt power and water supplies.

One of the most vulnerable forms of construction to damage in earthquakes is unreinforced masonry. The 1989 Newcastle, Australia, earthquake was a recent event that demonstrated this vulnerability. Page et al (1990) noted that the majority of damage in Newcastle was to older load bearing masonry construction or to non-structural masonry. Page et al, however, also noted that a large number of small and large unreinforced masonry buildings performed well during the earthquake.

With the generally poor performance of unreinforced masonry buildings when subjected to earthquake ground motion and evidence suggesting this that these buildings do not have to perform poorly, there is pressure on the engineering community to design and detail unreinforced masonry buildings to perform well in earthquakes. This study was devised to help engineers design and detail unreinforced masonry buildings that have an acceptable performance in earthquakes.

The general aim of this study was to investigate the susceptibility of unreinforced masonry buildings when subjected to earthquake ground motion, with special reference to the design magnitude earthquake in Adelaide and to provide an engineer with the tools necessary to provide unreinforced masonry with an acceptable level of performance under earthquake ground motion. The aim was achieved through an examination of the suitability of the earthquake design provisions included in The Australian Standard "Minimum design loads on structures - Part 4 : Earthquake loads" AS1170.4-1993 for use with unreinforced masonry construction common to Australia. The study was limited to unreinforced clay brick masonry. Unlike previous studies which concentrated on a single building, this study looked at eleven buildings

in order to try and ascertain trends from the predicted seismic behaviour of these buildings.

Generally earthquakes are considered to be the problem of areas on tectonic plate boundaries, California, Japan, and New Zealand, for example. For buildings not in areas on the tectonic plate boundaries earthquake loading may not be considered in the design process. While buildings constructed in areas near the tectonic plate boundaries are more likely to experience a large magnitude earthquake, to ignore the possibility of buildings in areas not near the tectonic plate boundaries experiencing earthquake ground motion could be disastrous. Again, the 1989 Newcastle earthquake demonstrated that areas not on tectonic plate boundaries are not immune from the dangers of earthquakes. There are differences in the properties of the earthquakes that occur at the tectonic plate boundaries, *interplate* earthquakes, and those that do not, *intraplate* earthquakes. While not directly part of this study, the properties of intraplate plate earthquakes will be considered when examining the earthquake design provisions of AS1170.4.

When examining the development of unreinforced masonry it becomes apparent that its development followed a different path to the other materials used in the construction of buildings and structures. The sophisticated use of unreinforced masonry has been found to date back 3000-4000 years (Hill (1984)) and the first codified rules for its use were by the Roman architect/engineer Vitruvius (Armytage (1961)). While structural engineering progressed rapidly in the 19th and 20th centuries, with the problems of bending and elasticity having been solved and the new principles of structural engineering being readily applied to the new building materials, iron, steel, and concrete, masonry buildings were still built using the basic rules developed 500 years earlier. In the late 19th and 20th centuries, isolated series of tests on masonry walls and piers were undertaken, though it was not until the 1950's that significant information was available to allow development of building codes based upon science and structural engineering theory. A new design approach for masonry was developed in Europe to cope with high rise residential buildings constructed in the period after the Second World War. No longer was each wall considered separately. Instead each wall was recognised as being part of the whole building. These new design approaches usually dealt with vertical and wind loads.

As has already been noted at the being of this section, unreinforced masonry has generally performed poorly in earthquakes and this poor performance was highlighted recently in Australia in the Newcastle, 1989, earthquake (magnitude 5.6).

Australia previously experienced earthquake damage to unreinforced masonry buildings during a magnitude 6.9 event in Meckering in 1968. Beresford (1969) observed that of fifty-two buildings with masonry walls of various types and quality, only one survived with damage that was economically repairable. Yet, of twenty-seven timber framed buildings, only two sustained worse than minor damage.

The Australian experience of unreinforced masonry performing poorly in earthquakes is not unique. United States earthquakes such as Long Beach, 1933, Anchorage, 1964, Whittier Narrows, 1987, Loma Prieta, 1989, and Northridge, 1994 also highlight the vulnerability of unreinforced masonry buildings to earthquake ground motion. Studies after the Whittier Narrows (Deppe (1988) and Comerio (1992)) also found that strengthened unreinforced masonry buildings generally had acceptable performance. Earthquakes in Canada, Iran, and Japan also confirmed the generally poor performance of unreinforced masonry when subjected to seismic actions.

Bruneau (1994) and Boussabah and Bruneau (1992) described the possible failure modes for unreinforced masonry buildings when subjected to earthquake induced loading:

(1) *Lack of Anchorage* : The lack of anchorage of the floors and roof to the walls results in the exterior walls behaving as cantilevers over the total height of the building. This can result in flexural stresses at the base of the walls that can cause out-of-plane failure. Another possibility is the overall failure of the structure as a result of the floors and roof sliding from their supports;

(2) *Anchor Failure* : The anchor between the walls and the roof or floors can fail. This can be through a failure of the anchor or rupture at the connection points;

(3) *In-Plane Failures* : In-plane failures of the walls may be induced by excessive bending or shear. In-plane shear failures are common and are usually evidenced by double diagonal (X) shear cracking. However, shear cracking, unless very severe, does not usually prevent the wall from continuing to carry gravity load. Unreinforced masonry facades with numerous window openings can also have short piers and spandrels fail in shear. Flexural failure is also possible in those elements, especially in slender unreinforced masonry columns. The cracking in both ends of an unreinforced masonry element transforms it into a rigid body of no further lateral load resisting capacity;

(4) *Out-of-Plane Failures* : The anchors between the horizontal elements of a structure and the walls provide out-of-plane support to the walls. These supports allow the walls to behave as one-storey high panels excited at each end by the movement in the horizontal diaphragms. Unreinforced masonry buildings are especially vulnerable to out-of-plane flexural failures and unlike in-plane shear failures, these failures prevent the wall from continuing to carry gravity loads. This type of failure also includes parapet failures where the parapet, if unrestrained, acts as a cantilever. They are also subject to the largest amplification of the base acceleration (being the tallest part of the building). Multiwythe walls which are improperly bonded to each other are also very vulnerable to out-of-plane failure;

(5) *Combined In-Plane and Out-of-Plane Effects* : As the principal direction of loading seldom coincides with the principal axis of buildings unreinforced masonry walls are generally subjected to combined in-plane and out-of-plane effects. As in-plane shear cracking occurs, the resultant triangular cantilever wedges have a considerably weaker out-of-plane strength than the original uncracked walls. It is difficult to identify this type of failure on site and the failures are generally attributed, incorrectly, to only out-of-plane forces; and

(6) *Diaphragm Related Failures* : The failure of the diaphragm is rarely observed following earthquakes. In most cases, damage to the diaphragm itself would not impair its gravity load carrying capacity. The failure of the diaphragm can, however, induce damage at the wall corners from the in-plane rotation of the diaphragm's ends.

The study was broken into three main parts:

(1) A study of the dynamic properties of twelve existing unreinforced masonry buildings using an ambient vibration field testing technique. The dynamic properties were used to calibrate finite element models of the buildings for use in part (3) of the study;

(2) A shaking table testing program aimed at determining the dynamic shear stiffness of a typical unreinforced brick masonry wall panel. The effect of four variables on the shear stiffness were examined. The results were used in the finite element modelling of the buildings from part (1) of the study in part (3); and

(3) The finite element modelling of eleven of the buildings from part (1) of the study. The finite element models were then used in response spectrum analyses using the design response spectrum from AS1170.4 for Adelaide. These results were compared to the results of an equivalent static force design of the buildings identifying differences in the results of the two approaches. From this comparison a simplified design methodology was developed based on the static force method.

A literature review of various aspects of earthquake design, unreinforced masonry construction, and the combination of both is undertaken in Chapter 2. The areas examined include period formula, full-scale building tests, dynamic load tests on unreinforced masonry, real earthquake data from unreinforced masonry buildings, strength and stiffness properties of unreinforced masonry, finite element modelling of brickwork, earthquake design models for unreinforced masonry buildings, floor flexibility, and response modification factors used in simplified earthquake design procedures. The reasons for studying these areas are described in the appropriate section of Chapter 2.

Key aspects of the ambient vibration tests are described in Chapter 3. These include the development of the testing methodology, and the testing program to measure the natural frequencies of twelve unreinforced masonry buildings in Adelaide. The suitability of the various period formulae from the literature review for use with unreinforced masonry buildings are then discussed.

Chapter 4 describes the shaking table testing phase of the study. The test set-up, testing procedure, testing program, and results of the shaking table test program are discussed. The reasons for choosing the four variables for the program and the construction of the test specimens are noted. The resulting dynamic shear stiffness values are compared to the values obtained by other researchers. The wall panels are then modelled using finite elements to establish an effective Young's Modulus for use in later finite element modelling work. The Young's Modulus was compared to those obtained by other researchers in Australia and overseas.

The results from Chapters 3 and 4 were then used to build finite element models of the buildings studied during the ambient vibration tests. These are described in Chapter 5. The development of the models to accurately represent the behaviour, based upon modal analyses, of the buildings is discussed. The models were then used in response spectrum analyses to determine the response of the buildings to the

Australian design earthquake response spectrum for Adelaide. In particular, the results were examined to determine whether trends in the pattern of failure exist, and if so, in which aspect of the response.

Chapter 6 presents the results of equivalent static force analyses which were performed on each of the buildings in accordance with AS1170.4. The results of the equivalent static force analyses are compared to the results of the response spectrum analyses from Chapter 5, in particular the results that influence the six failure modes described above, and refinements and simplifications of the code based design procedure are suggested.

Chapter 7 summarises the results of the study and makes recommendations as to further research that is required.

# 2 LITERATURE REVIEW

In this chapter a review of previous work carried out by other researchers into various subjects that are of relevance to this study is presented. Those subjects are:

(1) Period Formulae - An examination of previously published period formulae for use with unreinforced masonry structures in an earthquake analysis procedure;

(2) Full-Scale Building Tests - A review of tests conducted on actual buildings in order to determine their dynamic properties. The review encompasses both the ambient vibration method chosen for this study and the forced vibration testing method;

(3) Dynamic Loading Tests on Brick Walls and Structures - A review of dynamic loading (both shaking table and otherwise) tests conducted on unreinforced masonry walls and building models to both examine the results for input to an earthquake analysis procedure for unreinforced masonry and to guide the determination of a testing methodology for use in this study;

(4) Data from an Unreinforced Masonry Building subjected to Earthquake Ground Motion - A study of the reported data from an unreinforced masonry building subjected to the 1989 Loma Prieta Earthquake to provide some indication of the actual deformations and stresses experienced by an unreinforced masonry building in an actual earthquake;

(5) Brickwork Properties - A review of the material properties of unreinforced masonry including strength and stiffness values for use in an earthquake analysis procedure for unreinforced masonry;

(6) Finite Element Modelling of Brickwork - A review of finite element modelling of unreinforced masonry conducted by other researchers to guide the finite element modelling conducted as part of this research;

(7) Earthquake Design Models for Brickwork - A review of previously published models for the design of unreinforced masonry buildings subjected to earthquakes to either adopt for use, or guide the development of an earthquake analysis procedure for unreinforced masonry;

(8) Floor Flexibility/Stiffness - A review of previous studies into the effect of floor flexibility on the performance of unreinforced masonry buildings in earthquakes and the importance of floor flexibility in the finite element modelling of unreinforced masonry buildings; and

(9) Appropriate $R_f$ for Unreinforced Masonry - A study of a the $R_f$ factors used in various codes throughout the world and proposed by researchers for selection for an earthquake analysis procedure for unreinforced masonry.

There were some areas that have an effect on the performance of unreinforced masonry buildings that were not examined as they were considered not to be within the scope of this study. These subjects included soil-structure interaction, the use of sliding joints in unreinforced masonry buildings to reduce the earthquake induced forces, and the use of reinforcement to increase the strength of masonry buildings.

# 2.1 PERIOD FORMULAE

An examination of the equilibrium equations for a dynamic multi-degree-of-freedom system (Clough and Penzien (1993)) reveals that the natural period of a structure is an important factor in determining the response of that structure to earthquake ground motions. As such, it plays an important role in the determination of the induced earthquake forces in the various earthquake design procedures (time history, response spectra, and equivalent static force). In this section various period formula contained in several earthquake design codes or provided by researchers from around the world are described and evaluated for use to determine a reliable estimate of the natural period of an unreinforced masonry building. The symbols used by the various codes and researchers have been standardised for ease of comparison.

The Australian Standard "Minimum design loads on structures - Part 4 : Earthquake Loads" AS1170.4-1993 included two different formulae to determine the natural period of a building for use in an equivalent static load design.

$$T = \frac{h}{46} \tag{2.1.1}$$

for the fundamental translational period, and:

$$T = \frac{h}{58} \tag{2.1.2}$$

for the period in the orthogonal direction, where:

| | | |
|---|---|---|
| T | = | The natural period of the building, in seconds; and |
| h | = | The height of the building, in metres. |

It was expected that form of period formula suitable for use with an unreinforced masonry building was one in which the period is proportional the building's height (Equation 3.4.6) and both Equations 2.1.1 and 2.1.2 are of this form.

The original Australian earthquake code Australian Standard "SAA Earthquake Code" AS2121-1979, included the formula:

$$T = \frac{0.09h}{\sqrt{D}} \qquad (2.1.3)$$

for the determination of the natural period of a building , where:

D = The plan dimension of the building in the direction under consideration, in metres; and

h and D are as defined above. The code then noted that the natural period can be determined by Equation 2.1.3 except when the total horizontal force is resisted by a moment resisting frame and then the natural period can be determined by:

$$T = 0.010N \qquad (2.1.4)$$

where T is as defined above, and N is the number of storeys in the building. These formulae are for use in an equivalent static load design. Based upon Equation 3.4.6 it would appear that Equation 2.1.4 is of reasonable form for a shear walled building as the number of storeys can be seen to be proportional to the buildings height. The extra depth term in Equation 2.1.3 would suggest that the mass is not proportional to the depth and based upon Equations 3.4.1 to 3.4.6 would not seem to be of the correct form for use with an unreinforced masonry building.

Comparing Equations, 2.1.1 and 2.1.2, with Equation 2.1.4, it can be seen that with a story height of about three metres, a reasonable estimate for a modern multi-storey building, the three formulae will give approximately the same natural period.

The "Tentative provisions for the development of seismic regulations for buildings" (ATC (1984)) included the formula:

$$T = C_T h^{3/4} \qquad (2.1.5)$$

for moment resisting structures and for all other buildings:

$$T = \frac{0.05h}{\sqrt{D}} \qquad (2.1.6)$$

where T is as previously defined,

$C_T$ = 0.035 for steel framed structures and 0.025 for concrete framed structures; and

h and D are as for Equation 2.1.3 except that in this case the units are feet. Conversion of Equation 2.1.6 to SI units yields Equation 2.1.3. Equation 2.1.5 is similar to Equations 2.1.1, 2.1.2, and 2.1.4 in that the period is a function of the height of the building, though not a linear function as would be expected of a shear walled building as discussed in Section 3.4.

The "Recommended Lateral Force Requirements and Tentative Commentary" of the Seismology Committee, Structural Engineers Association of California (SEAOC (1988)) and "The Uniform Building Code" (UBC(1991)) provided, for the static lateral force procedure, Equation 2.1.5 except with:

$C_T$ = 0.035 for steel moment resisting space frames;
= 0.030 for reinforced concrete moment resisting space frames; and
= 0.020 for all other structures.

Further, as an alternative for structures with concrete or masonry shear walls:

$$C_T = \frac{0.1}{\sqrt{A_C}} \tag{2.1.7}$$

where:

$$A_C = \sum A_e \left[ 0.2 + \left( \frac{D_e}{h_n} \right)^2 \right] \tag{2.1.8}$$

with:

$$\frac{D_e}{h_n} \leq 0.9 \tag{2.1.9}$$

where:

$A_e$ = The effective horizontal cross sectional area, in square feet, of a shear wall in the first storey of a structure; and

$D_e$ = The length, in feet, of a shear wall element in the first storey in the direction parallel to the applied forces.

It should be noted that the shear wall masonry building mentioned in these codes could be a reinforced masonry building. The use of the coefficient as defined in Equation 2.1.7 would result in the depth of the building appearing in the denominator of the period formula. Referring to Equation 3.4.1 it can be seen that the square root of the shear area could appear in the denominator, but the depth would then be expected to appear on the top line of the equation.

SEAOC provided a second method for the determination of the fundamental period, their "properly substantiated analysis". Based upon the structural properties and the deformation characteristics of the resisting elements it used the formula:

$$T = 2\pi\sqrt{\left(\sum_{i=1}^{n} w_i\delta_i^2\right) \div \left(g\sum_{i=1}^{n} f_i\delta_i\right)} \qquad (2.1.10)$$

The values of $f_i$ represent any lateral force distributed approximately in accordance with any rational distribution. The elastic deflections, $\delta_i$ , are calculated using the applied lateral forces, $f_i$ . The period determined using this method is not allowed to be less than eighty percent of that obtained using the Equation 2.1.6. The calculation of the natural period by this method is suited to engineered structures but is not well suited for a simplified design procedure.

Aoyama (1981) stated the formula provided in the Japanese building code for the "first phase design" for earthquake forces:

$$T = (0.02 + 0.01\alpha)h \qquad (2.1.11)$$

where T and h are as defined for the AS1170.4 formulae and:

$\alpha$ = Ratio of the height of storeys, consisting of steel columns and girders, to the entire height, h.

For the case of unreinforced masonry buildings $\alpha = 0$ and Equation 2.1.11 becomes similar to Equations 2.1.1 and 2.1.2 from AS1170.4. As with these equations, Equation 2.1.11 would seem to be of the correct form for shear walled buildings.

Housner and Brady (1963) derived a form of equation to be used specifically with shear walled buildings. It was assumed that the plan dimensions of the building were sufficiently large compared to the height to ensure the building acted as a shear beam with negligible bending. The resulting formula:

$$T = Ch\sqrt{B} \qquad (2.1.12)$$

includes the term B which is the breadth of the building normal to the direction of vibration, h which is the height of the building, and C which is constant and is in a set of units consistent with h and B. This is the form of equation that would be expected for a unreinforced masonry building and Housner and Brady used the same justification for its form as was used in Section 3.4.

Housner and Brady then discussed the determination of the natural period of space frame buildings. While this is not directly related to shear walled buildings, the form of the equations may provide a basis for a formula for use with the buildings included in this study. Three types of space frame buildings were considered:

(1) where the stiffness of a storey is proportional to the weight above that storey;
(2) where the stiffness for each storey is the same and is proportional to the total number of storeys; and
(3) where the stiffness of each storey is the same and is independent of the total number of storeys.

For the first two cases the formula:

$$T = C\sqrt{h} \qquad (2.1.13)$$

was derived. For the third case the formula:

$$T = Ch \qquad (2.1.14)$$

was derived. T, C and h are as in Equation 2.1.12. The absence of any plan dimension in both equations was again explained by the terms being common to both

the mass term and the stiffness term and subsequently cancelling out when combined. Both of these equations are of the form that is expected for shear walled buildings, being proportional to the buildings height, and Equation 2.1.14 is in fact exactly as would be expected with the period being proportional to the buildings height (Section 3.4).

Housner and Brady went on further to compare Equations 2.1.3, 2.1.12, and 2.1.13 to the measured periods of a number of steel and reinforced concrete shear walled buildings along with a fourth equation which turned out to have the best fit to the data:

$$T = CN\sqrt{B}\sqrt{\left[1+16.4\left(\frac{1}{B}+\frac{1}{D}\right)\right]} \qquad (2.1.15)$$

The variables are all as previously defined. The difference between the standard deviation of the equation with the best fit, Equation 2.1.15, and the equation with the worst fit, Equation 2.1.3, was twenty-five percent. Housner and Brady then concluded that to achieve a significant improvement in the fit of the equation it would be necessary for the wall stiffness to appear explicitly in the equation and consequently provided the Japanese equation:

$$T = C\{4+h(1-4d)\} \qquad (2.1.16)$$

where T, C, and h are as previously defined by Housner and Brady and:

d = Total storey length of wall divided by the total area of all floors.

Because d makes an allowance for the actual length of walls, Housner and Brady concluded that Equation 2.1.16 came closer to allowing for the true stiffness of the wall. The units in Equation 2.1.16 are not consistent, however, and no guidance was given as to what units should be used for d.

Muria-Vila (1990), in a study involving ambient vibration testing of unreinforced masonry buildings in Mexico City, found, by fitting a curve to test data, the empirical relationship:

$$T = 0.039N \qquad (2.1.17)$$

where T and N are as defined previously. This equation gives a period only thirty-nine percent of that calculated by Equation 2.1.14. Equation 2.1.17 is also of the form expected of a period formula for a shear walled unreinforced masonry building.

Stafford-Smith and Crowe (1986) approached the problem of determining the natural period by different means. Rather than provide simple formulae for natural period a "hand method" was presented. The method was developed for tall structures having uniform properties through their height. The structures could consist of rigid frames, coupled walls, wall-frames, and braced frames. It is the coupled wall type that is most relevant for this study. A coupled wall consists of two shear walls in the same plan connected by beams along the height of the walls. The beams have known stiffness, length, and spacing. The basis of the method is that all the types of structures listed above behave as members of a family of shear-flexure structures whose static deflections can be predicted by coupled wall theory. The method involves sixteen lines of simple calculation and would be suitable for an engineered structure. This would limit its use for the unreinforced brick buildings in this study as the aim was to provide a simplified design approach. The method was tested against a series of computer analyses of coupled wall buildings and was within two percent of the period estimated by the computer model. The UBC formula, Equation 2.1.5, underestimated the same periods by an average of fifty-one percent.

Monge (1984) presented a method to determine the fundamental period of a tall building using a continuum model. The model was based on the hypothesis that the shear force in any vertical substructure of a building, such as a wall or rigid frame, is proportional to the first derivative and the second derivative of the displacement of the building multiplied by stiffness coefficients. Monge stated that the natural period could be calculated by hand in three hours using this method. The results from this method compared favourably with the results of matrix modal analysis, the Rayleigh method, and the UBC.

Cheung and Kasemset (1978) developed a model for determining the modal frequencies of a shear wall frame structure using the finite strip method. Two methods were proposed. In the first method the shear walls and frames were idealised as an assemblage of finite strips of varying thicknesses. In the second method the shears walls were idealised as finite strips while the frame elements were regarded as a number of long columns. The proposed methods showed good agreement with a finite element analysis in the determination of the modal frequencies.

Mukherjee and Coull (1974) and Coull and Mukherjee (1978) presented a method for the determination of the natural frequencies and mode shapes for a shear walled building, specifically those with complex geometric layouts. The method derived governing dynamic equations from energy principals using Vlasov's theory of thinned walled beams. The method can incorporate foundation flexibility in the determination of the natural frequencies. The method was compared with the results from experimental investigations of two model structures. The authors concluded that the correlation between the experimental results and the results from the proposed method was generally good.

In Chapter 3, the suitability of the above formulae for estimating the natural period of unreinforced masonry buildings was examined. This was done by comparing the periods given by the formulae to the measured values for sixteen unreinforced masonry buildings in Adelaide. The methods proposed by Stafford-Smith, Crowe and Monge, Cheung and Kasemset, and Coull and Mukherjee were not considered further in this study because of their complexity. Recall the criterion of a simple approach to the design of unreinforced masonry buildings for earthquake induced forces. They were included here only to show that more refined methods are available for the determination of the natural periods which do not require a finite element analysis, even if a structure has a complex geometry.

# 2.2 FULL-SCALE BUILDING TESTS

Testing of full-scale structures has long been recognised as a convenient method of determining for the first time or confirming the dynamic properties of structures (for example Ibanez and Shanman (1973)). Tests have been conducted in many parts of the world and on many different types of structures. The use of both ambient vibrations and vibrations induced by purpose made shaking machines to determine the dynamic properties have been reported. The mathematical justification behind the use of ambient vibration testing for the identification of structural system parameters is beyond the scope of this thesis but can be found in Gersch and Martinelli (1979) and Gersch and Brotherton (1982).

Tests conducted using a purpose made shaking machine to induce vibration in a structure, or forced vibration tests, were reported by Nielsen (1966), Reay and Shepherd (1971), Petrovski et al (1973), Chen et al (1977), Foutch and Jennings (1977), Ohta et al (1977), and Muto et al (1984) for reinforced concrete buildings; by Meyyappa and Craig (1984), and Ohta et al for steel framed buildings; and by Stephen and Bouwkamp (1977) for a reinforced masonry building. These tests were used to determine the accuracy of existing mathematical models and/or to determine parameters for new mathematical models of existing structures.

Briceno et al (1973) used pull back tests to study the dynamic response of a reinforced concrete building with different levels of non structural elements present.

Ward (1977) observed "It is convenient that the dynamic component of the wind acting on a bluff body can be considered to approximate a 'white noise' input to a multi-storey building. This means the lateral wind-induced vibrations of these structures can be interpreted in such a way that their natural periods, mode shapes and equivalent damping values can be measured". This dynamic component of wind results in ambient vibration of the structure.

Torkamani and Ahmadi (1988), and Kwok et al (1990) determined the natural periods of steel framed buildings from tests conducted without inducing additional vibrations in the buildings, ambient vibration tests. Kwok et al, and Mendoza et al (1991) undertook ambient vibration tests on reinforced concrete, and Muria-Vila (1990) on unreinforced masonry buildings, and Gates and Smith (1984), Nigbor (1984), and Brownjohn et al (1987) determined the dynamic properties of bridges

using ambient vibration tests. Diehl (1986) used ambient vibration tests to verify a mathematical model of a multistorey building.

Taoka et al (1973), and Williams (1984) determined the natural periods of reinforced concrete buildings by both a forced vibration test and an ambient vibration test. Boukamp and Stephen (1973) used both methods to determine the dynamic properties of a steel framed building, while Maguire et al (1984) performed both types of tests on a chimney structure, and Williams on a bridge.

Forced vibration tests are the traditional method of undertaking full-scale testing. An oscillating force is applied at a single frequency and the frequency varied until a resonance condition is reached in the structure. Conducting ambient vibration tests have some significant advantages over forced vibration as recognised by Stubbs and McLamore (1973) and Torkamani and Ahmadi "...the duration of testing and amount of labour needed in vibration generator tests are much greater than for ambient vibration tests". Gates and Smith noted "Ambient vibration testing is an economical means of testing structures for their dynamic response characteristics", and Brownjohn et al observed "The advantage of relying on this type of input (ambient) is that the test procedure is considerably simplified, as the only equipment required during the test is for data acquisition". Brownjohn et al also noted the disadvantage of ambient vibration testing "....the excitation is a non-stationary random process". However, Bouwkamp and Stephen, when comparing the results obtained during their forced and ambient vibration tests, noted that "The natural frequencies determined from the forced and ambient vibrations agree very closely". Maguire et al noted that "The results obtained from both ambient and impulse tests on the BRI chimney are presented in (their) Figure 5. The natural frequencies obtained from the two tests are similar,...". It would seem that both ambient vibration tests and forced vibration tests are legitimate methods of obtaining the dynamic properties of structures. Both methods were therefore considered for adoption in this project.

A concern raised by a number of researchers with the use of forced vibration tests, and especially ambient vibration tests, was the applicability of the results at the low levels of excitation during the tests to the higher levels of excitation associated with earthquakes. Ward observed, when discussing ambient vibration tests, that "The wind-induced vibrations in tall buildings are small, and it can be argued that the results from this type of study are not relevant to earthquake resistant design". Foutch and Housner (1977) noted that during the San Fernando earthquake buildings acted as non linear softening dynamic systems - "It was noted that the fundamental

periods of vibration of virtually all instrumented buildings were longer than those determined before the earthquake during ambient vibration tests at much lower levels of excitation.".

In a study into the identification of the modal parameters from forced vibration tests on a small model structure, Soucy and Deering (1989) noted a "slight, but steady" decrease in the natural frequency as the force level increased.

Nielsen noted "By exciting some of the modes at different amplitude levels it was found that the resonant frequency decreased slightly as the force level was increased, the shift in frequency being typically that of a 'softening spring' ". The lowest translational mode frequency decreased by a maximum of one percent for a seven and a quarter times increase in force. The second lowest mode frequency decreased by one and a half percent for a seven times increase in force. Foutch and Housner, in a follow up to the work of Nielsen, compared the results of the forced vibration testing to recordings of the behaviour of the structure during an earthquake and found "....the natural periods of vibration of the building were longer during the earthquake than they were either before or after the event". The explanation given by Foutch and Housner, however, rather than the building acting as a softening spring is that "....changes observed during the earthquake could be the result of the loss of stiffness due to cracking of the encasing concrete of the columns". It was noted that the damage sustained by the structure during the earthquake was repaired after the event. An important warning in the conclusion of Foutch and Housner should be noted for all full-scale dynamic tests "A prediction of the fundamental period of vibration of a particular structure may be 20 to 30 percent different from that observed during an earthquake".

Ohta et al also reported a difference in the fundamental natural period obtained from vibration tests and the fundamental natural period observed during earthquakes. The period during earthquakes was 1.13 times the natural period measured during vibration tests. Chen et al observed that "The increase of the period of the undamaged structure with increasing amplitude of response,.., indicates the structure has stiffness properties of a non linear softening spring system". Their results showed a twenty-five percent decrease in the frequency for a change in the roof velocity from just above zero to twenty cm/sec. The frequency converged to a constant value as the roof velocity (and hence force level) increased. It was also observed that the mode shape remained constant regardless of the force level of the test. Foutch and Jennings observed "it is not uncommon for the natural periods of a building to

lengthen by 20 to 30 percent during the large amplitudes of vibration experienced during response to strong motion".

Gates and Smith compared the natural periods determined from ambient vibration tests to those determined under earthquake conditions and under large force conditions for two of the bridges in their study. For the bridge subjected to a force vibration tests with large force levels it was found that the natural frequencies decreased by a maximum of eleven percent and by an average of five percent from ambient vibration tests to large scale vibration tests. The bridge subjected to earthquake excitation had a reduction in frequency of a maximum of eighty-five percent from ambient vibration tests to earthquake conditions in the longitudinal direction. For the vertical and translational direction the maximum reduction was thirty-seven percent for the first mode. The authors explained the significant difference in response between the ambient and earthquake results as a result of the non-linear response of the soils at the bridge abutments.

In contrast, however, Petrovski et al found the level of excitation did not have any effect on the first mode frequency, but the second mode frequencies decreased as the levels of excitation increased. A change of one percent in frequency was noted for fifty-nine percent increase in force level. Also noted was the fact that the mode shape was unaffected by changes in force level. Reay and Shepherd concluded from their comparison of results of a force vibration test and theoretically calculated dynamic characteristics that "...the dynamic characteristics determined from the small amplitude vibration tests undertaken by the authors are applicable to significantly higher strain levels".

Examination of the changes to the natural frequency due to changes in the level of vibration applied to a structure would suggest that the results of vibration tests at low levels would be of little use when considering the response to earthquake forces. However, when the errors in determining the frequency (experimental errors) are taken into account, the effect of the force level may not be as great. Further, the position of the structure's frequency on a response spectrum curve, especially on the constant acceleration region, could result in the change in frequency being insignificant. Finally, it was unanimously observed by those researchers which compared the results of tests conducted at high levels of excitation to those conducted at low levels of excitation, that there is an increase in the natural period (or decrease in the natural frequency) with an increase in the level of excitation. An examination of the design response spectrum, Figure 5.2.1, shows that an actual

period lower than the design period will either result in the design force being the same, if both are on the constant acceleration region of the design response spectrum, or a lower design force if they are not, which results in a conservative design force.

Gates and Smith raised a further problem with ambient vibration tests. Ambient vibrations could contain a predominant exciting force. When field data is obtained it is very difficult to identify and remove these unwanted frequencies from the response of the structure. A possible solution to this problem is also given by the authors. They suggest that to eliminate any dominant exciting force frequencies from the recorded response of the buildings multiple data be recorded and the results averaged. No other researchers mentioned this potential source of errors.

Hoerner and Jennings (1969) discussed the problem of the modes of vibration of a structure being close together and subsequently interference occurring between two adjacent modes. While the discussion was for forced vibration tests, some of the conclusions can be applied to ambient vibration tests. It was shown that there is no interference on the first mode and this was shown mathematically as well as with an empirical example. For all modes except the first, the possibility of modal interference was real and a method of separating the modes from the results of tests containing modes that have interference was presented. It can therefore be assumed that as long as the modes are excited the modal frequency and shape can be determined by either full-scale ambient or forced vibration testing.

Hoerner and Jennings also mentioned the important consideration of the location of the sensors of the vibration and in forced tests the location of the exciter. They observed that the "generators usually are located in the upper portion of the structure so that the exciting force will be away from any nodes of the lower modes of vibration,..". Chen et al found that the location of the vibration exciter had "a significant influence" on the deflected shape of the building undergoing testing. Nielsen noted that for the forced vibration tests conducted on a nine storey steel frame that "The exciter was located away from the center (sic) of the floor so that both translational and torsional modes could be excited." and further stated that "The main problems in gaining the most information from forced vibration tests are (1) to locate the vibration exciters far enough away from nodal points of the desired modes; and (2) to locate the vibration exciters such that interference between the response of modes that have frequencies close together is eliminated."

Kwok et al noted that the accelerometers in their series of ambient vibration tests were located, if possible, at the shear centres of the buildings so that torsional effects were eliminated and only lateral modes were recorded. Bouwkamp and Stephen observed for their forced and ambient vibration tests "..for the translational motions the accelerometers were located near the center (sic) of the floor and orientated so as to pick up the appropriate North-South or East-West accelerations. For recording the torsional motion accelerometers were properly oriented near the center (sic) of two opposite walls."

Diehl further simplified the ambient vibration method by restricting the location of the instrumentation to the roof, orientated so that both torsional and lateral modes were identified. Using this method, five modes were recovered for a structure, sufficient to verify a mathematical model. Diehl further observed that "....the mode ranking comes close to the 1,3,5 frequency sequence for structures dominated by shear deformation,..". This ratio of modal frequencies was not mentioned by other researchers.

Other important information provided by the authors of various studies into full-scale testing included Maguire et al noting "One of the greatest sources of error is (sic) any digitally computed spectrum results from the fact that the measured (transient) signal is not periodic in the measurement period chosen and therefore violates a prime requirement of the FFT. This results in the true spectral estimate at a particular frequency being modified by power leaking from other frequency components. ..... Leakage can be significantly reduced by 'windowing' the sampled time history record, ie shaping it to become periodic". Also mentioned was the problem of aliasing, the use of a too small sampling rate resulting in the structural frequencies being recorded as a lower frequency. (see Appendix A - Sampling Theorem).

Ohta et al used a 'Hanning' window to modify the data in their forced vibration tests of various buildings to modify the data to a periodic record. Torkamani and Ahmadi also used the 'Hanning' window. Further, they noted that they recorded 102.4 seconds of data at 40 samples per second, and a FFT was performed on 4096 points of their record. Brinceno et al used a sampling rate of 200 samples per second. Nigbor mentioned the use of low pass filtering to remove the frequencies from the record that are of no interest to the researchers. High pass filtering was performed on the record to remove the DC offset.

Either the ambient vibration test or the forced vibration test could have been used in this study. In Chapter 3 - Field Testing - the method adopted, and the reasons for that choice are discussed.

# 2.3 DYNAMIC LOADING TESTS ON BRICKS WALLS AND STRUCTURES

The 1970s saw a significant increase in the amount of research conducted on the earthquake performance of unreinforced masonry walls. Some of the research involved the dynamic testing of unreinforced masonry walls in the laboratory and this research is reviewed in this section. While this study is limited to unreinforced masonry, where the experimental test methods used on other materials are relevant to the current study they are included in the review.

### 2.3.1 In-Plane Tests

Researchers at the University of California at Berkeley have undertaken a number of tests on unreinforced and partially reinforced (i.e. reinforced only at critical sections) walls and scale-model buildings, including some shaking table tests.

Cyclic shear tests on masonry double piers were reported by Mayes et al (1976a), and Mayes et al (1976b) and on single piers by Hidalgo et al (1978) and Chen et al (1978). Four failure modes were observed in the tests; shear failure, shear failure with vertical cracks, shear and flexure failure, and flexure failure with crushing of compressive side. The unreinforced masonry panels failed by the first type, shear failure. All of the double piers experienced some type of ductile behaviour. A trend towards more ductile behaviour as bearing stress was increased was noted. However, the lateral displacement decreased with the increase in bearing stress so that the increased ductility was offset by an increased induced shear force. The ultimate strength of the panels was found to increase with increased amounts of reinforcement, or increased bearing stress. The shear stiffness of the piers was found to increase not only with increased bearing stress but also with an increased rate of loading.

Further tests on single piers were conducted at Berkeley and reported by Hidalgo et al (1978), Hidalgo et al (1979), and Chen et al (1978). From the unreinforced masonry piers tested it was found that for a height to width ratio of two, a flexural mode of failure occurred. For a height to width ratio of one, the unreinforced masonry specimens failed in shear.

Further dynamic testing of unreinforced clay brick masonry walls was carried out at Berkeley and reported in Mengi and McNiven (1989) and McNiven and Mengi

(1989). The shaking table tests conducted as part of this study (Chapter 4) were based upon the tests reported by Mengi and McNiven. The test set-up used for these tests at Berkeley is shown in Figure 2.3.1.

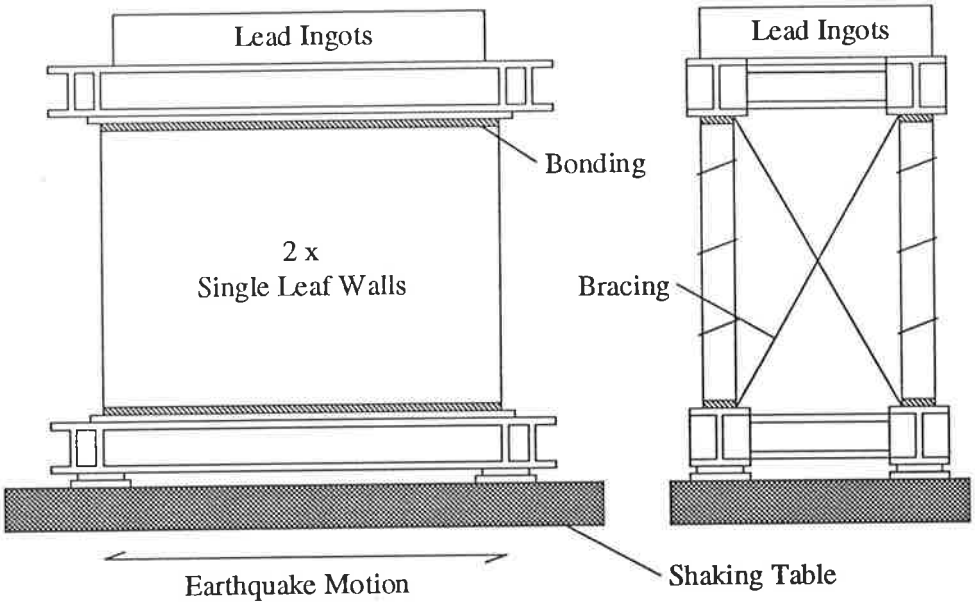


Figure 2.3.1 Mengi and McNiven test set-up.
(from Mengi and McNiven (1989))

The authors noted that the experiments were designed to produce pure shear in the wall so that the shear modulus was established. The most significant observation from the testing program was that "the values of the shear modulus which we (McNiven and Mengi) establish when the masonry is responding to dynamic forces are radically different from those when the masonry is responding to static forces". This has serious implications if the results of static tests are used to model the dynamic response of masonry buildings.

In 1984, similar tests conducted on unreinforced concrete block masonry were reported by Mengi et al (1984) and Sucuoglu et al (1984).

The last tests conducted at Berkeley of interest to this study were a series of shaking table tests on model masonry buildings. These tests were reported on by Gulkan et al

(1979), Clough et al (1979), Gulkan et al (1990), Clough et al (1990), and Manos et al (1983). The test specimens were a square arrangement of four wall panels. The authors noted the influence of workmanship on the properties of the masonry components. The load path shown in Figure 2.7.1 was observed for the buildings in these tests. The requirements for the different components of the model buildings were summarised as:

(1) Out-of-plane walls must have sufficient flexural strength to resist inertia forces due to their own self mass when acting as vertical beams supported top and bottom;

(2) In-plane walls must have the capacity to resist the inertia forces of the entire roof system plus the top half of the out-of-plane walls; and

(3) The roof structure must be strong enough to transmit the roof forces and the out-of-plane wall forces to the in-plane connection by membrane action.

Conclusions from the tests included that the "frequency characteristics of the earthquake input are not a major factor in its tendency to induce damage in a masonry house" and that "no significant deterioration in the overall performance can be seen" when the model buildings were orientated on the shaking table such that in-plane and out-of-plane responses were induced in the walls simultaneously.

In Italy, Benedetti and Benzoni (1984) undertook laboratory shaking table and static load testing on model stone masonry buildings for use with a non-linear finite element model. It was found that the failure of the buildings occurred at levels of base acceleration four to six times greater than the design level base acceleration for most of Australia.

Arya (1980) reported on a series of tests conducted on reinforced and unreinforced masonry wall specimens at the University of Roorkee in India from 1961 to 1978. The observations from these tests included:

(1) That the cracking of masonry largely occurred as a consequence of tension;

(2) Application of compressive load at the time of curing increased bond strength;

(3) Plain masonry walls, when tested as shear walls, had shear strengths 70 percent of the theoretical values; and

(4) Unreinforced masonry walls had no reserve strength beyond the first crack load.

Qamaruddin et al (1984) described further research conducted at the University of Roorkee aimed at determining the possible advantages of providing sliding joints in masonry walls at their bases. It was observed in these tests that the workmanship plays an important part in determining the strength of a masonry structure.

Research on the earthquake behaviour of brick masonry has also been undertaken in Europe. In Germany, Konig et al (1988) reported on shaking table and quasistatic tests conducted on unreinforced masonry walls. It was found that the crack pattern strongly depended on the axial load level.

In Slovenia, Tomazevic (1987) and Tomazevic and Zarnic (1984) reported on the earthquake simulator testing of a 1/7-scale 4-storey masonry building model. The tests were conducted to examine the feasibility of the storey mechanism model, noted in Section 2.7, to model masonry buildings subjected to earthquake excitation. It was concluded that the first natural mode was predominant in the response of the model to earthquake excitations.

Tomazevic and Weiss (1994) reported on the shaking table testing of two 3-storey plain and reinforced masonry 1/5 scale building models. Considering only the unreinforced masonry model it was found that at the ultimate state horizontal cracks developed at the joints between most walls and slabs. The model collapsed at the attained maximum response, showing no ductility.

Tomazevic and Velechovsky (1992) reported on the testing of a 1/7 scale model masonry buildings after finding that this was the most practical upper limit for the modelling for the modelling of masonry.

Also in Europe, in a joint research program between Macedonia and Italy, Jurukovski et al (1992) reported on three 1/3 scale 4-storey buildings tested on a biaxial shaking table. The aim of the testing program was to examine the effectiveness of strengthening techniques. The traditionally constructed model experienced intensive damage to the first floor, including the collapse of complete

walls, slight damage to the second floor, and almost no damage to the top two floors.

Magenes and Calvi (1992) conducted cyclic tests on unreinforced masonry walls in Italy. The tests were conducted to determine the effects of aspect ratio and vertical compression. Two failure modes were found for differing levels of axial stress. A frictional failure of the mortar joints was observed for lower axial stress levels and tensile cracking of the bricks was observed for higher axial stress levels.

In Britain, shaking table tests were conducted on twin unreinforced masonry wall specimens using a test set-up similar to that used at Berkeley and shown in Figure 2.3.1 and reported in Pomonis et al (1992). Pomonis et al concluded that the frequency content of the ground motion proved to be an important factor, along with the actual amplitude of the motion, in determining the response of the walls.

Shing et al (1989) reported on the testing of sixteen reinforced masonry specimens under dynamic shear forces at the University of Colorado. From the results of these tests it was concluded that the stiffness of a wall panel does not alter with the position of the induced displacements.

Cyclic in-plane loading tests were conducted on unreinforced masonry walls at the University of Illinios at Urbana-Champaign by Abrams (1992). Abrams noted that "it appeared as though the previous loading and damage had little to do with the subsequent behaviour". It was also found that the walls continued to resist sizeable lateral loads while deflecting beyond well beyond the linear range of response.

Jankulovski and Parsanejad (1994) undertook a similar study at the University of Technology, Sydney. It was found that the hysteresis behaviour of the walls varied within a broad range. The masonry walls exhibited a sizeable capacity for non-linear deformation and energy dissipation. The elastic limit for the horizontal displacement was about 0.2 percent of the height of the wall.

Similar tests were conducted in New Zealand by Priestley and Bridgeman (1974) on reinforced masonry walls. While the tests were not directly relevant to unreinforced masonry it was found that satisfactory ductility could be obtained by the provision of reinforcing steel in masonry walls.

### 2.3.2 Out-of-Plane Tests

It has been found by research on model structures with walls in both orthogonal plan directions that the walls subjected to out-of-plane forces are just as crucial to the satisfactory performance of unreinforced masonry buildings under seismically induced loads as the in-plane walls. This has been recognised in a number of research projects where the out-of-plane behaviour of masonry walls under cyclic loads has been investigated.

Bariola et al (1990) reported on the out-of-plane response of unreinforced clay brick walls during a shaking table test series. The walls were tested as cantilevers and failed by rocking as a rigid body after the bending strength of the base of the wall was exceeded.

Kariotis et al (1985) and Adham (1985) reported on a series of full-scale tests conducted on unreinforced masonry wall specimens to study the out-of-plane dynamic stability as part of a larger research program conducted in the United States aimed at mitigating the seismic hazards in existing unreinforced masonry buildings. The failure of the wall specimens was not sudden, but was characterised as a slow drift into instability during reversal of the dynamic motions of the ends of the walls.

Also in the United States, Davidson and Wang (1985) conducted cyclic lateral load tests on masonry wall panels. Both reinforced and unreinforced masonry wall specimens were tested and the unreinforced masonry specimen was found to absorb no energy and failed during the first cycle. The theoretical maximum moment for the specimens was found to be considerably greater than the measured maximum moment.

In New Zealand, Priestley et al (1979) reported on a series of out-of-plane tests conducted on masonry veneer panels. It was found that preformed horizontal and diagonal cracks had no apparent influence on the ultimate performance of the veneers.

### 2.3.3 Summary

The results of the previous research into the behaviour of unreinforced masonry construction can be summarised as:

(1) Unreinforced masonry walls exhibited some ductility;

(2) Ductility improved with increased bearing stress;

(3) Ultimate strength increased with increased bearing stress;

(4) The ultimate flexural strength determined from dynamic tests was less than or equal to the ultimate strength values from pseudo-static tests. This result was different to what has been observed for steel and concrete, where increased loading rate increases the flexural strength;

(5) Shear stiffness increased with increased bearing stress and an increased rate of loading;

(6) Height to width ratios of unreinforced masonry wall panels influenced the failure mode;

(7) The dynamic shear stiffness was radically different to the static shear stiffness;

(8) The influence of the workmanship was significant;

(9) Typical single storey masonry houses are so rigid that they do not develop complicated dynamic response mechanisms. The frequency characteristics of the input motion are not a major factor in the tendency to induce damage;

(10) The required strength of a wall to resist combined in-plane and out-of-plane loads was not significantly different to that required to resist the in-plane and out-of-plane actions independently;

(11) Out-of-plane strength was the critical design parameter. Shear stiffness was important in determining the forces induced in the structure;

(12) Unreinforced masonry walls have little reserve bending strength beyond the first crack load. Walls subjected to out-of-plane loads fail abruptly and have no energy absorption;

(13) Unreinforced masonry wall damage increased with increased in input energy, whether applied by one shock or in a series of smaller shocks;

(14) Crack patterns depended on the axial load level;

(15) The first mode response dominated the overall response of an unreinforced masonry building subjected to earthquake motion; and

(16) For walls subjected to out-of-plane loads, the theoretical upper bound of the centre displacement can be momentarily exceeded.

# 2.4 DATA FROM AN UNREINFORCED MASONRY BUILDING SUBJECTED TO EARTHQUAKE GROUND MOTION

A significant number of buildings around the world have been instrumented so that their performance in earthquakes can be monitored. Unfortunately, very few of these are unreinforced masonry buildings. However, one such unreinforced masonry building is a historic firehouse in Gilroy, California and reported in Tena-Colunga and Abrams (1992) and Abrams (1993). The Gilroy firehouse is a two-storey brick building typical of construction in the turn of the century in California and across the United States. Lateral load resistance is by unreinforced masonry bearing walls and timber diaphragm floor and roof systems. The building survived the 1906 San Francisco earthquake and was instrumented as part of the California Strong Motion Instrumentation Program. The data recorded by the instrumentation was a result of the 1989 Loma Prieta earthquake (Gilroy is within 15 km of the epicentre of the Loma Prieta earthquake).

### 2.4.1 Description of the Building

The Gilroy firehouse was initially constructed as a box, consisting of four exterior brick walls. A back room was later added to the building. The south and the west walls of the building contain several openings, while the west, north, and the interior walls are almost solid. The centre of the in-plane wall stiffness is offset from the centre of mass and therefore some torsional response would be expected during an earthquake. The plan of the building is shown in Figure 2.4.1.

The total wall thickness of 305 mm is made up of three wythes of brick. Mortar bed joints were 13 mm. Bricks were removed from the building and their properties were measured. The results are shown in Table 2.4.1.

Table 2.4.1 Measured Brick Properties from the Gilroy Firehouse (from Abrams (1993))

| | |
|---|---|
| density | 17.5 kN/m$^3$ |
| absorption | 13.8 percent |
| modulus of rupture | 1.79 MPa |
| compressive strength | 37.0 MPa |

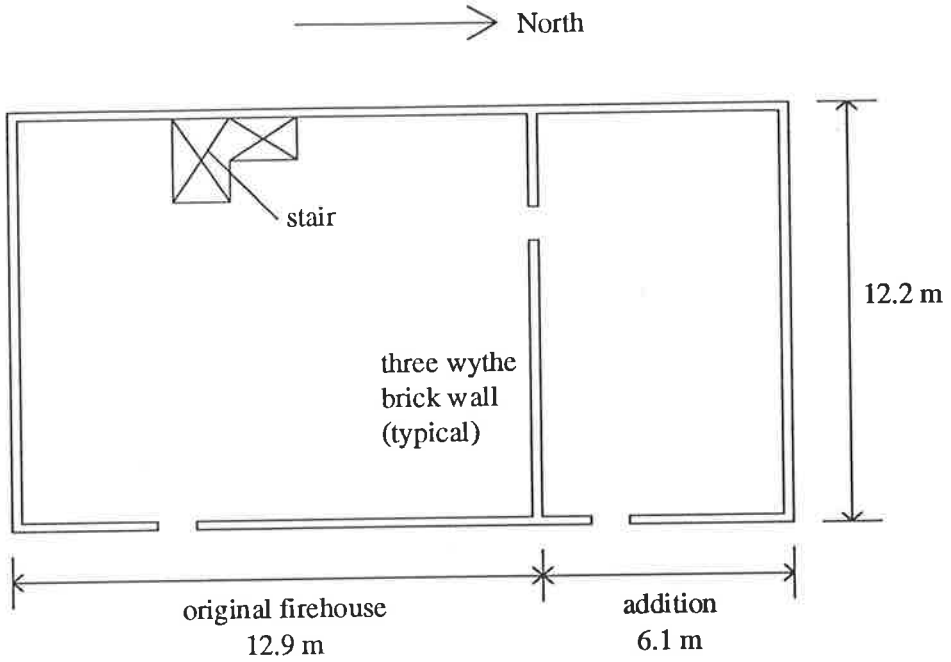


Figure 2.4.1 Plan of the Gilroy Firehouse.
(from Tena-Colunga and Abrams (1992))

In-situ shear strength tests were also carried out. It was found that the shear strength of the brickwork was 0.59 MPa.

### 2.4.2 Observed Behaviour

Damage to the building from the Loma Prieta earthquake was limited to diagonal cracking emitting from the top exterior corner of a window on the second floor. Cracking at the wall-ceiling interface was noted on the second floor level. No other structural damage was noted.

The horizontal accelerations were measured in three directions in the roof. The east-west acceleration was measured at the top of the interior wall and at the centre of the roof diaphragm. The recorded peak acceleration at the interior wall was 0.41g and at the centre of the roof diaphragm was 0.79g. These accelerations corresponded to

amplification factors of 1.4 and 2.7 respectively. A north-south acceleration of 0.55g was recorded at the centre of the roof diaphragm, corresponding to an amplification factor of 1.9.

It was noted by Abrams that the sequence and frequency content of the east-west wall motion was remarkably similar to the ground motion which suggested that the wall acting within its plane was "quite stiff". The Fourier spectra of the response of the structure lead to the determination of the dominant apparent period of the structure as 0.45 seconds. When a critical damping value of five to ten percent was assumed, excellent agreement was found between response spectra maxima and measured response values. This suggested to Abrams that linear response spectra are a viable means for estimating peak response, provided a reliable estimate of building period can be found, as was noted in Section 2.1.

Nominal shear and flexural stresses were estimated from the measured floor accelerations using masses derived from the estimated structural weight. The horizontal acceleration at the top of the walls was assumed to be equal to measured acceleration at the top of the interior wall in the east-west direction. This assumption was acknowledged by Abrams as being "rather crude" and the nominal stresses were only indicative of the approximate range. The stresses are shown in Table 2.4.2.

Table 2.4.2 Summary of Nominal Wall Stresses.
(from Abrams (1993))

| Wall | Shear Stress (MPa) | Flexural stress (MPa) | Gravity Stress (MPa) |
|---|---|---|---|
| South | 0.26 | 0.43 | 0.30 |
| Central | 0.24 | 0.71 | 0.28 |
| North | 0.09 | 0.27 | 0.17 |
| East | 0.24 | 0.54 | 0.28 |
| West | 0.15 | 0.31 | 0.20 |

The shear stresses in Table 2.4.2 were calculated using the entire wall section as the shear area, the flexural stresses were calculated by dividing the overturning moment by a section modulus based upon gross, uncracked sections. Gravity stresses were based upon minimum vertical dead loads alone.

Based upon the stresses reported in Table 2.4.2, it was reasonable that the walls of the Gilroy firehouse did not crack. The difference between the tensile flexural stress and the gravity stresses were nearly all less than the (United States) code allowable values. The central wall had the highest tensile stress (0.43 MPa) which was about 1.3 times the allowable values given in the various United States masonry codes of practice.

### 2.4.3 Computational Studies

As well as measuring the response of the firehouse to the Loma Prieta earthquake, Tena Colunga and Abrams also undertook computational studies into the performance of the building.

Firstly, a discrete multi-degree-of-freedom system was used to analyse the building for each horizontal direction. Dynamic degrees of freedom were assigned to lumped masses at the centroid of each wall and at the centre of the diaphragms for the floor and roof. Soil flexibility was modelled by generalised translational and rotational springs at the base. Tena Colunga and Abrams concluded from the results of several analyses that the dynamic response is sensitive to variations in diaphragm stiffness, wall stiffness, mass discretization, and damping assumptions. It was found that the measured acceleration histories at the roof could be "replicated reasonably well" using the discrete multi degree-of-freedom model, provided that diaphragm stiffness and soil flexibility were estimated accurately.

Secondly, a 3-dimensional finite element model was used to predict the behaviour of the building. The finite element model was confined to the linear range as the building was found to be largely uncracked after the earthquake. The finite element model was used to determine the mode shapes and frequencies. Further, it was used to undertake earthquake analyses using :

(1) Equivalent static forces (obtained from the multi degree-of-freedom dynamic discrete model);

(2) Response spectrum (from recorded ground motions); and

(3) a time-step integration of 20 modal coordinates using the measured ground motions.

Tena Colunga and Abrams reported good correlation between the three methods of analysis. It was further concluded that the discrete multi degree-of-freedom model may be suitable for estimating peak lateral forces and that a linear response spectrum is suitable once modes of vibration are identified.

### 2.4.4 Conclusions

Abrams concluded that the ground motion at Gilroy represented the upper limits to that which would be expected to experienced in the eastern United States. Similarly, the Loma Prieta earthquake would be at the upper limits of ground motion that a building in Australia might be expected to experience. As such, it suggests that unreinforced masonry can be designed to perform satisfactorily for the design level earthquakes in Australia.

Abrams further noted the importance of well tied roof and floor diaphragms. The importance of this observation cannot be underestimated based upon the observations in a number of earthquakes. Also noted by Abrams was the importance of a large ratio of wall to floor area.

# 2.5 BRICKWORK PROPERTIES

In order to model the behaviour of unreinforced masonry buildings under earthquake induced loads it is necessary to have an understanding of the properties of the clay brick unit, mortar, and the two phase material that results when brick units and mortar are used to construct a wall. In this section, the strength and stiffness properties of these two materials and the combined material, as reported in different studies, are examined. It should be noted that mean values of the properties are usually reported and that for masonry, the scatter can be large.

## 2.5.1 Axial Compressive Strength

Brickwork is usually designed for the axial loads applied to the structure, and therefore several studies have been conducted to investigate the axial strength of brick, mortar, and brickwork.

Considering first the clay brick unit, the results of tests conducted in Australia and overseas are summarised in Table 2.5.1.

Table 2.5.1 Compressive Strength of Brick.

| Compressive Strength (MPa) | Details (Origin) | Researcher |
|---|---|---|
| 83.2 | Full size normal brick with 3 cores (Australia) | Base and Baker (1973) |
| 66.3 | Full size normal brick with 17 cores (Australia) | Base and Baker (1973) |
| 36.3 | Normal brick (Australia) | Page (1978) |
| 22.9 | 3 core clay bricks (Australia) | Jankulovski and Parsanejad (1994) |
| 32.9 | Wire cut 3 hole brick (Britain) | Hendry (1973) |
| 31.8 | Wire cut 5 hole brick (Britain) | Hendry (1973) |
| 19.7 | Normal brick specimens (Italy) | Magenes and Calvi (1992) |
| 140 | Maximum commercial (United States) | Grimm (1975) |

It can be seen that the compressive strengths of commercially available clay brick units range from 20 MPa to 140 MPa. The variance in the strength is due to the differences in manufacturing techniques and raw materials from one country and manufacturer to the next.

Compared with the brick units, mortar has a considerably lower compressive strength. It is the weak link in the compressive strength of brickwork. The results of the compressive testing of mortar are summarised in Table 2.5.2. The mortar mix ratio refers to the ratio of cement to lime to sand in the mortar mix. A mortar mix ratio of 1:1:6 (1 part cement: 1 part lime: 1 part sand) corresponds to the typically used mix in Adelaide from the Australian Standard, "SAA Masonry Code" AS3700-1988.

Table 2.5.2 Compressive Strength of Mortar.

| Compressive Strength (MPa) | Mortar Mix Ratio | Details (Origin) | Researcher |
|---|---|---|---|
| 8.7 | 1:0.4:5 | 28 day strength (Australia) | Base and Baker (1973) |
| 3.2 | 1:1:6 | Standard Australian mix (Australia) | Page (1978) |
| 3.3 | 1:1:6 | (Australia) | Jankulovski and Parsanejad (1994) |
| 7.2 | 1:1:6 | (Britain) | Hendry (1973) |
| 16.7 | 1:0.25:3 | (Britain) | Hendry (1973) |
| 25.5 | 4 and 2 | Cement - lime ratio (United States) | Grimm (1975) |
| 14.0 | 1 | Cement - lime ratio (United States) | Grimm (1975) |
| 4.3 | 0:1:3 | (Italy) | Magenes and Calvi (1992) |
| 36.9 | 1:0.25:3 | 28 day strength (United States) | Mayes and Clough (1975a) |
| 17.1 | 1:1:6 | 28 day strength (United States) | Mayes and Clough (1975a) |
| 2.5 | 1:4:15 | 28 day strength (United States) | Mayes and Clough (1975a) |

Not surprisingly, the compressive strength of the mortar decreases with a decreasing proportion of cement in the mix. Mayes and Clough (1975a) also noted that the compressive strength of mortar is also a function of the gradation of the sand component of the mix. Table 2.5.3 shows the effect of the sand gradation on the compressive strength of the mortar based upon a 1:1:6 ratio.

It can be seen when comparing Table 2.5.2 to Table 2.5.3 that the effect of sand gradation is not as significant as that for the mortar mix ratios. The mortar mix ratio has a large effect on the compressive strength and for the mortars considered the lowest is an order of magnitude below the maximum.

Table 2.5.3 Compressive strength of mortar compared to sand gradation

| Compressive Strength (MPa) | Mortar Mix Ratio | Details (Origin) | Researcher |
|---|---|---|---|
| 13.0 | 1:1:6 | fine grain (United States) | Mayes and Clough (1975a) |
| 16.9 | 1:1:6 | medium grain (United States) | Mayes and Clough (1975a) |
| 18.7 | 1:1:6 | coarse grain (United States) | Mayes and Clough (1975a) |
| 16.4 | 1:1:6 | coarse to find blend (United States) | Mayes and Clough (1975a) |
| 15.8 | 1:1:6 | fine to coarse blend (United States) | Mayes and Clough (1975a) |

Now considering the combined brick-mortar material, an initial assumption may be that the brickwork strength is limited by the strength of the mortar. However, this is not the case. As Grimm (1975) explained, the uniaxial compressive strength and modulus of elasticity of mortar are considerably lower than that of the brick unit and the Poisson's ratio is higher for mortar than the brick unit. Therefore, under an axial compression, the unrestrained lateral strain in the mortar would be greater than that of brick. Between the brick and mortar exists shear and friction resistance and this acts to restrain the mortar. This results in the mortar being in triaxial compression while the brick is in axial compression and lateral tension. Therefore, the uniaxial compressive strength of brickwork exceeds the uniaxial compressive strength of the mortar. As the tensile strength of brick is low, the typical mode of failure of brick masonry in compression is by vertical longitudinal splitting. The reported brickwork compressive strengths are summarised in Table 2.5.4. The "good" masonry referred to by Jankulovski et al (1994) was described as laboratory made specimens.

Mayes and Clough (1975a) reported on two attempts to quantitatively predict the compressive strength of masonry prisms, one based on stress analysis considerations, the other on strain considerations. Both of the methods are approximate and have several limitations, including the assumption that there is perfect bond between the brick and mortar. Mayes and Clough also noted that the prism shape and the platen restraint provided by the compression testing apparatus influenced the compressive strength of a brickwork specimen and that results from one series of tests may not be directly comparable with other tests by other researchers.

Comparing the results in Table 2.5.4 with the results in Table 2.5.2 it can be seen that the effect of mortar type on the brickwork compressive strength is less than the effect on the mortar compressive strength. The order of magnitude of difference in mortar compressive strength is not reflected in the brickwork compressive strength

which has a upper value twice the lower. The effect of the mortar joint thickness is of the same order as the effect of the mortar type.

Table 2.5.4 Compressive Strength of Brickwork.

| Compressive Strength (MPa) | Mortar Mix Ratio | Details (Origin) | Researcher |
|---|---|---|---|
| 15.0 | - | "Good" masonry (Australia) | Jankulovski et al (1994) |
| 4.0 | - | "Poor" masonry (Australia) | Jankulovski et al (1994) |
| 16.7 | - | (Australia) | Jankulovski and Parsanejad (1994) |
| 1.7 | - | Prism strength (United States) | Grimm (1975) |
| 44.8 | - | Prism strength (United States) | Grimm (1975) |
| 40.0 | 1:0.25:3 | Brickwork prism (United States) | Mayes and Clough (1975a) |
| 37.9 | 1:0.5:4.5 | Brickwork prism (United States) | Mayes and Clough (1975a) |
| 26.9 | 1:1:6 | Brickwork prism (United States) | Mayes and Clough (1975a) |
| 20.0 | 1:2:9 | Brickwork prism (United States) | Mayes and Clough (1975a) |
| 45.2 | - | 6.4 mm Mortar joint (United States) | Mayes and Clough (1975a) |
| 40.3 | - | 9.5 mm Mortar joint (United States) | Mayes and Clough (1975a) |
| 33.7 | - | 12.7 mm Mortar joint (United States) | Mayes and Clough (1975a) |
| 27.9 | - | 15.9 mm Mortar joint (United States) | Mayes and Clough (1975a) |
| 21.7 | - | 19.1 mm Mortar joint (United States) | Mayes and Clough (1975a) |
| 9.2 | 1:0:3 | (India) | Arya (1980) |
| 6.0 | 1:0:6 | (India) | Arya (1980) |
| 5.3 | 1:0:12 | (India) | Arya (1980) |
| 5.8 | - | 1:2 Lime-surkhi mortar (India) | Arya (1980) |
| 5.2 | - | 1:2 Lime-cinder mortar (India) | Arya (1980) |
| 4.7 | - | Clay mud mortar (India) | Arya (1980) |
| 7.9 | - | (Italy) | Magenes and Calvi (1992) |
| 6.0 | - | (Italy) | San Bartolome et al (1992) |
| 5.3 | - | Full scale specimens (Slovenia) | Tomazevic and Weiss (1994) |

While masonry piers are used in practice as columns, the more normal method of carrying compressive loads in unreinforced masonry buildings is through walls. Brooks (1980) examined the behaviour of unreinforced masonry walls under vertical loading. Brooks noted that load tests on walls have indicated that there are two distinct types of failure mechanism. For short walls the failure pattern is a vertical tensile splitting at right angles to the compressive strain. Tall walls or walls loaded at

large eccentricities may fail in tension across the bed joints due to the flexural action associated with out-of-plane buckling. The failure mechanism for short walls is similar to that of the masonry prisms described earlier. Brooks noted that the compressive strength of a brick wall increases with increasing brick compressive strength, mortar compressive strength, increased bond strength, and reduction in joint thickness, all of which Mayes and Clough showed increased compressive strength of brickwork prisms, and by the use of solid bricks rather than cored bricks. If the failure of the wall is by buckling the brick and mortar compressive strengths are not important in the determination of the maximum load carrying capacity of the wall.

Pande et al (1994) discussed the derivation of the equation for the compressive strength of masonry as given in the Eurocode "Design of Masonry Structures", EC6. The EC6 equation is:

$$f_k = K(f_b')^{\alpha}(f_m)^{\beta} \qquad (2.5.1)$$

where

| | | |
|---|---|---|
| $f_k$ | = | Characteristic masonry compressive strength; |
| $f_m$ | = | Average mortar compressive strength; |
| $f_b$ | = | Normalised unit compressive strength, which was defined as the compressive strength of the masonry unit modified by a moisture factor and a shape factor; |
| K | = | 0.4; |
| $\alpha$ | = | 0.75; and |
| $\beta$ | = | 0.25. |

Evaluating Equation 2.5.1 with the range of values for compressive strength of the brick and mortar materials as already discussed in Tables 2.5.1 and 2.5.2 (brick compressive strength from 31.8 MPa to 83.2 MPa and mortar compressive strength from 2.5 MPa to 36.9 MPa) yields a range of values for the compressive strength of brickwork from 6.7 MPa to 27.2 MPa. The reported values of the compressive strength in Table 2.5.4 range from 4.7 MPa to 45.2 MPa, which is a larger range than that estimated by EC6.

### 2.5.2 Flexural Strength

The actual flexural strength of the components in brickwork have not been widely reported. Reported values of the modulus of rupture of brick are reported in Table 2.5.5 and reported values for the tensile strength of mortar are presented in Table 2.5.6.

Table 2.5.5 Modulus of Rupture of Brick.

| Modulus of Rupture (MPa) | Details (Origin) | Researcher |
|---|---|---|
| 4.7 | Five hole wire cut brick (Britain) | Hendry (1973) |
| 5.6 | Three hole wire cut brick (Britain) | Hendry (1973) |

Table 2.5.6 Tensile Strength of Mortar.

| Tensile Strength (MPa) | Mortar Mix Ratio | Details (Origin) | Researcher |
|---|---|---|---|
| 2.1 | 1:0.25:3 | 28 day (United States) | Mayes and Clough (1975a) |
| 1.0 | 1:0.5:4.5 | 28 day (United States) | Mayes and Clough (1975a) |
| 0.4 | 1:1:6 | 28 day (United States) | Mayes and Clough (1975a) |
| 1.2 | 1:1:6 | (Britain) | Hendry (1973) |
| 1.8 | 1:0.25:3 | (Britain) | Hendry (1973) |

When considering brickwork there is two values related to the strength in flexural and/or tension. The flexural tensile strength, also known as the modulus of rupture, is determined from bending tests. The tensile strength is a measure of the strength of the brickwork in tension, usually determined from a test such as the bond wrench test.

Grimm (1975) reported that the flexural tensile strength of brick masonry is a function of the tensile bond strength of mortar to brick, mortar cement ratio, mortar bed joint thickness, and orientation of the mortar bed joints with respect to span.

Base and Baker (1973) observed that three modes of failure are possible in brickwork subjected to flexure across perpend joints:

(1) Bending failure of the bricks;

(2) Failure of bond in bending on the perpend joint; and

(3) Failure of bond in torsional shear on the bed joints.

Base and Baker noted that in tests of brickwork subject to flexure the modulus of rupture decreased with increasing span. Three hypothesis were given:

(1) Any horizontal restraint of the rollers would have given rise to arching action which would have had greater effect on the shorter spans;

(2) Deep beam action was approached on shorter spans; or

(3) With high moment gradient, in the shorter spans only two joints were subject to maximum or near maximum moment.

Reported values of the tensile strength of brickwork are presented in Table 2.5.7.

Table 2.5.7 Tensile Strength of Brickwork.

| Tensile Strength (MPa) | Mortar Mix Ratio | Details (Origin) | Researcher |
|---|---|---|---|
| 0.10 | - | "Poor" masonry (Australia) | Jankulovski et al (1994) |
| 1.0 | - | "Good" masonry (Australia) | Jankulovski et al (1994) |
| 1.2 | - | (Australia) | Jankulovski and Parsanejad (1994) |
| 0.69 | 1:0:3 | (India) | Arya (1980) |
| 0.24 | 1:0:6 | (India) | Arya (1980) |
| 0.04 | 1:0:12 | (India) | Arya (1980) |
| 0.09 | 1:2 | Lime : surkhi (India) | Arya (1980) |
| 0.06 | 1:2 | Lime : Cinder (India) | Arya (1980) |
| 0.03 | - | Clay mud (India) | Arya (1980) |
| 0.07 | - | (Italy) | Magenes and Calvi (1992) |
| 0.5 | - | (Slovenia) | Tomazevic and Weiss (1994) |

The moduli of rupture of brickwork reported by a number of researchers are presented in Table 2.5.8.

Table 2.5.8 Modulus of Rupture of Brickwork.

| Modulus of Rupture (MPa) | Mortar Mix Ratio | Details (Origin) | Researcher |
|---|---|---|---|
| 2.5 | - | Flexural failure in perpends (Australia) | Base and Baker (1973) |
| 0.34 | - | (United States) | Grimm (1975) |
| 3.4 | - | (United States) | Grimm (1975) |
| 0.62 | 1:1:6 | 0 degrees - Figure 2.5.1 (Britain) | Hendry (1973) |
| 0.22 | 1:1:6 | 45 degrees - Figure 2.5.1 (Britain) | Hendry (1973) |
| 0.08 | 1:1:6 | 90 degrees - Figure 2.5.1 (Britain) | Hendry (1973) |
| 0.94 | 1:0.25:3 | 0 degrees - Figure 2.5.1 (Britain) | Hendry (1973) |
| 0.49 | 1:0.25:3 | 45 degrees - Figure 2.5.1 (Britain) | Hendry (1973) |
| 0.20 | 1:0.25:3 | 90 degrees - Figure 2.5.1 (Britain) | Hendry (1973) |
| 2.10 | 1:0.25:3 | Normal to bed joint (Britain) | West et al (1977) |
| 0.73 | 1:0.25:3 | Parallel to bed joint (Britain) | West et al (1977) |
| 2.14 | 1:1:6 | Normal to bed joint (Britain) | West et al (1977) |
| 0.71 | 1:1:6 | Parallel to bed joint (Britain) | West et al (1977) |
| 1.86 | 1:2:9 | Normal to bed joint (Britain) | West et al (1977) |
| 0.57 | 1:2:9 | Parallel to bed joint (Britain) | West et al (1977) |
| 1.59 | - | (Italy) | Magenes and Calvi (1992) |

It can be seen from Table 2.5.7 that the tensile strength of the brickwork is very small compared to the compressive strengths given in Table 2.5.4.

Hendry (1973) also reported on the results of tests to determine the modulus of rupture of brick walls using two types of mortar. These results are shown in Table 2.5.8. The angles given were the direction of bending and are shown in Figure 2.5.1

It can be seen that the modulus of rupture was significantly higher for bending parallel to the bedding planes than for bending perpendicular to the bedding joints.

It can be seen that there is considerable variation in the magnitude of the moduli of rupture and the tensile strengths reported by the various researchers. This can be partially explained by the difference in material properties from test to test. As research was done at different times in different countries there is no likelihood of the materials having identical properties to allow direct comparison. The other important factor is the workmanship. The workmanship involved in the construction

of brickwork has a significant influence on its properties and this can explain some of the differences in the properties measured by the various researchers.

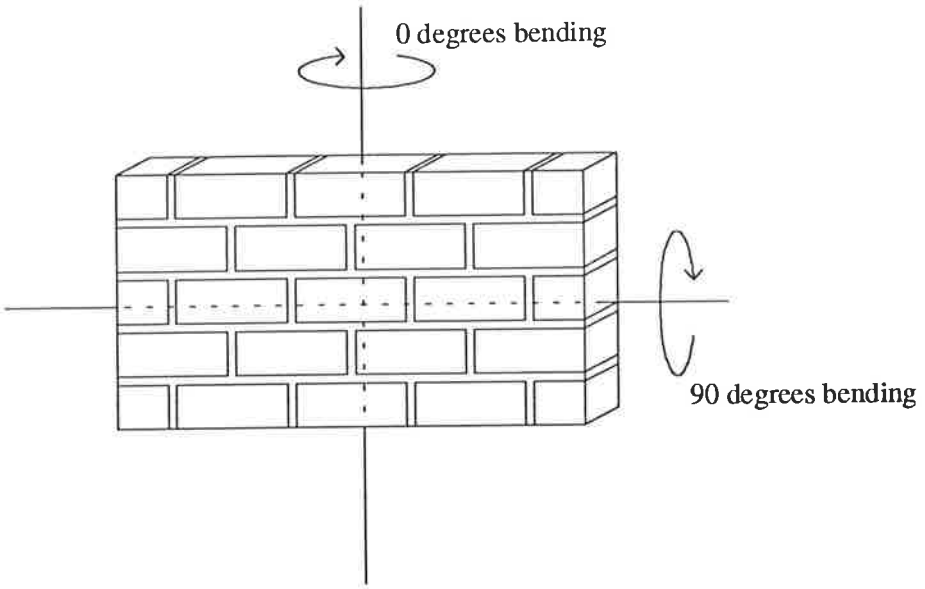


Figure 2.5.1 Orientation of bending for results in Table 2.5.8.

### 2.5.3 Shear Strength

In order to establish the seismic resistance of a shear wall structure such as an unreinforced masonry building the shear strength of the resisting elements is needed. Ghazali and Riddington (1988) and Riddington and Ghazali (1990) described an hypothesis for the shear failure of masonry walls. It was noted that the widely accepted explanation for the strength of a masonry joint is that it is derived from a combination of bond shear strength and friction between the brick and the mortar. The ultimate shear strength is then expressed by:

$$\tau_u = \tau_o + \mu\sigma_c \qquad (2.5.2)$$

where $\tau_u$ is the ultimate shear strength, $\tau_o$ is the bond shear strength between brick and mortar, $\mu$ is the coefficient of internal friction at the brick mortar interface, and $\sigma_c$ is the axial compressive stress. The results of tests have shown that the rate of

increase in shear strength starts to reduce at higher compression stresses. This decrease often occurs at around 2 MPa compressive stress. This would suggest that the coefficient of friction reduces with increasing compressive stress. Riddington and Ghazali proposed that the shear failure in the mortar-brick interface is initiated by joint slip at compression stresses below approximately 2 MPa, but at higher stress levels, shear failure is initiated by tensile failure within the mortar. This hypothesis was supported by finite element modelling and shear testing. Yokel and Fattal (1976) also advanced the hypothesis of shear failure proposed by Riddington and Ghazali. The hypothesis was again in good agreement with test results.

Mayes and Clough (1975b), in a literature review on the shear strength of masonry, reported on a proposal to predict the shear strength of a masonry assemblage that identified three failure modes. The first two are similar to those identified by Riddington and Ghazali and Yokel and Fattal. The third failure occurs for an axial compressive stress higher than that which defines the second type of failure, tensile failure. The third mode is governed by a Mohr type failure, where the shear strength is equal to Poisson's Ratio multiplied by the compressive stress. The proposed failure mechanisms were supported by the results of laboratory testing. Mayes and Clough also noted that an increase in mortar strength resulted in an increase in the shear strength of masonry. Further, they provided evidence from other investigations that supported the hypothesis for shear strength given in Equation 2.5.2, where an increase in the bearing load increases the shear strength.

The results of tests to determine the shear strength of brickwork walls are summarised in Table 2.5.9. The results from tests to determine the coefficient of internal friction, $\mu$, are presented in Table 2.5.10.

Most brickwork walls built in Australia include a damp proof membrane at the base. This membrane results in no bond shear strength and the shear resistance is only derived from frictional resistance based on the axial load. Page (1994) conducted a series of tests that determined the shear capacity of membrane type damp proof courses. The tests were conducted with the damp proof course placed on the brick and the mortar placed on top and with the damp proof course in the middle of the mortar layer. The results of these tests are shown in Tables 2.5.11 and 2.5.12.

Page concluded that the friction coefficients are all greater than the default value of 0.30 specified in Australian Standard, "SAA Masonry Code" AS3700-1988 except for the Polyethylene Bitumen Coated Aluminium.

Table 2.5.9 Shear Strength of Brickwork.

| Shear Strength (MPa) | Mortar Mix Ratio | Details (Origin) | Researcher |
|---|---|---|---|
| 0.7 | - | "Good" masonry (Australia) | Jankulovski et al (1994) |
| 0.1 | - | "Poor" masonry (Australia) | Jankulovski et al (1994) |
| 1.0 | - | (Australia) | Jankulovski and Parsanejad (1994) |
| 0.35 | - | (Britain) | Riddington and Ghazali (1990) |
| 1.19 | - | (Britain) | Riddington and Ghazali (1990) |
| 0.21 | - | (Italy) | Magenes and Calvi (1992) |
| 0.4 | - | (United States) | Grimm (1975) |
| 4.7 | - | (United States) | Grimm (1975) |
| 0.8 | - | (Italy) | San Bartolome et al (1992) |

Table 2.5.10 Internal friction Coefficient, μ, of Brickwork.

| Internal Friction Coefficient, μ | Mortar Mix Ratio | Details (Origin) | Researcher |
|---|---|---|---|
| 0.4 | - | (United States) | Yokel and Fattal (1976) |
| 0.6 | - | (United States) | Grimm (1975) |
| 1.33 | - | (United States) | Grimm (1975) |
| 0.68 | - | Suggested value (United States) | Grimm (1975) |

Comparison of the shear strength of brickwork with membranes to that of normal brickwork reveals that the shear strength of brickwork with the membranes is considerably lower than normal brickwork (two orders of magnitude in some cases). This lower shear strength occurs at the critical location in the load path for lateral loads, the base of the building where the total lateral load is transferred to the ground.

### 2.5.4 Biaxial Stress Behaviour

It is obvious that masonry elements are rarely subjected to only one type of load at any time. Walls are generally in a complex state of stress produced by in-plane loading and/or out-of-plane loading. This loading is normally cyclic, such as wind and earthquake induced loading. Thus, the wall experiences cyclic biaxial stress states which can be tensile and/or compressive.

Naraine and Sinha (1991 and 1992), Page (1981), and Dhanasekar et al (1985a and 1985b) all examined the bi-axial stress behaviour of unreinforced masonry walls. This is generally beyond the scope of this study and will not be investigated further.

Table 2.5.11 Friction coefficients for the shear capacity of brickwork. (from Page (1994))

| Damp Proof Course Type | In Plane | | Out of Plane | |
|---|---|---|---|---|
| | In Joint | On Brick | In Joint | On Brick |
| Standard Bitumen Coated Aluminium | 0.41 | 0.49 | 0.50 | 0.47 |
| Super Bitumen Coated Aluminium | 0.60 | 0.41 | 0.57 | 0.48 |
| Polyethylene Bitumen Coated Aluminium | 0.26 | 0.26 | 0.31 | 0.35 |
| Embossed Polythene (Supercourse 500) | 0.68 | 0.59 | 0.59 | 0.56 |
| Embossed Polythene (Supercourse 750) | 0.71 | 0.58 | 0.60 | 0.59 |

Table 2.5.12 Shear Strengths of brickwork with membranes. (from Page (1994))

| Damp Proof Course Type | In Plane | | Out of Plane | |
|---|---|---|---|---|
| | In Joint | On Brick | In Joint | On Brick |
| Standard Bitumen Coated Aluminium | 0.18 | 0.01 | 0.12 | 0.00 |
| Super Bitumen Coated Aluminium | 0.10 | 0.07 | 0.03 | 0.01 |
| Polyethylene Bitumen Coated Aluminium | 0.08 | 0.04 | 0.07 | 0.05 |
| Embossed Polythene (Supercourse 500) | 0.09 | 0.02 | 0.07 | 0.02 |
| Embossed Polythene (Supercourse 750) | 0.10 | 0.03 | 0.11 | 0.02 |

### 2.5.5 Stiffness

In order to develop mathematical models of brick masonry walls it is important to have the value of the stiffness of the materials making up the structure. Brickwork walls can be modelled as one-phase or two-phase materials and therefore the stiffness properties of both the one-phase material and both phases of the two-phase material are examined.

Reported values for the Young's Modulus of clay bricks are presented in Table 2.5.13.

Table 2.5.13 Young's Modulus of Clay Bricks

| Young's Modulus (MPa) | Details (Origin) | Researcher |
|---|---|---|
| 9,750 | (Australia) | Brooks et al (1979) |
| 18,000 | Used in 2 phase finite element model (Australia) | Payne et al (1990) |
| 16,000 | (Australia) | Brooks and Payne (1990) |
| 24,750 | (Australia) | Base and Baker (1973) |
| 5,920 | Loading parallel to bed joint (Australia) | Page (1978) |
| 7,550 | Loading perpendicular to bed joint (Australia) | Page (1978) |
| 14,700 | (Australia) | Zhuge et al (1993) |
| 27,000 | Wire cut brick (Britain) | Riddington and Ghazali (1990) |
| 10,400 | Single frogged pressed common brick (Britain) | Riddington and Ghazali (1990) |

The reported Young's Modulus of mortar are presented in Table 2.5.14.

The values of Young's Modulus of brickwork determined from experimental work and/or used by researchers in the modelling of brickwork elements are summarised in Table 2.5.15.

The Choice of Young's Modulus of brickwork is not easy. Priestley (1985) used a Young's Modulus of 1,000 MPa in a sample calculation for the earthquake resistance of unreinforced masonry. Robinson (1986), in a discussion of Priestley, suggested a more appropriate Young's Modulus of 10,000 MPa based on the fact that most of the deformation of a brick wall is in the mortar which makes up only a small percentage of the total height of a wall. Priestley countered that Robinson offered no

proof of the 10,000 MPa value and that 1,000 MPa is backed up by test results from the United States and New Zealand.

Table 2.5.14 Young's Modulus of Mortar

| Young's Modulus (MPa) | Mortar Mix Ratio | Details (Origin) | Researcher |
|---|---|---|---|
| 8,300 | 1:1:6 | (Australia) | Brooks et al (1979) |
| 8,000 | 1:1:6 | (Australia) | Payne et al (1990) |
| 6,000 | - | Typical range (Australia) | Brooks and Payne (1990) |
| 10,000 | - | Typical range (Australia) | Brooks and Payne (1990) |
| 7,400 | - | (Australia) | Zhuge et al (1993) |
| 8,130 | 1:0.4:5 | (Australia) | Base and Baker (1973) |
| 9,100 | 1:0:3.5 | (Britain) | Riddington and Ghazali (1990) |

The values given for the Young's Modulus of brickwork by various researchers in Table 2.5.15 shows the large variability in the properties of unreinforced masonry. It was this variation in properties that was the motivation behind the shaking table tests conducted as part of this research and discussed in Chapter 4.

Finally, the Poisson's Ratio of brickwork given by researchers ranged from 0.11 to 0.25.

Table 2.5.15 Young's Modulus of Brickwork

| Young's Modulus (MPa) | Mortar Mix Ratio | Details (Origin) | Researcher |
|---|---|---|---|
| 15,120 | - | Compression (Australia) | Base and Baker (1973) |
| 21,200 | - | Bending vertically (Australia) | Base and Baker (1973) |
| 19,240 | - | Bending horizontally (Australia) | Base and Baker (1973) |
| 2,000 | - | "Good" masonry (Australia) | Jankulovski et al (1994) |
| 900 | - | "Poor" masonry (Australia) | Jankulovski et al (1994) |
| 5,800 | - | (Australia) | Page et al (1985) |
| 13,240 | - | From 2 phase modelling (Australia) | Zhuge et al (1993) |
| 1,000 | - | Used in calculation (New Zealand) | Priestley (1985) |
| 10,000 | - | Discussion of above (New Zealand) | Robinson (1986) |
| 2,991 | - | (Italy) | Magenes and Calvi (1992) |
| 1,510 | - | (Peru) | San Bartolome et al (1992) |
| 4,500 | - | (Slovenia) | Tomazevic and Weiss (1994) |
| 17,750 | - | Perpendicular to bed joint (Britain) | Duarte and Sinha (1992) |
| 13,500 | - | Parallel to bed joint (Britain) | Duarte and Sinha (1992) |
| 13,910 | - | (United States) | Anand and Yalamanchili (1988) |
| 1,000 | - | (Italy/United States) | Calvi et al (1994) |
| 1,652 | 1:0:3 | Static (India) | Arya (1980) |
| 1,161 | 1:0:6 | Static (India) | Arya (1980) |
| 1,085 | 1:0:12 | Static (India) | Arya (1980) |
| 2,266 | 1:0:3 | Dynamic (India) | Arya (1980) |
| 1,638 | 1:0:6 | Dynamic (India) | Arya (1980) |
| 1,422 | 1:0:12 | Dynamic (India) | Arya (1980) |

# 2.6 FINITE ELEMENT MODELLING OF BRICKWORK

Brickwork is a two phase material. When researchers and designers modelled brickwork panels using the finite element method it was usual to have a model that separated the two phases of the brickwork. The model would therefore consist of a mortar phase, divided into many elements, and a brick phase, also divided into many elements. This led to models of brickwork panels having a large number of elements, increasing the size of the model and the time taken to analyse the problem. In this section finite element models for the two phase modelling of brickwork, as well as various methods for modelling brickwork as an equivalent one phase model to overcome the problem of model size and complexity, are examined.

Page (1978) looked at a two phase finite element model for masonry walls subjected to in-plane loads. A finite element model was modified to take into account the specific properties of masonry. The material properties and characteristics were obtained from a laboratory testing program. The masonry wall was modelled using a continuum of plane stress elements with superimposed linkage elements simulating the mortar joints. The bricks were modelled using conventional plane stress elements with isotropic elastic properties. A typical finite element subdivision is shown in Figure 2.6.1.

Because of the joint elements being extremely thin, the pairs of nodes, (1,3) and (2,4), are specified by the same coordinates of nodes A and B and the thickness, t, is used in computing joint element properties. The technique used to add the joint element stiffness to the total structural stiffness was originally used in reinforced concrete and rock mechanics. The joint element stiffness was determined by minimising the potential energy with respect to the element displacements. An iterative process was then used to model material non-linearities, solving until convergence is achieved after checking the solution against failure criterion.

Another two phase finite element model was developed by Sved et al (1982). This model differed from the Page model in that it only used standard finite elements. Brickwork that was part of a typical wall element was subdivided into small brick-mortar "modules" as shown in Figure 2.6.2.

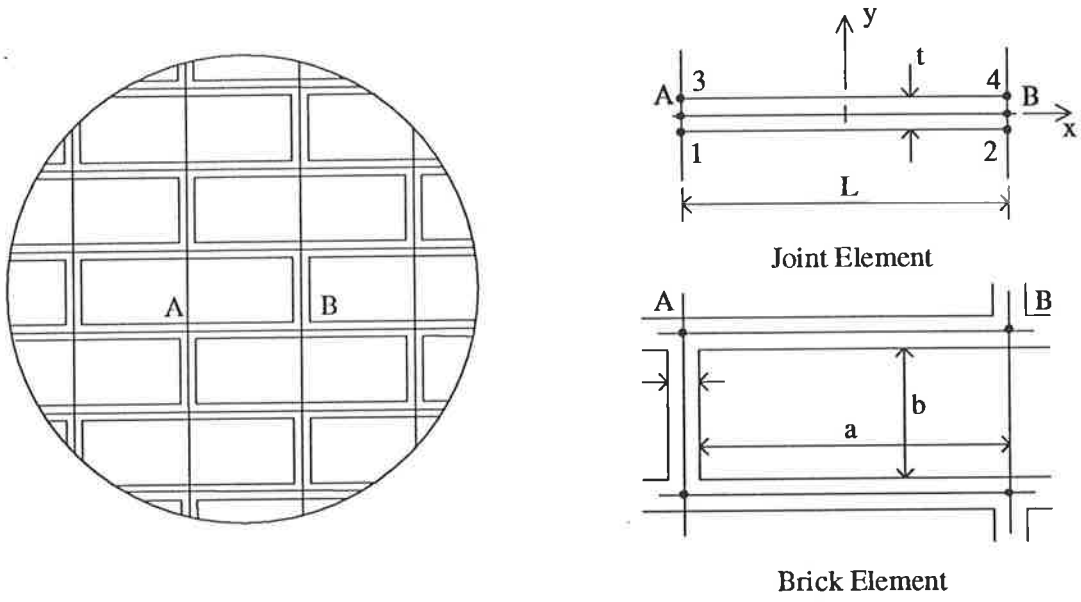


Figure 2.6.1 Finite element subdivision.
(from Page (1978)).

The properties of a single module were used to analyse the behaviour of a whole panel by the investigation of the load-deformation characteristics of a module with the brickwork in the uncracked and cracked state. The stiffness values obtained from the module were substituted into differential equations describing the behaviour of plates of variable thickness. For the uncracked condition the elements making up the module were coupled at the brick-mortar interfaces, and uncoupled whenever tension stresses occurred at the brick-mortar interfaces. The model had good agreement with the properties of a brickwork wall panel determined from an experimental test program.

Shing et al (1992) used both a one phase model and a two phase model in the finite element analysis of masonry wall panels. The one phase model used a smeared crack model to simulate distributed tension and compression failure of masonry units. This is an approach that has been used for reinforced concrete members. It has the

advantage of computational efficiency. The study concluded that the failure of reinforced and unreinforced masonry wall panels, with and without confining frames, can be adequately modelled with a combination of smeared crack and interface elements. The later was used to model the separation of a confining frame and masonry wall. The results were verified by an experimental program.

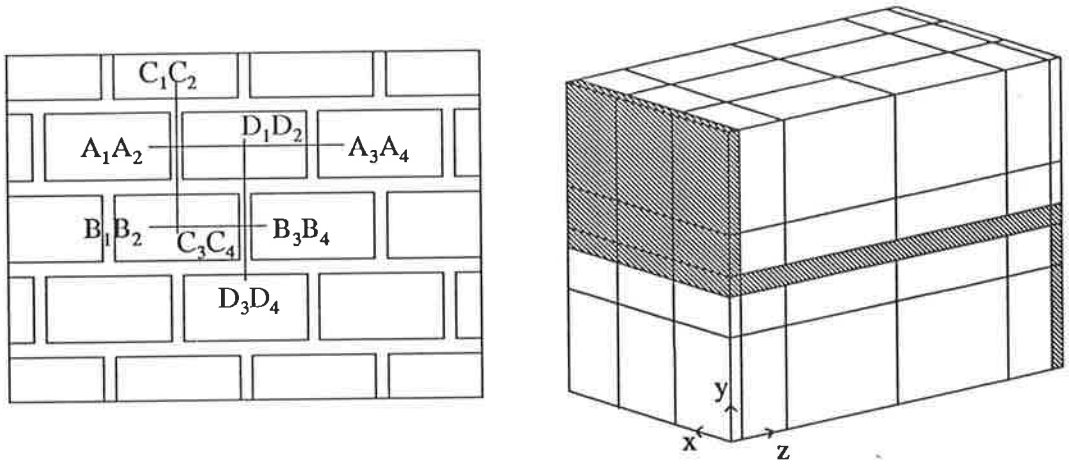


(a) brickwork in stretcher bond (b) finite element details

Figure 2.6.2 Finite element details.
(from Sved et al (1982)).

Page et al (1985) described a one phase finite element model that incorporated material characteristics taken from biaxial stress tests on masonry panels. The model reproduced the inelastic deformations typical of brick masonry and used a failure criterion that included the orientation of the jointing planes and the state of stress. Page et al noted an advantage of the one phase model is that a relatively course grid could be adopted which led to computational advantages when analysing a large wall panel. The finite element results were compared to the results from an experimental test program on five infilled steel frames. The predicted results from the finite element model for the load-deflection behaviour, the modes of failure, failure loads,

and local stress-strain behaviour were all in good agreement with the experimental results.

Zhuge et al (1993) used a one phase finite element model to model masonry walls. The model was based on conventional four node plane stress rectangular elements. An equivalent elastic modulus was derived for the one phase material based on the formula:

$$E_O = cE_B + (1-c)E_M \qquad 0.5 \leq c \leq 1.0 \qquad (2.6.1)$$

where $E_O$ is the equivalent elastic modulus for a one phase material, $E_B$ is the elastic modulus of brick, and $E_M$ is the elastic modulus of mortar. To test Equation 2.6.1 and to determine a suitable value of "c" a wall was modelled as a two phase material using the appropriate material properties. A one phase model was then run with an elastic modulus derived from Equation 2.6.1 with various values of "c". Good agreement between the two phase model and the one phase model was obtained when c = 0.8.

Anand and Yalamanchili (1988) used a one phase model for the brickwork component of a composite masonry wall (a composite masonry wall consists of a brick leaf, and concrete block leaf separated by a grouted cavity). The finite element model was used to examine the behaviour of the composite wall when subjected to earthquake induced forces. A 2016 node, 1547 element grid was used to model the three phases of a 3.05m x 3.05m composite wall. The results of the finite element model were not confirmed by experimental data.

It can be seen from the research discussed in this section that the finite element modelling of masonry can take two paths. First, a two phase model, where the masonry unit and the mortar are treated as separate materials and the finite element mesh is constructed so as to allow for the individual materials. The alternative method is to adopt a single material to represent both the masonry unit and the mortar phase of the masonry construction. This later method has the advantage of being considerably less computer intensive than the two phase model as a courser mesh can be adopted. The one phase method has been adopted successfully by Shing et al (1992), Page et al (1985), Zhuge et al (1993), and Anand and Yalamanchili (1988).

# 2.7 EARTHQUAKE DESIGN MODELS FOR BRICKWORK

There have been previous attempts by researchers to model the behaviour of masonry buildings under earthquake induced loadings. While most have focused om reinforced masonry buildings, some have studied unreinforced masonry buildings. In this section some of the models proposed by previous researchers are presented.

Priestley (1985) outlined the traditional method of seismic analysis of unreinforced masonry buildings. It was noted that ductility considerations were traditionally inappropriate in the design of unreinforced masonry. Further, it was stated that the seismic capacity of unreinforced masonry was not governed by material strength but rather by stability and energy considerations. Priestley also provided the energy path for an unreinforced masonry building subjected to earthquake excitation (Figure 2.7.1).

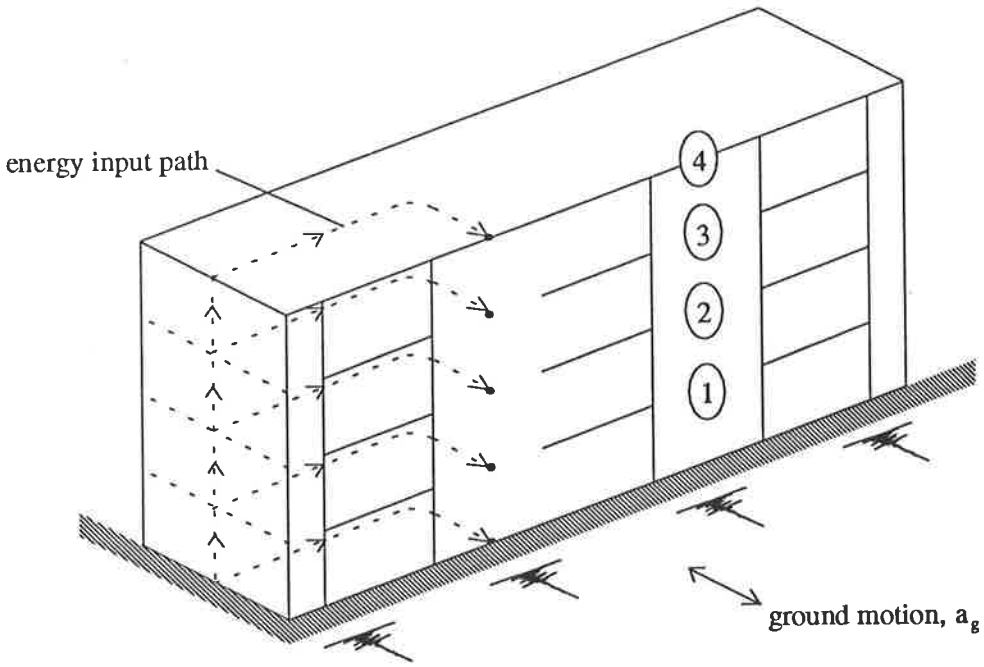


Figure 2.7.1 Energy path for a masonry building resisting seismic loads.
(from Priestley (1985))

Jankulovski et al (1994) presented a simple approach for the non-linear dynamic response analysis of an unreinforced masonry building. The basic assumption of the model was that the vertical elements are connected at the floor and roof levels by a rigid diaphragm.

Kwok and Ang (1987) reported on research conducted at The University of Illinios at Urbana-Champaign on the seismic damage analysis and design of unreinforced masonry buildings. Kwok and Ang first noted that collapse of an unreinforced masonry wall element was equivalent to failure. It was further noted that under cyclic loading walls can resist lateral loads through friction mechanisms even after severe cracking. Two aims of the seismic design of masonry buildings were noted:

(1) Prevention of catastrophic collapse of a structure; and

(2) Damage should not be concentrated in any particular storey but should be uniformly distributed among the various stories.

Kwok and Ang then simplified the procedure such that it became the basis for a modified equivalent lateral force procedure as used in many earthquake codes.

Mengi et al (1984), in research conducted at Berkeley, developed a linear mathematical model for the in-plane behaviour of brick masonry walls based on the experimental program already reported in Section 2.3. Two models for masonry were used; a two phase mixture model (MM) and a one phase effective modulus model (EMM). It was concluded for ground motions with a lower frequency content than the first modal frequency of the wall element, the EMM should be used. If, however, the frequency content of the ground motion is higher than the first modal frequency of the wall element, the MM should be used.

Further work on the modelling of unreinforced masonry by researchers at Berkeley was reported by Mengi and McNiven (1989) and McNiven and Mengi (1989). As with Mengi et al a testing program was undertaken (Section 2.3). A linear isotropic model was used to model the unreinforced masonry.

Wesley et al (1980) used the "reserve energy" technique for the analysis of the collapse capacity of unreinforced masonry wall structures. Wesley et al identified the collapse mechanism of unreinforced masonry walls as cracking occurring at the base

of the wall followed by rigid body rocking of the wall-roof system as an inverted pendulum.

A brief summary of several proposed modelling methods for reinforced masonry buildings follows.

Tomazevic (1987) looked at the dynamic modelling of horizontally reinforced masonry buildings by the storey mechanism model. Good correlation was found between the storey mechanism model and the results of a scale-model testing program. Tomazevic and Sheppard (1987) used the storey mechanism model to model masonry buildings damaged in earthquakes and found that the behaviour of these buildings was best described by the storey mechanism model.

Qamaruddin et al (1985) developed a mathematical model of a multi-storey reinforced brick building. Another study of reinforced masonry was conducted by Soroushian et al (1988). The main emphasis of the study was the determination of a model for the hysteretic behaviour of a reinforced masonry shear wall. The building was idealised as a single degree of freedom system.

The work of Goel and Chopra (1990) examined a number of one-storey buildings with asymmetric plans. It was found that the linear elastic response of a one-storey asymmetric plan system depends on the lateral and torsional vibration frequencies of the corresponding symmetric plan system.

In summary, it can be seen that some researchers used an equivalent linear model to simulate the non-linear behaviour of unreinforced masonry. This was accomplished by various methods such as the "Reserve Energy" technique. In Section 2.9 it will be seen that another method of achieving this type of model is the use of a response modification factor, $R_f$. Some researchers only modelled the in-plane elements of the structure to simplify the model. Single and two phase models were used by researchers with no conclusive proof that either was better. It would seem that a single phase masonry material model using an equivalent linear elastic model can give a reasonably accurate model for unreinforced masonry buildings subjected to earthquake excitation.

# 2.8 FLOOR FLEXIBILITY/STIFFNESS

The stiffnesses (EA) and the related flexibilities of floor and roof diaphragms play an important part in the determination of the overall stiffness of a building and the distribution of the forces and the moments in the building.

In this section a review was conducted on various studies into the effect of the horizontal-vertical element connection on the properties of a building. Also, a review of studies into the sensitivity of the structural behaviour to floor/roof stiffness was also undertaken.

Moon and Lee (1994) reported on a study to investigate the effects of in-plane floor slab flexibility on natural periods, mode shapes, seismic base shear, and the distribution of seismic base shear. The study involved two structures, a 6-bay 5-storey building, and a 10-storey building with set back. Two types of structural system were considered for each building, a frame system, and a frame plus shear wall system. The buildings were each modelled with a rigid floor diaphragm (no in-plane floor flexibility, EA = infinity) and a semi-rigid floor diaphragm (some in-plane floor flexibility).

Moon and Lee found that for frame type structures that in-plane floor slab flexibility did not have a significant effect on the natural period of structures. For the frame plus shear wall structures the inclusion of in-plane floor slab flexibility increased the natural period of the structure. Moon and Lee concluded that the period for the semi-rigid floor diaphragm was up to 2.5 times that for the rigid floor diaphragm. In-plane floor slab flexibility also led to mode shifts for the buildings.

In order to compare the seismic behaviour of the two types of floor slab flexibility, Moon and Lee undertook modal analysis of the structures using the Applied Technology Council (ATC (1984)) design spectra. For the frame type structure, the effect of floor slab flexibility on the base shear was not significant. For the frame plus shear wall structures, floor slab flexibility reduced the seismic base shear. This was attributed to two things:

(1) Increase in period associated with the in-plane floor slab flexibility results in the structure being on the descending portion of the design response spectra (see Figure 5.2.1); and

(2) Decrease in the effective weight for the lower modes.

It was also found that the use of rigid floor diaphragms in models of low rise building structures with end walls can result in underestimation of the storey shears and column axial forces.

Adham and Ewing (1978) studied the effect of roof diaphragms of various stiffness on the behaviour of unreinforced masonry buildings. Three floor diaphragm stiffness values were used, with diaphragm stiffness values in the ratio 20:4:1. It was found that the natural period of the structure increased with increasing period, similar to what was found by Moon and Lee. Similar base shear conclusions to Moon and Lee were also found by Adham and Ewing.

It can be seen that the stiffness of the horizontal elements of the structure play an important part in the determination of the response of a structure to earthquakes. In the later parts of this study, the influence will be investigated further to determine the effects of the properties of the horizontal elements.

# 2.9 APPROPRIATE $R_f$ FOR UNREINFORCED MASONRY

An important consideration in the equivalent static load approach to earthquake design is the choice of the structural response factor, or response modification factor, $R_f$. This is a factor included in the calculation of the base shear, and subsequently, the loads applied to the various levels of a structure to simulate earthquake induced inertia forces, that allows for structural over-strength, damping, and the ability of a structure to support load into the inelastic behaviour range of its materials. It is a factor that varies with material type and the structural system.

Prior to examining the various recommended and proposed values of $R_f$ an examination of the meaning of $R_f$ is presented. The explanation is based on Uang (1991).

Figure 2.9.1 shows the structural response idealised by a elastic-perfectly plastic curve. The structural ductility factor is defined as:

$$\mu_s = \frac{\Delta_{max}}{\Delta_y} \tag{2.9.1}$$

where the deformation is expressed in terms of inter storey drift, $\Delta$. Because of this ductility (or energy dissipation capacity), the design force can be reduced to $C_y$ by a ductility reduction factor, $R_\mu$.

$$C_y = \frac{C_{eu}}{R_\mu} \tag{2.9.2}$$

This reduction factor is usually computed with an equivalent viscous damping ratio, usually five percent of critical. $C_y$ is then reduced to $C_s$ by an over-strength factor, $\Omega$, such that:

$$C_s = \frac{C_y}{\Omega} \tag{2.9.3}$$

and $C_s$ is the minimum required design base shear ratio corresponding to the first significant yield level defined by Uang (1991) as *a level beyond which the first plastic hinge forms and the global structural response starts to deviate significantly from the elastic response.* Codes such as the "Uniform Building Code" (UBC

(1991)) specifies the seismic force level for allowable stress design by reducing further the $C_s$ level to the $C_w$ level by a factor Y. The $R_f$ factor in the Australian Standard "Minimum design loads on structures - Part 4 : Earthquake Loads" AS1170.4-1993 incorporates the ductility reduction factor, the over-strength factor, and a correction for the assumed five percent critical damping.

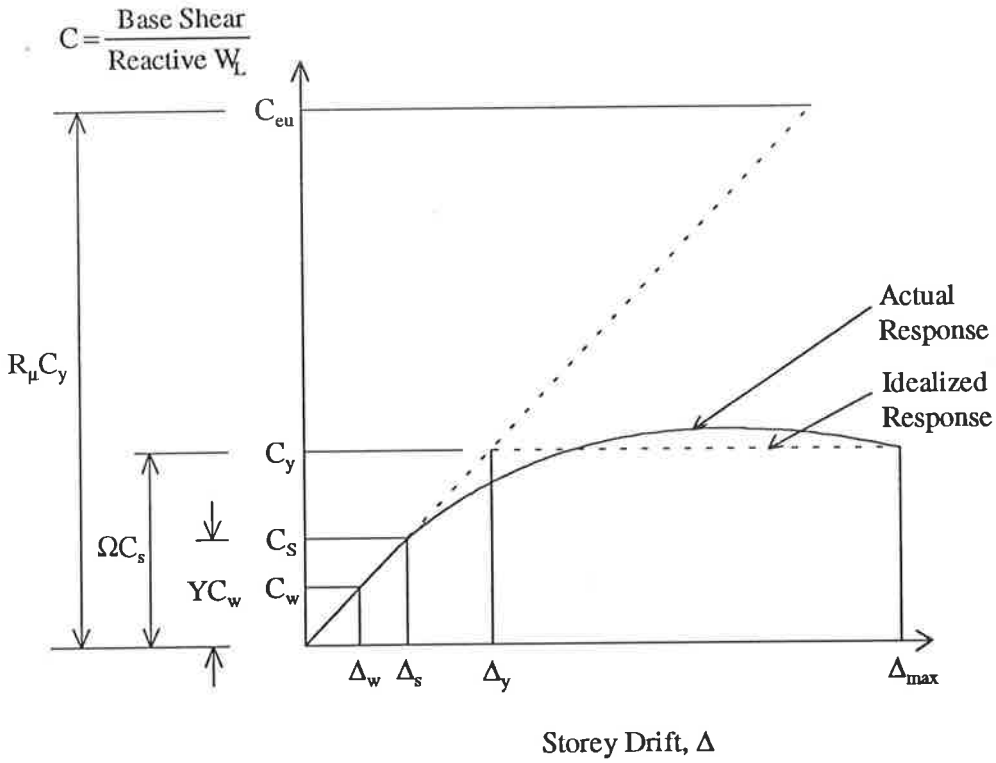


Figure 2.9.1 General Structural Response.
(from Uang (1991))

AS1170.4 specifies an $R_f$ of 1.5 for use with any unreinforced masonry lateral load resisting system when used with the equivalent static load design approach and the response spectrum method. This is the smallest $R_f$ allowed in AS1170.4 and only considers over-strength and damping and assumes masonry buildings do not exhibit any ductile behaviour. The maximum $R_f$ in AS1170.4 is 8.0 for reinforced concrete and steel moment resisting frames. Hutchinson et al (1994) noted that the $R_f$ factors in AS1170.4 are taken from the "Uniform Building Code" and are modified to reflect the ultimate limit state condition used in the Australian loading codes and a slight

difference between the two codes in the proportion of live load included in the overall weight of the structure.

The "NEHRP Recommended Provisions for the Development of Seismic Regulations for New Buildings Part 1" (NEHRP (1991)) has a $R_f$, or in the case of the NEHRP an R factor, of 1.25. The "NEHRP Recommended Provisions for the Development of Seismic Regulations for New Buildings Part 2 : Commentary" (NEHRP (1991)) described the R factor as taking into account damping and ductility. There is no mention of over-strength. This factor is close to the AS1170.4 factor and with the inclusion of over-strength the NEHRP factor would increase and could become closer to the AS1170.4 value. The other earthquake code used in the United States is the "Uniform Building Code" and it is from this code, as noted previously, that the AS1170.4 $R_f$ values are taken (Hutchinson et al (1994)).

In the 1985 National Building Code of Canada (Zhu et al (1989)) the equivalent static load approach uses a form of equation that is different to the usual form found in most of the world's earthquake codes and subsequently the factor that is the equivalent of AS1170.4's $R_f$ is not directly comparable to the values from other codes. The factor, K, is 2.0 for unreinforced masonry buildings. Rainer (1987) calculated an equivalent R (or $R_f$) factor based on the "Tentative provisions for the development of seismic regulations for buildings" (ATC (1984)) for a K = 2.0 of 2.27 which is considerably greater than the AS1170.4 value which means a lower elastic force demand and an assumed higher level of over-strength, damping and/or post-elastic behaviour. Rainer, noting this discrepancy, suggested that the 1985 Canadian Code be changed to a R factor and brought in line with the ATC.

The 1990 National Building Code of Canada (Tso and Naumoski (1991) and Chandler (1991)) changed from the K factor of the 1985 code to a form of equivalent base shear formula that is similar to the form used by AS1170.4 and the ATC. There is one major difference between the response modification factor, R, from the Canadian code and $R_f$ used in AS1170.4. The R in the Canadian code is the ratio of the elastic strength to actual strength (Tso and Naumoski) and is therefore only a ductility factor. Another factor is used to take into account over-strength. $R_f$ is both the over-strength and ductility factor. Tso and Naumoski report that the over-strength factor has an assigned value of 0.6 and that R varies between 1 for a non-ductile system to 4 for a ductile system. Combining these two factors into an effective $R_f$ for a non-ductile system, such as unreinforced masonry, yielded a $R_f$ = 1.667, very close to the AS1170.4 value.

The regulations for the seismic design of buildings in Mexico City were discussed by Fukuta (1991). A reduction factor for the ductility of structures is included in the Mexico City design requirements and for unreinforced masonry structures such as those in this study a reduction factor of 1.0 is specified (under structure type - other structures). The largest reduction factor in the Mexico City code is 6.0. This is similar to the factor in AS1170.4 where the $R_f = 1.5$ reflects no ductility and is just an over-strength and damping factor.

The Chilean seismic code, as reported in Moroni et al (1992), has a more sophisticated approach to the determination of a seismic force reduction factor than the previously noted codes. A formula is given in the Chilean code that uses a factor dependant on the soil conditions, $T_o$, the period of the structure, T, and a parameter, $R_o$, related to the structural ductility. The formula is given as Equation 2.9.4.

$$R = 1 + \frac{T}{0.10T_o + \frac{T}{R_o - 1}} \qquad (2.9.4)$$

Moroni et al did not give values of $T_o$ or $R_o$.

Riddell et al (1989) proposed the use of a response modification factor that is partially consistent with the Chilean code in that it uses the building's period as a variable. A bi-linear response modification factor is proposed which consists of a linearly increasing response modification factor from 1.0 at a period of 0, to a maximum value depending on a ductility factor, $\mu$. The curve then remains constant for increasing period. The period at which this maximum first occurs also depended on $\mu$. The response modification factor was expressed as:

$$R = 1 + \frac{R^* - 1}{T^*} T \qquad \text{for } 0 \le T < T^* \qquad (2.9.5)$$

$$R = R^* \qquad \text{for } T \ge T^* \qquad (2.9.6)$$

where the values of $R^*$ and $T^*$ are given in Table 2.9.1 for various values of $\mu$.

The use of a structural response factor that is period dependant was also noted in Hutchinson et al (1994) as a way of correcting reported increased ductility demands in short period structures.

Table 2.9.1 Values of the parameters of the bi-linear relation for the response modification factor, R
(from Riddell (1989))

| Ductility factor, μ, for a single-degree-of-freedom system | R* | T* (seconds) |
|---|---|---|
| 2 | 2.0 | 0.1 |
| 3 | 3.0 | 0.2 |
| 4 | 4.0 | 0.3 |
| 5 | 5.0 | 0.4 |
| 6 | 5.6 | 0.4 |
| 7 | 6.2 | 0.4 |
| 8 | 6.8 | 0.4 |
| 9 | 7.4 | 0.4 |
| 10 | 8.0 | 0.4 |

It can be seen that the response modification factor in the Australian earthquake code, AS1170.4, has a similar value to the other earthquake codes around the world that have a similar approach to design. It is suggested by some researchers, however, that the structural response factor should be period dependant. For unreinforced masonry buildings the periods may be found to be in a small range (Chapter 3) and a constant value of the structural response factor may still be appropriate.

# 3. FIELD TESTING

## 3.1 INTRODUCTION

As outlined in Section 2.1, earthquake design requires reliable estimates of the natural period of a structure to calculate an earthquake design force. The applicability of existing earthquake code formulae for the natural period when applied to unreinforced masonry buildings was examined. The natural periods of a series of buildings were measured and the results compared to the periods determined by period formulae from building codes and proposed by other researchers. These period formulae have already been discussed in Section 2.1.

The only way to determine the actual natural period of a structure, as opposed to that determined by some form of mathematical modelling, is to measure it. In order to conduct tests on existing unreinforced masonry buildings it was first necessary to devise a testing methodology that was reliable, non-destructive, and had minimal impact on the occupants, as well as addressing the problems highlighted by other researchers and noted in Section 2.2.

The procedure to be used was broken down into five components:

(1) Source of vibration to record;
(2) Data collection on site;
(3) Digitisation of the data;
(4) Conversion of the data to the frequency domain; and
(5) Examination of the data.

While each component was dealt with separately, the interaction and compatibility of the components was carefully considered.

# 3.2 DEVELOPMENT OF TESTING METHODOLOGY

### 3.2.1 Source of Vibration

The source of the vibration to be recorded and subsequently analysed to determine the natural frequencies was the first part of the testing procedure to be considered.

Initially, the use of a small dynamic oscillator was considered, located either in the building, or on the ground near the building. This is the same method employed by various authors in forced vibration tests. However, it had three main disadvantages:

(1) Setting up and removal time on site;
(2) Disruption to occupants; and
(3) Possibility of damage, or blame for damage to the building due to extra stresses induced in the structure as part of the test.

These three disadvantages ruled out forced vibration testing for this project.

It was decided to use ambient vibration as the source for the vibration measurements of the buildings. This immediately overcame the three disadvantages of the forced vibration method listed above. Ambient vibrations have been used successfully by a number of researchers to obtain a reasonable estimation of the natural period, as has previously been noted in Section 2.2. No external vibration source was required and the on site set-up consisted of only the basic instrumentation required for the recording of the building response.

### 3.2.2 Data Collection on Site

The measurement of vibration can be achieved by the measurement of one of three physical actions:

(1) Displacement;
(2) Velocity; or
(3) Acceleration.

Ideally the measurement of vibration was to be achieved by the use of existing departmental resources, provided no compromises in the quality of the data was

encountered. This ensured the most optimum use of the project's resources. No equipment existed for the measurement of velocity so this was immediately ruled out. Both displacement and acceleration have been used by previous researchers without problem.

To measure the displacement of a structure the use of a displacement transducer is required. The displacement is measured relative to a fixed datum. This datum would need to be very stiff to ensure it will not move relative to ground. While this would present no problem in a laboratory, the setting up and dismantling of such a frame on site would counteract the main advantages of using ambient vibration, namely, the ease with which the tests could be set-up and conducted.

Hence, acceleration proved to be the best solution. Absolute acceleration was measured by attaching accelerometers directly to the building. The accelerometers chosen were the KISTLER 305A model. These accelerometers have an upper acceleration limit of fifty times the acceleration of gravity and a lower limit of 0.0005 times the acceleration of gravity. While it was not expected that the upper limit would be reached, the recorded accelerations were expected to be around the lower limit so all recorded accelerations were compared with the lower limit to ensure the results were within the linear operating range of the accelerometers.

The accelerometers were attached to the buildings using plastic mounts and 'Plasti-Bond' two part adhesive compound. The mounts were easily removed after the completion of the test by gentle hammering. This also removed the 'Plasti-Bond' and left no trace of the test having been conducted. The accelerometers could be mounted on any material usually found on a building, concrete, masonry, timber, or steel. This ensured that the location of the accelerometers was not compromised by any difficulties in attaching them.

The positioning of the accelerometers was critical. Incorrect positioning could lead to the localised modes of the building elements being recorded with the desired overall building modes (refer Figure 3.2.1). Separation of the two types of modes from the combined recording would be impossible. To overcome this problem the accelerometers were placed at the floor and roof levels of the building as these were node points of the local vertical modes of vibration of the walls (a node is a point of no relative displacement for the mode shape - see points labelled (2) in Figure 3.2.1) and ensured that these local modes were not present in the recorded data. The horizontal location of the accelerometers was at the corners of the building as these

were node points of the local horizontal modes of vibration for the walls and again ensured that these vibrations were not present in the recorded data. By recording the data from the corners of the building, torsional modes were expected to be present in the data. These modes were identified because of their presence in the recorded data of both axes.

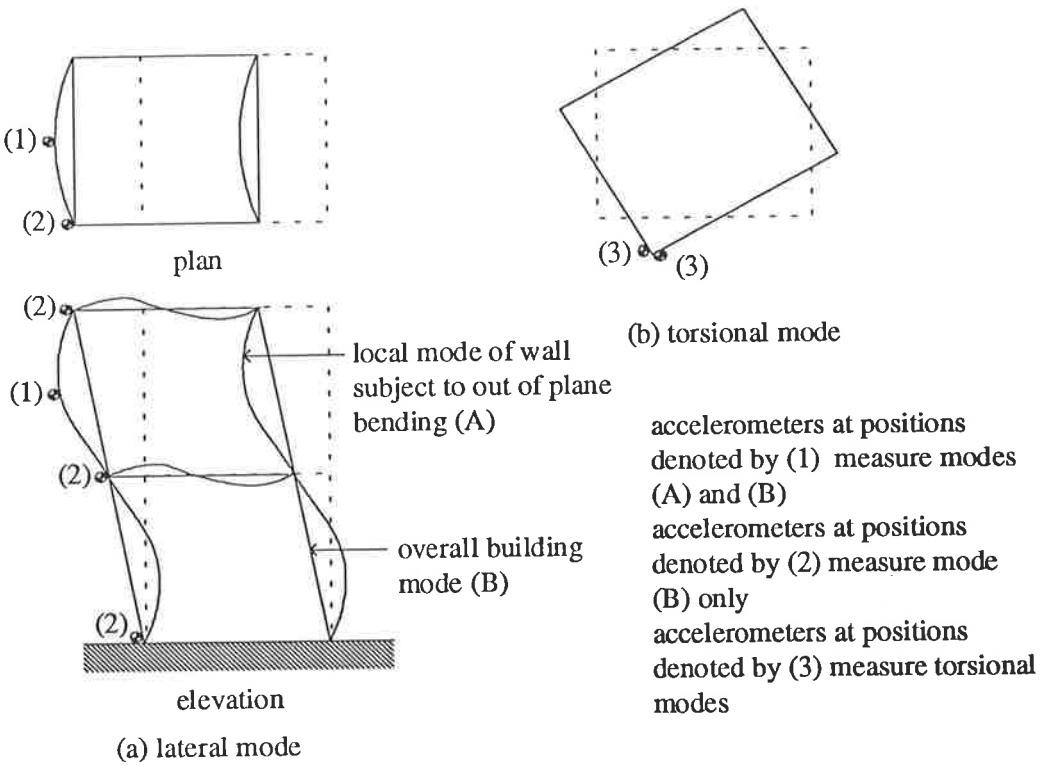


Figure 3.2.1 Effect of accelerometer location on recorded modes.

Accelerometers were also placed in both directions at the ground level of the buildings to identify the exciting vibrations in the recorded data. This ensured that the exciting frequency was easily identified in the upper level records.

It was necessary to position the accelerometers in a vertical line so that the mode shapes of the building could be determined. This was easily accomplished along the corners of the building. The data for one direction was recorded simultaneously so that the magnitude of the exciting force was constant for all levels of the building and the relative magnitudes at each level were compatible.

The accelerometers were connected to a servo-amplifier operating in the 0.2 g per volt range. This setting was found by trial and error during initial tests to result in the best resolution of the data for the levels of excitation experienced under ambient vibration conditions. After the attachment of the accelerometers to the building the gain of the servo-amplifiers was adjusted to 'zero' the output. This meant adjusting the gain until the acceleration was centred about zero volts. While it was not possible to exactly 'zero' the accelerometers, the 'zero' level was set within $\pm 10$ millivolts.

Two of the major requirements for the data collection and recording device were reliability and portability. One possible solution would have been the use of analogue tape recorders as used by previous researchers. A better alternative was provided by the computer program 'Chart' with the 'Maclab' data collection device running on an Apple Macintosh SE personal computer. 'Chart' is a computer simulation of an analogue chart recorder. This system provided the capacity to record up to eight channels of data, which was more than sufficient for the unreinforced masonry buildings in Adelaide. The data was recorded on a 3.5 inch computer floppy disk for further processing.

### 3.2.3 Digitisation and Filtering of the Data

To be able to undertake further processing of the data after it was collected on site the data was converted from an analogue to a digital format. The 'Maclab' system digitised the data prior to recording and therefore no further actions were required.

With the acceleration data being recorded with respect to time, the 'Sampling Theorem' (Appendix A) was invoked. As the periods of interest were low, because of the high stiffness and relatively low height of the unreinforced masonry buildings, the frequencies measured were expected to be in the 2 to 10 Hertz range so a low pass filter with a cut-off of 20 Hertz was used. To keep the frequencies of interest and the filtering frequency well below the Nyquist frequency of the digitising device a sampling rate of 100 Hertz was adopted (resulting in a Nyquist frequency of 50 Hertz). The filter used was a 5 pole Butterworth filter.

As will be explained later, 20.5 seconds of data was recorded. At 100 Hertz this resulted in at least 2048 (2k) points of data being available for conversion to the frequency domain.

### 3.2.4 Conversion of the data to the frequency domain

A Fourier transform was used to convert data in the time domain to the frequency domain. Various algorithms exist in different computer packages for the Fourier transformation of data. Three readily available in the Civil and Environmental Engineering Department were considered for use in this study.

(1) Hewlett Packard Structural Dynamics Analyser;
(2) 'Maclab Scope' program; and
(3) 'Lab-Workbench' computer software.

However, after consideration of the compatibility between the format of the recorded data and the format required for the input of the data to the three alternatives, as well as the format of the output data from the Fourier transformation, it was decided to use 'Lab-Workbench'.

'Lab-Workbench' is a UNIX based data collection and manipulation program. It is run on a MASSCOMP real time UNIX computer and is controlled from a graphics terminal using a flow chart and icon system. The transfer of the data from Maclab to MASSCOMP was relatively simple. The data was saved in text mode in the 'Chart' program and transferred to the UNIX operating system via the 'Macintosh' program 'MacKermit'. This program transferred the data serially while altering the data format to UNIX. There is no restriction on the number of channels to be transferred simultaneously. A header file similar to that produced by the 'Lab-Workbench' program when storing data was created using the UNIX system editor 'vi'. This allowed the use of the 'playback' module in 'Lab-Workbench' to load the data. The 'power spectral density' module was used to change the data from the time domain to the frequency domain. The output of the 'power spectral density' module was saved in the same format as the input data. At the time of testing, no "hard" copy output from the MASSCOMP was possible. It was necessary to transfer the data from the UNIX system to a MS-DOS PC and load the data into either of the spreadsheet 'Excel' or the program 'C-Plot' for output in graphical form to a laser printer. This transfer was completed using the standard 'Ethernet' computer connection.

The 'Lab-Workbench' provided a sharp and clear power spectrum of the data. From a trial and error approach with various lengths of input data it was found that 2048 points per channel provided the sharpest image. While less points provided the power spectrum peaks at the same frequency with the same magnitude, the peaks

were more easily distinguishable with 2048 points. More points had no significant effect on the resolution of the output. As outlined in Section 2.2 it is necessary to use a window to make the data periodic. The options included in the program for windowing were all tried and, while none were significantly better than the others, the Blackman-Harris window was adopted for this study.

### 3.2.5 Examination of the Data

The power spectra of the data were examined. Firstly, the peaks in each spectrum were identified as the natural frequencies of the building. A peak was always present at the 0 Hertz point representing the DC offset of the accelerometers. Even though the accelerometer output was 'zeroed' prior to the test, a small voltage at zero acceleration was always present. The lateral and torsional modes were identified from the data as discussed in Section 3.2.2. If a peak was common to both axes of the building it was not possible to determine whether the mode was a torsional mode or a combined torsional and lateral mode.

In order to estimate the mode shapes for each of the buildings in this study, the magnitude of the response spectrum peaks for each frequency at each level were normalised and plotted against the height of the building.

## 3.3 TESTING PROGRAM

### 3.3.1 The Physics Building Annex

The first unreinforced masonry building to be tested was a five storey annex to the Physics Building on the University of Adelaide's North terrace campus. The results of this test indicated that the fundamental natural frequency of this building was 3.1 Hertz (see Figure 3.3.1). This result was promising because the annex is located more than 500m from any street and was expected to be subject to very low levels of ambient vibration. Thus, the method was established as being capable of determining the structural periods for buildings subject to low levels of excitation.

An estimate of the normalised first mode shape was also determined (see Figure 3.3.1) based upon the power spectral density values at each floor. It was not possible to determine the second mode shape because the power spectrum data did not include enough information to estimate the point at which the mode shape crossed the vertical axis.

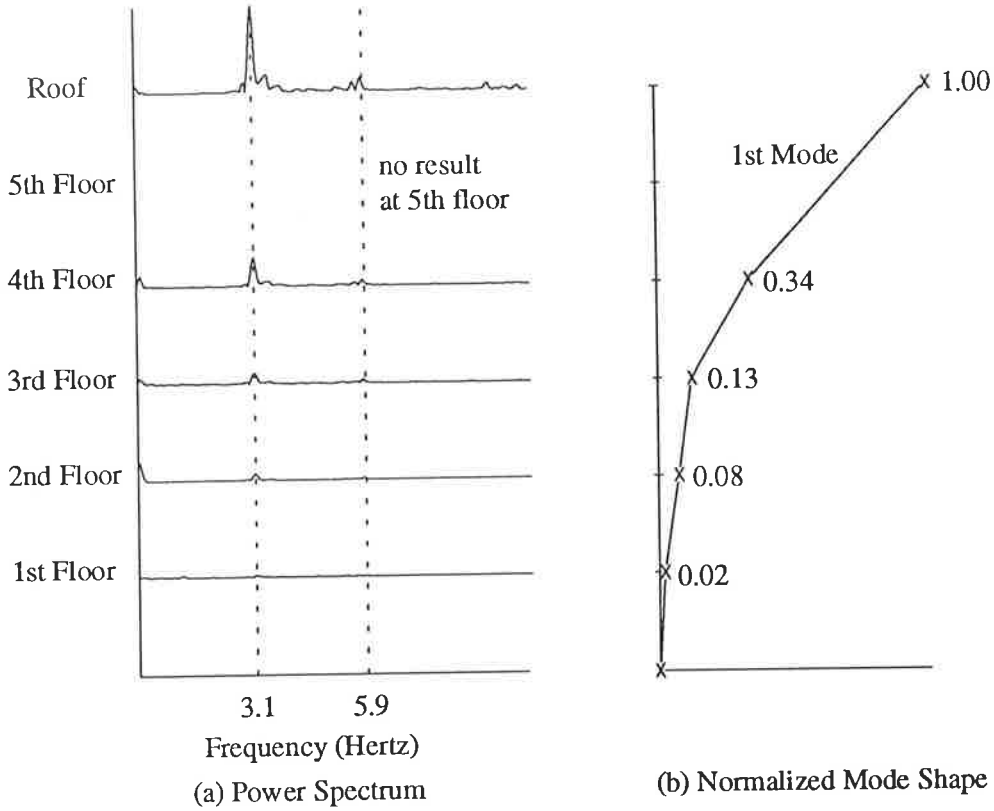


Figure 3.3.1 Physics Annex Results

### 3.3.2 The Engineering Building Annex

After the Physics Building Annex test, the annex of the Engineering Building at the University of Adelaide was also tested. This building is a steel moment resisting frame. It was chosen because it contained a gantry crane. The gantry crane was used to impart a pulse excitation to the structure by running it into its end stops. This caused a pulse excitation and the structure responded at its natural frequencies. The results from the pulse excitation tests were compared to the results from an ambient vibration test on the same structure. The natural frequencies determined by both tests agreed, hence providing further confidence that the ambient vibration tests were suitable to obtain period estimates.

### 3.3.3 General Testing Program

Ambient vibration testing was conducted on fifteen unreinforced masonry buildings, including the Physics Building annex, in the Adelaide central business district and metropolitan area using the method outlined above. The data was recorded

concurrently for both directions of the building, except in one case where there was insufficient accelerometers, on the MACLAB system.

The raw data was transferred to the MASSCOMP system. After calibration, the data from three buildings was found to be below the lower limit of the accelerometers and were discarded from the data set. All three buildings were single storey. One building in the remaining twelve, a city social club (IAC), has two results included in the final data set because it was considered to have two parts with differing dynamic properties and the accelerometers were placed to record the vibration modes associated with each part seperately.

The thirteen results from the twelve buildings not eliminated from the testing program are given in Table 3.3.1 along with various parameters associated with the period formulae given in Section 2.1. Full details, and plans of the buildings are given in Appendix B.

# 3.4 EXPECTED FORM OF PERIOD FORMULA

The natural period of a structure is a function of the ratio of the structure's mass to its stiffness (Clough and Penzien (1993)). Assuming that the deflection of an unreinforced masonry building, or any panel or shear walled building, is predominantly a result of the shear deflection of the walls then the deflection of the building could be expected to be of a similar form to the equation for the shear deflection of a beam, Equation 3.4.1, as shown in Figure 3.4.1. This makes the simplifying assumption that the earthquake induced load acts at the top of the wall only, and hence, the wall has a straight deflected shape.

$$\Delta = k\frac{Ph}{AG} \tag{3.4.1}$$

where $\Delta$ is the shear deflection, P is the force, h is the height, A is the cross sectional area, G is the shear modulus, and $k$ is a constant.

The shear stiffness of a wall, K, is given by:

$$K = \frac{P}{\Delta} \tag{3.4.2}$$

Table 3.3.1 Results of ambient tests

| Building Description | Plan   | Building Height, h (metres) | Building Plan Dimensions, $D_x$ and $D_y$ (metres) | Measured Period, $T_x$ and $T_y$ (seconds) | Floor Type Concrete/Timber |
|---|---|---|---|---|---|
| 2 storey vacant city commercial building (EE2) | | 7.8 | 3.9 x 7.3 | 0.208 and 0.200 | timber |
| 2 storey vacant city commercial building (EE3) | | 7.8 | 7.3 x 12.2 | 0.278 and 0.200 | timber |
| 2 storey vacant city commercial building (EE4) | | 7.8 | 7.3 x 12.2 | 0.270 and 0.200 | timber |
| 1 storey suburban residence (WARD) | | 3.9 | 20.6 x 11.5 | 0.057 and * | timber |
| 3 storey school building (CBC) | | 8.8 | 10.9 x 32.4 | 0.182 and * | concrete |
| 1 storey city social club (IAC) | | 3.6 | 19.8 x 14.5 | 0.073 and 0.072 | concrete |
| 2 storey city social club (IAC) | | 6.5 | 19.8 x 36.1 | 0.092 and 0.089 | concrete |
| 3 storey city commercial building (LTI) | | 13.0 | 23.5 x 29.0 | 0.313 and 0.270 | concrete |
| 2 storey city commercial building (NSC) | | 8.0 | 11.4 x 28.8 | 0.099 and * | concrete |
| 2 storey city retail building (STP) | | 9.3 | 10.0 x 27.0 | 0.135 and 0.133 | timber |
| 5 storey university building (OLW) | | 19.1 | 12.2 x 48.8 | 0.323 and * | concrete |
| 2 storey suburban apartment building (KIDA) | | 4.6 | 5.5 x 15.0 | 0.139 and 0.137 | concrete |
| 2 storey suburban apartment building (KIDB) | | 4.6 | 5.5 x 20.0 | 0.139 and 0.139 | concrete |

* denotes result not available for this direction.

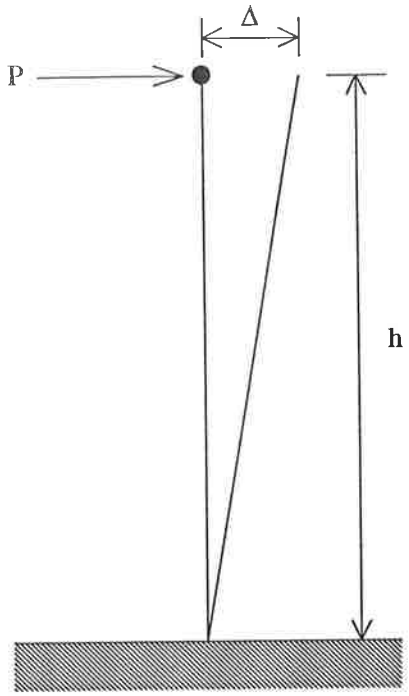


Figure 3.4.1 Shear Deflection of a Beam.

The shear area is proportional to the depth of the building, D, so that:

$$K \propto \frac{D}{h} \tag{3.4.3}$$

where G and *k* are constants in Equation 3.4.1. In addition, the mass of the building is proportional to the breadth, B, depth, D, and height, H so that substituting into the equation for natural period gives:

$$T \propto \sqrt{\frac{BDh}{D/h}} \tag{3.4.4}$$

So that it could be expected that a period formula for unreinforced masonry, or any panel type building, would take the form:

$$T \propto h\sqrt{B} \tag{3.4.5}$$

To take this analysis further, it could also be assumed that the stiffness of the building would be proportional to its breadth, B, as a wider building would be expected to have more walls parallel to the direction of interest which would contribute to the shear stiffness. Hence, Equation 3.4.5 would reduce to the period being proportional to the building's height:

$$T \propto h \tag{3.4.6}$$

# 3.5 COMPARISON WITH PERIOD FORMULAE

The tested buildings were divided into two categories; those buildings where the floor was a concrete slab and those where the floor was timber. The distinction was considered important because of the detail of the connection between the floor and the wall for the two types of floor system were expected to lead to different types of behaviour between the wall and the floors. Considering the concrete slab floor system first. The typical connection detail for the buildings in the study with concrete floors is shown in Figure 3.5.1(a). It can be seen that rotation would not be expected to occur between the floor and wall for this type of connection. The typical connection detail of a timber floor to a masonry wall is shown in Figure 3.5.1(b). It can be seen that rotation can occur between the wall and the floor for this type of connection. The building's type of floor system is included in Table 3.3.1.

As previously stated, the aim of this part of the research project was to ascertain the accuracy of various formulae for the estimation of the natural period of unreinforced masonry buildings for use in earthquake design. To accomplish this, the natural periods determined from the field tests were plotted against the various parameters from the period formula discussed in Section 2.1.

Three linear regressions were carried out for each of the forms of period formula:

(1) Using all the data;
(2) Using the data from the buildings with concrete floor systems; and
(3) Using the data from the buildings with timber floor systems.

The linear regressions were performed so that the resulting regression line passed through the origin (0,0) of the plot (Appendix C). The confidence intervals corresponding to the various period formulae were also calculated. It can be seen

that for the Australian design response spectrum (Figure 5.2.1) an underestimation of the fundamental natural period will result in a design earthquake force either equal to, or less than, that corresponding to the actual fundamental natural period. For this reason the calculated confidence intervals were single sided. That is, a 30 percent confidence interval meant that period formula predicted a fundamental natural period less than or equal to the actual fundamental period for 30 percent of the data. The resulting plots of the parameters from the various forms of the period formulae against the measured periods can be seen in Figures 3.5.2 to 3.5.22. The various period formulae are also plotted on the appropriate graphs along with the regression curves. The results are summarised in Table 3.5.1 along with the values of $R^2$ (a measure of the fit of the form of the formula to the measured data) for each of the forms of the period formula and for each of the three sub-sets of data.

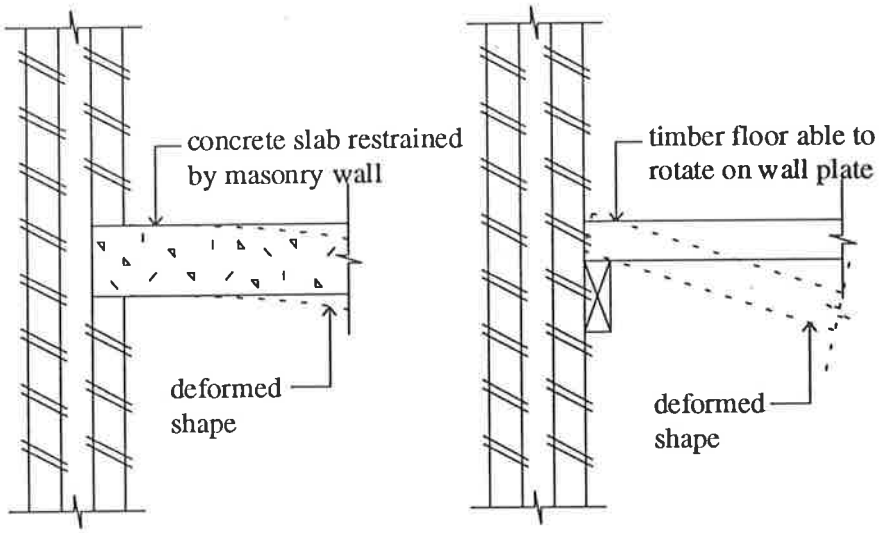


(a) Concrete Floor System (b) Timber Floor System

Figure 3.5.1 Concrete and Timber Floor System Connections to Walls.

The first form of period formula to be compared was that found in The Australian Standard "Minimum design loads on structures - Part 4 : Earthquake Loads" AS1170.4 (Equations 2.1.1 and 2.1.2). The three comparisons are shown in Figures 3.5.2, 3.5.3, and 3.5.4. Next form of period formula to be compared was that found

in The Australian Standard "SAA Earthquake Code" AS2121 (Equation 2.1.3). The three comparisons are shown in Figures 3.5.5, 3.5.6, and 3.5.7.

The alternative form of period formula from AS2121 (Equation 2.1.4) was compared next. The three comparisons are shown in Figure 3.5.8, 3.5.9, and 3.5.10. The next comparison was for the form of equation used in the "Tentative provisions for the development of seismic regulations for buildings" (ATC(1984)), Equation 2.1.5. These comparisons are shown in Figures 3.5.11, 3.5.12, and 3.5.13. The revised form of the ATC formula (Equations 2.1.5 and 2.1.7) was compared to the measured periods in Figures 3.5.14, 3.5.15, and 3.5.16. The next form of period formula compared was the expected form of period formula for a masonry building (Equation 3.4.5). The comparisons are shown in Figures 3.5.17, 3.5.18, and 3.5.19. The final form of period formula compared was that given by Housner and Brady (1963), Equation 2.1.15. The comparisons are shown in Figures 3.5.20, 3.5.21, and 3.5.22.

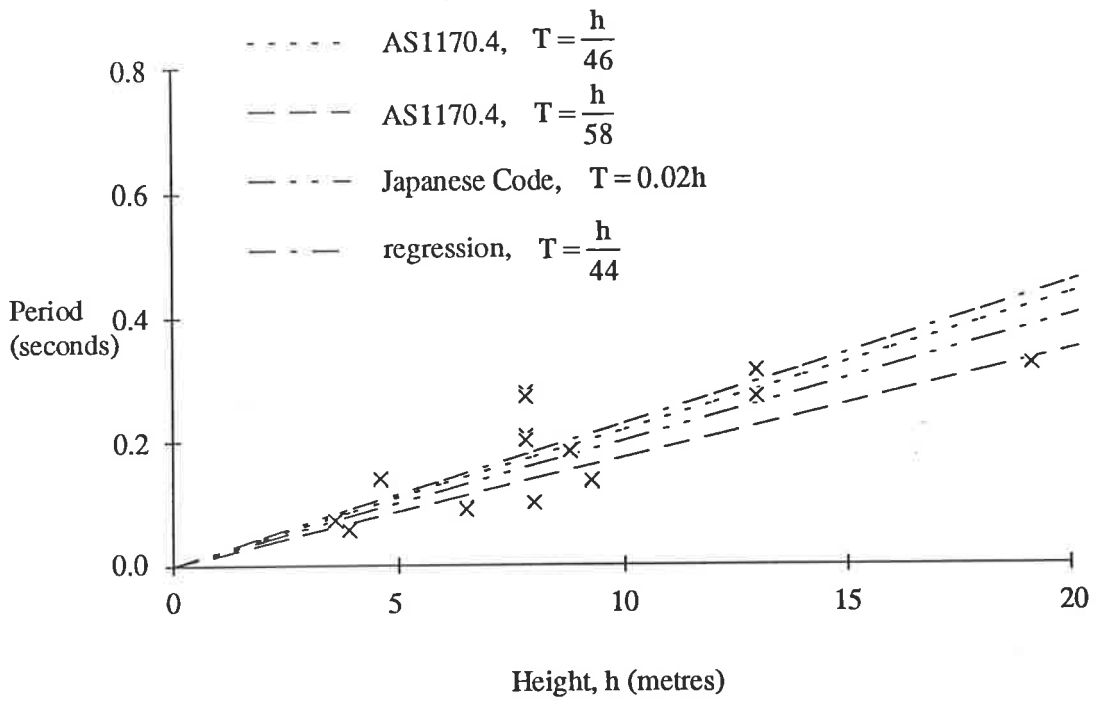


Figure 3.5.2 Plot of Period versus Building Height, h - All Data.

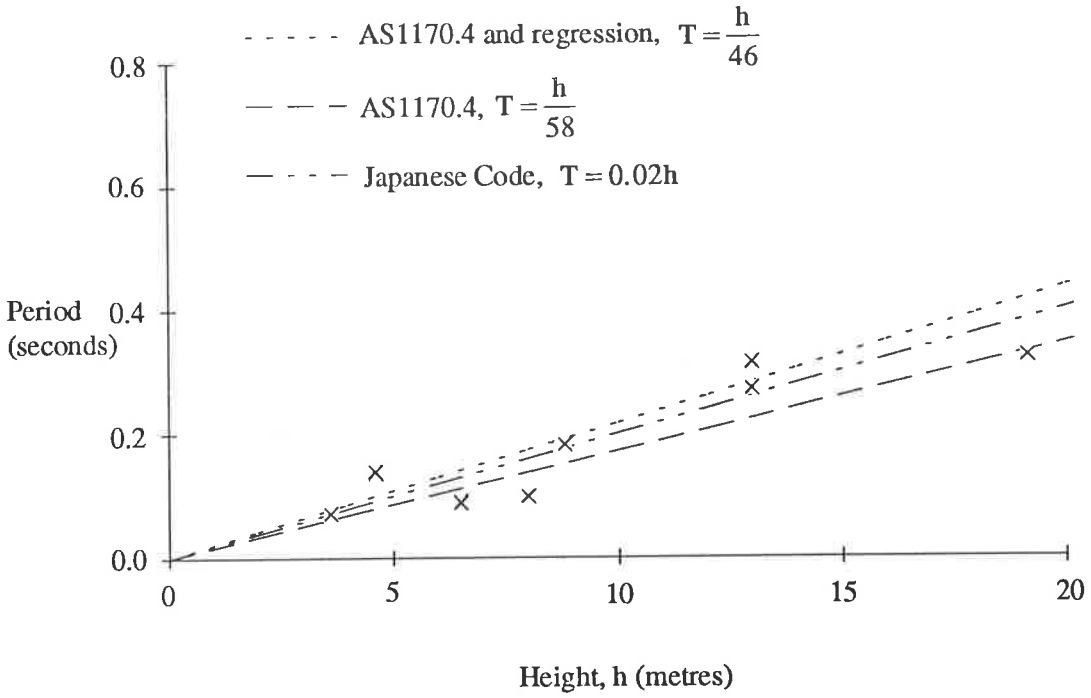


Figure 3.5.3 Plot of Period versus Building Height, h - Concrete Floor Systems.

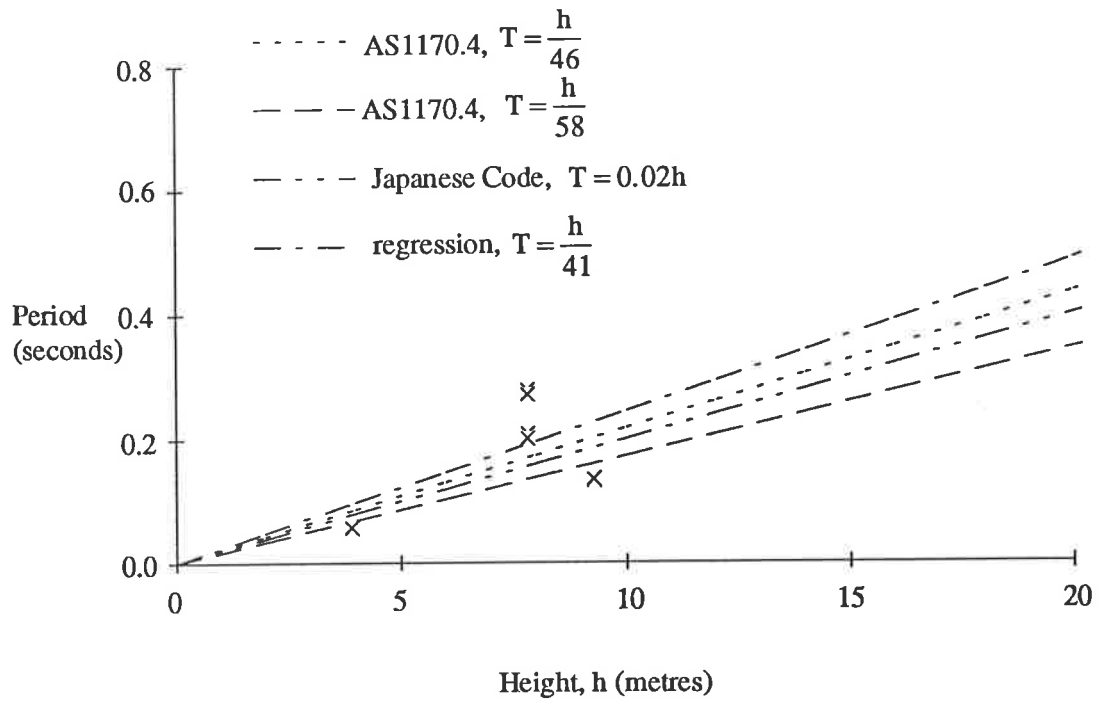


Figure 3.5.4 Plot of Period versus Building Height, h - Timber Floor Systems.

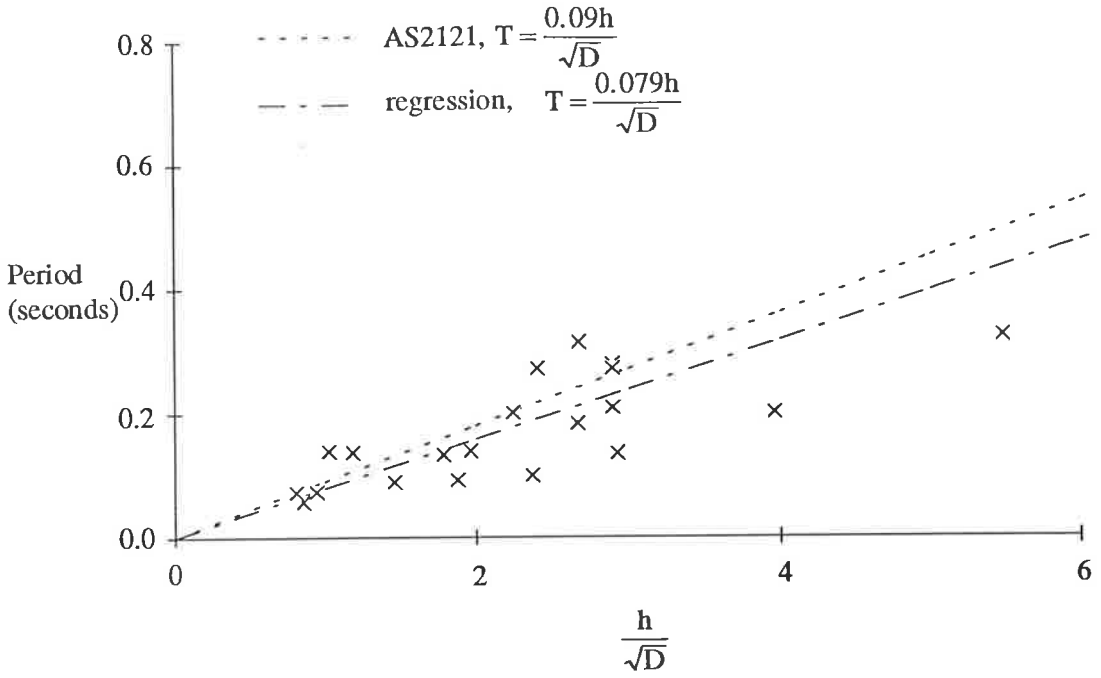


Figure 3.5.5 Plot of Period versus $\frac{h}{\sqrt{D}}$ - All Data.

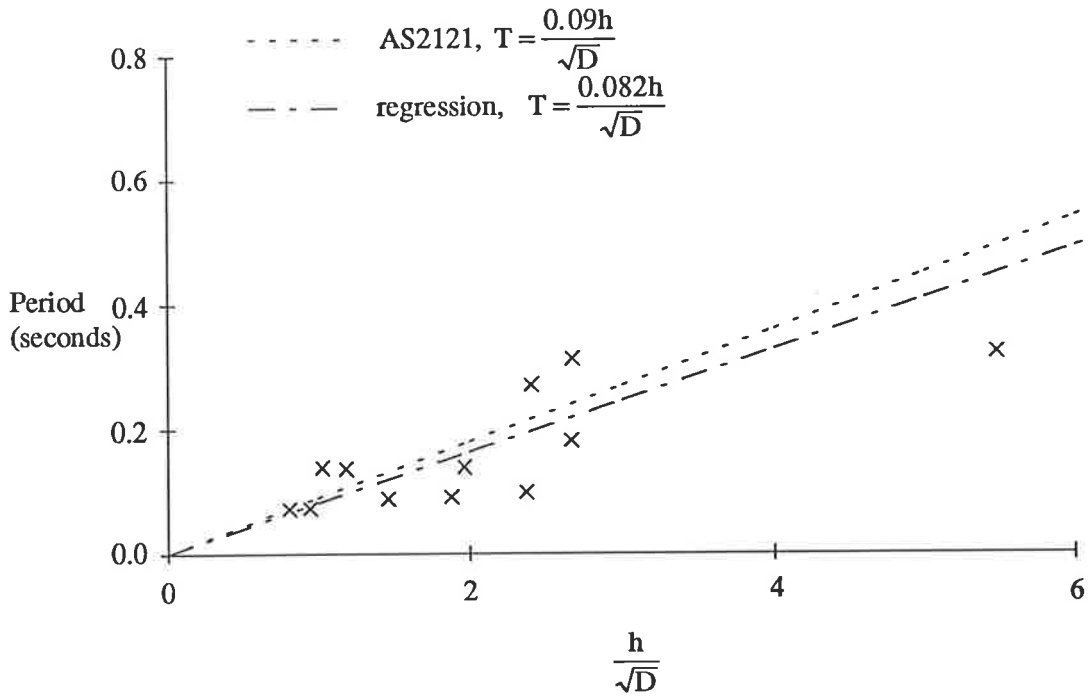


Figure 3.5.6 Plot of Period versus $\frac{h}{\sqrt{D}}$ - Concrete Floor Systems.

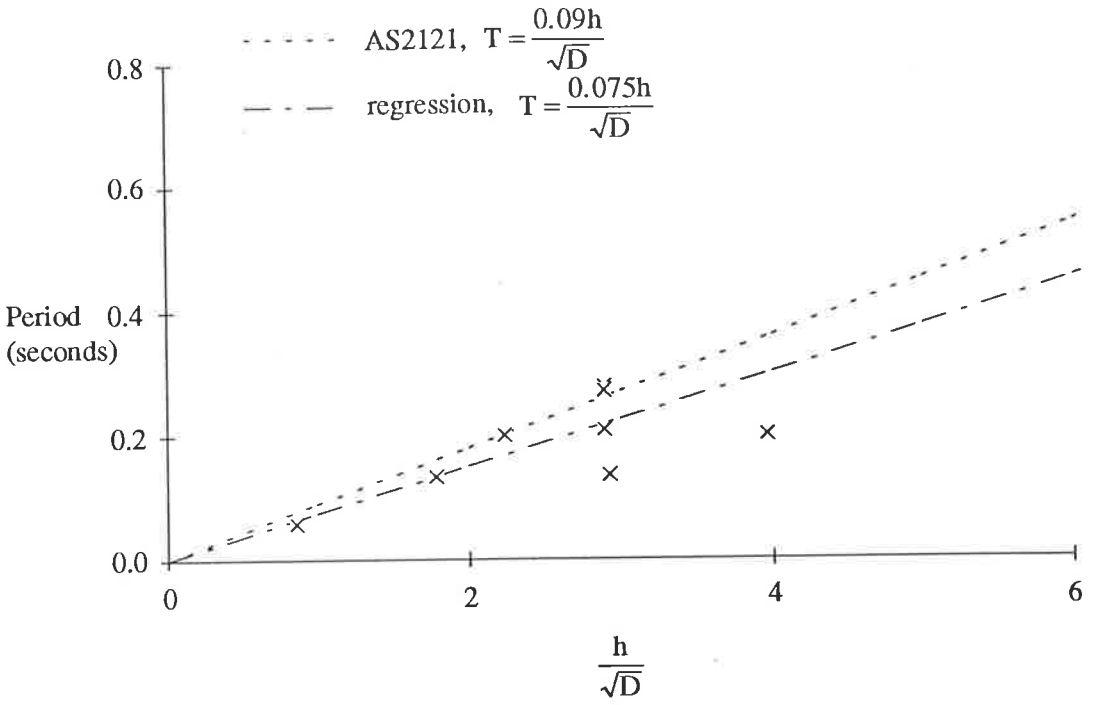


Figure 3.5.7 Plot of Period versus $\frac{h}{\sqrt{D}}$ - Timber Floor Systems.

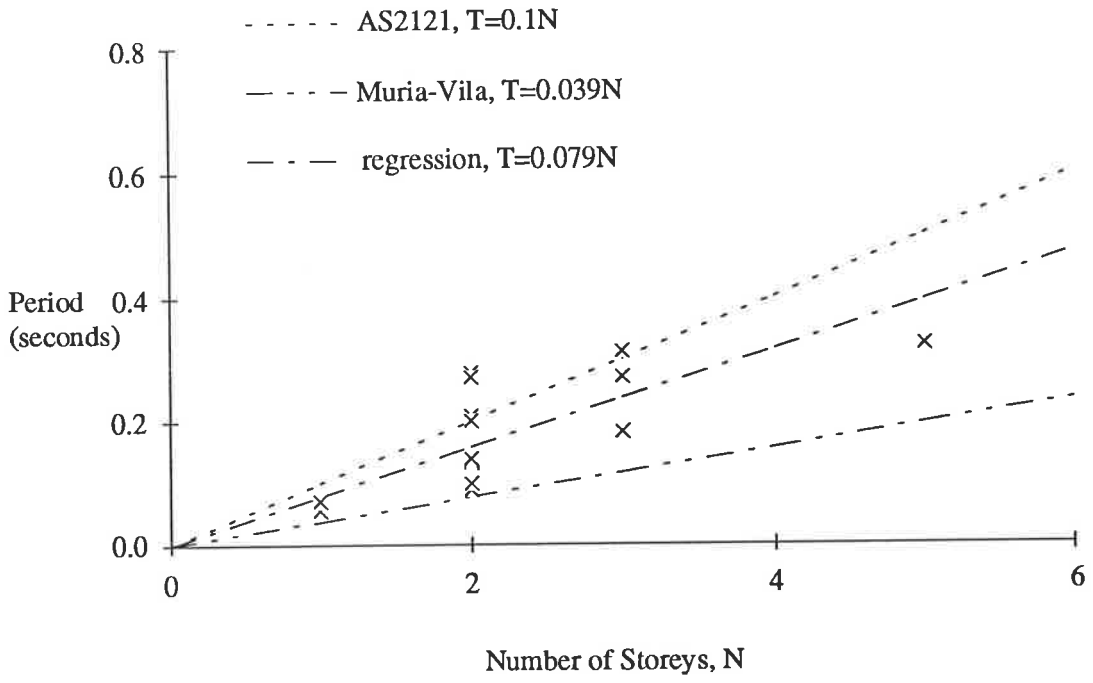


Figure 3.5.8 Plot of Period versus Number of Stories, N - All Data.

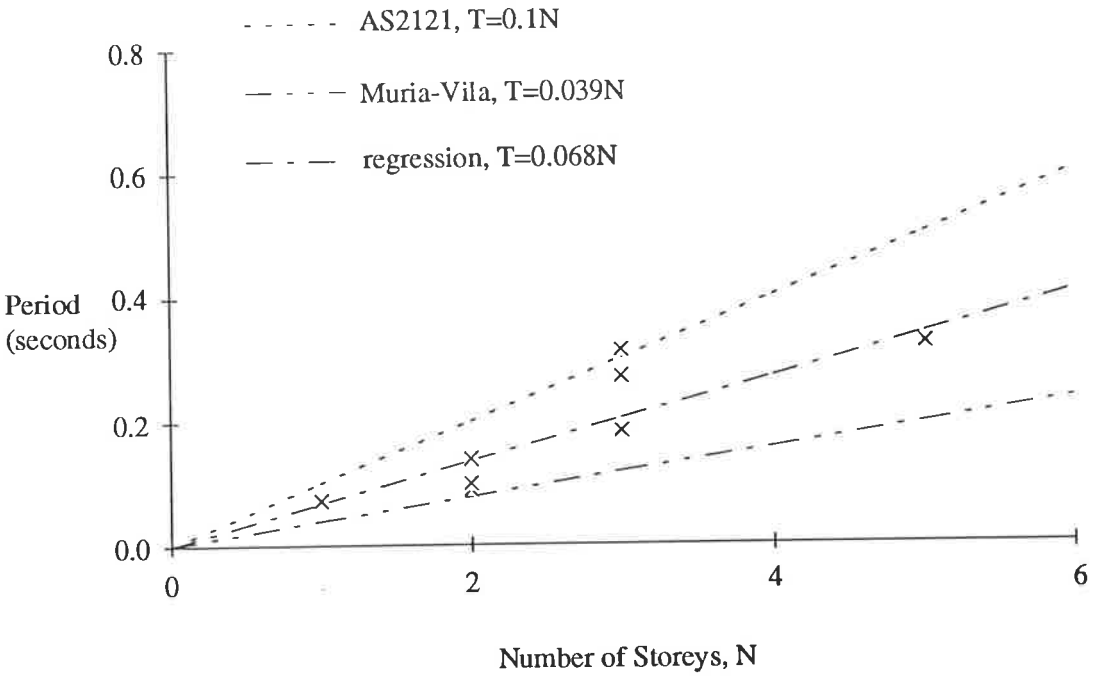


Figure 3.5.9 Plot of Period versus Number of Stories, N - Concrete Floor Systems.

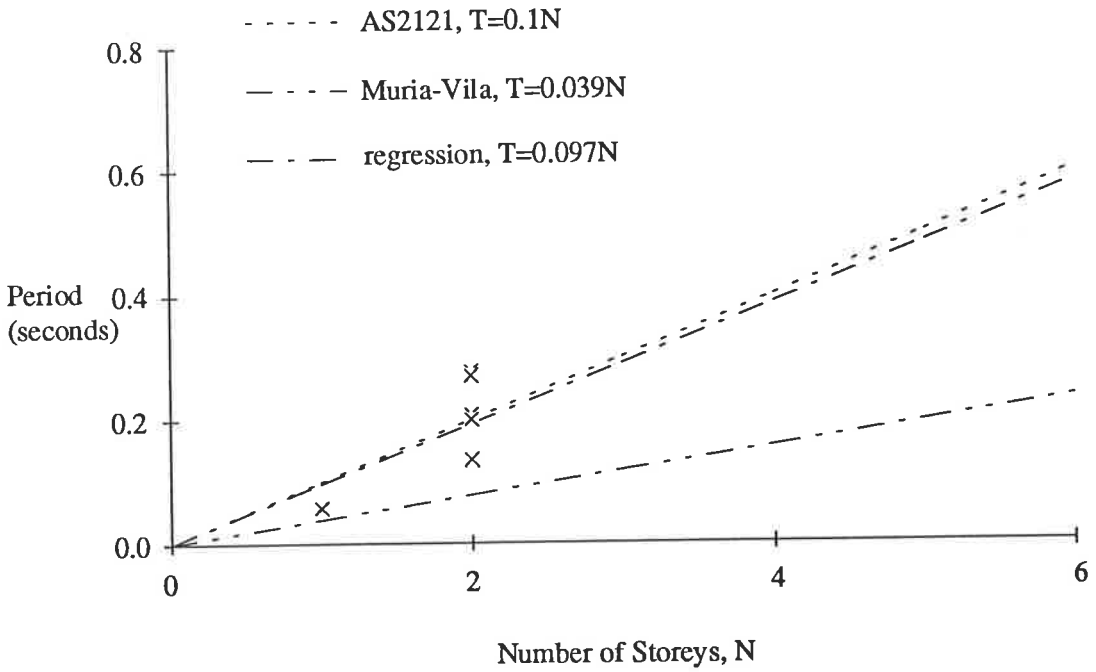


Figure 3.5.10 Plot of Period versus Number of Stories, N - Timber Floor Systems.

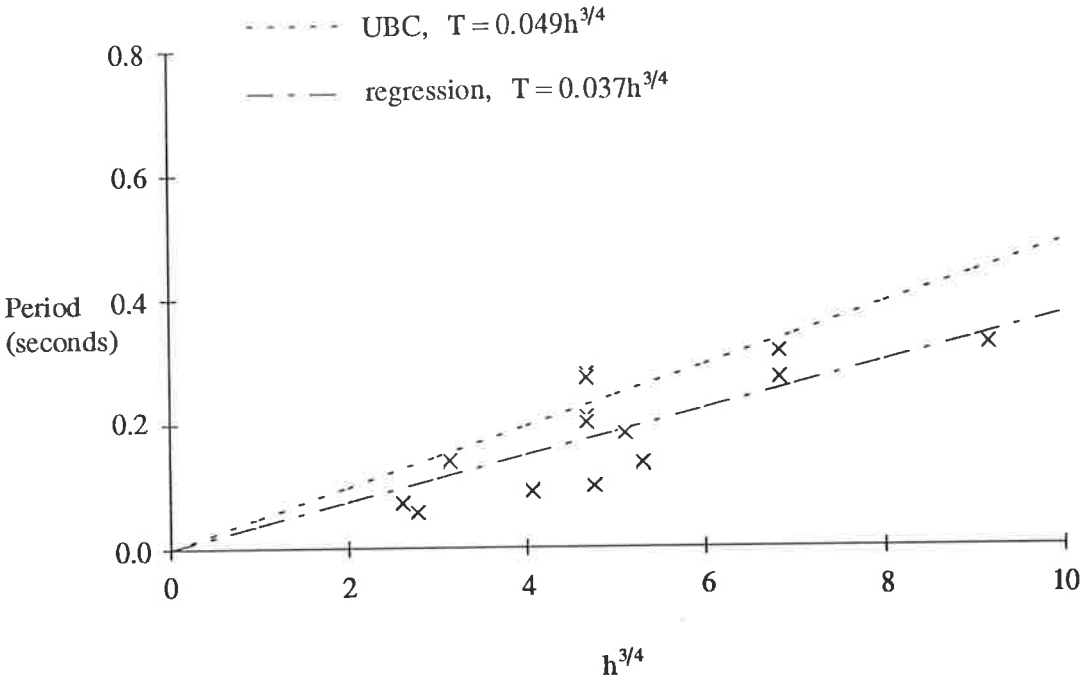


Figure 3.5.11 Plot of Period versus $h^{3/4}$ - All Data.

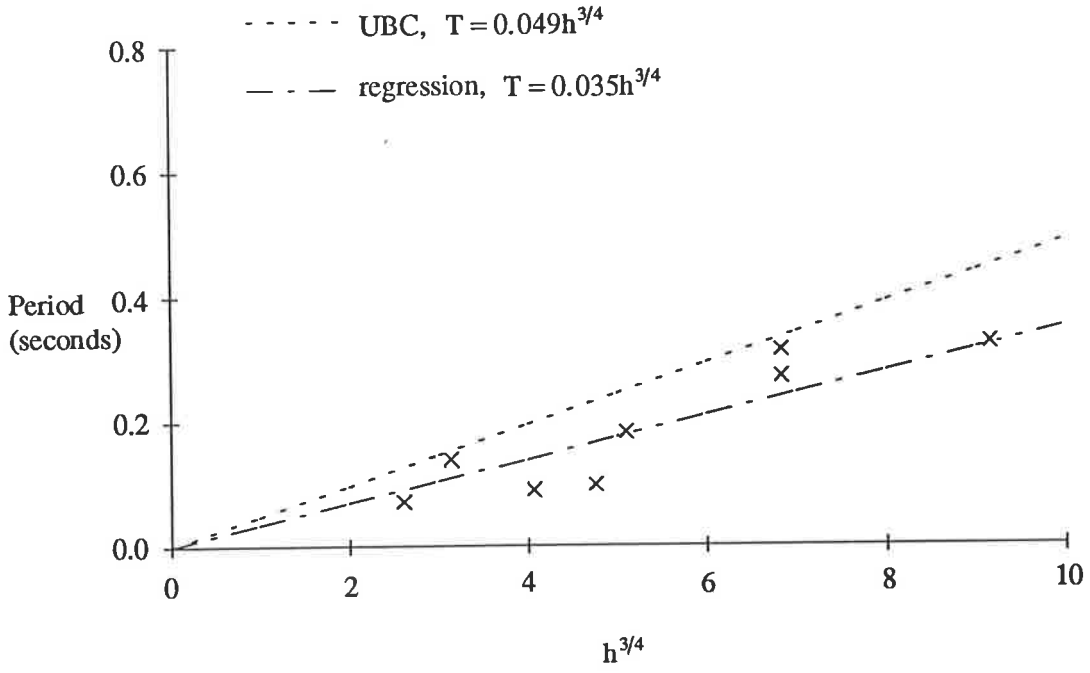


Figure 3.5.12 Plot of Period versus $h^{3/4}$ - Concrete Floor Systems.

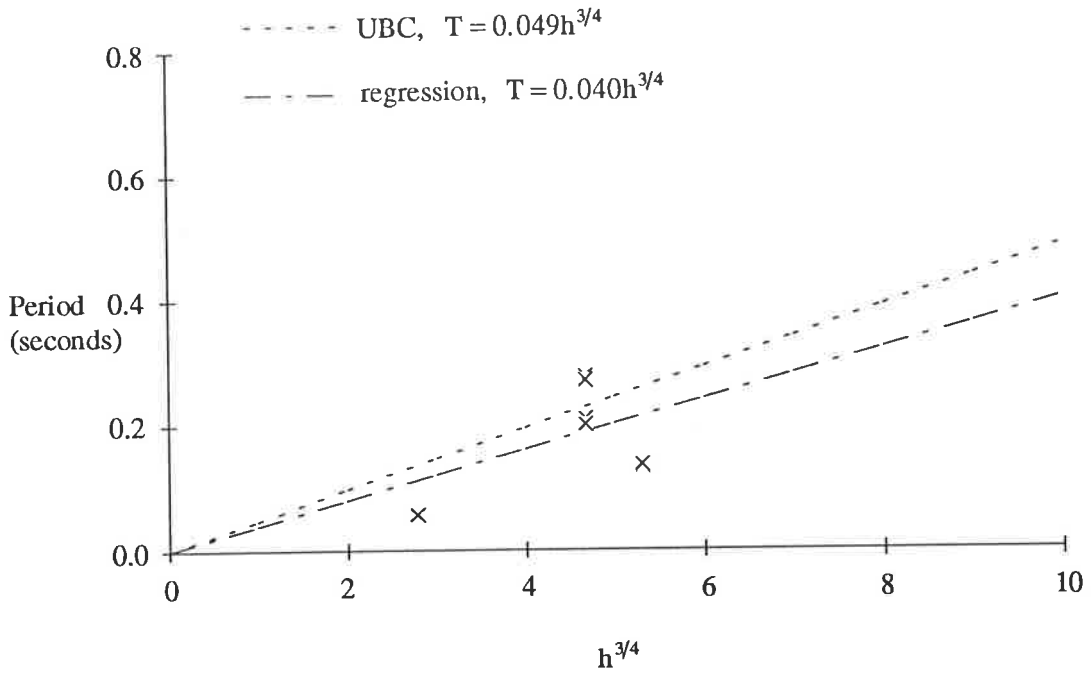


Figure 3.5.13 Plot of Period versus $h^{3/4}$ - Timber Floor Systems.

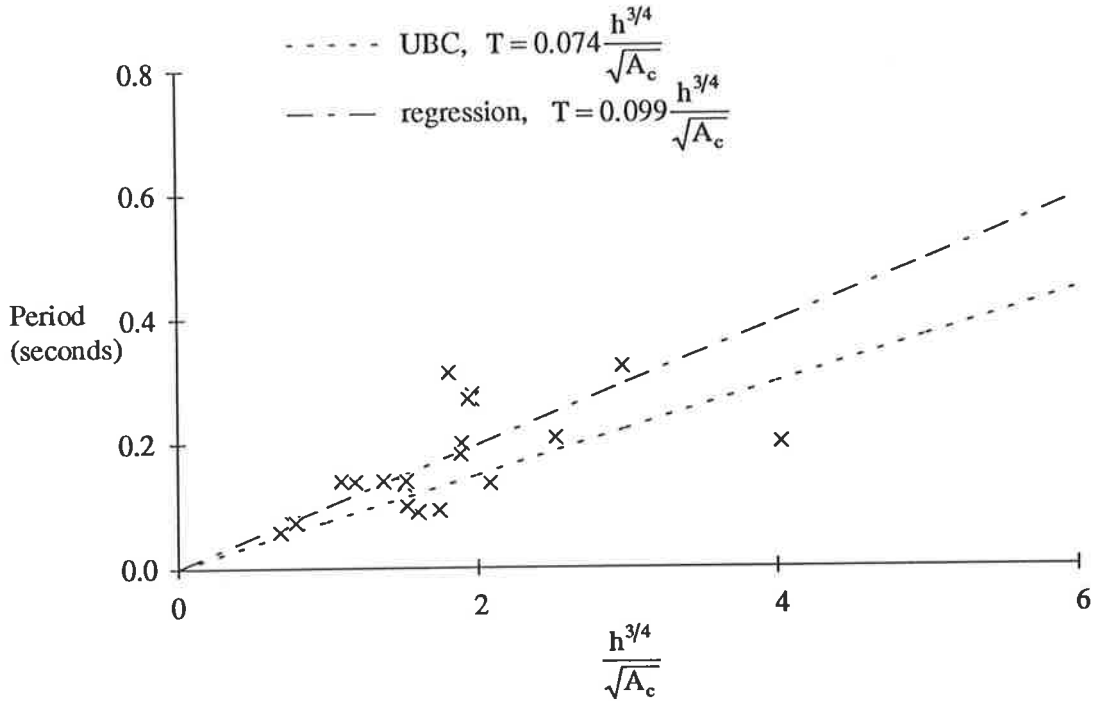


Figure 3.5.14 Plot of Period versus $\frac{1}{\sqrt{A_c}}h^{3/4}$ - All Data.

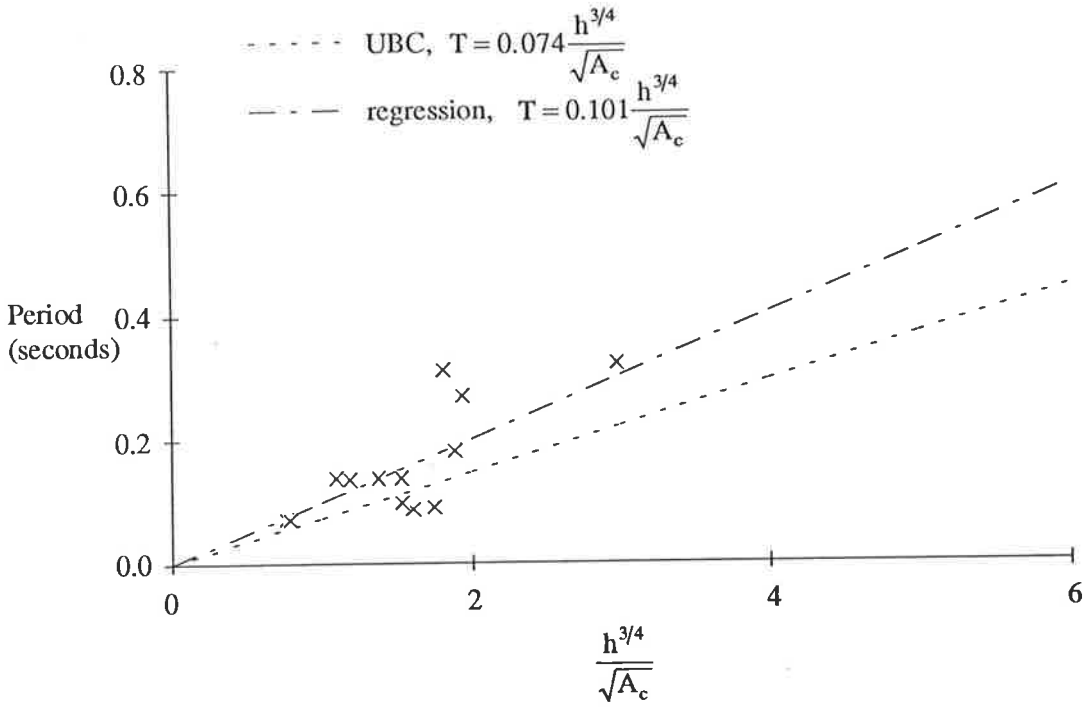


Figure 3.5.15 Plot of Period versus $\frac{1}{\sqrt{A_c}}h^{3/4}$ - Concrete Floor Systems.

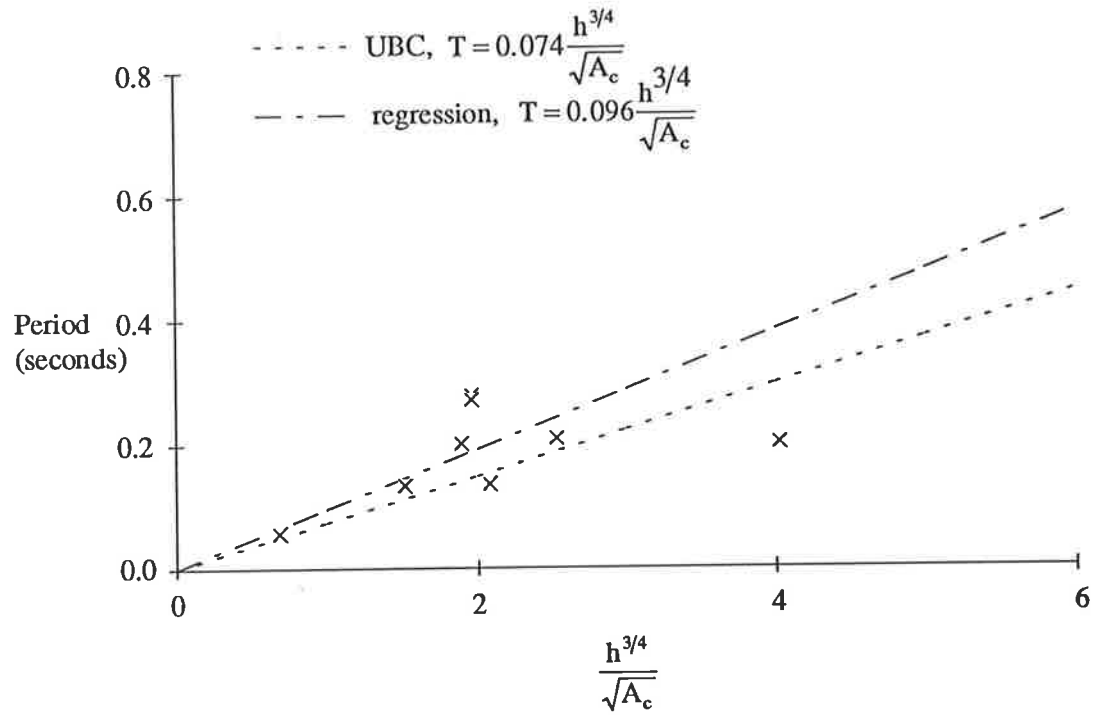


Figure 3.5.16 Plot of Period versus $\frac{1}{\sqrt{A_c}}h^{3/4}$ - Timber Floor Systems.

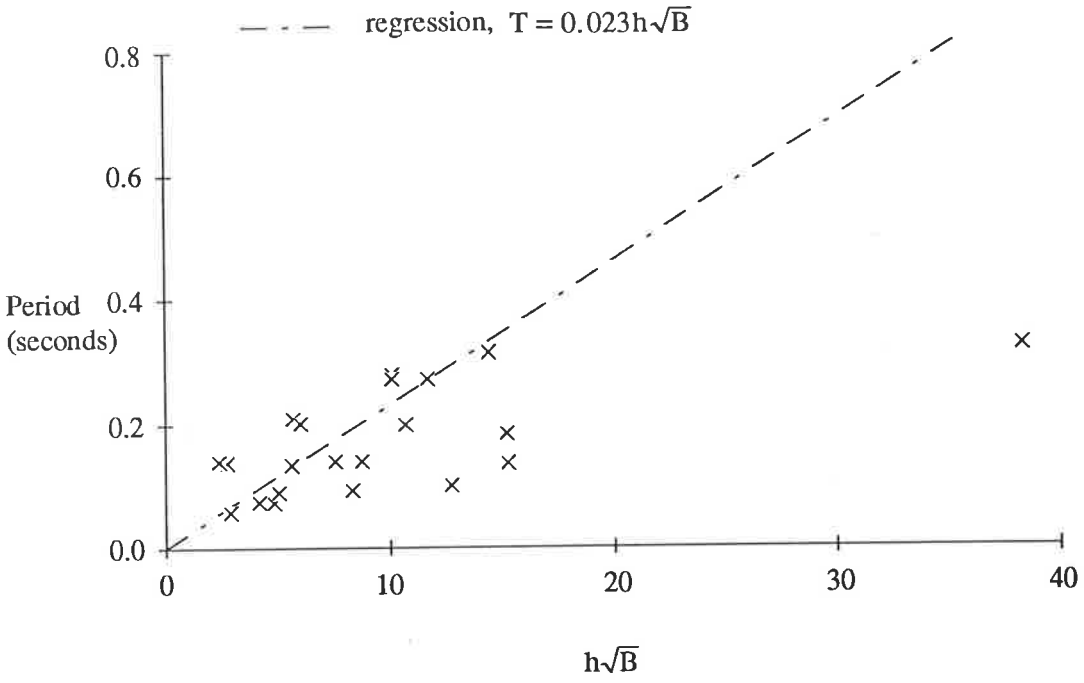


Figure 3.5.17 Plot of Period versus $h\sqrt{B}$ - All Data.

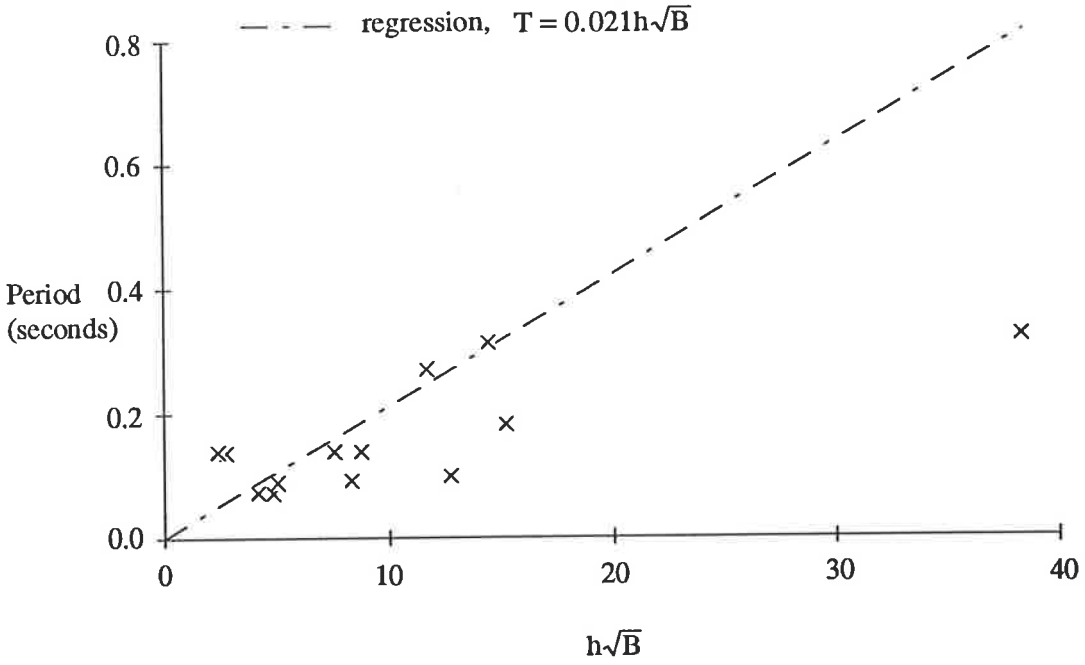


Figure 3.5.18 Plot of Period versus $h\sqrt{B}$ - Concrete Floor Systems.

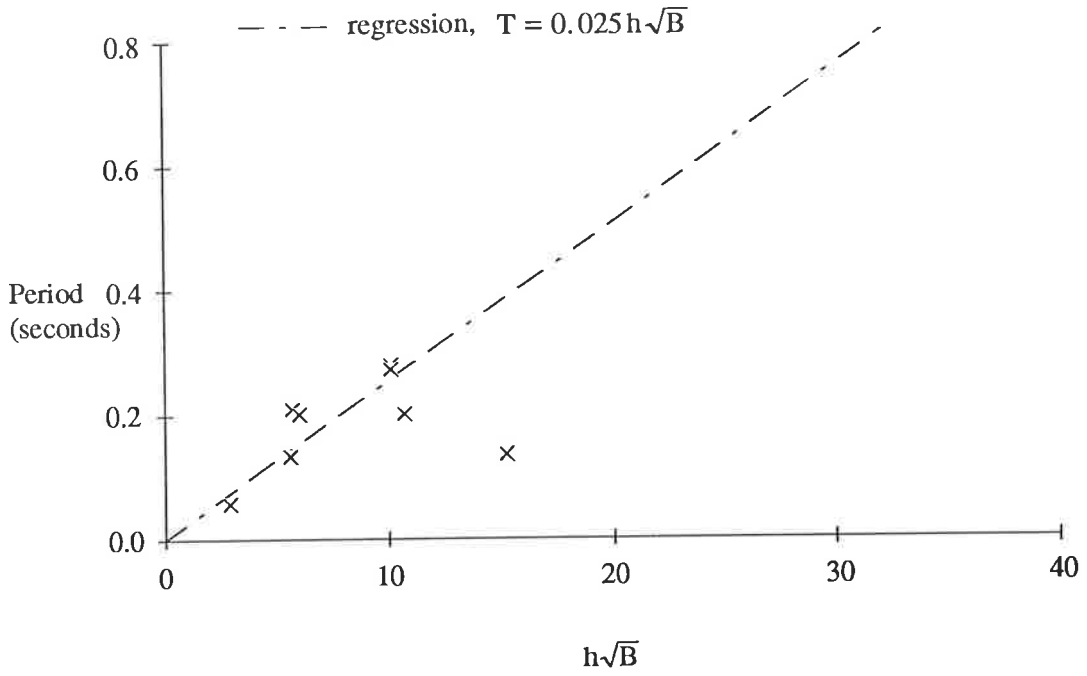


Figure 3.5.19 Plot Period versus $h\sqrt{B}$ - Timber Floor Systems.

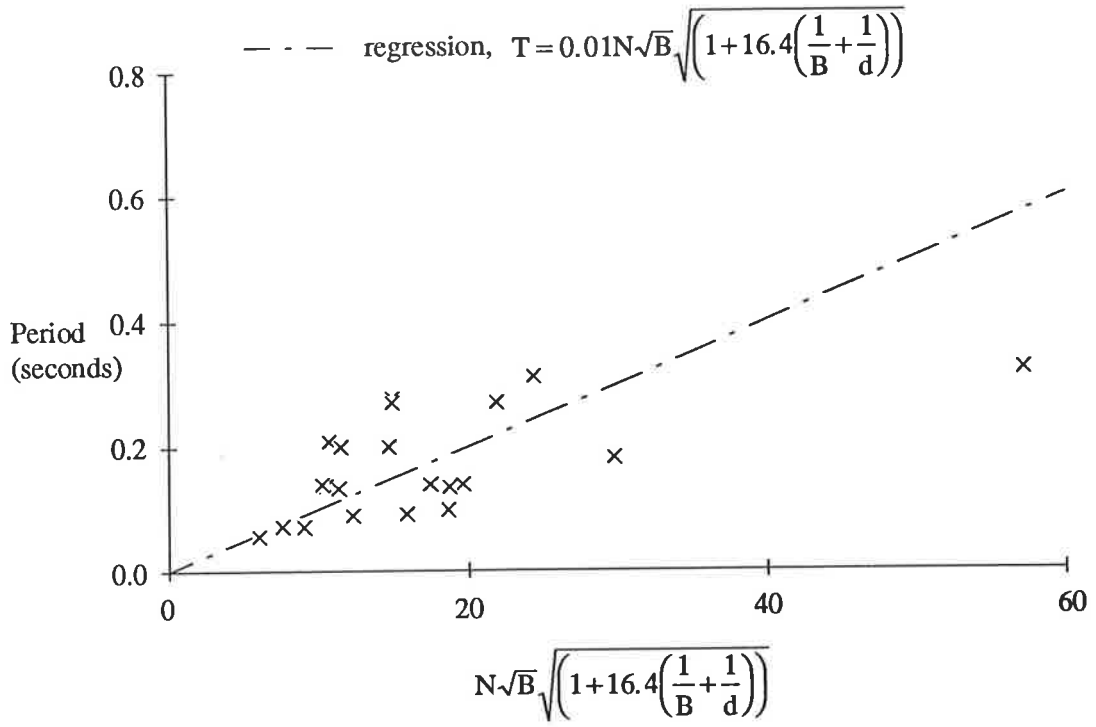


Figure 3.5.20 Plot of Period versus $N\sqrt{B}\sqrt{\left[1+16.4\left(\frac{1}{B}+\frac{1}{D}\right)\right]}$ - All Data.

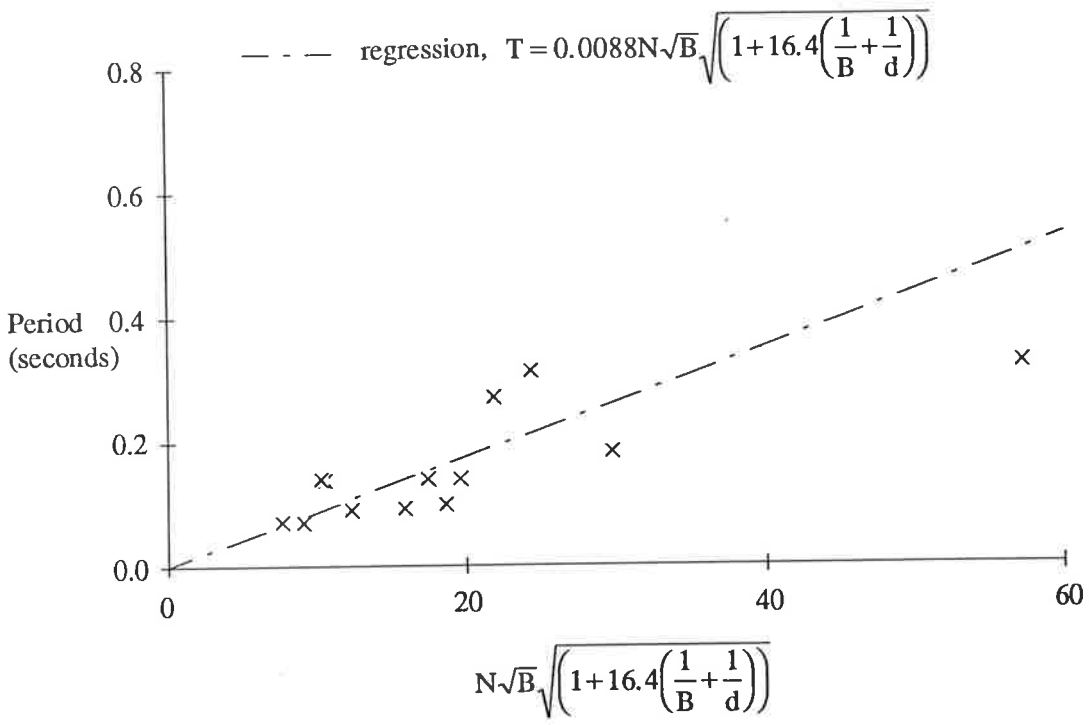


Figure 3.5.21 Plot of Period versus $N\sqrt{B}\sqrt{\left[1+16.4\left(\frac{1}{B}+\frac{1}{D}\right)\right]}$ - Concrete Floors.

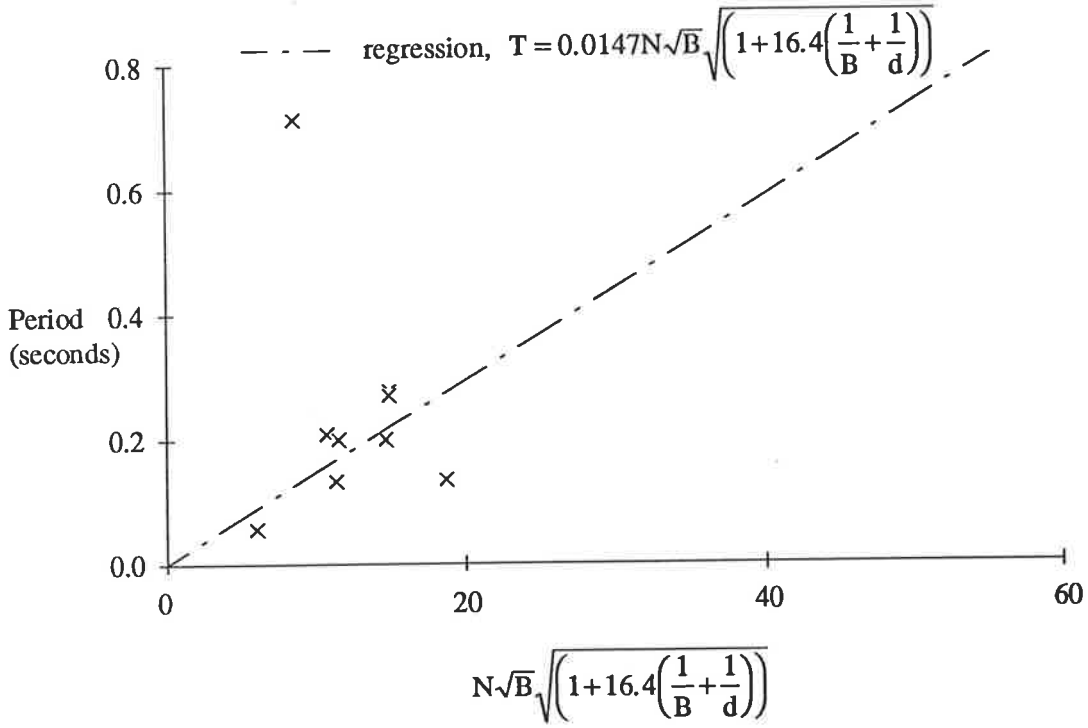


Figure 3.5.22 Plot of Period versus $N\sqrt{B}\sqrt{\left[1+16.4\left(\frac{1}{B}+\frac{1}{D}\right)\right]}$ - Timber Floor.

# 3.6 IMPLICATIONS

Examination of the fit of the forms of period formulae to the measured data ($R^2$) noted in Table 3.5.1 revealed that the form of equation:

$$T \propto h\sqrt{B} \tag{3.6.1}$$

had no fit to the data regardless of which of the three data sets was considered. This contrasts with the discussion in Section 3.4 where this form of equation was the expected form of period formula (Equation 3.4.5) for unreinforced masonry buildings.

The form of equation:

$$T \propto N\sqrt{B}\sqrt{\left[1+16.4\left(\frac{1}{B}+\frac{1}{D}\right)\right]} \tag{3.6.2}$$

also has poor fit to the data for the three sets of data. Both of these formulae (Equations 3.6.1 and 3.6.2) were, therefore, considered unsuitable for the estimation of the natural period of an unreinforced masonry building.

The five remaining forms of equation have very similar fit (54.2 percent to 49 percent) when all the data is considered. When considering only the data for the buildings with concrete floor systems, the five remaining forms of equation had improved fit to the data (55.2 percent to 72.2 percent) and three of the forms of equation stood out from the other two with significantly improved fit:

$$T \propto h^{3/4} \tag{3.6.3}$$

$$T \propto N \tag{3.6.4}$$

and

$$T \propto h \tag{3.6.5}$$

with fits of 72.2 percent, 67.7 percent, and 67.1 percent respectively.

Table 3.5.1 Details of Period Formulae Comparison

| Form of Formula | | Data Set | | |
|---|---|---|---|---|
| | | All Data | Concrete Floor | Timber Floor |
| $T = k\,h$ | Linear Regression Line | $k = 0.0227$ | $k = 0.0217$ | $k = 0.0244$ |
| | AS1170.4 Equation 2.1.1 | 52.5% | 50.0% | 60.0% |
| | AS1170.4 Equation 2.1.2 | 76.0% | 73.0% | 77.5% |
| | Japanese Equation 2.1.11 | 64.3% | 59.0% | 65.0% |
| | $R^2$ (ranking) | 53.1% (2) | 67.1% (3) | 9.1% (3) |
| $T = k\frac{h}{\sqrt{D}}$ | Linear Regression Line | $k = 0.079$ | $k = 0.082$ | $k = 0.075$ |
| | AS2121 Equation 2.1.3 | 34.5% | 55.2% | 51.3% |
| | $R^2$ (ranking) | 52.9% (3) | 55.2% (5) | 51.3% (1) |
| $T = k\,N$ | Linear Regression Line | $k = 0.079$ | $k = 0.068$ | $k = 0.097$ |
| | AS2121 Equation 2.1.4 | 23.0% | 8.5% | 46.9% |
| | Muria-Vila Equation 2.1.17 | 92.5% | 89.0% | 92.5% |
| | $R^2$ (ranking) | 49.0% (5) | 67.7% (2) | 3.4% (4) |
| $T = kh^{3/4}$ | Linear Regression Line | $k = 0.037$ | $k = 0.035$ | $k = 0.040$ |
| | UBC Equation 2.1.5 | 16.0% | 11.0% | 30.0% |
| | $R^2$ (ranking) | 54.2% (1) | 72.2% (1) | 1.4% (5) |
| $T = k\frac{1}{\sqrt{A_c}}h^{3/4}$ | Linear Regression Line | $k = 0.099$ | $k = 0.101$ | $k = 0.096$ |
| | UBC Equation 2.1.7 | 77.5% | 78.0% | 73.0% |
| | $R^2$ (ranking) | 51.2% (4) | 61.2% (4) | 18.9% (2) |
| $T = kh\sqrt{B}$ | Linear Regression Line | $k = 0.023$ | $k = 0.021$ | $k = 0.025$ |
| | $R^2$ (ranking) | 0.0% (7) | 0.0% (7) | 0.1% (6) |
| $T = kN\sqrt{B}\sqrt{\left[1+16.4\left(\frac{1}{B}+\frac{1}{D}\right)\right]}$ | Linear Regression Line | $k = 0.010$ | $k = 0.009$ | $k = 0.015$ |
| | $R^2$ (ranking) | 18.5% (6) | 28.1% (6) | 0.0% (7) |

In Section 3.4, the derivation of Equation 3.4.5 was taken further and it was determined that a reasonable form of equation for the estimation of the natural period of unreinforced masonry buildings would be an expression where the period was proportional to the building's height. Two of the best performed of the period formulae are for formulae where the period is proportional to the buildings height, or the number of storeys, which is generally related to the buildings height. However, the best performed of the forms of period formulae when all the buildings were considered, or when the data for the buildings with concrete floor systems were considered was a formula where the period is a function of the height only, but not directly proportional.

For the case of the buildings with timber floor systems, the fit of the data was worse than when either of the other two data sets were considered. The fits of all the forms of period formulae bar:

$$T \propto \frac{h}{\sqrt{D}} \tag{3.6.6}$$

were very low (all less than 20 percent). Equation 3.6.6 has the best fit for this data, by a large margin, of 51.3 percent.

It can be seen then that the two types of unreinforced masonry buildings, that is buildings with concrete floor systems and buildings with timber floor systems, have different requirements for a formula for the reliable estimation of the natural period. The concrete floor system buildings require a formula that has the period as a function of the building's height and the timber floor system buildings require a formula that has the period as a function of the building's height and its depth. Therefore, it could be necessary to split the buildings into two categories and provide two equations for the determination of the natural period.

Further examination of the performance of the various period formulae contained with the various earthquake codes reveals that, in general, the formula from AS1170.4, Equation 2.1.1, performs as well as any of the other equations considered. The formula corresponds to the linear regression line for the data from buildings with concrete floor systems and, as already discussed, has a high level of fit to the data. The period formula associated with Equation 3.6.3, that is Equation 2.1.5, only corresponds to the 11 percent confidence interval for the data, and is therefore unsuitable for use in design. The formula provided by Muria-Vila (1990), Equation 2.1.17, corresponds to the 89 percent confidence interval for the data.

It has already been discussed that the only form of period formula suitable, of those considered in this study, for use with unreinforced masonry buildings with timber floor systems is that shown in Equation 3.6.6. The formula from AS2121, Equation 2.1.3, corresponds closely to the linear regressed line for the data.

In summary, it can be seen that for unreinforced masonry buildings generally, and specifically unreinforced masonry buildings with concrete floor systems, the period formula provided with AS1170.4 provides a reasonable estimate of the natural period for use in earthquake design. Further, an examination of the measured periods from the buildings in the study and the design response spectrum from AS1170.4 (Figure 5.2.1) reveals that the periods for all but one of the buildings correspond to the constant acceleration region of the response spectrum and, as such, the estimate of the period becomes a moot point when calculating equivalent static force design approach earthquake loads in accordance with AS1170.4.

# 4 DYNAMIC TESTS ON BRICK PANELS

## 4.1 INTRODUCTION

One of the properties required for an accurate structural model, and generally not examined in detail in previous work, is the dynamic in-plane stiffness of unreinforced masonry walls. The in-plane stiffness is as defined in Figure 4.1.1. The dynamic stiffness depends upon:

(1) The geometrical layout and size of the components making up the structure; and
(2) The Youngs Modulus and Poisson's Ratio.

The geometrical properties are readily available for a given structure. However, the determination of material properties presents more of a challenge. As was explained in Sections 2.6 and 2.7, an equivalent modulus, or single phase model, for the brick and mortar unit can be used rather than using the respective moduli for the brick units and the mortar to create a model of an unreinforced masonry structure. It has already been seen in Section 2.5 that there is a large variation in the reported values for the Young's Modulus of brickwork and very few Young's Moduli from dynamic tests have been reported. In order to undertake the modelling of the unreinforced masonry structures in Chapter 5 it was decided to perform dynamic tests of unreinforced masonry wall panels to determine an appropriate Young's Modulus for the dynamic loading of Adelaide brickwork.

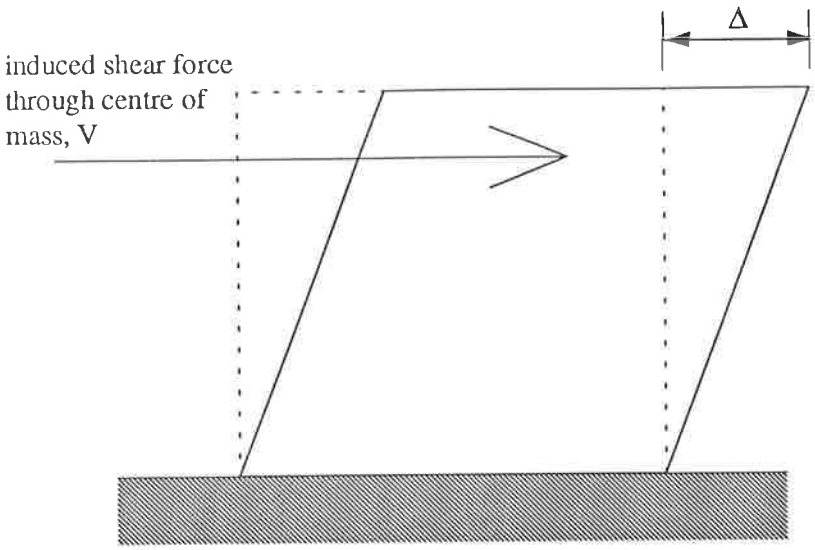


$V = k\Delta$

k = in-plane stiffness

Figure 4.1.1 Definition of Shear Stiffness.

# 4.2 DEVELOPMENT OF TESTING METHODOLOGY

The discussion of results of previous in-plane dynamic testing of unreinforced masonry panels in Section 2.3 highlighted three variables as critical to the stiffness of a wall panel:

(1) Axial compressive stress;
(2) Workmanship; and
(3) Rate of loading.

The dynamic testing undertaken as part of this research was required, therefore, not only to determine the in-plane stiffness of a masonry wall panel but also to study the influence of axial load and the rate of loading. It was also decided to vary the height of some specimens since the in-plane stiffness is also a function of the geometry of the panel tested.

One method to determine the in-plane stiffness of a masonry panel is by a static load test. This involves applying a monotonically increasing in-plane force to the top of the wall panel and measuring the corresponding panel displacements. The in-plane stiffness can then be determined from the load-deflection plot for this test. Mengi and McNiven (1989) and McNiven and Mengi (1989) noted, however, that the dynamic shear modulus was radically different from the static shear modulus (Section 2.3). As earthquakes induce dynamic loading in a structure, the dynamic modulus was required for a more accurate structural model. Hence, it was decided to conduct dynamic tests of masonry panels to establish appropriate dynamic in-plane stiffness values.

The dynamic tests were conducted on the earthquake simulator in The University of Adelaide's Structural Engineering Laboratory. This was considered to be the easiest way to apply dynamic in-plane loading to a masonry panel. This approach had the added advantage that it also more accurately modelled the true nature of earthquake induced forces.

### 4.2.1 Laboratory Test Set-up

The test configuration was chosen so that the masonry test panels were subjected only to in-plane shear, and allowed variable axial loads. Mengi and McNiven (1989) and McNiven and Mengi (1989) had already devised a test set up that achieved this, as shown in Figure 2.3.1. Hence, a similar arrangement was adopted for these tests.

The Adelaide test set-up is shown in Figure 4.2.1. The panel size was dictated by the size and capacity of the shaking table. The University of Adelaide's Structural Engineering Laboratory's shaking table consists of a 1400 mm by 2200 mm steel plate mounted on bearings on a concrete base. The plate is orientated such that a hydraulic actuator provides motion parallel to the plate's 1400 mm side. The actuator is controlled by an 200 kN INSTRON load/displacement hydraulic testing machine. The actuator can be controlled such that it applies a specified displacement (displacement control) or specified load (load control). The INSTRON control panel has pre-defined analog signals which are used to drive the hydraulic actuator with sinusoidal, pulse wave, square wave, static, or any arbitrary displacement or load pattern, such as an earthquake ground motion. The maximum vertical load capacity of the shaking table, as governed by the bearings, is 66 kN. The maximum horizontal displacement is $\pm 125$ mm.

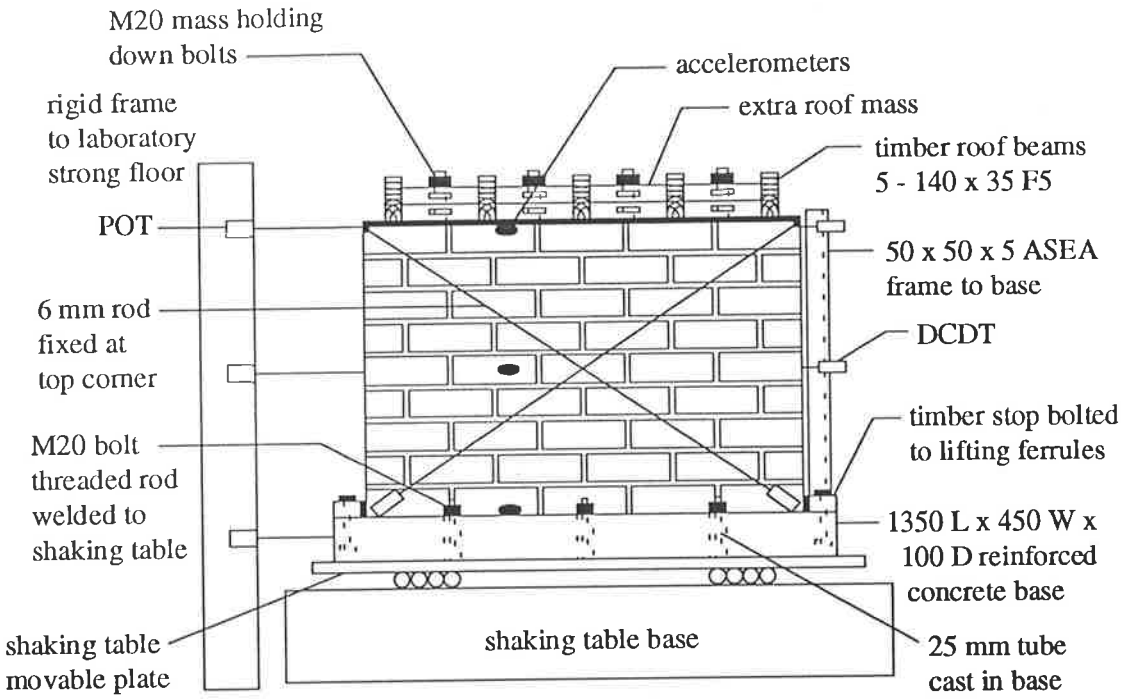


(a) side elevation

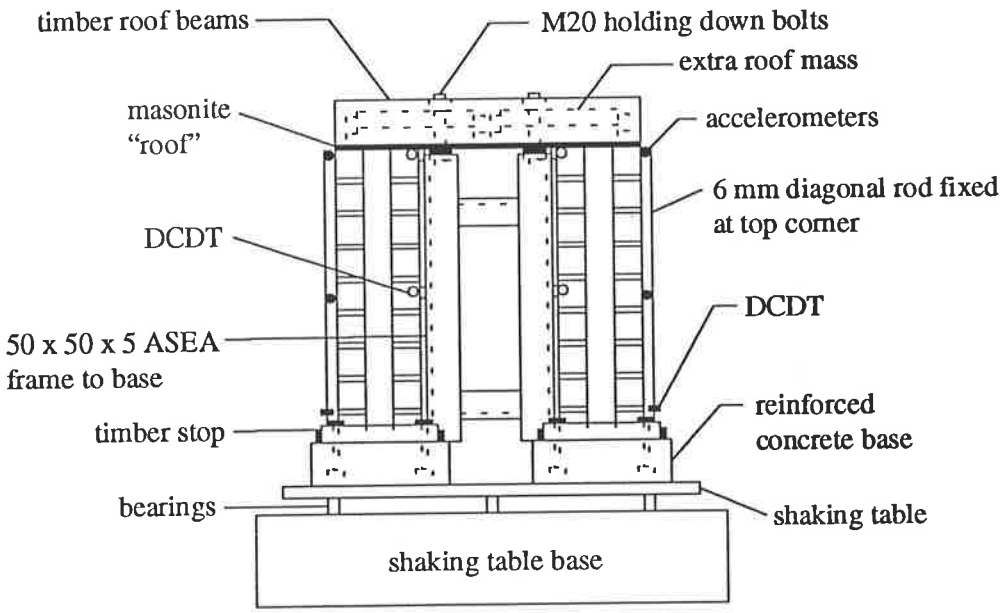


(b) end elevation

Figure 4.2.1 Shaking table test set up.

A roof structure was placed on top of the wall panels. It consisted of a 3 mm thick masonite sheet with four 100 mm deep x 35 mm wide timber "beams" evenly spaced across the walls. The roof structure was attached to the wall panels to prevent sliding by four M8 Ramset "Dynabolts" in each wall panel. The roof structure had a mass of 21.5 kg. Additional mass was placed on the roof structure to more accurately represent the axial stresses in a real wall (see Appendix D for the calculation of a realistic level of stress). The additional mass consisted of a number of 400 Newton steel weights. The weights were attached to the roof structure by M20 bolts.

To prevent sliding of the wall panels along the concrete bases a timber stop was attached to the end of the concrete bases and "dental paste" was placed between the stop and the wall panel.

### 4.2.2 Brick Masonry Panels

Single and double leaf specimens were tested as both types of construction are used in masonry buildings, double leaf on outside walls, and single leaf on internal walls. The original test specimens were 13 courses high and five bricks long (Figure 4.2.1 only shows the nine course specimen). For reasons given in Section 4.4, nine course high specimens were also tested. Full details of the test specimens are given in Section 4.3. The specimens were constructed individually on concrete bases that allowed the panels to be moved within the laboratory by gantry crane. The concrete bases were attached to the shaking table by six M20 holding down bolts. As adopted by Mengi and McNiven (1989), the panels were tested in pairs. Each pair of test panels were identical and symmetrically positioned on the table to minimise the amount of torsion induced in the specimen.

The panels were constructed from standard commercially available nominal 110 mm x 70 mm x 90 mm clay bricks purchased from an Adelaide brick manufacturing company that uses clay quarried in the Adelaide Hills. The bricks used were typical of those used in the Adelaide metropolitan area on a variety of building projects ranging from family homes to cladding on multi storey commercial buildings. The mortar used was a standard mix used in Adelaide and around Australia consisting of one part portland cement, one part lime, and six parts building sand as specified in the Australian Standard, "SAA Masonry Code" AS3700-1988. Sufficient water was added to ensure a workable mix. Brick ties were used on the double leaf specimens in accordance with AS3700 and typical practice.

The bricklaying and mixing of mortar was done by an experienced Adelaide bricklaying contractor in one week. It was stressed to the bricklayers that the workmanship was to be of the same standard as used in practice on a building site. Subsequently the mortar was batched using shovels and water was added until the bricklayer felt the mix was "right". While this lead to larger variations in the properties of the masonry than if a tight quality control had been imposed on the mixing of mortar and brick laying, it was decided to make the investigation on realistic examples of brickwork. Comparison of the quality of the brickwork construction of the laboratory test panels to that observed on building sites in Adelaide lead to the conclusion that the laboratory test panels were representative of the range of quality observed on site, and would be in the middle to upper part of the quality range, with respect to joint thickness, grooving of mortar, and consistency of the finished wall.

The panels were constructed in the structure's laboratory of the Civil and Environmental Engineering Department near the shaking table so as to limit the amount of handling prior to testing. The panels were cured in the laboratory for 35 days prior to testing and were subject to ambient temperature and humidity during curing. Prior to testing, the panels were painted white so that cracks could easily be identified. Sixteen reinforced concrete bases were built and a total of thirty-one wall panels were constructed in two batches. The initial series of panels were all double leaf and thirteen courses high. Subsequently, four courses were removed for the reasons outlined in Section 4.4. The final series of panels consisted of single and double leaf panels, nine courses high.

Brick and mortar specimens were tested to determine their individual properties. Randomly selected brick units were tested in a compression testing machine. The units were placed with a thin layer of dental paste on their top and bottom to provide a more even load distribution. The units were loaded and unloaded three times while the force-displacement relationship was recorded on a chart recorder. The displacement was measured using a Direct Current Differential Transducer (DCDT) and the force using a force transducer. The average Young's Modulus for the bricks was 1400 MPa, with values ranging from 766 MPa to 3065 MPa. The compressive strength was 43 MPa. Comparing the Young's Modulus determined here with the values published by other researchers (Section 2.5.5) it can be seen that the Young's Modulus determined here was substantially less than that given by other researchers.

Three mortar specimens were made while the walls were being constructed. The mortar specimens were made using standard 100 mm concrete cylinders. The mortar specimens were tested immediately after the wall tests were conducted using the standard procedure for determining the Young's Modulus for concrete. The average Young's Modulus for the mortar specimens was 1079 MPa, with values ranging from 840 MPa to 1680 MPa. Similar to the brick values, the Young's Modulus determined from the laboratory tests was significantly less than that published by other researchers (Section 2.5.5).

The final test conducted on the brick and mortar was to take a part of the failed walls and to subject them to a bond wrench test. The tests were conducted on random samples of brickwork from different panels. The average bond strength was 0.04 MPa with values ranging from 0.02 MPa to 0.07 MPa. Again, these values are less than those published by other researchers (Section 2.5.2). It can be concluded that the brickwork used in these tests had properties significantly different to brickwork used overseas and in other parts of Australia.

### 4.2.3 Instrumentation

In order to determine the in-plane stiffness of the panels it was necessary to measure the displacement of the top of the panel relative to the base. Recall that the definition of in-plane stiffness adopted for this study uses the total base shear divided by the top displacement relative to the base (Figure 4.1.1). To measure the relative displacements Linear Voltage Displacement Potentiometers (POTs) were attached to a rigid frame connected to the laboratory floor and were mounted to the frame in line with the top and mid height of each of the wall panels. A fifth POT was mounted on the frame in line with the shaking table to measure its displacement relative to the laboratory floor. The difference between the displacements of the top POTs and the shaking table displacement was the displacement of the wall panel relative to its base. The POTs were Honston Scientific model 1850-050 types with a maximum displacement of 500 mm. The POTs were powered by a 10 volt DC power supply unit and the output was a voltage.

The main difficulty with this method was the relatively low level of relative displacement expected in the walls. Using the results of Mengi and McNiven (1989) and McNiven and Mengi (1989) as a guide to the in-plane stiffness of a panel, it was estimated that the expected relative displacement at the top of the panel was 0.12 mm for a 0.5g acceleration. This was less than 0.02 % of the maximum absolute

displacement of the POTs. The ability of the POTs to measure this small level of displacement was questionable (A comparison of the results of Mengi and McNiven (1989), and McNiven and Mengi (1989) to this study was undertaken in Appendix E). To overcome this problem a second rigid frame was attached directly to the reinforced concrete bases that the walls were constructed on. This rigid frame moved with the shaking table so that there was no relative displacement between the frame and the shaking table. Attached to this frame were four Direct Current Differential Transducers (DCDTs) which measured the top and mid height wall displacements relative to the base for both wall panels. The DCDTs were $\pm 10$ mm and $\pm 5$ mm Sangamo Schlumberger models and used the same 10 volt power supply as the POTs.

The in-plane shear distortion of the panels was also measured using 6 mm diameter steel rod positioned diagonally on each wall panel, the rods were fixed at the top corners of both panels. Guides were placed along the length of the diagonal of the wall panels with the rod free to move in the guides. At the opposite corner of the panels DCDTs were mounted to measure the in-plane distortion as the rod moved with the top of the wall.

Finally, horizontal acceleration at the top and mid height of the wall panels, and the horizontal acceleration of the shaking table were measured using Kistler Servo-Accelerometers model 305A. In later tests, an accelerometer was also placed on the reinforced concrete base to measure the acceleration in the vertical direction to ensure the table was not rocking on the bearings when the panels started to rock. The accelerometers were powered by a servo amplifier and the output was low pass filtered with a Butterworth filter of 20 Hertz in order to ensure compliance with the Sampling Theorem (Appendix A).

The instruments were calibrated before and after the first series of tests and before and after the second series of tests. No changes were observed in any of the calibration factors.

The voltage outputs from the instruments were recorded using the Civil and Environmental Engineering Department's Real Time Unix Masscomp computer. The computer has an inbuilt analogue to digital converter so the output from the instruments could be fed directly to the computer's input channels. "Labworkbench", the computer package discussed in Chapter 3 with respect to data processing, was also used here, to sample the data. The data was sampled at 100 Hertz and 2048

points for each channel were collected. It was found from previous work that 2048 points was the optimum amount of data for Fourier Transformation. To facilitate post processing, the data was transferred to the "DADiSP" program on an IBM compatible personnel computer. "DADiSP" was used to apply calibration factors to the data and any other processing required. The data from "Labworkbench" was transferred to a personnel computer as text files using an ethernet card and were read directly into the "DADiSP" program after writing a standard input heading file.

"DADiSP" used a system of workbooks to display and process data. A workbook consisted of a number of windows each containing a data set. Each data set was manipulated by performing functions on its window or a series of windows, similar to a spreadsheet. A default workbook was written to receive the data from a test and to calibrate it. The data was then plotted on a laser printer.

# 4.3 TESTING PROGRAM

As explained in Section 4.2.2, the walls were constructed in two series of sixteen panels. This meant eight tests per series. However, one of the first series of panels was damaged while being placed on the simulator and only seven tests were conducted during the first test series. Test pairs numbered one to seven comprised the first series of tests and test pairs numbered eight to fifteen comprised the second test series. The panels were tested by moving the shaking table horizontally in a sinusoidal fashion such that the base motion could be described by the equation:

$$u_g(t) = A \sin(2\pi ft) \qquad (4.3.1)$$

The frequency (f) of the base motion was varied from panel to panel. The amplitude (A) of base motion was first applied at a low level and subsequently increased until failure occurred in the panel. Details of the testing program are shown in Table 4.3.1. The sine wave frequency (f) refers to the frequency of the sinusoidal displacement of the shaking table. The superimposed load is the weight of the extra mass placed on the roof.

Table 4.3.1 Shaking Table Test Program.

| Wall Test Pair Number | Number of Courses | Double or Single Leaf (D/S) | Superimposed Load (kN) | Sine Wave Frequency (f) (Hertz) |
|---|---|---|---|---|
| 1 | 13 | D | 4.8 | 1.0 |
| 2 | 13 | D | 4.8 | 2.0 |
| 3 | 13 | D | 4.8 | 1.0 |
| 4 | 9 | D | 4.8 | 1.0 |
| 5 | 9 | D | 4.8 | 2.0 |
| 6 | 9 | D | 4.8 | 5.0 |
| 7 | 9 | D | 4.8 | 0.625 |
| 8 | 9 | D | 4.8 | 1.0 |
| 9 | 9 | S | 2.4 | 0.625 |
| 10 | 9 | S | 2.4 | 1.0 |
| 11 | 9 | S | 2.4 | 2.0 |
| 12 | 9 | S | 2.4 | 5.0 |
| 13 | 9 | S | 6.4 | 1.0 |
| 14 | 9 | D | 0 | 1.0 |
| 15 | 9 | D | 6.4 | 1.0 |

# 4.4 RESULTS

The first test panel was tested and found to fail by rocking. Rocking was defined as a vertical tensile failure of the panel in the mortar-brick interface at the first mortar course level or at the mortar-concrete base interface (Figure 4.4.1). This type of tensile failure occurred at both ends of the panel and moved inward as the shaking of the base continued. After experiencing this failure, the panel began to rock as a rigid body about its base.

After the first panel failed in this manner it was thought that the failure may have been caused by the panel overturning. However, subsequent calculations of the overturning moment and resistance to overturning indicated that uplift should not occur (see Appendix F). Prior to the onset of rocking the panel was subjected to a sinusoidal base displacements of A = ±11 mm, 19 mm, 34 mm, 49 mm, and 65 mm. Rocking commenced at A = ±70 mm. The test was continued after the onset of

rocking but this data did not give a measure of the in-plane stiffness and was subsequently discarded from the data set. In addition, some of the initial tests had very small relative displacement of the walls. If the values in the data were below the resolution of the instrumentation the results were not used for the calculation of the dynamic in-plane stiffness. In order to calculate the in-plane stiffness it was first necessary to calculate the induced shear force. This calculation was based upon the measured accelerations at base, mid, and full height levels of the wall. Figure 4.4.2 shows the shear force (V) plotted against the top wall displacement (Δ) for test panel number 1.

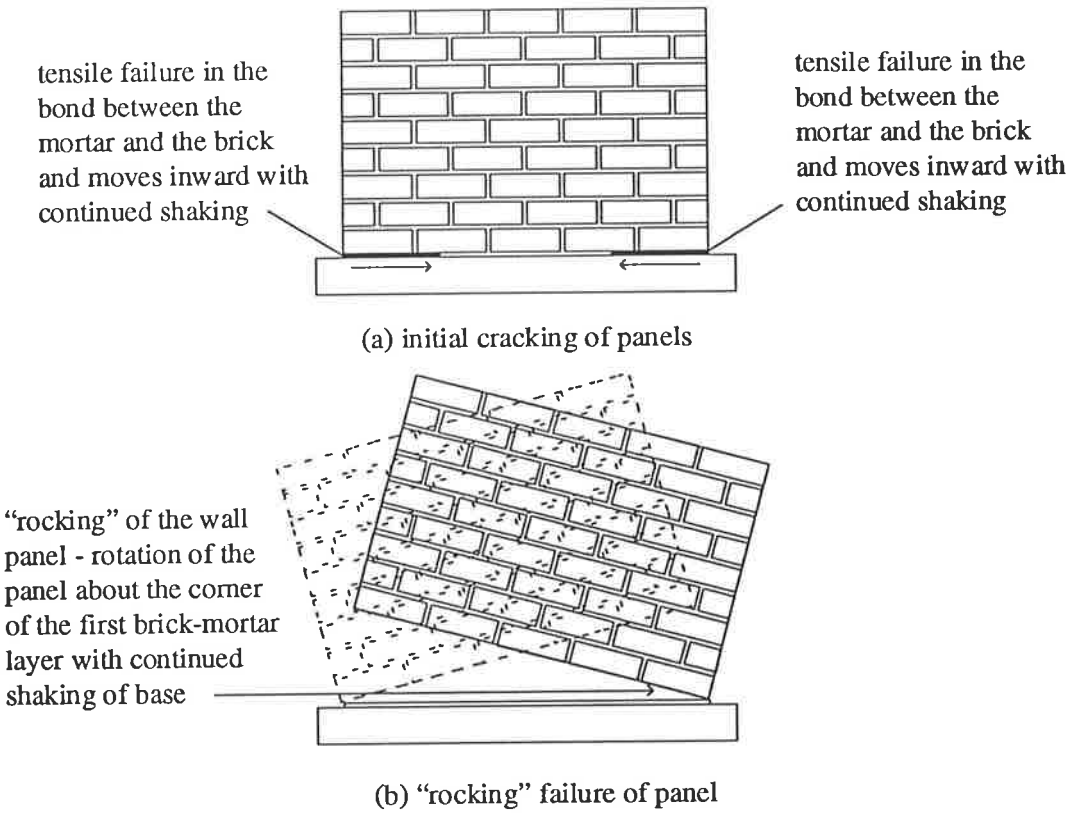


Figure 4.4.1 Tensile failure and rocking of wall panels.

While undertaking the first test it was noted that manual control of the amplitude of base displacement to which the model was subjected was difficult. The 'coarseness' of the displacement control for the shaking table made small changes in the table displacement difficult to achieve. This problem was expected to be magnified when dealing with the panels to be tested at a higher frequency.

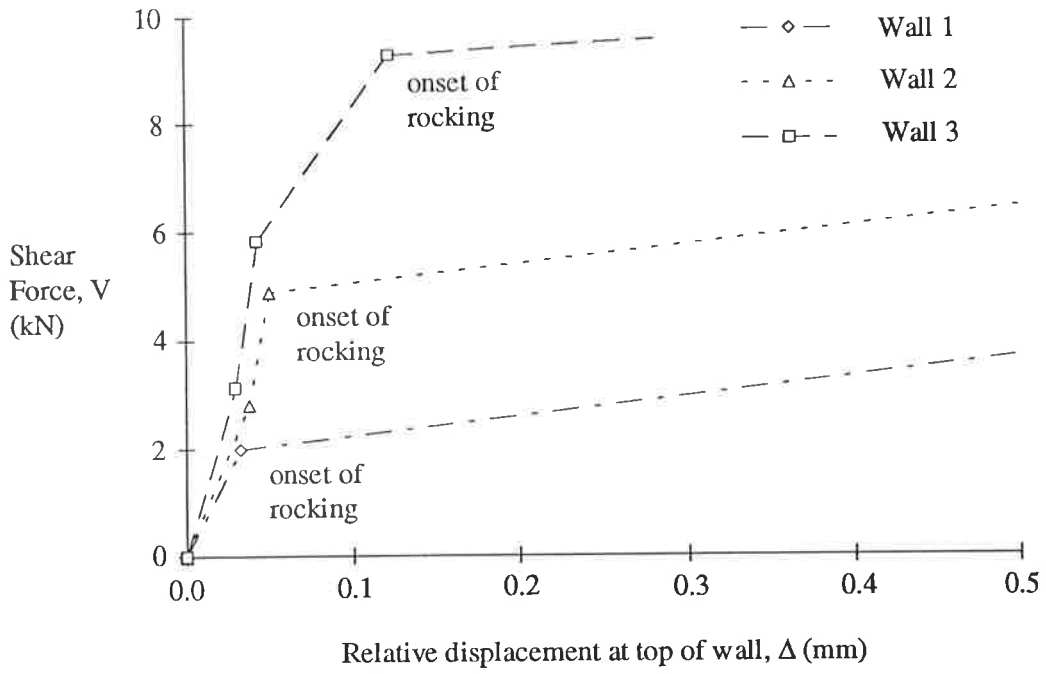


Figure 4.4.2 Induced shear force versus in-plane displacement - Walls 1, 2 and 3.

The second panel was tested using the same set-up as the first panel but subjected to a higher frequency base motion. The adverse effect in the ability to control the table manually of the increased frequency was confirmed when the panel was only able to be subjected to two base displacements, A = ±12 mm and ±21 mm, prior to the onset of rocking. Rocking commenced at A = ±30 mm. Figure 4.4.2 shows the induced shear force plotted against the top relative displacement for wall panel number 2.

It was decided for the third panel to try to prevent the onset of rocking to gather more stiffness data. The test used similar parameters to the first panel. Holes were drilled through the bottom course of both leaves of the panels at each end. Steel rods were placed through the holes and grouted in place. The rods were then fixed to the concrete bases using a timber bracket. A test was then conducted to determine the onset of rocking. It was found that rocking started at A = ±80 mm, 10 mm more than for the first panel. This increase was small and the rods were not used on the later panels. The induced shear force versus the in-plane displacement in the panel for this wall is also shown in Figure 4.4.2.

Another method to prevent the onset of rocking was tried with the fourth panel. In this test, the top four courses of the panel were removed. The aim was to lower the centre of mass of the panel to reduce the tensile force induced in the edges of the panel from the horizontal inertia force. This panel was also tested using the same parameters as the first and third panels. Prior to the onset of rocking this panel was subject to sinusoidal displacements varying between A = ±20 mm and 80 mm. Rocking commenced at A = ±83 mm. It was then decided to remove the top four courses of the remaining five pairs of walls from the first constructed batch and to have the second batch constructed to nine instead of thirteen courses. The induced shear force plotted against the panel's in-plane displacement is shown in Figure 4.4.3.

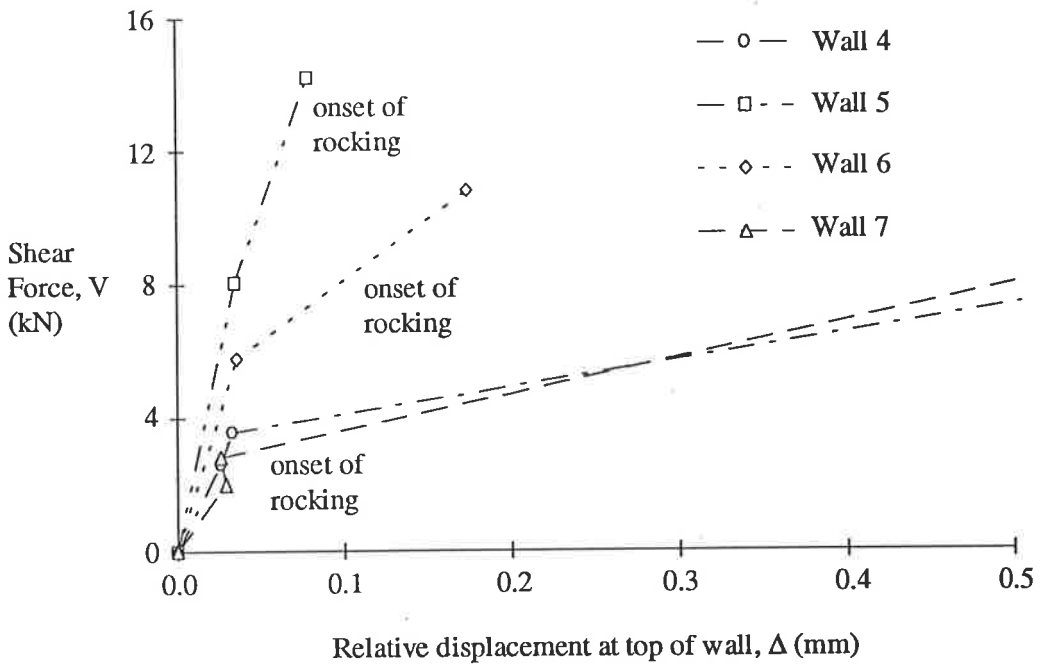


Figure 4.4.3 Induced shear force versus in-plane displacement - Walls 4, 5, 6 and 7.

Panels five to seven were then tested using the parameters as described in Table 4.3.1. All of the panels failed by rocking. The second batch of panels was then tested and again all of the panels failed by rocking. The induced shear force plotted against the top relative displacement for panels five to fifteen are given in Figures 4.4.3 to 4.4.5.

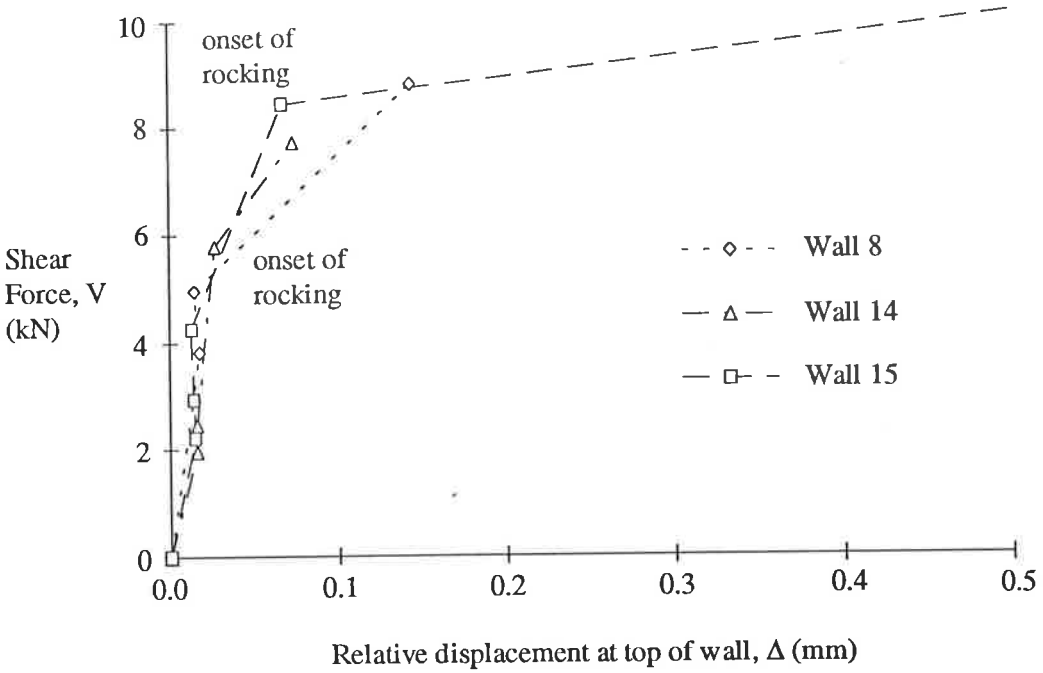


Figure 4.4.4 Induced shear force versus in-plane displacement - Walls 8, 14 and 15.

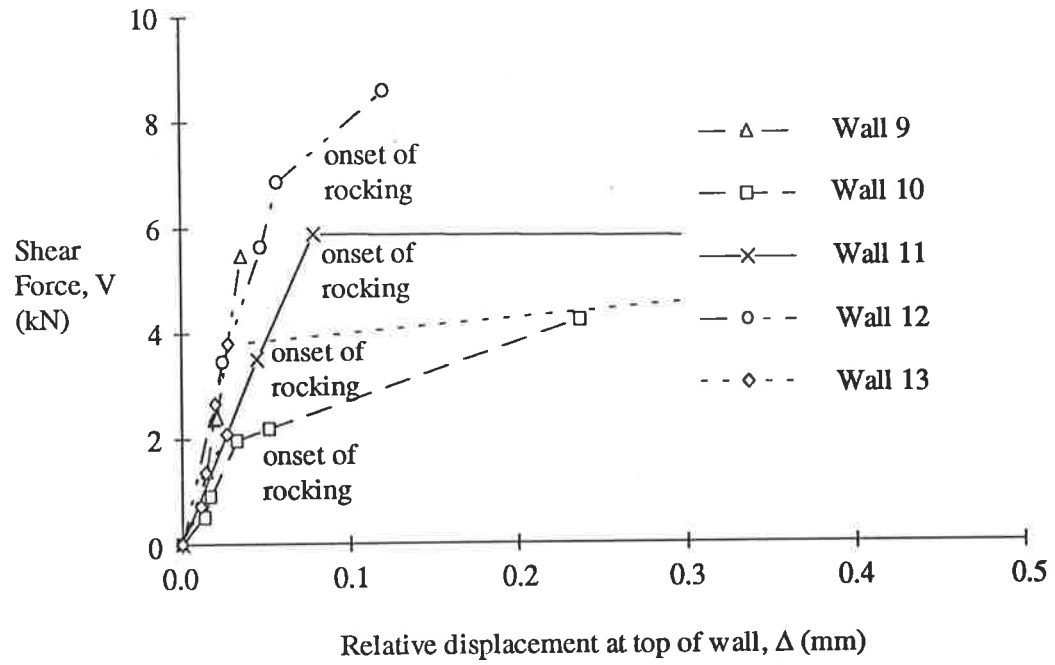


Figure 4.4.5 Induced shear force versus in-plane displacement- Walls 9, 10, 11, 12 and 13.

# 4.5 DISCUSSION OF RESULTS

As noted in Section 4.1, the tests were conducted in order to determine the dynamic in-plane stiffness for unreinforced masonry wall sections. The measured in-plane stiffness values are listed in Table 4.5.1 and were calculated from the induced shear force and in-plane displacement data given in Figures 4.4.2 to 4.4.5 using the regression analysis technique as defined in Appendix C for fitting a curve that passes through the origin. The definition of in-plane stiffness used was that shown in Figure 4.1.1. Also listed in Table 4.5.1 was the ratio of induced shear force to the panel weight at the onset of rocking for each panel. The values in Table 4.5.1 are for one panel of the pair of panels tested. That is, for the double leaf tests the stiffness is for two leafs of brickwork and for the single leaf tests the stiffness is for one leaf of brickwork.

Table 4.5.1 Calculated in-plane stiffness from laboratory tests.

| Wall Test Pair Number | Axial Stress (MPa) | Shear Stiffness, k (kN/m) | Ratio of Induced Shear Force to Panel Weight at rocking |
|---|---|---|---|
| 1 | 0.032 | 61,500 | 0.651 |
| 2 | 0.032 | 44,600 | 0.861 |
| 3 | 0.032 | 30,150 | 0.689 |
| 4 | 0.026 | 52,400 | 0.868 |
| 5 | 0.026 | 102,400 | 1.256 |
| 6 | 0.026 | 80,250 | 0.947 |
| 7 | 0.026 | 54,100 | 0.735 |
| 8 | 0.026 | 149,600 | 0.771 |
| 9 | 0.026 | 68,400 | 0.944 |
| 10 | 0.026 | 28,250 | 0.377 |
| 11 | 0.026 | 37,650 | 1.001 |
| 12 | 0.026 | 59,900 | 1.475 |
| 13 | 0.044 | 62,200 | 0.719 |
| 14 | 0.015 | 99,350 | 1.168 |
| 15 | 0.029 | 163,300 | 0.648 |

It can be seen from Table 4.5.1 that the measured in-plane stiffness values vary over a large range. This is most evident in the comparison of Wall 4 to Wall 8, a control specimen included in the second batch for which the test parameters were the same. Wall 8 had almost three times the in-plane stiffness of Wall 4. This variability was attributed to a combination of workmanship and material variability. The variability in the properties of the brick units and mortar was noted previously in Section 4.2.2.

The first of the parameters noted in Section 4.2 to be examined were the frequency of excitation and the effect of single and double leaf. The axial stress was kept constant for the comparison at 0.026 MPa. The comparison is summarised by the data in Table 4.5.2.

Table 4.5.2 Comparison of Frequency of Excitation and Single or Double Leaf on Shear Stiffness.

| Frequency of Excitation (Hertz) | Single Leaf Shear Stiffness (kN/m) | Double Leaf Shear Stiffness (kN/m) | Ratio of Single to Double Stiffness |
|---|---|---|---|
| 0.625 | 68,400 | 54,100 | 1.26 |
| 1 | 28,250 | 52,400 & 149,600 | 0.54 & 0.19 |
| 2 | 37,650 | 102,400 | 0.37 |
| 5 | 59,900 | 80,250 | 0.75 |
| Average | 48,550 | 87,750 | 0.55 |

It was expected that the in-plane stiffness of the double leaf walls would be twice that of the single leaf walls as the in-plane stiffness was assumed to be proportional to the wall's cross sectional area for shear type deformation and proportional to the width of the wall for bending type deformation. The average values of the in-plane stiffness seemed to show this. The ratio of 0.55 was very close to the expected value of 0.5, especially considering the variability in materials and workmanship already discussed. The individual ratios vary considerably, but this was not surprising considering the variability in panel properties. As only one panel of each type was tested, individual comparisons were dangerous. This was best illustrated by the comparison of results at 0.625 Hertz, where the single leaf wall was stiffer than the double leaf wall. What was important, however, was that the overall trend of in-plane stiffness follows the expected pattern of twice the in-plane stiffness for a double brick panel compared with a single brick panel.

The effect of the excitation frequency on the in-plane stiffness was more difficult to determine because of the variability in materials and workmanship. It has already been noted that the in-plane stiffness of the 0.625 Hertz specimens were inconsistent with the expectation that a double leaf specimen would be twice as stiff as a single leaf specimen. Whether the single leaf specimen was at the upper limits of the possible range of in-plane stiffness, or the double leaf specimen was at the lower limits, or a combination of both is difficult to determine. If the data from the 0.625 Hertz test is momentarily ignored, the single leaf specimens suggested a trend of increasing in-plane stiffness with increasing frequency of excitation. However, inclusion of the 0.625 Hertz data meant this trend could have been a result of the variability of the materials and workmanship. Examination of the data for the double leaf specimens also did not lead to a definite conclusion. Careful selection of the data for the double leaf specimens could have in fact resulted in the conclusion that there was a trend of decreasing in-plane stiffness with increasing excitation frequency. Therefore, the only conclusion that could be reached, based on the test data, was that there was no clear trend in the effect of the excitation frequency on the in-plane stiffness in the range of testing frequencies, 0.625 to 5 Hertz. To establish definite statistically valid trends, a much larger number of test specimens would be required.

The third variable considered was the level of axial stress in the walls. The axial stress was varied for a set of specimens tested with an excitation frequency of 1 Hertz. It was expected that the specimens would show a trend of increasing stiffness with increasing axial stress as was noted by other researchers (Section 2.3). There were two results for the double leaf specimens tested with an axial stress of 0.026 MPa. Firstly, using the result from the panel with the higher stiffness (149,600 kN/m) and comparing with the results from the other panels with the same excitation frequency and geometry there was a trend of increasing in-plane stiffness with increasing axial stress levels. If, however, the other panel tested with 0.026 MPa axial stress was used in the comparison the trend was no longer observable. Again, the variability of the materials and workmanship seemed to mask any trends in the relationship between axial stress and in-plane stiffness.

The final parameter checked was the specimen panel height. The first three panels were, as already noted in Table 4.3.1, thirteen courses high and the rest of the test specimens were nine courses high. If the walls were acting as a simple cantilever shear beam it would be expected that the stiffness values were inversely proportional to the panel heights and in this case that would mean the thirteen course panels would have lower values of stiffness than the nine course panels, in the ratio of nine

to thirteen, 0.69. Comparing the thirteen course panels to the nine course panels tested with excitation frequencies of 1 and 2 Hertz, it was seen that there was no observable trend in the stiffness of the panels. It would seem that any trend is masked by the variability in the materials and workmanship.

In summary, it would appear the main parameter affecting the dynamic in-plane stiffness of unreinforced masonry wall panels was material and workmanship variability. This variability and its effect on the properties and behaviour of unreinforced masonry has been recognised by many previous researchers as noted in Chapter 2. The effects of material and workmanship variability masked the effects of other parameters. From the tests conducted as part of this research the expected trend of a double leaf wall having double the stiffness of a single leaf wall was confirmed and the trend of increasing stiffness for increasing axial stress was partially observed. Any trends in in-plane stiffness with panel height and excitation frequency could not be identified from these tests. Further testing, with a larger number of panels, is required to ascertain these trends. The main objective, however, of this testing was to determine the in-plane stiffness of the wall panels for latter use with a mathematical model of masonry walls and this was accomplished.

## 4.6 DETERMINATION OF AN EFFECTIVE YOUNG'S MODULUS

In order to determine the effective Young's Modulus of brickwork to be used in the later modelling of unreinforced masonry buildings, the shaking table test results were used to calibrate a mathematical model of the laboratory wall specimens. A single leaf laboratory wall specimen was modelled using the IMAGES3D finite element program. The geometrical parameters and material densities were all based on data obtained from the laboratory test specimens. An in-plane load was applied through the centre of mass of the wall panel (including the roof mass). The combined brickwork material was assumed to have a Poisson's Ratio of 0.2 and the Young's Modulus was varied until the in-plane stiffness of the model of the laboratory wall panel matched the range of in-plane stiffness values determined from the shaking table tests (7,538 to 40,825 kN/m for a single leaf of wall).

Three different finite element grids were used to determine the sensitivity of the model to the number of elements. As the walls were rectangular, the chosen grids consisted of rectangular elements having the same number of elements vertically and

horizontally. Grids of 1 x 1, 4 x 4, and 16 x 16 elements were used. The 1 x 1 grid did not allow for the load to be applied at the centre of mass which was calculated to be 540 mm from the bottom of the nine course (760 mm high) panels for 12 x 400 N superimposed roof load. This centre of mass was close to 75% of the total height and on the 4 x 4 and 16 x 16 grids the horizontal load was applied to the nodes along the line representing 75% of the panel height, that is the 4th row of nodes for the 4 x 4 grid and the 13th row of nodes for the 16 x 16 grid. The 4 x 4 grid model was also tested with the horizontal load applied at the top of the panel for comparison to the 1 x 1 grid. The models are shown in Figure 4.6.1.

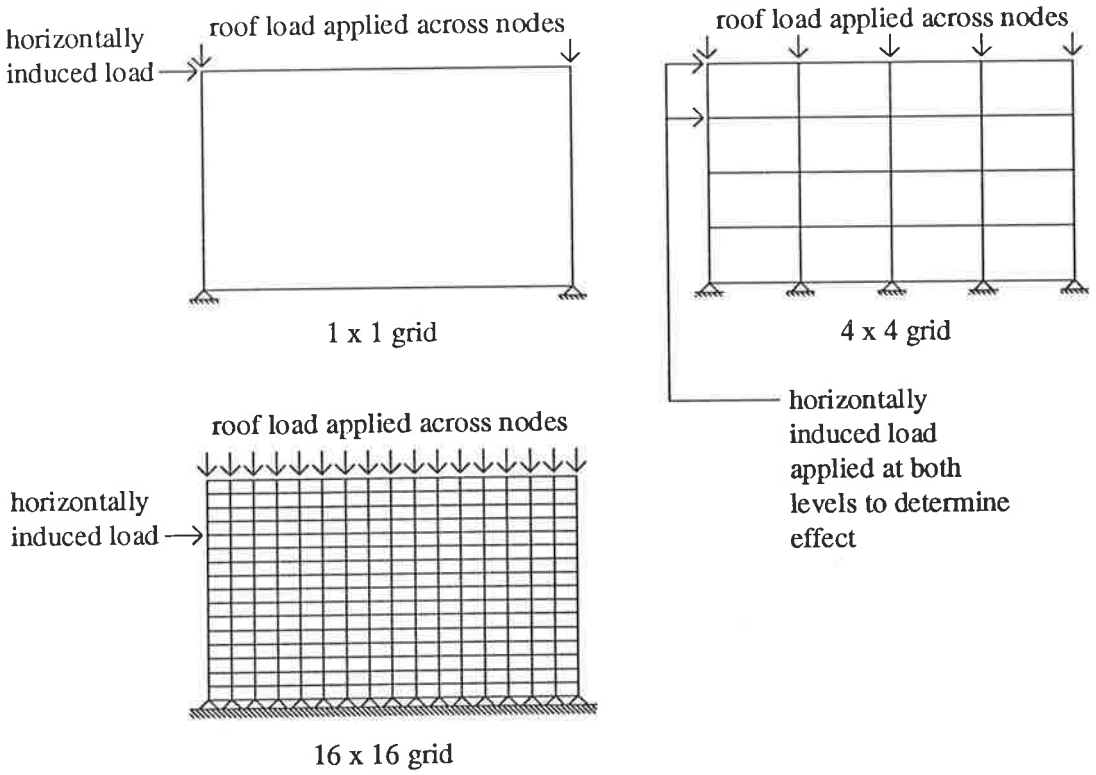


Figure 4.6.1 Mathematical models of the test specimens.

It was decided to load the panel with the load induced in wall panel 4 just prior to the onset of rocking, 3550 N. The 3,550 Newton load was resisted by four single leafs so that the load applied to the model panels was 890 N.

The first modelling parameter to be studied was the number elements used in the grid. This was carried out by comparing the results of analyses for the three models with a constant Young's Modulus. The comparison is shown in Figure 4.6.2. It can

be seen that the number of elements had little influence on the in-plane stiffness. Considering a Young's Modulus of 2,000 MPa it can be seen the difference in in-plane stiffness between the three models was 6,800 kN/m which is less than the influence of the workmanship and material variability and could be considered to be insignificant from a practical point of view. A 4x4 element grid was used for all subsequent models.

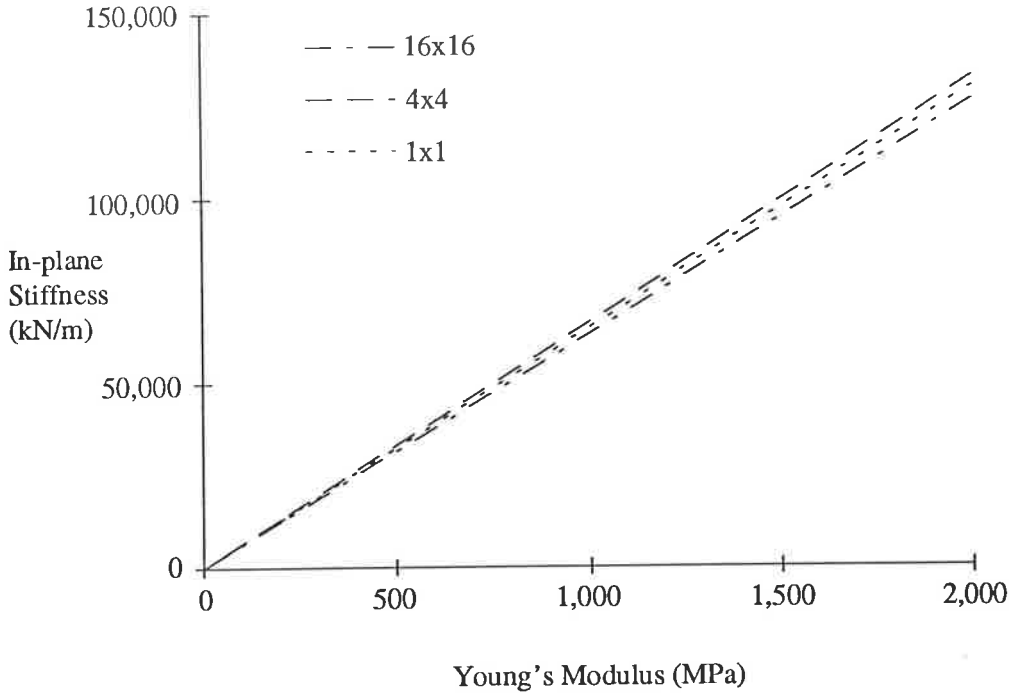


Figure 4.6.2 Comparison of Number of Elements.

The 4x4 model was used to determine the sensitivity of the results to the position of the applied horizontal load. The load was applied first at the top of the wall and then at 75 percent of the wall's height, corresponding to the centre of mass. The load was applied at the top in one case to permit direct comparison of the results to those from the 1x1 model which, by necessity, was constrained to have its horizontal load applied at the top of the wall. It was noted that the in-plane stiffness values determined from the top loaded model varied significantly from those determined from the centre of mass loaded model. Hence, care was taken in all subsequent modelling to ensure that the inertia forces would be concentrated at nodes very near to the centre of mass.

The 4x4 model was then used to study the sensitivity of the results to values for Young's Modulus. The results of these analyses are given in Figure 4.6.3. The measured values of in-plane stiffness, given in Table 4.5.1, for the double leaf specimens were divided by two to give an estimate of the in-plane stiffness for a single leaf wall. It can be seen that for the measured values of the in-plane stiffness, the corresponding values of Young's Modulus were 220 to 1250 MPa. These values were then used in mathematical models of real buildings as an effective Young's Modulus for the composite brick and mortar material.

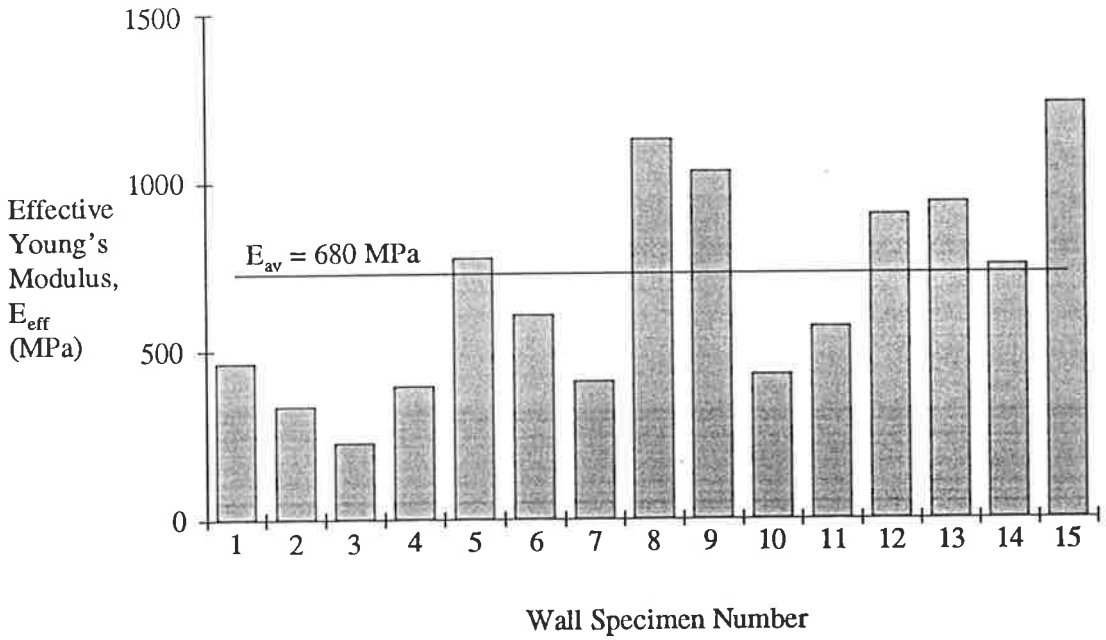


Figure 4.6.3 Effective Young's Modulus for wall specimens.

# 4.7 SUMMARY OF LABORATORY TESTS

From the laboratory tests conducted as part of this research it was seen that the in-plane stiffness and the Young's Modulus of an unreinforced brick masonry wall vary considerably with workmanship and material variability. The variation of these properties due to workmanship and materials tends to mask any relationship between the frequency of excitation, axial stress level, and wall height with the in-plane stiffness. Only the expected relationship between the number of leafs and the in-plane

stiffness could be confirmed from the tests. In order to ascertain any relationships between the frequency of excitation, axial stress level, and wall height a large number of tests would need to be conducted and average results used to minimise the effects of workmanship and material variability.

The results from the laboratory tests were used to calibrate a mathematical model which relates the range of values for in-plane stiffness to a range of values for an effective Young's Modulus for a combined brick and mortar material.

The range of values determined for the brickwork Young's Modulus, 220 to 1250 MPa, are of the order expected for brickwork based upon some of the work reported in Section 2.5.5, for example Arya (1980), Jankulovski et al (1994), Priestley (1985), San Bartolome et al (1992), and Calvi et al (1994). It should be noted, however, that there was no consensus between other researchers who have conducted tests on unreinforced masonry walls as to an effective Young's Modulus and as many researchers whose results agree with the order of magnitude of Young's Modulus determined from these tests disagree and suggest and/or measure a Young's Modulus an order of magnitude greater.

# 5 MODELLING OF BUILDINGS

## 5.1 INTRODUCTION

As was noted in the introduction, part three of this study involved an examination of the force and stress demands placed on unreinforced masonry buildings when subjected to the design earthquake ground motion. The major weaknesses of unreinforced masonry construction when subjected to earthquake ground motion have already been identified in Chapter 1 as connection failure between the walls and the floor and roof diaphragms, in-plane (shear) failures in the walls, and out-of-plane (bending) failures in the walls. In order to study these weaknesses the following model responses were examined in detail:

(1) Base shear;
(2) Storey shears;
(3) Connection forces and corresponding required connection friction coefficients;
(4) In-plane and out-of-plane wall stresses; and
(5) Deflections.

The connection forces and corresponding connection friction coefficients are related to the interaction between the unreinforced masonry walls and the roof and floor diaphragms. Whilst the roofs often had a mechanical connection to the walls, usually due to the need to hold the roof down under wind loading, the concrete floor to wall connections normally relied on friction between the floor and wall to transfer lateral loads. On the other hand, timber floors were usually connected to the walls with a type of mechanical connection. Two connection details between the concrete floors and the unreinforced masonry walls were observed in the buildings in this study. The two types of connections are shown in Figure 5.1.1.

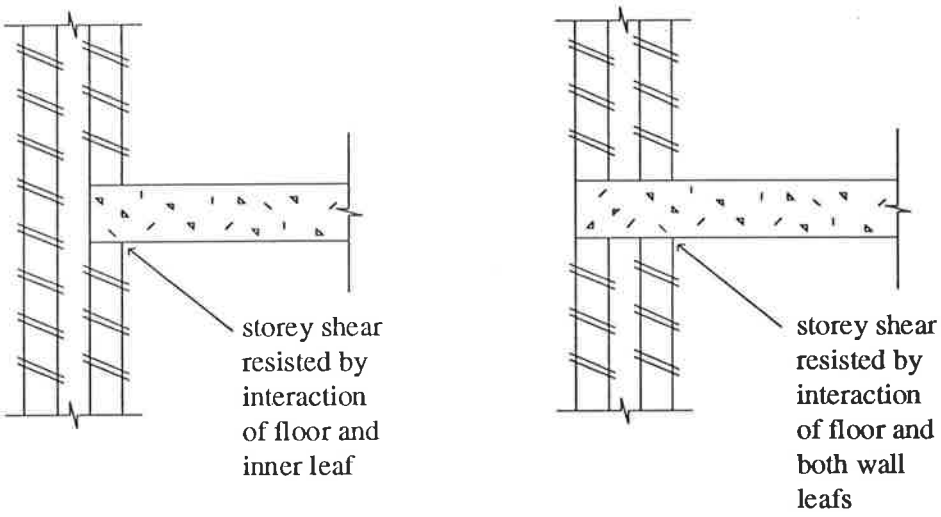


(a) Type I - concrete floor on inner leaf only

(b) Type II - concrete floor on both leafs

Figure 5.1.1 Concrete Floor to Wall Connection Details.

From Figure 2.7.1 it can be seen that the storey shear is transferred from the floor and roof diaphragms to the in-plane walls. The main difference between the two types of concrete floor to wall connections, shown in Figure 5.1.1, is how this storey shear is transferred. For Type I connections, the storey shear is transferred by friction from the concrete floor to the inner leaf of the two leaf wall. For Type II connections the storey shear is transferred by friction from the concrete floor to both leafs of the double leaf wall. The use of a Type I or Type II connection also has an important implications on the level of vertical load that contributes to the frictional resistance of the induced horizontal earthquake load.

The typical connection for a timber floor to a masonry wall was shown in Figure 3.5.1. It can be seen that the shear from the floor system is transferred into the inner

leaf of the double leaf wall similar to the connection in Figure 5.1.1 (a), although the loads will be concentrated at rafter locations and not uniformly distributed along the wall.

The response spectrum method (Clough and Penzien (1993)) was chosen to carry out the earthquake analyses for the unreinforced masonry buildings. The choice of an appropriate response spectrum has an important bearing on the validity of the results of the analysis. In the absence of actual Australian earthquake strong ground motion data it was decided to use the design response spectra included in The Australian Standard "Minimum design loads on structures - Part 4 : Earthquake Loads" AS1170.4-1993 as the basis for the dynamic analyses. The use of this design response spectrum also permitted easy comparisons to be made between the results obtained from the code's equivalent static force provisions and the results of response spectrum analyses.

# 5.2 RESPONSE SPECTRUM ANALYSIS DETAILS

The AS1170.4 response spectrum is shown in Figure 5.2.1. It can be expressed mathematically as:

$$C = \frac{1.25aS}{T^{2/3}} \leq 2.5a \qquad (5.2.1)$$

where S is a site factor, taking into account the soil profile; a is an acceleration coefficient; and T is the natural period of the building. The response spectrum is then multiplied by the ratio:

$$\frac{I}{R_f} \qquad (5.2.2)$$

to account for the importance of the structure (I) and the ductility and over-strength of the building material ($R_f$ - see Section 2.9).

Four variables from Equations 5.2.1 and 5.2.2 had to be defined prior to undertaking the analysis. It was considered that unreinforced masonry is unlikely to be used for buildings that have post disaster functions, such as hospitals. Hence, the importance factor, I, was chosen to be 1.0. The site factor, S, was taken as 1.0 corresponding to

a firm soil site. The response modification factor, $R_f$, was taken as 1.5 in accordance with the recommendations for unreinforced masonry buildings in AS1170.4. This low value assumed that an unreinforced masonry building had little ductility (see Section 2.9) and so is greater than 1 mainly due to a small amount of over-strength. The ground acceleration coefficient, a, was taken to be that which AS1170.4 specifies for Adelaide, South Australia, that is a = 0.1g, and is the highest ground acceleration specified for any Australian capital city.

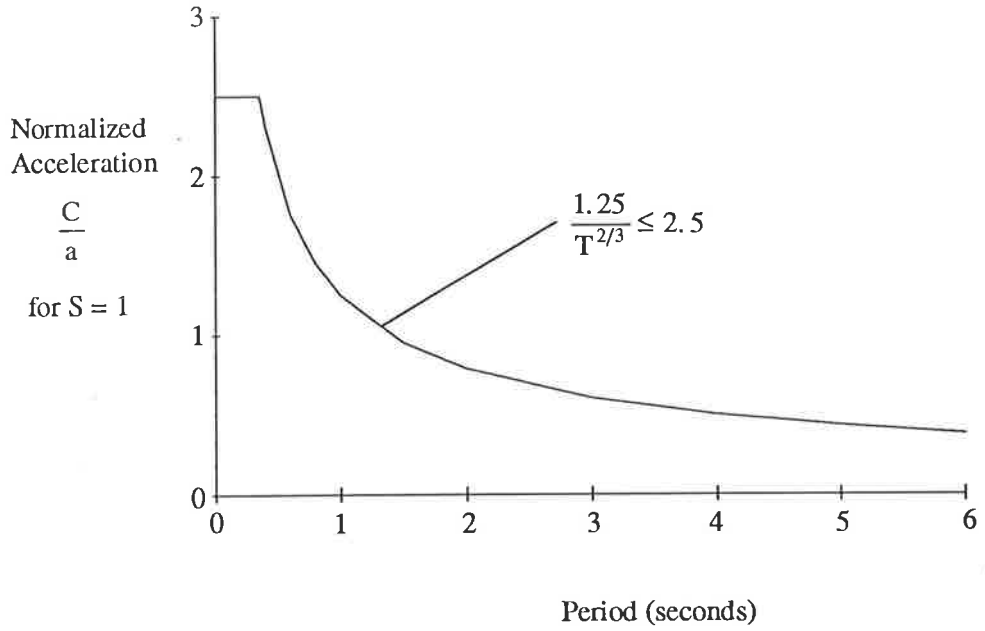


Figure 5.2.1 AS1170.4 Design Response Spectrum.

The use of a commercial analysis package to undertake the response spectrum analysis was decided upon in the interests of reliability and time. The computer package chosen to undertake the analysis was the IMAGES3D program already used to model the wall specimens from the laboratory testing as described in Section 4.6.

# 5.3 IMAGES3D MODEL DETAILS

As was already noted in Section 4.6, IMAGES3D is a finite element based structural analysis program. As with other finite element programs, the structure to be analysed must be defined in terms of nodes, elements, and geometrical and material properties of the structure. The package then automatically assembles a stiffness matrix for the structure. In order for dynamic analyses to be performed, IMAGES3D also assembles a mass matrix so that the dynamic equilibrium equation can be solved.

There were three parameters that could be varied in the IMAGES3D models of the unreinforced masonry buildings. The parameters were:

(1) Type of plate element used;
(2) Young's Modulus of the brickwork; and
(3) Wall geometry.

Two types of plate element are available with IMAGES3D. A "membrane" plate is a plate element with two degrees-of-freedom at each node of the element representing the in-plane distortion of the element. The other type of plate element available, the "membrane plus bending" plate, has three additional degrees-of-freedom at each node representing the out-of-plane displacement of the element and the bending about the two in-plane axes. As out-of-plane bending failure is common in unreinforced masonry walls the "membrane plus bending" plate type elements were chosen to model the unreinforced masonry walls. Concrete floors and metal deck roofs can behave similarly so that "membrane plus bending" plates were also used to model the concrete floors and metal deck roofs. Timber floors were considered to act mainly as a diaphragm, with very little bending stiffness. Therefore, it was initially decided to model timber floors using "membrane" plates. This assumption was tested on one building (East End Market Building 2 - EE2) where the timber floors were also modelled with "membrane plus bending" plates to examine the effect of the extra stiffness provided by the "membrane plus bending" plates had on the structural response and it was found that there was little difference between the two types of plates.

The variability of the Young's Modulus of brickwork has already been discussed in Section 2.5 and Chapter 4. Any value from the range of values for the Young's Modulus of brickwork determined from the shaking table testing could be used for the building models. One of the buildings in the study (two-storey apartment building

- KIDA) was used to determine the sensitivity of the modal properties (frequency, mode shape, and effective modal mass) and the earthquake response, determined by the computer model, to the value of Young's Modulus.

The unreinforced masonry buildings in this study had double leaf (two 110 mm leafs) external walls. Simply defining the elements modelling the external walls to have the same thickness as the wall would yield incorrect results. It was decided that the shear stiffness of the walls was the most important aspect of the model to have correct as the in-plane stiffness of the unreinforced masonry walls was considered to be the major component of the overall structural stiffness of the building. It was therefore decided to set the wall thickness at 220 mm for the correct evaluation of the wall area and shear stiffness (GA). However, this had implications for the wall bending deformations. A 220 mm thick element has the same cross-sectional area as two 110 mm thick elements. Since shear and axial stresses in the wall are proportional to the cross-sectional area of the element then the axial and shear stresses calculated by IMAGES3D for a single 220 mm thick element model should be the same as for two 110 mm thick elements.

The bending stresses, however, will not be calculated correctly for a single element model. For example, consider two walls, one consisting of two plate elements of thickness "d", and the other consisting of a single element "2d" thick. The moment of inertia, I, for the twin "d" thick wall model is:

$$I_{total} = 2 \times \left( \frac{bd^3}{12} \right) \tag{5.3.1}$$

Dividing by the depth to the neutral axis gives the bending modulus, z:

$$z = \frac{2 \times \left( \frac{bd^3}{12} \right)}{\frac{d}{2}} \tag{5.3.2}$$

which reduces to:

$$z = \frac{bd^2}{3} \tag{5.3.3}$$

Considering the "2d" thick single wall, the moment of inertia is:

$$I = \frac{b(2d)^3}{12} \tag{5.3.4}$$

dividing by the depth to the neutral axis, d, gives the bending modulus, z:

$$z = \frac{\frac{b(2d)^3}{12}}{d} \tag{5.3.5}$$

this reduces to:

$$z = \frac{2bd^3}{3} \tag{5.3.6}$$

which is twice the value for the twin "d" wall model. Applying this to the models of the buildings in this study it can be seen that the buildings modelled with the single 220 mm thick wall elements will have twice the bending modulus of the same building modelled with twin 110 mm thick elements. This will lead to the single 220 mm thick element models having half the bending stress of the twin 110 mm thick element model. As the twin wall model more accurately represents the real situation of the buildings, that is two independently acting walls, then the bending stress results from the models, using single 220 mm thick wall elements, need to be doubled to accurately model the buildings. The bending deformations for the "2d" elements will be one-quarter of those for an equivalent model with two "d" walls. Basically, for ease of modelling, single 220 mm elements were used to model the double leaf brick walls, but the bending stresses were doubled to reflect the actual bending stresses expected. The same building used for the comparison of different values of Young's Modulus (KIDA) was also used to confirm the effects of using a single 220 mm wall element model by comparison with a model of the building using two parallel 110 mm elements to represent the double leaf walls.

The comparisons described above for the three variable parameters in the models of the buildings are reported in Section 5.4.

Further details of the models of the buildings included:

(1) The restraint provided by the foundation of the building on the building structure was modelled by restraining the displacement of the nodes at the base of the building in the three global axes, that is, pinned supports;

(2) The properties of the materials used in the horizontal elements of the buildings were taken as the typical values used in design. These properties were:

| | | |
|---|---|---|
| Concrete | Young's Modulus | 30,000 MPa |
| | Poisson's Ratio | 0.3 |
| | Weight Density | 24 kN/m$^3$ |
| Steel | Young's Modulus | 200,000 MPa |
| | Poisson's Ratio | 0.2 |
| | Weight Density | 79 kN/m$^3$ |
| Timber | Young's Modulus | 8,000 MPa |
| | Poisson's Ratio | 0.3 |
| | Weight Density | 11 kN/m$^3$ |
| Ceiling | Young's Modulus | 10,000 MPa |
| | Poisson's Ratio | 0.3 |
| | Weight Density | 17 kN/m$^3$ |

(3) The material properties used for the masonry walls were also taken from typical design values. The Poisson's Ratio was taken as 0.2 and the weight density was taken as 19 kN/m$^3$. The Young's Modulus was determined from the comparison noted previously for building KIDA and detailed in Section 5.4; and

(4) The thickness of the concrete floor slabs were taken to be actual thickness of the slabs. Timber floors were modelled using an effective thickness to take into account the floor boards and flooring joists.

After each model was defined, IMAGES3D was used to carry out modal analyses of the structures. The modal analyses identified the natural periods of the structure, the mode shapes, the modal participation factors, and the effective modal masses. Where

possible, sufficient modes were identified in each of the two major horizontal axes such that 90 percent of the total mass was represented in each direction. The 90 percent value corresponded to the requirements of the AS1170.4.

In many cases, IMAGES3D calculated a number of local modes as well as the desired global building modes. To minimise the number of local modes determined by IMAGES3D, and therefore maximise the number of global modes, the weight of the horizontal building elements, such as floors, roof, and ceiling, were not generated by the program from the defined weight densities for these elements. Instead, weights were defined in the global horizontal directions only at each floor level. This eliminated many of the local modes in the horizontal elements which did not contribute to the overall behaviour of the building with regard to earthquake induced forces.

After each modal analysis was carried out a response spectrum analysis was performed using the modal analysis data and the design response spectrum from AS1170.4 (Section 5.2). The modal maxima were combined using the CQC method (Wilson et al (1981)), assuming five percent damping. The results of the modal analyses are given in Section 5.5. The results of the response spectrum analyses are given in Section 5.6.

# 5.4 PRELIMINARY ANALYSES RESULTS

As noted in Section 5.3, the effect of the variation of three parameters on both the results of the modal analyses and the response spectrum analyses is reported in this section.

### 5.4.1 Plate Element Type

The first aspect of the IMAGES3D models to be checked was the use of "membrane" or "membrane plus bending" plates to model timber floors. A two storey city commercial building (EE2) was chosen for this test. The model was first analysed with the floor diaphragm modelled using "membrane plus bending" plates. The model was then re-analysed with the floor diaphragm modelled using "membrane" plates. The results are shown in Table 5.4.1.

It can be seen from Table 5.4.1 that the change of the type of element used in the floor plates from "membrane" to "membrane plus bending" had little effect on the main lateral modes in each direction. There is a third short direction lateral mode that is very close to the second lateral mode (7.8 Hertz) and has an effective modal mass of 4 percent of the total mass for the "membrane plus bending" plate model. It was concluded from this exercise that only "membrane plus bending" plates would be used in all of the subsequent analyses.

Table 5.4.1 Two Storey Commercial Building (EE2) - Effect of Horizontal Plate Type on Modal Properties.

| Element Type | Modal Frequency (Hertz) and Effective Modal Weights (% total mass) | | |
|---|---|---|---|
| | 1st Short | 2nd Short | 1st Long |
| "membrane" | 5.1 (77.3%) | 7.6 (8.0%) | 7.5 (73.9%) |
| "membrane plus bending" | 4.8 (74.9%) | 7.7 (2.1%) | 7.5 (74.0%) |

### 5.4.2 Young's Modulus of Brickwork

The value of Young's Modulus for unreinforced masonry which was used in the models for all of the unreinforced masonry buildings was obtained by finding the value of Young's Modulus which resulted in a natural period which matched the measured value of one building from the ambient vibration tests (Chapter 3). The chosen Young's Modulus was selected to be in the upper half of the range of Young's Modulus to reflect the fact that walls constructed on future buildings which had earthquake induced forces considered as part of the design would also have a reasonable level of supervision in the construction of the walls and therefore, have stiffness properties in the upper part of the range. The second to last building in Table 3.3.1 was used for this purpose as it was one of the first buildings modelled. The results of the modal analyses for different values of Young's Modulus are shown in Table 5.4.2.

It can be seen from Table 5.4.2 that the Young's Modulus used for the unreinforced masonry walls of a building has a significant effect on the modal frequencies of the building. The modal frequencies calculated using a Young's Modulus of 1500 MPa were almost three times larger than those calculated using a Young's Modulus of 200

MPa. A value of Young's Modulus of 1065 MPa was found to give a reasonable estimate of the natural period in the short direction. This value was subsequently used in all future models of the buildings.

Table 5.4.2 Two Storey Apartment Building (KIDA) - Effect of Young's Modulus of the unreinforced masonry walls on the modal frequencies.

| Mode | Young's Modulus, E (MPa) | | | |
|---|---|---|---|---|
| | 200 | 500 | 1065 | 1500 |
| 1st (lateral short) | 4.9 | 7.7 | 11.1 | 13.1 |
| 2nd (torsional) | 6.9 | 10.8 | 15.7 | 18.4 |
| 3rd (lateral long) | 7.4 | 11.7 | 17.0 | 20.1 |

It should be noted that the modal frequencies determined by the modal analyses for all of the values of Young's Modulus considered all corresponded to a modal period of less than 0.35 seconds and when the design earthquake response spectra to be used in the analysis was considered (Figure 5.2.1) the periods all corresponded to the constant acceleration region of the design earthquake response spectra and the choice of a Young's Modulus between 220 MPa and 1,250 MPa (the range derived from the laboratory tests) would have no effect on the induced design earthquake force calculated using the design response spectrum for this two storey building.

In order to determine the effect of adopting a Young's Modulus value corresponding to that given by a number of researchers (Section 2.5) that was an order of magnitude greater than that determined from the shaking table tests one of the buildings in the study (OLW) was analysed with the adopted Young's Modulus of 1,065 MPa and with a Young's Modulus of 20,000 MPa. For a Young's Modulus of 1,065 MPa the first lateral mode frequency in the short direction was 2.4 Hertz, for a Young's Modulus of 20,000 MPa the frequency increased to 10.7 Hertz. The measured frequency (Table 3.3.1) was 3.1 Hertz which was close to that predicted by the IMAGES3D model with a Young's Modulus of 1,065 MPa. The frequency

predicted by the IMAGES3D model with a Young's Modulus of 20,000 MPa was more than three times greater than the measured frequency.

Also varied was the Young's Modulus of the reinforced concrete floor to determine its effect on the modal properties. The comparison was undertaken using building KIDA, with the Young's Modulus of the unreinforced masonry walls equal to the value adopted for use in this study, 1,065 MPa. When the reinforced concrete floor was given a Young's Modulus of 30,000 MPa, the value adopted as standard for this study, a modal frequency of 11.1 Hertz was obtained for the first mode (a short direction lateral mode). When the Young's Modulus was increased to 60,000 MPa (an unrealistically high value for concrete) the first modal frequency was 11.2 Hertz. Hence, it was concluded that the value of the Young's Modulus adopted for the horizontal elements had little effect on the overall modal properties of the unreinforced masonry building and the values adopted for the properties of the materials used in the horizontal elements were acceptable for use in this study.

### 5.4.3 Wall Geometry

The final check undertaken on the IMAGES3D models before the commencement of the modelling program was to examine the effect of modelling double leaf walls with a single 220 mm thick plate element. The two storey apartment building (KIDA) used in the comparison of the effect of the Young's Modulus on the modal properties was used in this comparison. As has already been described in Section 5.3, the building was modelled using the 220 mm plate elements for the double leaf walls. A second model of the building was completed with two 110 mm thick elements replacing the single 220 mm thick elements of the first model for the double leaf walls. The use of two 110 mm thick walls ensured that IMAGES3D correctly calculated the bending stiffness, shear stiffness, and bending modulus for the walls. The results for the 220 mm thick single element model are given in Table 5.4.2. The results for the twin 110 mm thick element model are given in Table 5.4.3.

In the short direction the two models gave similar results (11.1 Hertz compared with 10.7 Hertz). In the long direction the twin element model was characterised by a number of modes close together (15.1, 15.4 and 15.4 Hertz). The single element model had a mode at a similar frequency, 17.0 Hertz, with a low effective modal mass (5.5 percent).

The results of a response spectrum analysis on the twin wall model were compared to the results of a response spectrum analysis on the single wall model. The comparison was carried out for the first mode in the short direction. The first comparison was for base shear. For mode one of the single wall model the base shear was 161 kN. For the twin wall model, the first mode base shear was 157 kN, a difference of 2.5 percent. This difference was considered to be negligible in light of the variability of the properties of unreinforced masonry as reported in Chapter 4 and in Section 2.5. The next result compared was the connection force that was experienced at the connection of the floors to the walls of the building. The apartment building had a connection detail similar to Figure 5.1.1(b). The out-of-plane connection forces were very low (< 0.3 kN/m) in both cases. The in-plane connection forces were considerably greater than the out-of-plane connection forces for both models. In the case of the twin wall specimen, the connection force was assumed to be divided evenly between the two concurrent wall elements. The connection forces are shown in Figure 5.4.1, where the connection forces in each of the concurrent walls for the twin wall specimen were summed to obtain a total connection force for comparison to the single element model. It can be seen from Figure 5.4.1 that the connection forces are essentially the same for both models.

Table 5.4.3 - Results for 110 mm Twin Element Model (KIDA).

| | Modal Frequency (Hertz) and Effective Modal Weights (% total mass) | | | | |
|---|---|---|---|---|---|
| | 1st Short | 1st Long | 2nd Long | 3rd Long | 4th Long |
| Twin 110 mm Wall Model | 10.7 (88.4%) | 14.4 (2.1%) | 15.1 (5.0%) | 15.4 (6.6%) | 15.4 (47.3%) |

The last response to be compared was the wall stresses. The results for the twin 110 mm wall model and the single 220 mm wall model were compared to determine if the ratio of the bending stress would be approximately half. It was found that the single 220 mm model bending stresses were indeed half those of the twin 110 mm wall model as was expected. Hence, single 220 mm thick element models were used to model the double 110 mm thick walls for all buildings in the study. However, the calculated bending stresses were adjusted to compensate for the overestimate of the bending stiffness and section modulus.

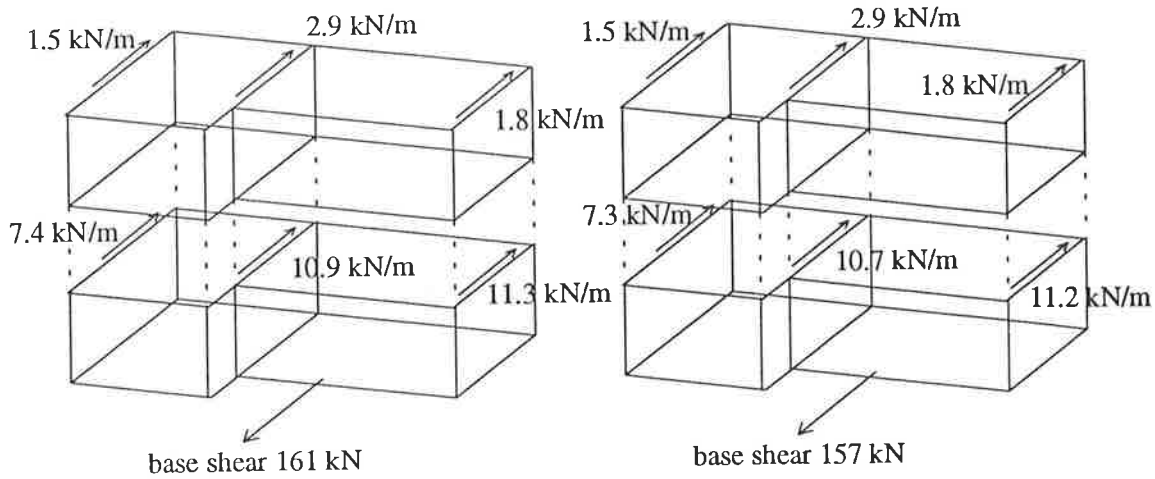


(a)single 220 mm thick wall model

(b) twin 110 mm thick wall model

Figure 5.4.1 Two Storey Apartment Building - Connection Force Comparison : Single Wall versus Twin Wall.

# 5.5 MODAL ANALYSES RESULTS

After the comparisons described in Section 5.4 were completed, modal analyses were performed for each of the buildings in Table 3.3.1. The results of these analyses are listed in Table 5.5.1.

The descriptions given for the buildings in Table 5.5.1 correspond to the descriptions given to the same buildings in Table 3.3.1.

The first mode frequencies for the buildings were compared with those determined from the field experiments (Chapter 3) and are presented in Table 5.5.2.

Table 5.5.1 - Results of Modal Analyses on Buildings.

| Building Description | Direction | Modal Frequency (Hertz) and Percentage of Total Mass | | | | Percentage of Total Mass |
|---|---|---|---|---|---|---|
| | | Mode 1 | Mode 2 | Mode 3 | Mode 4 | |
| 2 storey vacant city commercial building (EE2) | short | 4.8 (74.9%) | 7.7 (2.1%) | 7.8 (4.0%) | - | 81.0% |
| | long | 7.5 (74.0%) | - | - | - | 74.0% |
| 2 storey vacant city commercial building (EE3) | short | 6.8 (48.0%) | 7.4 (23.3%) | - | - | 71.3% |
| | long | 7.6 (8.5%) | 7.7 (5.7%) | 7.9 (6.7%) | 8.1 (64.9%) | 85.8% |
| 2 storey vacant city commercial building (EE4) | short | 6.6 (22.5%) | 7.4 (58.9%) | - | - | 81.4% |
| | long | 7.6 (7.3%) | 7.9 (6.0%) | 8.2 (71.7%) | - | 85.0% |
| 3 storey school building (CBC) | short | 5.9 (88.7%) | - | - | - | 88.7% |
| | long | 7.0 (11.0%) | 7.6 (71.9%) | 19.4 (10.3%) | - | 93.2% |
| 2 storey city social club (IAC) | short | 10.7 (89.7%) | - | - | - | 89.7% |
| | long | 11.5 (83.9%) | 19.3 (10.0%) | - | - | 93.9% |
| 3 storey city commercial building (LTI) | short | 4.3 (75.4%) | 11.1 (9.7%) | - | - | 85.2% |
| | long | 5.1 (74.9%) | - | - | - | 76.3% |
| 2 storey city commercial building (NSC) | short | 6.5 (78.8%) | 7.7 (9.9%) | - | - | 88.7% |
| | long | 10.4 (79.6%) | 11.3 (11.7%) | - | - | 91.3% |
| 2 storey city retail building (STP) | short | 4.2 (47.8%) | 4.9 (32.3%) | 9.1 (6.6%) | - | 86.7% |
| | long | 9.5 (81.4%) | - | - | - | 81.4% |
| 5 storey university office building (OLW) | short | 2.4 (76.3%) | 6.8 (19.5%) | - | - | 95.8% |
| | long | 3.5 (81.9%) | - | - | - | 81.9% |
| 2 storey suburban apartment building (KIDA) | short | 11.1 (90.4%) | - | - | - | 90.4% |
| | long | 15.7 (5.5%) | 17.0 (86.4%) | - | - | 91.9% |
| 2 storey suburban apartment building (KIDB) | short | 5.2 (81.9%) | 8.2 (2.1%) | - | - | 84.0% |
| | long | 8.8 (46.4%) | 9.2 (18.2%) | - | - | 64.6% |

Table 5.5.2 - Comparison of Experimentally Determined Natural Frequencies to those Determined from Modal Analyses.

| Building Description | Direction | Measured Frequency (Hertz) | IMAGES3D Frequency (Hertz) |
|---|---|---|---|
| 2 storey vacant city commercial building (EE2) | short<br>long | 5.0<br>4.8 | 5.1<br>7.5 |
| 2 storey vacant city commercial building (EE3) | short<br>long | 3.6<br>5.0 | 4.8<br>7.5 |
| 2 storey vacant city commercial building (EE4) | short<br>long | 3.7<br>5.0 | 6.8<br>7.6 |
| 3 storey school building (CBC) | short<br>long | 5.5<br>- | 5.9<br>7.0 |
| 2 storey city social club (IAC) | short<br>long | 13.9<br>- | 10.7<br>11.5 |
| 3 storey city commercial building (LTI) | short<br>long | 3.2<br>3.7 | 4.3<br>5.1 |
| 2 storey city commercial building (NSC) | short<br>long | 10.1<br>- | 6.5<br>10.4 |
| 2 storey city retail building (STP) | short<br>long | 7.4<br>7.5 | 4.2<br>9.5 |
| 5 storey university office building (OLW) | short<br>long | 3.1<br>- | 2.4<br>3.5 |
| 2 storey suburban apartment building (KIDA) | short<br>long | 7.2<br>7.3 | 11.1<br>15.7 |
| 2 storey suburban apartment building (KIDB) | short<br>long | 7.2<br>7.2 | 5.2<br>8.8 |

Comparison of these results are probably best aided by a plot of the form of Figure 5.5.1. From this it can be seen that there is no clear trend in the data. In some cases the ambient vibration tests determined a lower frequency than the IMAGES3D analyses and in some cases the ambient vibration tests resulted in a higher frequency than the IMAGES3D analyses. For most buildings the measured and calculated frequencies were within 25 percent of each other although the overall correlation was probably only fair. In certain cases the agreement was very good (OLW, KIDB, EE2, and CBC).

The modal properties were then used in the response spectrum analysis conducted on the unreinforced masonry buildings and described in Section 5.6.

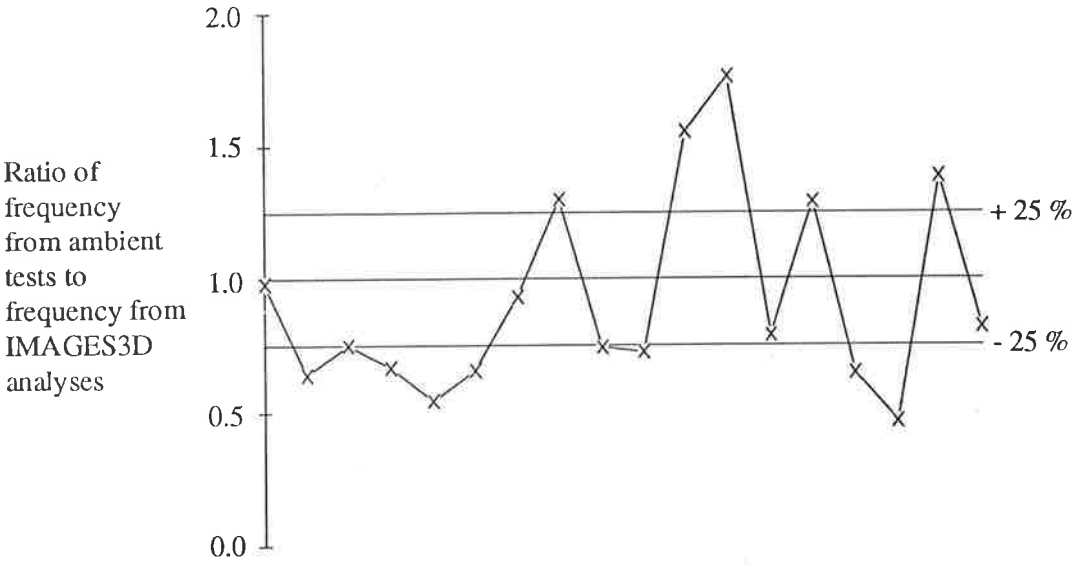


Figure 5.5.1 Plot of the ratio of the results of the ambient vibration tests to the results of the IMAGES3D analyses.

# 5.6 RESPONSE SPECTRUM ANALYSES RESULTS

As noted in Section 5.2, the unreinforced masonry buildings were subjected to a response spectrum analysis using the design earthquake response spectrum from AS1170.4 for a firm soil site in Adelaide (S = 1.0, a = 0.1 and $R_f$ = 1.5).

The results from the previous modal analyses were used as the basis for the response spectrum analyses and the modes given in Table 5.5.1 corresponded to the modes used in these analyses. Each building was analysed for earthquake effects in the directions of both major plan axes of the buildings.

It was found from the analytical results that the buildings tended to behave as described by Priestley (1985) (Section 2.7). The induced earthquake force was resisted by in-plane shear in walls running parallel to the direction of the earthquake

ground motion. The primary response of the walls at right angles to the seismic input was in bending.

The results of the response spectrum analyses are examined here in the order in which the buildings were presented in Tables 5.5.1 and 3.3.1. The dimensions of the buildings are given in Table 3.3.1 and details in Appendix B. The main building responses examined were:

(1) The base shear;

(2) The storey shear;

(3) The maximum and average connection forces along the in-plane walls and the friction coefficient, $\mu$, required to resist that connection force (the roof connections do not rely on friction so no friction coefficient was given for the roof levels); and

(4) The corrected wall bending stresses. The bending stresses are given about a horizontal axis and a vertical axis.

The required friction coefficients were compared to those determined by Page (1994) and described in Section 2.5. The friction coefficients given in Page are for walls with a damp proof membrane and it would be expected that brickwork without a membrane, such as that which would exist at the floor connection, would be able to achieve even greater friction coefficients than those published by Page. The bending stresses were compared to those given in Section 2.5 by various researchers to determine if a tensile failure might be expected.

Also presented for the buildings in the study was the total sway of the buildings and the corresponding average shear strain, $\gamma$ (total sway divided by the height of the building). The shear strain was presented so that it could be compared to the shear strain corresponding to a shear failure in the walls. The shear strain corresponding to shear failure was calculated by taking the failure shear stress and dividing by the shear modulus, G. The shear modulus was calculated from the Young's Modulus, E, used in this study, 1,065 MPa, and the assumed Poisson's Ratio, 0.2. The range of shear strength presented by Jankulovski et al (1994), 0.1 MPa to 0.7 MPa, was used to calculate the range of shear strains corresponding to failure. The calculated range was 270 microstrain to 1900 microstrain. For reasonably good levels of

workmanship it would be expected that the shear strength would be in the upper part of the shear strength range and correspondingly, the upper level of the shear strain range.

### 5.6.1 2-Storey Commercial Building (EE2)

The first building was a 2-storey commercial building (EE2). It had a timber floor and a timber truss and metal deck roof. The results for the response spectrum analysis are shown in Table 5.6.1.

Table 5.6.1 Response Spectrum Analysis Results : Building EE2

| | Short Direction | | | | Long Direction |
|---|---|---|---|---|---|
| | Mode 1 | Mode 2 | Mode 3 | CQC | Mode 1 |
| Base Shear (kN) (W = self weight of the building) | -103 (0.12W) | -11 (0.01W) | 9 (0.01W) | 104 (0.12W) | -98 (0.11W) |
| Storey Shear (kN) | | | | | |
| 1st Floor | 99 | 4 | -6 | 99 | 93 |
| Roof | 55 | -1 | 6 | 55 | 50 |
| In-plane Connection Force - Maximum (kN/m) and μ | | | | | |
| 1st Floor | 12.7 μ = 0.71 | 0.5 μ = 0.03 | -0.8 μ = 0.04 | 12.8 μ = 0.71 | 6.4 μ = 0.25 |
| Roof | 7.1 | -0.1 | 0.8 | 7.1 | 2.8 |
| In-plane Connection Force - Average (kN/m) and μ | | | | | |
| 1st Floor | 12.7 μ = 0.71 | 0.5 μ = 0.03 | -0.8 μ = 0.04 | 12.8 μ = 0.71 | 6.4 μ = 0.25 |
| Roof | 7.1 | -0.1 | 0.8 | 7.1 | 2.8 |
| Wall Stresses (MPa) - horizontal and vertical | | | | | |
| 1st Floor - Hori | 0.015 | 0.009 | 0.019 | 0.032 | 0.012 |
| - Vert | 0.059 | 0.025 | 0.052 | 0.100 | 0.038 |
| Roof -Hori | 0.032 | 0.008 | 0.015 | 0.040 | 0.053 |
| - Vert | 0.042 | 0.021 | 0.043 | 0.078 | 0.077 |

The connection force was evenly distributed between the two in-plane walls. The required friction coefficients are all generally achievable in practice, based upon the results of Page (1994). The only required friction coefficient that may cause a problem in practice and lead to a possible failure at the connection of the floor to the wall was for mode 1 in the short direction. It should be noted, however, that this building has timber floors and the connection of timber floors to walls was generally achieved with a positive connection between the floor joist and wall by use of a mechanical fastener, such as bolts. The out-of-plane connection forces were all less than 1 kN/m and were not considered to be a problem.

The most common form of damage to unreinforced masonry buildings when subjected to earthquake excitation is due to out-of-plane failure of the walls. This building had an average axial compressive pre-load due to self weight of 0.11 MPa for the walls between the roof and the first floor and 0.18 MPa for the walls between the first floor and the ground. It can be seen that the none of the bending stresses given in Table 5.6.1 would be expected to cause a wall bending failure in a properly constructed building, especially when taking into account the axial compressive stresses.

The last important response of the buildings to earthquake excitations is the sway. The building sway in the short direction was 2.1 mm and 1.1 mm in the long direction, both small enough not to initiate pounding with adjacent buildings. The corresponding shear strains were 260 microstrain and 100 microstrain respectively. These shear strains were both less than the expected range of shear strain corresponding to a shear failure in the in-plane walls based on the work of Jankulovski et al (1994).

### 5.6.2 2-Storey Commercial Building (EE3)

The second building analysed was part of the same development as the first. It had similar details but was larger and had an internal double leaf wall. The results of the response spectrum analysis are shown in Table 5.6.2.

As with the first building, the friction coefficients required to resist the in-plane connection force for this building were all smaller than should be able to be achieved in practice. In this case the extra (interior) wall resisting the earthquake induced forces in the short direction resulted in a smaller connection force in the walls and a subsequent lower friction coefficient demand than the first building.

The axial compressive self weight stress in the walls of this building were 0.175 MPa for the walls from the first floor to the ground and 0.102 MPa for the walls from first floor to the roof. From the results in Table 5.6.2, it can also be seen that there is unlikely to be an out-of-plane wall failure due to bending about a horizontal axis. However, the bending stress about a vertical axis in the walls was nearly equal to the stress that would cause failure. This aspect of the performance of the walls will be examined further in Chapter 6 when the requirements of the AS1170.4, and the Australian Masonry Code, AS3700, are examined. It can be seen then that the walls

of this building may experience out-of-plane failures, which are catastrophic, and would lead to collapse.

Table 5.6.2 Response Spectrum Analysis Results : Building EE3

| | Short Direction | | | Long Direction | | | | |
|---|---|---|---|---|---|---|---|---|
| | Mode 1 | Mode 2 | CQC | Mode 1 | Mode 2 | Mode 3 | Mode 4 | CQC |
| Base Shear (kN) (W = self weight of the building) | -128 (0.07W | -62 (0.04W) | 171 (0.10W) | 23 (0.01W) | 15 (0.01W) | 18 (0.01W) | -157 (0.09W) | 118 (0.07W) |
| Storey Shear (kN) | | | | | | | | |
| 1st Floor | 132 | 46 | 163 | -32 | -19 | -17 | 124 | 83 |
| Roof | 55 | 25 | 72 | -14 | -8 | -4 | 49 | 34 |
| In-plane Connection Force - Maximum (kN/m) and μ | | | | | | | | |
| 1st Floor | 6.8 | 2.8 | 8.7 | -1.1 | -0.7 | -0.7 | 5.9 | 4.2 |
| | μ = | μ = | μ = | μ = | μ = 0.04 | μ = | μ = | μ = 0.23 |
| Roof | 0.25 | 0.10 | 0.32 | 0.06 | -0.4 | 0.04 | 0.33 | 1.5 |
| | 3.1 | 1.1 | 3.8 | -0.7 | | -0.4 | 2.4 | |
| In-plane Connection Force - Average (kN/m) and μ | | | | | | | | |
| 1st Floor | 6.0 | 2.4 | 7.6 | -1.1 | -0.7 | -0.7 | 5.9 | 4.2 |
| | μ = | μ = | μ = | μ = | μ = 0.04 | μ = | μ = | μ = 0.23 |
| Roof | 0.22 | 0.09 | 0.28 | 0.06 | -0.4 | 0.04 | 0.33 | 1.5 |
| | 2.7 | 1.0 | 3.4 | -0.7 | | -0.4 | 2.4 | |
| Wall Stresses (MPa) - horizontal and vertical | | | | | | | | |
| 1st Floor - Hori | 0.080 | 0.074 | 0.137 | -0.055 | -0.042 | -0.045 | 0.103 | 0.040 |
| - Vert | 0.185 | 0.171 | 0.315 | -0.150 | 0.109 | 0.116 | 0.290 | 0.622 |
| Roof -Hori | 0.101 | 0.064 | 0.147 | -0.049 | -0.036 | -0.039 | 0.075 | 0.186 |
| - Vert | 0.233 | 0.143 | 0.336 | -0.141 | 0.102 | 0.105 | 0.201 | 0.514 |

The sway for this building, determined by CQC, was about 2 mm for both directions of excitation, well within limits that would prevent pounding between adjacent buildings. The corresponding shear strains were 260 microstrain in both directions and as with the first building in the study, these shear strains are not expected to lead to in-plane failures in the walls.

### 5.6.3 2-Storey Commercial Building (EE4)

The third building analysed was the last building from the same development as the first two and it had the same details as EE2 and EE3 as well as an internal double leaf wall. The results are shown in Table 5.6.3.

This building had a very similar layout to building EE3, with the main difference being the internal wall which was offset from the centre-line of the building. This led to some torsional response in the building. Again, the required friction coefficients

should be able to be met in practice. The self weight axial compressive stresses for this building were the same as those for the previous building. The only bending stress that may cause a failure in the walls was bending about a vertical axis in the short direction above the first floor. The sways for this building were the same as the previous building, about 2 mm. The corresponding shear strains were the same as for building EE3, 260 microstrain, and again were not expected to lead to any in-plane failures in the walls.

Table 5.6.3 Response Spectrum Analysis Results : Building EE4

| | Short Direction | | | Long Direction | | | |
|---|---|---|---|---|---|---|---|
| | Mode 1 | Mode 2 | CQC | Mode 1 | Mode 2 | Mode 3 | CQC |
| Base Shear (kN) (W = self weight of the building) | -59 (0.03W) | -156 (0.09W) | 189 (0.11W) | 19 (0.01W) | 16 (0.01W) | -190 (0.11W) | 164 (0.09W) |
| Storey Shear (kN) | | | | | | | |
| 1st Floor | 68 | 120 | 161 | -27 | -19 | 140 | 109 |
| Roof | 24 | 59 | 73 | -12 | -7 | 54 | 42 |
| In-plane Connection Force - Maximum (kN/m) and μ | | | | | | | |
| 1st Floor | 3.4 μ = 0.12 | 6.7 μ = 0.25 | 8.7 μ = 0.32 | -1.0 μ = 0.06 | -0.7 μ = 0.04 | 6.5 μ = 0.36 | 5.3 μ = 0.29 |
| Roof | 1.6 | 2.9 | 3.9 | -0.6 | -0.4 | 2.7 | 2.0 |
| In-plane Connection Force - Average (kN/m) and μ | | | | | | | |
| 1st Floor | 3.0 μ = 0.11 | 6.1 μ = 0.22 | 7.9 μ = 0.28 | -1.0 μ = 0.06 | -0.7 μ = 0.04 | 6.5 μ = 0.36 | 5.3 μ = 0.29 |
| Roof | 1.4 | 2.6 | 3.4 | -0.6 | -0.4 | 2.7 | 2.0 |
| Wall Stresses (MPa) - horizontal and vertical | | | | | | | |
| 1st Floor - Hori | 0.069 | 0.090 | 0.135 | -0.047 | -0.050 | 0.092 | 0.057 |
| - Vert | 0.171 | 0.247 | 0.355 | -0.125 | -0.130 | 0.263 | 0.159 |
| Roof -Hori | 0.079 | 0.074 | 0.129 | -0.041 | -0.042 | 0.064 | 0.048 |
| - Vert | 0.197 | 0.182 | 0.321 | -0.118 | -0.116 | 0.172 | 0.135 |

### 5.6.4 3-Storey School Building (CBC)

The fourth building analysed was a 3-storey school building. It had concrete flat slab floors, metal deck and steel beam roof and was not symmetrical. The results for the response spectrum analysis are shown in Table 5.6.4.

The connection forces in this building required friction coefficients that should be able to be met in practice. The bending stresses were also sufficiently low that an out-of-plane wall failure was not expected. The building responded torsionally as there was a wall present in the long direction of the building on the ground floor that was not present in the upper floors. Because of this, it is the only building which

could have a problem with out-of-plane connection forces. The calculated out-of-plane connection force in the second storey was 2.4 kN/m.

Table 5.6.4 Response Spectrum Analysis Results : Building CBC

| | Short Direction | Long Direction | | | |
|---|---|---|---|---|---|
| | Mode 1 | Mode 1 | Mode 2 | Mode 3 | CQC |
| Base Shear (kN) (W = self weight of the building) | -812 (0.12W) | 100 (0.01W) | -659 (0.09W) | -94 (0.01W) | 608 (0.09W) |
| Storey Shear (kN) | | | | | |
| 1st Floor | 812 | -100 | 658 | 95 | 607 |
| 2nd Floor | 553 | -83 | 463 | -44 | 416 |
| Roof | 145 | -23 | 125 | -46 | 120 |
| In-plane Connection Force - Maximum (kN/m) and μ | | | | | |
| 1st Floor | 24.2 | -3.3 | 11.2 | 1.3 | 9.5 |
| | μ = 0.38 | μ = 0.07 | μ = 0.23 | μ = 0.03 | μ = 0.20 |
| 2nd Floor | 13.1 | -2.5 | 11.6 | -1.1 | 10.2 |
| | μ = 0.26 | μ = 0.10 | μ = 0.47 | μ = 0.04 | μ = 0.41 |
| Roof | 4.4 | -0.9 | 3.8 | -1.2 | 3.5 |
| In-plane Connection Force - Average (kN/m) and μ | | | | | |
| 1st Floor | 21.3 | -1.2 | 8.4 | 1.2 | 7.8 |
| | μ = 0.34 | μ = 0.03 | μ = 0.18 | μ = 0.03 | μ = 0.17 |
| 2nd Floor | 11.1 | -0.9 | 7.5 | -0.7 | 7.0 |
| | μ = 0.22 | μ = 0.04 | μ = 0.31 | μ = 0.03 | μ = 0.29 |
| Roof | 3.3 | -0.7 | 1.4 | -0.7 | 1.3 |
| Wall Stresses (MPa) - horizontal and vertical | | | | | |
| 1st Floor - Hori | 0.009 | 0.001 | -0.002 | 0.001 | 0.002 |
| - Vert | 0.045 | 0.005 | -0.010 | 0.004 | 0.009 |
| 2nd Floor - Hori | 0.001 | 0.002 | -0.002 | 0.000 | 0.002 |
| - Vert | 0.005 | 0.010 | -0.007 | 0.001 | 0.008 |
| Roof -Hori | 0.002 | 0.003 | -0.004 | 0.000 | 0.003 |
| - Vert | 0.011 | 0.015 | -0.020 | 0.001 | 0.015 |

The sway of this building was 2 mm in the short direction and 1 mm in the long direction. The corresponding shear strains were 230 microstrain and 110 microstrain respectively. Neither of these corresponded to the level of shear strain expected to correspond to an in-plane failure of the walls.

### 5.6.5 2-Storey Social Club Building (IAC)

The fifth building was a 2-storey building with a concrete suspended floor slab and a one storey area which houses a social club in the city. The results of the response spectrum analysis are given in Table 5.6.5.

Table 5.6.5 Response Spectrum Analysis Results : Building IAC

| | Short Direction | Long Direction | | |
|---|---|---|---|---|
| | Mode 1 | Mode 1 | Mode 2 | CQC |
| Base Shear (kN) (W = self weight of the building) | -558 (0.11W) | -522 (0.10W) | 62 (0.01W) | 523 (0.10W) |
| Storey Shear (kN) | | | | |
| 1st Floor | 556 | 524 | -57 | 525 |
| Roof | 111 | 133 | 41 | 140 |
| In-plane Connection Force - Maximum (kN/m) and μ | | | | |
| 1st Floor | 9.6 μ = 0.60 | 8.4 μ = 1.01 | -0.7 μ = 0.08 | 8.4 μ = 1.01 |
| Roof | 2.9 | 4.8 | 1.5 | 5.1 |
| In-plane Connection Force - Average (kN/m) and μ | | | | |
| 1st Floor | 6.0 μ = 0.37 | 4.6 μ = 0.55 | -0.5 μ = 0.06 | 4.6 μ = 0.55 |
| Roof | 2.8 | 4.6 | 1.5 | 4.9 |
| Wall Stresses (MPa) - horizontal and vertical | | | | |
| 1st Floor - Hori | 0.035 | 0.002 | 0.002 | 0.003 |
| - Vert | 0.018 | 0.010 | 0.003 | 0.011 |
| Roof -Hori | 0.073 | 0.003 | 0.003 | 0.004 |
| - Vert | 0.010 | 0.015 | 0.006 | 0.016 |

The connection force requirements for this building were complicated by the fact that the upper floor only covers part of the ground floor plan. This resulted in a fairly low compressive stress in the ground floor walls and high friction coefficient requirements ($\mu > 1$). In the long direction, a failure was predicted between the floor and wall for in-plane forces. The bending stresses were all low enough that out-of-plane wall failures were not expected. The sway of the building in both directions was less than 1 mm due to the large plan area and low height providing a very stiff structure to resist the lateral loads. The corresponding shear strain in both directions was 150 microstrain; well less than that required for an in-plane wall failure.

### 5.6.6 3-Storey Commercial Building (LTI)

The sixth building analysed was a 3-storey commercial building that had concrete floors, unreinforced masonry stair and lift shafts, and a metal deck roof. The results of the response spectrum analysis are given in Table 5.6.6.

The friction coefficients ($\mu$) required to resist the in-plane forces in this building were all less than 0.5. The out-of-plane bending stresses were also low and would not be expected to result in a tensile failure in the brickwork. The low stress levels may be

due to the relatively (to the other buildings in the study) small storey height. The sway in both directions was less than 3.0 mm and would not be considered a problem to adjoining buildings. The corresponding shear strains were both 230 microstrain, which was not expected to correspond to a shear failure in the in-plane walls.

Table 5.6.6 Response Spectrum Analysis Results : Building LTI

| | Short Direction Mode 1 | Mode 2 | CQC | Long Direction Mode 1 |
|---|---|---|---|---|
| Base Shear (kN) (W = self weight of the building) | -1480 (0.10W) | 190 (0.01W) | 1490 (0.10W) | 1470 (0.10W) |
| Storey Shear (kN) | | | | |
| 1st Floor | 1474 | -190 | 1484 | 1470 |
| 2nd Floor | 1410 | -124 | 1414 | 1406 |
| 3rd Floor | 1003 | 132 | 1013 | 989 |
| Roof | 309 | 106 | 328 | 291 |
| In-plane Connection Force - Maximum (kN/m) and μ | | | | |
| 1st Floor | 27.7 μ = 0.24 | -3.4 μ = 0.03 | 27.9 μ = 0.24 | 20.6 μ = 0.17 |
| 2nd Floor | 26.2 μ = 0.34 | -2.0 μ = 0.03 | 26.3 μ = 0.34 | 19.8 μ = 0.24 |
| 3rd Floor | 19.7 μ = 0.50 | 2.1 μ = 0.05 | 19.8 μ = 0.50 | 14.9 μ = 0.34 |
| Roof | 6.6 | 2.2 | 7.0 | 5.4 |
| In-plane Connection Force - Average (kN/m) and μ | | | | |
| 1st Floor | 23.9 μ = 0.21 | -3.1 μ = 0.03 | 24.1 μ = 0.21 | 17.5 μ = 0.14 |
| 2nd Floor | 22.8 μ = 0.30 | -2.0 μ = 0.03 | 22.9 μ = 0.30 | 16.7 μ = 0.20 |
| 3rd Floor | 16.3 μ = 0.41 | 2.3 μ = 0.06 | 16.5 μ = 0.42 | 11.8 μ = 0.27 |
| Roof | 5.0 | 1.7 | 5.3 | 3.5 |
| Wall Stresses (MPa) - horizontal and vertical | | | | |
| 1st Floor - Hori | 0.003 | 0.001 | 0.003 | 0.005 |
| - Vert | 0.012 | 0.003 | 0.012 | 0.024 |
| 2nd Floor - Hori | 0.002 | 0.001 | 0.002 | 0.001 |
| - Vert | 0.003 | 0.002 | 0.004 | 0.003 |
| 3rd Floor - Hori | 0.002 | 0.001 | 0.002 | 0.007 |
| - Vert | 0.006 | 0.002 | 0.006 | 0.004 |
| Roof -Hori | 0.002 | 0.001 | 0.002 | 0.005 |
| - Vert | 0.004 | 0.002 | 0.004 | 0.005 |

### 5.6.7 2-Storey Commercial Building (NSC)

The seventh building analysed was a 2-storey commercial building with a suspended slab that is part reinforced concrete and part timber and a metal deck roof. The results of the response spectrum analysis are given in Table 5.6.7.

Table 5.6.7 Response Spectrum Analysis Results : Building NSC

| | Short Direction | | | Long Direction | | |
|---|---|---|---|---|---|---|
| | Mode 1 | Mode 2 | CQC | Mode 1 | Mode 2 | CQC |
| Base Shear (kN) (W = self weight of the building) | -487 (0.12W) | -61 (0.01W) | 506 (0.12W) | 386 (0.09W) | -57 (0.01W) | 353 (0.08W) |
| Storey Shear (kN) | | | | | | |
| 1st Floor | 445 | 21 | 451 | -361 | 35 | 340 |
| Roof | 80 | 7 | 82 | -78 | 10 | 72 |
| In-plane Connection Force - Maximum (kN/m) and μ | | | | | | |
| 1st Floor | 15.7 μ = 0.53 | 1.5 μ = 0.05 | 16.1 μ = 0.54 | -6.6 μ = 0.23 | 0.8 μ = 0.03 | 6.1 μ = 0.21 |
| Roof | 4.5 | 0.2 | 4.6 | -1.7 | 0.1 | 1.6 |
| In-plane Connection Force - Average (kN/m) and μ | | | | | | |
| 1st Floor | 13.5 μ = 0.46 | 1.3 μ = 0.04 | 13.9 μ = 0.47 | -6.3 μ = 0.22 | 0.8 μ = 0.03 | 5.8 μ = 0.20 |
| Roof | 3.4 | 0.1 | 3.4 | -1.6 | 0.1 | 1.5 |
| Wall Stresses (MPa) - horizontal and vertical | | | | | | |
| 1st Floor - Hori | 0.017 | 0.032 | 0.040 | 0.018 | 0.031 | 0.045 |
| - Vert | 0.057 | 0.145 | 0.169 | 0.051 | 0.117 | 0.154 |
| Roof -Hori | 0.054 | 0.026 | 0.066 | 0.042 | 0.027 | 0.063 |
| - Vert | 0.231 | 0.115 | 0.283 | 0.180 | 0.096 | 0.252 |

This building's connection force requirements should be able to be met in practice. However, the calculated bending stresses were of concern. For both directions of ground motion the bending stresses in the walls between the first floor and the roof were high for bending about a vertical axis. The contribution of the self weight axial stresses to the resistance of these bending stresses is less than that for the bending about a horizontal axis. An out-of-plane wall failure in the upper walls of this building would therefore be a possibility.

The sway of the building (<3 mm) will not cause problems to adjacent buildings in either direction. The corresponding shear strain was 370 microstrain for both directions. Unlike the other buildings examined so far, this exceeded the lower bound of the range of shear strain that corresponded to a shear failure in brickwork based on the work of Jankulovski et al (1994). It is therefore possible that this building could experience an in-plane wall shear failure.

### 5.6.8 2-Storey Retail Building (STP)

The eighth building analysed was a 2-storey retail building which had a suspended timber ground and upper floor and a metal deck roof. The results of this analysis are given in Table 5.6.8

Table 5.6.8 Response Spectrum Analysis Results : Building STP

| | Short Direction | | | | Long Direction |
|---|---|---|---|---|---|
| | Mode 1 | Mode 2 | Mode 3 | CQC | Mode 1 |
| Base Shear (kN) (W = self weight of the building) | -241 (0.07W) | 138 (0.04W) | 33 (0.01W) | 246 (0.07W) | -409 (0.12W) |
| Storey Shear (kN) | | | | | |
| Ground Floor | 241 | -162 | -32 | 254 | 409 |
| 1st Floor | 241 | -142 | 12 | 245 | 351 |
| Roof | 50 | -67 | -16 | 74 | 139 |
| In-plane Connection Force - Maximum (kN/m) and μ | | | | | |
| Ground Floor | 13.0 μ = 0.32 | -10.6 μ = 0.27 | -1.6 μ = 0.04 | 14.5 μ = 0.36 | 7.6 μ = 0.21 |
| 1st Floor | 13.0 μ = 0.62 | -8.6 μ = 0.41 | 0.6 μ = 0.03 | 13.6 μ = 0.65 | 6.6 μ = 0.35 |
| Roof | 3.5 | -3.7 | -0.8 | 4.5 | 2.7 |
| In-plane Connection Force - Average (kN/m) and μ | | | | | |
| Ground Floor | 12.5 μ = 0.32 | -8.4 μ = 0.21 | -1.3 μ = 0.03 | 13.2 μ = 0.34 | 7.6 μ = 0.21 |
| 1st Floor | 12.1 μ = 0.58 | -7.3 μ = 0.35 | 0.3 μ = 0.01 | 12.4 μ = 0.59 | 6.5 μ = 0.34 |
| Roof | 2.8 | -3.3 | -0.7 | 3.8 | 2.6 |
| Wall Stresses (MPa) - horizontal and vertical | | | | | |
| Ground Floor - Hori | 0.308 | 0.236 | 0.030 | 0.436 | 0.003 |
| - Vert | 0.050 | 0.102 | 0.056 | 0.139 | 0.005 |
| 1st Floor - Hori | 0.778 | 0.523 | 0.009 | 1.046 | 0.005 |
| - Vert | 0.401 | 0.263 | 0.013 | 0.535 | 0.003 |
| Roof -Hori | 0.469 | 0.256 | 0.011 | 0.592 | 0.005 |
| - Vert | 0.167 | 0.035 | 0.031 | 0.183 | 0.008 |

The connection force requirements for this building should be able to be met in practice. The connection forces that required a friction coefficient of about 0.6 may be of some concern and may lead to an in-plane connection failure. The axial compressive stresses due to the buildings self weight were 0.092 MPa for the wall between the roof and the first floor, 0.176 MPa for the walls between the first floor and the ground floor, and 0.211 MPa for the wall from the ground floor to footing level. The plan of this building given in Appendix B shows that for two corners of the building the floor does not meet the wall. This meant that the walls were

spanning from the roof to the floor (9300 mm) which was a span considerably greater than the other buildings in the study. It can be seen from the results given in Table 5.6.8 that the upper level walls risk out-of-plane failure when the building was excited in the short direction. The span of the out-of-plane walls for earthquake excitation in the long direction were the floor to floor height, and coupled with the short horizontal span resulted in bending stress levels that would not be expected to lead to failure.

The short direction had a large sway, about 8 mm, which, though large compared the majority of buildings in the study, would not be expected to result in pounding problems. The long direction sway was 0.6 mm. The corresponding shear strains were 860 microstrain and 60 microstrain respectively. The shear strain in the short direction could be expected to lead to an in-plane failure of some walls.

### 5.6.9 5-Storey University Building (OLW)

The ninth building analysed was a 5-storey university office building which had reinforced concrete flat slab floors and roof. The results of the analysis are given in Table 5.6.9.

This building was the tallest in the study. The required friction coefficients for the in-plane connection forces were all less than 0.6. This was due to the building having a high self weight, including a concrete roof. The only connection force that may be of concern in an earthquake was for the fifth floor in the long direction, where a friction coefficient of about 0.6 was required. Prior to analysis, it was thought that the height of this building would lead to the possibility of out-of-plane failures in the upper floors. This turned out to not be the case. This was due to the regular spacing of the internal walls that kept the span of the out-of-plane walls small enough that the bending stresses remained low.

Naturally, for the tallest building the sways were relatively large, 4 mm in the long direction, and nearly 10 mm in the short direction. The corresponding shear strains were 520 microstrain and 209 microstrain, respectively. A shear failure in the short direction was a possibility if the wall shear strength was in the lower part of the range.

Table 5.6.9 Response Spectrum Analysis Results : Building OLW

| | Short Direction Mode 1 | Mode 2 | CQC | Long Direction Mode 1 |
|---|---|---|---|---|
| Base Shear (kN) (W = self weight of the building) | -3105 (0.11W) | 868 (0.03W) | 3218 (0.12W) | -3647 (0.13W) |
| Storey Shear (kN) | | | | |
| 1st Floor | 3014 | -836 | 3122 | 3641 |
| 2nd Floor | 2875 | -566 | 2926 | 3381 |
| 3rd Floor | 2593 | -179 | 2598 | 2961 |
| 4th Floor | 2137 | 153 | 2144 | 2351 |
| 5th Floor | 1495 | 314 | 1530 | 1559 |
| Roof | 679 | 233 | 720 | 703 |
| In-plane Connection Force - Maximum (kN/m) and μ | | | | |
| 1st Floor | 35.9 μ = 0.40 | -11.5 μ = 0.13 | 37.6 μ = 0.42 | 33.6 μ = 0.42 |
| 2nd Floor | 21.7 μ = 0.30 | -4.1 μ = 0.06 | 22.1 μ = 0.30 | 22.0 μ = 0.34 |
| 3rd Floor | 19.5 μ = 0.34 | -1.3 μ = 0.02 | 19.5 μ = 0.34 | 19.9 μ = 0.40 |
| 4th Floor | 15.9 μ = 0.39 | 1.2 μ = 0.03 | 16.0 μ = 0.40 | 16.2 μ = 0.47 |
| 5th Floor | 11.1 μ = 0.46 | 2.4 μ = 0.10 | 11.4 μ = 0.47 | 11.6 μ = 0.59 |
| Roof | 5.5 | 1.8 | 5.8 | 6.1 |
| In-plane Connection Force - Average (kN/m) and μ | | | | |
| 1st Floor | 20.9 μ = 0.24 | -6.1 μ = 0.07 | 21.7 μ = 0.24 | 22.4 μ = 0.28 |
| 2nd Floor | 10.7 μ = 0.15 | -2.0 μ = 0.03 | 10.9 μ = 0.15 | 13.2 μ = 0.20 |
| 3rd Floor | 9.6 μ = 0.17 | -0.6 μ = 0.01 | 9.6 μ = 0.17 | 11.3 μ = 0.23 |
| 4th Floor | 8.0 μ = 0.20 | 0.6 μ = 0.01 | 8.0 μ = 0.20 | 8.7 μ = 0.25 |
| 5th Floor | 5.6 μ = 0.23 | 1.2 μ = 0.05 | 5.7 μ = 0.23 | 5.7 μ = 0.29 |
| Roof | 2.7 | 0.9 | 2.9 | 2.1 |
| Wall Stresses (MPa) - horizontal and vertical | | | | |
| 1st Floor - Hori | 0.008 | 0.004 | 0.010 | 0.010 |
| - Vert | 0.042 | 0.015 | 0.044 | 0.043 |
| 2nd Floor - Hori | 0.012 | 0.012 | 0.017 | 0.001 |
| - Vert | 0.010 | 0.005 | 0.011 | 0.009 |
| 3rd Floor - Hori | 0.014 | 0.012 | 0.018 | 0.001 |
| - Vert | 0.009 | 0.003 | 0.009 | 0.003 |
| 4th Floor - Hori | 0.018 | 0.007 | 0.019 | 0.000 |
| - Vert | 0.002 | 0.003 | 0.004 | 0.002 |
| 5th Floor - Hori | 0.024 | 0.001 | 0.024 | 0.001 |
| - Vert | 0.003 | 0.001 | 0.003 | 0.003 |
| Roof -Hori | 0.030 | 0.009 | 0.032 | 0.000 |
| - Vert | 0.003 | 0.002 | 0.003 | 0.002 |

### 5.6.10 2-Storey Apartment Building (KIDA)

The tenth building analysed was a 2-storey apartment building. This building consisted of a reinforced concrete flat slab and a metal deck roof. The results of the analysis are given in Table 5.6.10.

Table 5.6.10 Response Spectrum Analysis Results : Building KIDA

| | Short Direction Mode 1 | Long Direction Mode 1 | Mode 2 | CQC |
|---|---|---|---|---|
| Base Shear (kN) (W = self weight of the building) | -161 (0.13W) | 10 (0.01W) | -153 (0.12W) | 147 (0.12W) |
| Storey Shear (kN) | | | | |
| 1st Floor | 141 | -10 | 136 | 130 |
| Roof | 25 | -1 | 23 | 22 |
| In-plane Connection Force - Maximum (kN/m) and μ | | | | |
| 1st Floor | 11.3 μ = 0.60 | -1.1 μ = 0.06 | 5.3 μ = 0.28 | 4.7 μ = 0.25 |
| Roof | 2.9 | -0.3 | 1.1 | 0.9 |
| In-plane Connection Force - Average (kN/m) and μ | | | | |
| 1st Floor | 9.9 μ = 0.52 | -0.6 μ = 0.03 | 4.4 μ = 0.23 | 4.1 μ = 0.21 |
| Roof | 2.1 | -0.1 | 0.7 | 0.6 |
| Wall Stresses (MPa) - horizontal and vertical | | | | |
| 1st Floor - Hori | 0.014 | 0.002 | 0.014 | 0.015 |
| - Vert | 0.036 | 0.004 | 0.031 | 0.034 |
| Roof -Hori | 0.013 | 0.002 | 0.018 | 0.020 |
| - Vert | 0.045 | 0.005 | 0.054 | 0.057 |

The connection force friction coefficient requirements for this building were all less than 0.6. The out-of-plane bending stresses were all small so that an out-of-plane failure was not expected. Sways of less than 0.5 mm were calculated and these corresponded to shear strains of 109 microstrain for both directions. Shear strains of this level would not be expected to lead to an in-plane failure in the walls.

### 5.6.11 2-Storey Apartment Building (KIDB)

The last building analysed was part of the same development as the previous building. The difference between the two buildings is that KIDB was longer and had a staircase at one end. The results of the analysis are given in Table 5.6.11.

Table 5.6.11 Response Spectrum Analysis Results : Building KIDB

| | Short Direction | | | Long Direction | | |
|---|---|---|---|---|---|---|
| | Mode 1 | Mode 2 | CQC | Mode 1 | Mode 2 | CQC |
| Base Shear (kN) (W = self weight of the building) | -276 (0.17W) | -7 (0.00W) | 276 (0.17W) | -156 (0.09W) | -61 (0.04W) | 212 (0.13W) |
| Storey Shear (kN) | | | | | | |
| 1st Floor | 234 | -6 | 234 | 139 | 37 | 173 |
| Roof | 63 | 0 | 63 | 29 | 10 | 38 |
| In-plane Connection Force - Maximum (kN/m) and μ | | | | | | |
| 1st Floor | 13.8 μ = 0.78 | -0.3 μ = 0.02 | 13.8 μ = 0.78 | 3.7 μ = 0.20 | 1.2 μ = 0.06 | 4.8 μ = 0.25 |
| Roof | 6.1 | -0.1 | 6.1 | 1.1 | 0.3 | 1.4 |
| In-plane Connection Force - Average (kN/m) and μ | | | | | | |
| 1st Floor | 12.8 μ = 0.72 | 0.1 μ = 0.01 | 12.8 μ = 0.72 | 3.4 μ = 0.18 | 1.1 μ = 0.06 | 4.4 μ = 0.32 |
| Roof | 4.0 | -0.1 | 4.0 | 0.9 | 0.2 | 1.1 |
| Wall Stresses (MPa) - horizontal and vertical | | | | | | |
| 1st Floor - Hori | 0.029 | 0.020 | 0.036 | 0.040 | 0.130 | 0.166 |
| - Vert | 0.096 | 0.073 | 0.123 | 0.057 | 0.294 | 0.348 |
| Roof -Hori | 0.062 | 0.075 | 0.099 | 0.173 | 0.050 | 0.219 |
| - Vert | 0.212 | 0.053 | 0.220 | 0.385 | 0.086 | 0.464 |

This building may have problems achieving the required in-plane friction coefficients at the first floor level for excitation in the short direction. Bending stresses for bending about a vertical axis were also near the value where tensile failure could become a possibility, especially in the long direction.

The sway for both directions was calculated to be about 2 to 3 mm. This corresponded to shear strains of 430 microstrain to 650 microstrain. Both of these exceeded the lower bound of the expected range of shear strains that corresponded to shear failure in the walls.

# 5.7 SUMMARY

A single phase finite element model was used to model the dynamic behaviour of eleven unreinforced masonry buildings. The dynamic properties of the buildings were estimated using single 220 mm thick elements to model twin 110 mm thick walls. The only response property to be incorrectly modelled by this procedure was the wall bending stress, which was doubled to obtain a more accurate value of bending stress.

It was found that the in-plane connection force requirements could generally be met by friction. This conclusion was based upon the results of Page (1994). The predicted failure mechanism for an in-plane failure was that the connection force at a particular point of the wall exceeded the capacity of the floor-wall connection. This resulted in the floor trying to slide along the wall at this location. Because the floor is a rigid diaphragm, the floor cannot slide at this point until the rest of the floor-wall connection slides. So rather than a local failure, an in-plane connection force failure can not occur until the whole floor-wall connection reaches its capacity. This meant that the friction from the weight of all of the parts of the building contributing to the dead load on these walls was available to resist the total storey shear on that wall.

For new buildings it would be expected that a reasonably high level of workmanship would be present in the unreinforced masonry walls and that the shear strength of an unreinforced masonry wall in a new building would be at the upper end of the 0.1 MPa to 0.7 MPa range reported by Jankulovski et al (1994). In-plane wall shear failures would then not be a likely failure mechanism in an unreinforced masonry building subjected to earthquake excitation based upon the results of these buildings. However, if the shear strength of the walls was at the lower part of the range of shear strength then there is the possibility of some in-plane wall failures. However, in-plane shear type wall failures are generally do not lead to collapse.

A failure mechanism that is more likely is an out-of-plane wall failure, particularly in the upper walls were the self weight is the lowest and the acceleration, and hence the inertia force, is the greatest. Five of the buildings in the study had bending stresses that would suggest that an out-of-plane failure was a possibility based upon the tensile strengths reported in Section 2.5. Unlike in-plane wall failures, the out-of-plane failure of walls are generally a collapse condition.

No correlation was observed between the building height and the possibility of an out-of-plane failure from the results of the response spectrum analyses. However, it was obvious that as the height of a buildings increased, so will the induced acceleration, and hence, the induced inertia force. Also important in predicting the possibility of an out-of-plane wall failure was the floor-to-floor height, and the horizontal span of the walls. Obviously, the greater the span of the wall between supports, the greater the out-of-plane deflections and bending moment induced in the wall by the earthquake ground motion, and the greater the bending stress.

The sway of all the buildings in the study was sufficiently small that the buildings would not be expected to pose a problem for neighbouring buildings through pounding. This was the result of the buildings having a very large shear stiffness due to the in-plane walls.

Comparison of the results of this study to the results gained from a real earthquake acting on an unreinforced masonry building, as outlined in Section 2.4, from Tena-Colunga and Abrams (1992) and Abrams (1993), was difficult because the ground acceleration at the firehouse studied was 0.29g, almost three times that used in this study, and is further complicated by the fact that an $R_f$ factor of 1.5 was used in the response spectrum analyses.

Nevertheless, a comparison of the shear and bending stresses in Table 2.4.2 for the firehouse showed that the bending stresses and shear stresses (and hence, connection forces) obtained from the response spectrum analyses carried out in this study were of a similar order of magnitude for the base acceleration and in many cases, about one third of the firehouse values.

It was concluded that the calculated responses of the buildings in this study to the earthquake ground motion represented by the response spectrum provided a reasonable prediction of the behaviour of the buildings to earthquake ground motion. These results will be further compared to the requirements of AS1170.4 in the next chapter.

# 6 EQUIVALENT STATIC FORCE ANALYSIS OF BUILDINGS

## 6.1 INTRODUCTION

To achieve the overall aim of this project, that is to evaluate and, if necessary, refine the current simplified methods for the earthquake analysis of unreinforced masonry buildings, it was first necessary to examine a number of existing methods available to the designer. In Australia, this meant the design procedures given in The Australian Standard "Minimum design loads on structures - Part 4 : Earthquake Loads" AS1170.4-1993. The code contains two methods for the analysis of a structure when subjected to earthquake induced forces. The first method is an equivalent static load approach and the second method is by a dynamic analysis. The second method allows the use of either a response spectrum analysis (Chapter 5) or a time history analysis.

This chapter presents the results of an investigation where the equivalent static load approach was used to analyse the buildings from Chapter 5. These results are then compared to the results of the response spectrum analyses described in Chapter 5. From this comparison it was concluded that the equivalent static load approach required refinement to take into account the particular properties of unreinforced masonry and unreinforced masonry buildings.

## 6.2 CODE BASED ANALYSIS

All the buildings in the study were analysed in accordance with the equivalent static force procedures in AS1170.4. All the buildings were classified as Type I structures except for the five-storey university office building (OLW) and the two-storey city

social club (IAC) which are both Type II buildings, because of the office building's height and the social club's potential for holding a large number of people.

The AS1170.4 equivalent static force base shear is given by the formula:

$$V = I\left(\frac{CS}{R_f}\right)G_g \leq I\left(\frac{2.5a}{R_f}\right)G_g \qquad (6.2.1)$$

where:

$$C = \frac{1.25aS}{T^{2/3}} \qquad (6.2.2)$$

and I is an importance factor, S is a site factor, taking into account the soil profile, a is an acceleration coefficient, T is the natural period of the building, and $R_f$ is a response modification factor (Section 2.9). $G_g$ is the gravity load, given by:

$$G_g = G + \psi_c Q \qquad (6.2.3)$$

where G is the dead load, Q the live load, and $\psi_c$ is a live load combination factor from the Australian Standard "SAA Loading Code - Part 1 : Dead and live loads and load combinations" AS1170.1-1989.

The variables, a, S, and I, were all taken to be the same values as used for the response spectrum analyses in Chapter 5; that is, for a firm soil site in Adelaide (a = 0.10g, S = 1.0, and I = 1.0).

The earthquake design category given in AS1170.4 for Type I buildings with aS = 0.1 is category B, and for the Type II buildings is category C. The requirements for category B and C buildings are very similar for non-ductile construction, such as unreinforced masonry. The buildings are required to be designed by either the equivalent static force method or by dynamic analysis.

There is a further requirement for buildings that are four or more storeys high. That is, unreinforced masonry is not allowed to be used for the earthquake force resisting mechanism for these buildings. This requirement meant that the five storey university office building in this study does not comply with the current earthquake code and the analysis procedures do not apply to it. However, for completeness, the equivalent

static force analysis was also carried out for this building for comparison to the results of the response spectrum analysis presented in Chapter 5.

The calculated base shear was applied to the building using the procedures given in AS1170.4. The method used the formula:

$$F_x = C_{vx} V \tag{6.2.4}$$

to distribute the base shear up the building. $F_x$ is the force applied at level x and

$$C_{vx} = \frac{G_{gx} h_x^k}{\sum_{i=1}^{n} G_{gi} h_i^k} \tag{6.2.5}$$

where $G_{gx}$ and $G_{gi}$ are the proportions of the load $G_g$ at levels x and i respectively, $h_x$ and $h_i$ are the distance from the base to levels x and i respectively, and n is the total number of storeys. k is a period dependant exponent that for periods less than 0.5 seconds (all of the buildings in this study) is equal to 1.0.

The torsional effects created in the buildings due to centre of mass and the centre of shear not being coincident were also evaluated using the provisions in AS1170.4. The static eccentricity, that due to the distance between the centre of mass and the centre of shear, was calculated and then the design eccentricity was calculated using the procedures in AS1170.4. Torsion tends to increase the force to be resisted by individual members of a structure compared to the case where only lateral modes are considered.

AS1170.4 also specifies a minimum wall anchorage requirement for the connection of walls to floors and the roof. The minimum anchorage is 10(aS) kN per metre run of wall. This requirement applies to the out-of-plane resistance of the wall-floor connection rather the in-plane connection force. 10(aS) is equal to 1 kN/m for all the buildings in this study. For the in-plane connection force no other requirements are included. Through a simple analysis of the structure, assuming the structure acts as described by Priestley (1985) (Figure 2.7.1), it would appear that the storey shear should be distributed to the in-plane walls in proportion to their stiffness with an additional correction for eccentricity.

# 6.3 RESULTS OF STATIC ANALYSIS

In this section the results of the equivalent static force procedure are presented and compared with the results of the response spectrum analyses reported in Chapter 5. The response quantities compared were:

(1) Natural periods;
(2) Base shear;
(3) Distribution of base shear;
(4) Connection forces; and
(5) Out-of-plane effects.

### 6.3.1 Natural Periods

The first result to be investigated was the natural periods calculated using Equations 2.1.1 and 2.1.2. It was noted that the periods calculated from these equations corresponded to the constant acceleration region of the Design Response Spectrum (Figure 5.2.1) for all buildings except the five-storey office building, OLW. This resulted in the design base shears for these buildings being equal in both directions. Further, the constant acceleration region of the Design Response Spectrum is expressed as the upper limit in Equation 6.2.1, so that the acceleration in this region is independent of the site factor, S. Hence, the soil type under the building does not effect the calculated design base shear for these buildings. The soil type under the building only changes the length of the constant acceleration region as it effects the building period at which the upper limit to the acceleration is reached.

### 6.3.2 Base Shear

The calculated design base shears from the equivalent static load method are compared to the base shears calculated from the response spectrum method in Table 6.3.1.

AS1170.4 specifies that the base shear determined by a response spectrum analysis must not be less than the base shear determined from the equivalent static force approach if the building is classed, in accordance with the code, as "irregular". If the building is classed as "regular", then the base shear calculated by the response spectrum method should not be less than 90 percent of that determined from the static force approach in the code. The only exception to this requirement for regular

buildings is if the response spectrum analysis was performed using the natural periods for the building determined from the period formulae included in the code (Equations 2.1.1 and 2.1.2). In this case, the base shear calculated by the response spectrum method should not be less than 80 percent of that determined from the static force approach in the code. The code also states that the base shear determined from the response spectrum method need not exceed the 100, 90, and 80 percent levels described above. The buildings that the code considers "regular" are denoted by "reg" in the Building description column of Table 6.3.1 whilst those considered "irregular" are denoted by "irreg". The minimum allowable base shear for a response spectrum analysis (90 or 100 percent) is also shown in Table 6.3.1 under the values for the AS1170.4 determined base shear for each building. Also shown in Table 6.3.1 is the percentage of the required minimum base shear for each of the base shears calculated by the base shears expressed as a percentage of the required minimum base shear under the response spectrum base shear values.

For the buildings in this study the base shear determined using the response spectrum method never exceeded the values determined using the equivalent static force approach. In fact, the response spectrum results for all the buildings in this study would be required to be factored up to the minimum levels of base shear (either 100 percent for irregular buildings or 90 percent for regular buildings) specified in AS1170.4. However, for the purpose of comparison, the response spectrum results were not altered. There was a large discrepancy in the difference in the base shears from the two types of analyses between the buildings. In some cases, notably KIDB, the response spectrum base shear and the AS1170.4 base shear were very close, in others, such as STP and LTI, the AS1170.4 base shears were considerably higher than the base shear from the response spectrum analysis. In the case of STP the code base shear was three times the response spectrum base shear in the short direction. It was expected that the differences will be least when the participating mass all occurred in a single mode and greatest when it occurred in a large number of modes. This was best illustrated with building KIDB where, for the short direction, the majority of the mass was in one mode (Table 5.5.1) and the response spectrum analysis predicted 94 percent of the AS1170.4 base shear compared to the long direction where the mass was spread amongst multiple modes and the response spectrum analysis predicted a base shear 72 percent of that determined by AS1170.4.

Table 6.3.1 Summary of base shears by static and dynamic analyses.

| Building Description | Base Shear (kN) | | | |
|---|---|---|---|---|
| | Short Direction | | Long Direction | |
| | AS1170.4 1993 | Response Spectrum | AS1170.4 1993 | Response Spectrum |
| 2 storey vacant city commercial building (EE2) - reg[1] | 154<br>90%[2] = 139 | 104<br>(75%)[3] | 154<br>90% = 139 | 98<br>(71%) |
| 2 storey vacant city commercial building (EE3) - reg | 318<br>90% = 286 | 171<br>(60%) | 318<br>90% = 286 | 118<br>(41%) |
| 2 storey vacant city commercial building (EE4) - reg | 318<br>90% = 286 | 189<br>(66%) | 318<br>90% = 286 | 164<br>(57%) |
| 3 storey school building (CBC) - irreg | 1343<br>100% = 1343 | 812<br>(60%) | 1343<br>100% = 1343 | 608<br>(45%) |
| 2 storey city social club (IAC) - irreg | 951<br>100% = 951 | 558<br>(59%) | 951<br>100% = 951 | 523<br>(55%) |
| 3 storey city commercial building (LTI) - reg | 2955<br>90% = 2660 | 1490<br>(56%) | 2955<br>90% = 2660 | 1470<br>(55%) |
| 2 storey city commercial building (NSC) - reg | 771<br>90% = 694 | 506<br>(73%) | 771<br>90% = 694 | 353<br>(51%) |
| 2 storey city retail building (STP) - reg | 759<br>90% = 683 | 246<br>(36%) | 759<br>90% = 683 | 409<br>(60%) |
| 5 storey university office building (OLW) - irreg | 4544<br>100% = 4544 | 3218<br>(71%) | 5094<br>100% = 5094 | 3647<br>(72%) |
| 2 storey suburban apartment building (KIDA) - irreg | 224<br>100% = 224 | 161<br>(72%) | 224<br>100% = 224 | 147<br>(66%) |
| 2 storey suburban apartment building (KIDB) - irreg | 294<br>100% = 294 | 276<br>(94%) | 294<br>100% = 294 | 212<br>(72%) |

1 The buildings denoted "reg" were classified as regular according to AS1170.4. The buildings denoted "irreg" were classified as irregular according to AS1170.4.

2 Minimum base shear for a response spectrum analysis. The base shear was required to be a minimum of 90% of that determined from an equivalent static load approach for a regular building and 100% for an irregular building.

3 The base shear from the response spectrum analyses expressed as a percentage of the required minimum base shear (see [2] above).

### 6.3.3 Distribution of the Base Shear

The third building response to be compared was the distribution of the base shear up the height of the building. This was compared by looking at the storey shear for the buildings and assuming that the connection type was that shown in Figure 5.1.1(b) as Type II and behaved as described in Section 5.1. As the base shears for the two types of analyses were different it was inconsistant to compare the absolute values of the storey shears. What was compared was the storey shear expressed as a percentage of the base shear. For the AS1170.4 analyses the distribution of the base shear up the height of a building was calculated using Equation 6.2.4. This equation relied on the distribution of the mass of the building and the building's storey heights. Subsequently, the force distribution was the same for the long and short directions using the AS1170.4 approach. The results for the code and response spectrum analyses are shown in Table 6.3.2.

In the majority of cases the AS1170.4 analyses had a greater percentage of the base shear applied to the upper levels of the buildings than did the response spectrum analyses. This was not the case for OLW in both directions and IAC in the long direction. For OLW this could be due to the assumption that the mode shape, and hence the shear force distribution, was based on a linear function. That is, in Equation 6.2.5 k = 1.0. For the taller OLW building this assumption may not hold as more bending could be present in the mode shape than would be expected in the other buildings where their height is low compared with their plan dimensions and shear type deflection would tend to dominate the mode shape. For the IAC building, the upper floor only covered part of the lower floor and this may be contrary to some of the assumptions implicit in the use of Equation 6.2.5. Generally, however, it should be noted that a building designed according to the requirements of AS1170.4 would have a greater percentage of its base shear applied higher up the building and would, therefore, predict that the upper walls experienced higher connection forces and shear stresses than the same building analysed using the response spectrum method for the same base shear. Similarly, the overturning moments calculated from the results of the code based analyses would be greater than those determined from the results of the response spectrum analyses.

Table 6.3.2 Storey Shear Results from static and dynamic analyses

| Building Description | Location | AS1170.4 Storey Shear as percentage of Base Shear | Response Spectrum Storey Shear as percentage of Base Shear | |
|---|---|---|---|---|
| | | | Short Direction | Long Direction |
| 2 storey vacant city commercial building (EE2) - reg | roof to 1st floor<br>1st to ground | 0.63<br>1.00 | 0.52<br>0.95 | 0.51<br>0.95 |
| 2 storey vacant city commercial building (EE3) - reg | roof to 1st floor<br>1st to ground | 0.58<br>1.00 | 0.42<br>0.95 | 0.29<br>0.70 |
| 2 storey vacant city commercial building (EE4) - reg | roof to 1st floor<br>1st to ground | 0.58<br>1.00 | 0.39<br>0.85 | 0.26<br>0.66 |
| 3 storey school building (CBC) - irreg | roof to 2nd floor<br>2nd to 1st floor<br>1st to ground | 0.22<br>0.74<br>1.00 | 0.18<br>0.68<br>1.00 | 0.20<br>0.68<br>1.00 |
| 2 storey city social club (IAC) - irreg | roof to 1st floor<br>1st to ground | 0.21<br>1.00 | 0.20<br>1.00 | 0.27<br>1.00 |
| 3 storey city commercial building (LTI) - reg | roof to 3rd floor<br>3rd to 2nd floor<br>2nd to 1st floor<br>1st to ground | 0.33<br>0.73<br>0.96<br>0.99 | 0.22<br>0.68<br>0.95<br>1.00 | 0.20<br>0.67<br>0.96<br>1.00 |
| 2 storey city commercial building (NSC) - reg | roof to 1st floor<br>1st to ground | 0.40<br>1.00 | 0.16<br>0.89 | 0.20<br>0.96 |
| 2 storey city retail building (STP) - reg | roof to 1st floor<br>1st to ground<br>ground to base | 0.35<br>0.87<br>1.00 | 0.30<br>1.00<br>1.00 | 0.34<br>0.86<br>1.00 |
| 5 storey university office building (OLW) - irreg | roof to 5th floor<br>5th to 4th floor<br>4th to 3rd floor<br>3rd to 2nd floor<br>2nd to 1st floor<br>1st to ground | 0.13<br>0.42<br>0.65<br>0.83<br>0.94<br>1.00 | 0.22<br>0.48<br>0.67<br>0.81<br>0.91<br>0.97 | 0.19<br>0.43<br>0.65<br>0.81<br>0.93<br>1.00 |
| 2 storey suburban apartment building (KIDA) - irreg | roof to 1st floor<br>1st to ground | 0.39<br>1.00 | 0.16<br>0.88 | 0.15<br>0.88 |
| 2 storey suburban apartment building (KIDB) - irreg | roof to 1st floor<br>1st to ground | 0.39<br>1.00 | 0.23<br>0.85 | 0.18<br>0.82 |

### 6.3.4 Connection Forces

Whilst the greater AS1170.4 analysis base shears ensured the average connection force for a level of a building is greater than or equal to the average connection force calculated by a response spectrum analysis, the maximum connection forces calculated from the AS1170.4 analysis may not have been equal to or greater than the response spectrum analysis value. The difference between the average and the

maximum connection force in the AS1170.4 analysis was due to torsional effects. The ratio of the maximum connection force to the average connection force calculated using the torsional requirements of AS1170.4 are shown in Table 6.3.3. Where the plan of the building changes with height (such as building IAC and building CBC) the calculations were done for the floor level that had the maximum torsional response. The ratio of maximum connection force to average connection force from the response spectrum analyses are also shown in Table 6.3.3.

Table 6.3.3 Summary of maximum connection forces.

| | Short Direction | | | Long Direction | | |
|---|---|---|---|---|---|---|
| | Ratio of maximum to average connection force | | geometric eccentricity (percentage of width of building)[1] | Ratio of maximum to average connection force | | geometric eccentricity (percentage of width of building) |
| | AS1170.4 1993 | Response Spectrum | | AS1170.4 1993 | Response Spectrum | |
| 2 storey vacant city commercial building (EE2) - reg | 1.05 | 1.00 | 0 | 1.05 | 1.00 | 0 |
| 2 storey vacant city commercial building (EE3) - reg | 1.09 | 1.14 | 1.6 | 1.05 | 1.00 | 0 |
| 2 storey vacant city commercial building (EE4) - reg | 1.10 | 1.10 | 2.4 | 1.05 | 1.00 | 0 |
| 3 storey school building (CBC) - irreg | 1.13 | 1.13 | 3.4 | 1.00 | 1.21 | 24.7 |
| 2 storey city social club (IAC) - irreg | 1.16 | 1.60 | 4.5 | 1.08 | 1.82 | 1.0 |
| 3 storey city commercial building (LTI) - reg | 1.05 | 1.32 | 0 | 1.05 | 1.54 | 0 |
| 2 storey city commercial building (NSC) - reg | 1.12 | 1.35 | 3.8 | 1.05 | 1.07 | 0 |
| 2 storey city retail building (STP) - reg | 1.05 | 1.18 | 0 | 1.05 | 1.04 | 0 |
| 5 storey university office building (OLW) - irreg | 1.06 | 2.03 | 0.4 | 1.07 | 2.90 | 0.6 |
| 2 storey suburban apartment building (KIDA) - irreg | 1.16 | 1.38 | 4.7 | 1.10 | 1.50 | 4.0 |
| 2 storey suburban apartment building (KIDB) - irreg | 1.09 | 1.53 | 2.0 | 1.07 | 1.27 | 3.4 |

[1] geometric eccentricity is the difference between the shear centre and the centre of mass

For the buildings where the centre of mass and the shear centre coincide AS1170.4 specifies a minimum "accidental" eccentricity of five percent of the plan dimension of the building in the direction perpendicular to the direction under consideration. This resulted in the maximum connection force being five percent greater than the average connection force for these buildings when the building only has two external walls. The response spectrum analysis did not take into account this "accidental" eccentricity and as such had maximum connection forces equal to the average where the contributing modes were purely lateral. When a torsional response was included as one of the modes that are combined using the CQC technique then the maximum connection force will be greater than the average connection force.

For the buildings where the shear centre and the centre of mass did not coincide the ratio of maximum connection force to average connection force for the response spectrum analysis results was greater than that for the AS1170.4 results. This suggested that the AS1170.4 analysis procedure may have underestimated the effect of the torsional component of the response of the buildings to earthquake ground motion. The maximum connection force was nearly three times greater than the average connection force for the OLW building. Building IAC, which had the largest eccentricity of all the buildings in the study, had the next largest increase in connection force of up to eighty percent. The increase was generally less than fifty percent of the average connection force for the rest of the buildings in the study.

Table 6.3.3 also gives the geometric eccentricities for the buildings in the study. This was the distance between the shear centre and the centre of mass expressed as a percentage of the width of the building. It can be seen in Table 6.3.3 that there seemed to be no correlation between the geometric eccentricity of the building and the differences between the ratio of the maximum connection force to the average connection force for the two analysis methods examined.

Comparing the lower maximum connection force to the higher base shear predicted by the AS1170.4 analysis method to the response spectrum method it could be seen that the higher base shear for the AS1170.4 analysis would, for the majority of the buildings in the study, ensure that the connection forces calculated by the AS1170.4 method would be greater than the maximum connection forces calculated by the response spectrum analyses. The only exceptions were for building OLW and for building KIDB in the short direction.

### 6.3.5 Out-of-Plane Effects

The last structural response to be compared and one of the most critical was the out-of-plane wall bending. It has already been seen in Chapter 5 that applying earthquake induced forces to some of the buildings in the study resulted in stress levels in the upper walls exceeding the estimated tensile capacity of the brickwork.

The analysis of earthquake forces on out-of-plane walls is given in Section 5.2 of AS1170.4. The inertia force to be applied to a wall is given by the formula:

$$F_p = aSa_c a_x C_{cl} I G_c \leq 0.5 G_c \qquad (6.3.1)$$

where:

| | | |
|---|---|---|
| $a$ | = | Acceleration coefficient, as per Equation 6.2.1; |
| $S$ | = | Site factor, as per Equation 6.2.1; |
| $a_c$ | = | Attachment amplification factor, a variable that takes into account the flexibility of the connection between the component and the building. For the case of out-of-plane walls it would be equal to 1.0; |
| $a_x$ | = | The height amplification factor as given in Equation 6.3.3; |
| $C_{cl}$ | = | Earthquake coefficient for architectural components. For non-ductile out-of-plane walls it is 1.8; |
| $I$ | = | Importance factor, as per the one in Equation 6.2.1; and |
| $G_c$ | = | Weight of the component. |

For a firm soil site in Adelaide Equation 6.3.1 simplifies to:

$$F_p = 0.18 a_x G_c \leq 0.5 G_c \qquad (6.3.2)$$

The height amplification factor is given as:

$$a_x = 1 + \frac{h_x}{h_n} \qquad (6.3.3)$$

where $h_x$ is the height above the base of the structure at which the component is attached and $h_n$ is the total height above the base of the structure. Dividing Equation 6.3.1 by the weight of the component yields the acceleration applied to the component. The acceleration of an out-of-plane wall versus the height of the wall

above the base of the wall (expressed as a percentage of the total height) is plotted in Figure 6.3.1.

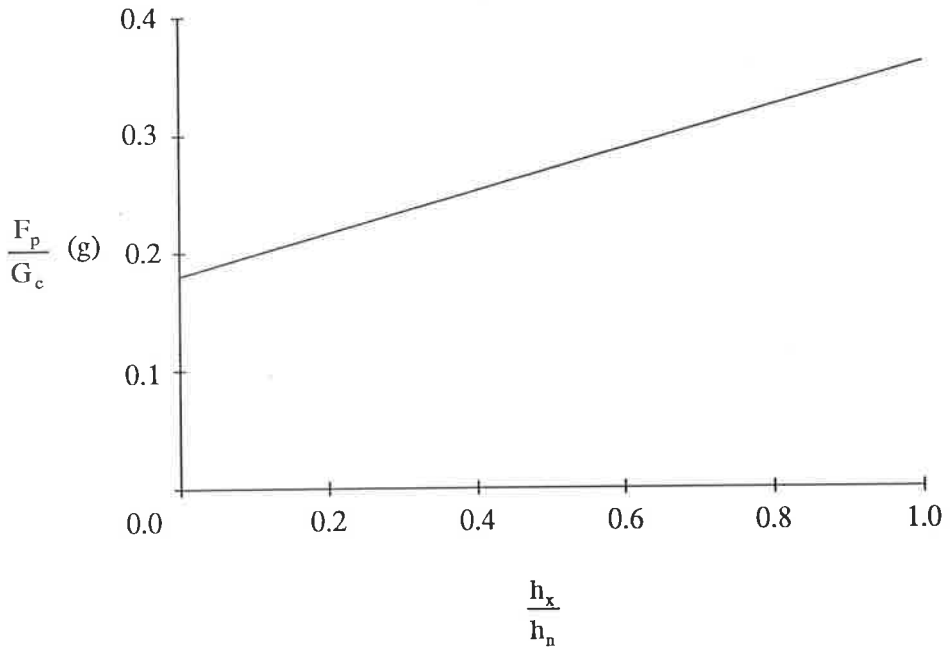


Figure 6.3.1 Plot of component acceleration versus relative height.

Examining Figure 6.3.1 it can be seen that for an out-of-plane wall attached to the building at ground level the level of acceleration applied to the building is 0.18 g compared to 0.1 g for the building structure and the maximum level of acceleration that an out-of-plane wall can be subjected to is 0.36 g. This acceleration is to be applied through the centre of mass of the wall.

The analysis of a brick wall subjected to out-of-plane forces can be undertaken by two simple methods. Firstly, the wall can be analysed as a plate element subjected to a point load at the centre of mass of the wall. The wall could then be taken to be in either one or two way bending, depending on the height to width ratio of the wall panel. The height is the storey height and the width is the width between points of support for horizontal bending. Traditionally, one way action is deemed to be applicable when either the height or the width is twice the perpendicular dimension. Design tables can then be used to determine the bending moments and bending stresses in the wall.

The second method requires the wall to be broken down into smaller sub walls. The design acceleration is then applied through the centroid of these new sub walls. As the number of sub walls approaches infinity the out-of-plane forces become a distributed load over the area of the wall, a similar situation to that of lateral wind loading on the wall. The Australian Standard, "SAA Masonry Code" AS3700-1988 has provision for the determination of the lateral wind load capacity and this can then be used to determine whether the wall's capacity is exceeded.

The vertical bending capacity of an unreinforced masonry wall is given in AS3700 as the lesser of:

$$M_{cv} = C_m f'_{mt} Z_d + f_d Z_d \tag{6.3.4}$$

and

$$M_{cv} = 3.0 C_m f'_{mt} Z_d \tag{6.3.5}$$

where:

| | | |
|---|---|---|
| $C_m$ | = | A capacity reduction factor given as 0.6; |
| $f'_{mt}$ | = | The characteristic flexural tensile strength of masonry, given as 0.2 MPa for masonry not subjected to axial tension; |
| $Z_d$ | = | The section bending modulus; and |
| $f_d$ | = | The minimum design compressive stress on the bed joints of the masonry at the cross section under consideration. |

The horizontal bending capacity of an unreinforced masonry wall is given in AS3700 as the lesser of:

$$M_{dh} = 2.0 C_m K_p \sqrt{f'_{mt}} \left(1 + \frac{f_d}{f'_{mt}}\right) Z_d \tag{6.3.6}$$

$$M_{dh} = 4.0 C_m K_p \sqrt{f'_{mt}} Z_d \tag{6.3.7}$$

and

$$M_{dh} = C_m (0.44 f'_{ut} r_z + 0.56 f'_{mt}) Z_d \tag{6.3.8}$$

where, in addition to the definitions for terms given for Equations 6.3.4 and 6.3.5:

$K_p$ = A perpend spacing factor;

$f'_{ut}$ = The characteristic lateral modulus of rupture of the masonry units; and

$r_z$ = The ratio of the lateral section modulus of the masonry units per millimetre of height to the lateral section modulus of the perpend joints per millimetre height.

For the walls of the buildings in this study, the AS1170.4 out-of-plane forces were calculated and the resulting forces were compared to the capacity of the walls as calculated in accordance with AS3700. Only the top walls were checked as these were subjected to the highest accelerations and hence the highest out-of-plane forces (the $a_x$ factor is maximised for the top wall). The $a_x$ factor from Equation 6.3.1 was calculated for the mid height of the wall, as the wall is connected at two points to the building; at its top and base. It was considered then that the wall element would be subjected to the average of these two accelerations, which for the linear function shown in Figure 6.3.1, is equal to the force calculated using the mid height of the wall.

The majority of the walls in the buildings in the study acted in predominantly one way vertical bending as the restraints in the horizontal direction were usually widely spaced. The results of the AS1170.4 and AS3700 evaluation of the performance of the out-of-plane walls, summarised in Table 6.3.4, revealed that all of the walls acting in one way bending would be expected to fail in the event of the design magnitude earthquake. The only walls not expected to suffer out-of-plane failure were in OLW, for excitation in the short direction, in KIDA and KIDB for excitation in the long direction, and in EE2 for excitation in the long direction. The OLW walls did not fail because of the significant number of cross walls in this building making the walls act in two way bending. The KIDA and KIDB did not fail because they have height to width ratios that allow them to act in two way bending. The EE2 walls also did not failure because the height to width ratio ensures two way action.

In comparison with the results of the response spectrum analysis (Section 5.6), it can be seen that the AS1170.4 equivalent lateral force analysis predicted more of the buildings to experience out-of-plane bending failures. This could be due to the requirements of AS3700 introducing a capacity reduction factor, $C_m$, that was not used in the evaluation of the bending stresses in the response spectrum analyses. This

lowered the allowable tensile stresses and subsequently increased the number of walls that were likely to experience out-of-plane failures. It should be noted that according to the AS1170.4 analysis the level of acceleration expected in the top level of the six storey OLW building is the same as that for the AS1170.4 analysis of the two storey KIDA building ($F_p$ is not proportional to the total height of the building - see Equation 6.3.3).

Table 6.3.4 Summary of Out-of-Plane Tensile Stresses for AS1170.4 and Response Spectrum Analyses.

| | Maximum Out-of-Plane Tensile Stress (including dead load stress) (MPa) | | | |
|---|---|---|---|---|
| | AS1170.4 Analyses | | Response Spectrum Analyses | |
| | Short Direction | Long Direction | Short Direction | Long Direction |
| 2 storey vacant city commercial building (EE2) - reg | 0.20[1] | 0.08 | 0.10 | 0.077 |
| 2 storey vacant city commercial building (EE3) - reg | 0.20[1] | 0.18[1] | 0.34 | 0.62 |
| 2 storey vacant city commercial building (EE4) - reg | 0.20[1] | 0.18[1] | 0.36 | 0.16 |
| 3 storey school building (CBC) - irreg | 0.21 | 0.25 | 0.05 | 0.02 |
| 2 storey city social club (IAC) - irreg | 0.28 | 0.30 | 0.07 | 0.02 |
| 3 storey city commercial building (LTI) - reg | 1.40 | 1.40 | 0.01 | 0.02 |
| 2 storey city commercial building (NSC) - reg | 0.37 | 0.52 | 0.28 | 0.25 |
| 2 storey city retail building (STP) - reg | 0.33 | 0.51 | 1.05 | 0.01 |
| 5 storey university office building (OLW) - irreg | 0.05 | 0.75 | 0.04 | 0.04 |
| 2 storey suburban apartment building (KIDA) - irreg | 0.15[1] | 0.11 | 0.05 | 0.06 |
| 2 storey suburban apartment building (KIDB) - irreg | 0.15[1] | 0.11 | 0.22 | 0.46 |

[1] Value exceeds AS3700 design stress ($C_m f'_{mt}$) but not AS3700 tensile strength ($f'_{mt}$)

# 6.4 SUMMARY OF CODE BASED ANALYSES

Comparing the two sets analyses for each building it was seen that generally the code based method predicted higher levels of force and stress than the response spectrum method.

The first aspect of the code based analysis procedure to be examined was the natural period. The natural periods calculated by the code based formulae and the response spectrum analysis have already been discussed in Chapters 3 and 5.

For all of the buildings in the study, the AS1170.4 code based analyses resulted in a greater base shear than that obtained from the response spectrum analyses. A similar situation occurred for the storey shears, except for two buildings where the response spectrum analyses distributed a larger proportion of the base to the upper floors than the AS1170.4 analysis. One of these cases was the OLW building. The other case was for a building that had an extremely irregular plan (IAC) and a smaller upper floor than lower floor. The larger base shear predicted by the code based analysis ensured, however, that the storey shears calculated by AS1170.4 were greater than the storey shears calculated by the response spectrum method for all but two buildings.

The connection force calculations for the in-plane walls were based on the storey shears. Hence, the average connection force, being the storey shear divided by the total length of in-plane walls on a floor, was always greater for the AS1170.4 analyses than the response spectrum analyses. However, the average connection forces were increased due to torsional effects to create local maximum forces. Two of the buildings in the study had a greater maximum connection force from the response spectrum analysis than the AS1170.4 analysis, even taking into account the greater base shears associated with the code based analyses. One was the OLW building which, as discussed previously, had a greater number of storeys than is allowed by the code for unreinforced masonry building. The other was the KIDB building, where the maximum connection force was thirty percent greater for the response spectrum analysis than the code analysis even though the base shear associated with the response spectrum analysis was six percent lower than the code base shear force.

The last comparison made was for out-of-plane failures of the walls. In all cases the AS1170.4 analyses resulted in larger values of stress than the response spectrum analyses.

## 6.5 REFINED CODE BASED ANALYSIS

From this work, it appeared that the analysis procedure in AS1170.4 was sufficient to ensure a conservative design for the majority of unreinforced masonry buildings. It was, however, complicated by the fact that it was applicable for a wide variety of building types and as such has a number of variables that for the case of an unreinforced masonry building were constants. In order to simplify the requirements of the code a number of refinements could be considered. The results for the OLW building were ignored in this section as the building did not comply with the requirement of the code that limited unreinforced masonry buildings to be less than or equal to three storeys.

Firstly, considering the code formula for base shear and the effect of the building's natural period on the calculated base shear (Equation 6.2.1). Every unreinforced masonry building in the study had natural periods for both major axes, from both the ambient vibration tests (Chapter 3) and by calculation by the code period formulae (Equations 2.1.1 and 2.1.2), that placed them in the constant acceleration region of the design response spectra (Figure 5.2.1). This resulted in the base shear for the buildings in the study being independent of the site factor, S, since the only effect S had on the constant acceleration region of the response spectrum curve was to extend the length of the plateau from T = 0.35 seconds for S = 1.0 to T = 1 second for S = 2.

Assuming that all unreinforced masonry buildings have a natural period that places them on the constant acceleration region of the design response spectrum resulted in a simplification of the base shear formula. The design base shear of a unreinforced masonry buildings became independent of the natural period of a building, T, the site factor, S, and the design coefficient, C. Further, for unreinforced buildings the response modification factor, $R_f$, is 1.5. The base shear formula from AS1170.4 (Equation 6.2.1) then reduced to:

$$V = 1.667 I a G_g \qquad (6.5.1)$$

This compared with the requirement for a "domestic" structure in the code where the design base shear is $0.15G_g$ which meant that an unreinforced masonry "domestic" structure (as defined in AS1170.4) is allowed to be designed for a slightly lower base shear force than an unreinforced masonry "general" structure.

Whether the use of unreinforced masonry construction is suitable for buildings that have a post disaster function given the poor performance of unreinforced masonry buildings in past earthquakes is beyond the scope of this study. However, it can be seen from the results of the response spectrum analysis and from reports of the performance of recently built unreinforced masonry construction that it is possible to design and detail an unreinforced masonry building to perform adequately in design magnitude earthquakes in regions of low to moderate earthquake hazard. Whether it is possible to design and detail unreinforced masonry buildings economically to be able to function after an earthquake is another matter that requires further investigation. In the meantime, the importance factor, I, can be retained as a variable in Equation 6.5.1 and the formula could possibly be used for AS1170.4 Type III structures.

The distribution of the base shear force up the height of the building for subsequent design can be undertaken using Equation 6.2.4. For unreinforced masonry buildings k = 1.0 as all of the measured and calculated building periods were less than 0.5 seconds. Equation 6.2.4 then reduces to:

$$C_{vx} = \frac{G_{gx} h_x}{\sum_{i=1}^{n} G_{gi} h_i} \qquad (6.5.2)$$

where $C_{vx}$, $G_{gi}$, and $h_i$ are as defined for Equation 6.2.4.

The storey shears are distributed to the walls as in-plane connection forces and shear stresses using general structural mechanics. Whether the storey shears are transmitted through the floor slabs into the walls or down the outside walls without using the floor slab depends upon whether the detail at the floor-wall connection was Type I or Type II from Figure 5.1.1. The increase in some of the wall shear stresses and the in-plane connection forces due to torsion in the building response can be taken into account by increasing the average connection force and shear stresses by thirty percent. This brings the torsional effects requirements for unreinforced masonry buildings in line with the general requirements for AS1170.4 Type I regular structures with shear resisting elements without static eccentricity. A limit to the type

of structure that can be analysed using this requirement would be needed to prevent buildings such as IAC from being analysed using this simple rule, though the rule could be less restrictive than AS1170.4's "regular" and "irregular" distinction.

The out-of-plane connection force can be calculated using the AS1170.4 equation (10aS kN/m run of wall). As was already noted the acceleration applied to the buildings in the study are independent of the site factor, S. This meant that the results for the response spectrum method will not change with a change in the site factor and the out-of-plane connection force will be independent of the site factor. This meant that the site factor, S, could be removed from the connection force formula for consistency with the calculated base shear. Applying this to the connection force formula resulted in:

$$\text{force} = 10a \text{ kN per metre of wall} \qquad (6.5.3)$$

where a is as was defined for Equation 6.2.1. However, as will be discussed in Chapter 7, the removal of the site factor from the base shear formula may be inappropriate based on the observations in recent earthquakes. On this basis, the site factor probably should be kept in Equation 6.5.3.

The out-of-plane bending forces in the walls can be best determined using the AS1170.4 requirements. The out-of-plane inertia force on an unreinforced masonry wall is given by:

$$F_p = 1.8a\left(1+\frac{h_x}{h_n}\right)G_c \qquad (6.5.4)$$

where the variables are as defined for Equations 6.3.1 and 6.3.3. The capacity of the wall to resist this out-of-plane force can be checked using the lateral wind loading requirements of AS3700.

This procedure should ensure that an unreinforced masonry building is accurately designed for the forces induced in the structure by an earthquake that can be represented by the design response spectra. Whether the shape of the current design response spectra is appropriate for Australia and whether the constant acceleration region of the response spectra should be independent of the site factor for non-ductile structures are questions that require further attention.

# 7 SUMMARY AND CONCLUSIONS

## 7.1 SUMMARY

The overall aim of this project was to provide the tools for an engineer to use with confidence to design an unreinforced masonry building to perform acceptably when subjected to earthquake ground motion.

This was accomplished by firstly undertaking a series of ambient vibration tests on unreinforced masonry buildings in Adelaide. The ambient vibration tests involved recording the vibrations induced in a structure due to wind, traffic, and other common low levels of excitation. The recorded vibrations were then converted from the time domain to the frequency domain using a Fourier Transform. From frequency domain plots, the natural periods were identified. The measured natural periods of the buildings were then compared to the natural periods estimated using period formulae from various earthquake codes from around the world, including The Australian Standard "Minimum design loads on structures - Part 4 : Earthquake Loads" AS1170.4-1993. It was found that none of the period formulae considered had a very high level of fit. Of particular interest here were the formulae included in the Australian Earthquake Code (Equations 2.1.1 and 2.1.2). The fit the ambient test data, $R^2$, to these forms of period formula were 67 percent for buildings with concrete floors, 9 percent for the buildings with timber floors, and 53 percent for all the buildings in the study. This level of fit was as good as for any of the other period formulae examined. It was further noted that using the measured periods in conjunction with the Australian Earthquake code requirements and the design response spectrum (Figure 5.2.1) meant that the periods of all buildings were in the constant acceleration region of the design response spectra.

The next part of the study involved undertaking shaking table tests of unreinforced brick masonry wall panels to determine a realistic value for the dynamic in-plane shear stiffness of a brickwork wall panel. This stiffness was subsequently used in finite element modelling of the buildings from the first part of the study. The experimental test procedure was based on that used in a similar study on block and brick masonry in the United States. The shaking table tests were used to study the effect of axial stress, rate of loading (the excitation frequency), and panel geometry of the on the dynamic in-plane stiffness. It was found from the tests that increased axial compressive stress increased the dynamic in-plane stiffness. This confirmed results of other researchers. Unfortunately, material and workmanship variability between the panels masked any relationship between the dynamic in-plane stiffness and frequency of loading. The observed changes in the dynamic in-plane stiffness with changes in testing panel geometry were not consistent with classical structural theory, possibly due to material and workmanship variability. Finally, the dynamic in-plane stiffness of the panels were noted to be consistent with the values from shaking tests conducted in the United States.

The shaking table test panels were then modelled using the finite element method. The walls were modelled as a one phase material model (brick and mortar combined as one type of material) rather than a two phase (brick and mortar as individual phases) model. The finite element model was calibrated to establish an effective Young's Modulus for a one phase material model for use in subsequent one phase modelling of the buildings from the first part of the study. The most important result from the shaking table tests was that the calibrated value for Young's Modulus (1065 MPa) was considerably less than that commonly accepted for design in Australia. This has also been observed by Australian and overseas researchers where values of Young's Modulus for brickwork of approximately 1000 MPa have been reported.

The results from the first two parts of the study were then used in the final part of the study where response spectrum analyses of the buildings from the first part of the study were carried out. The stiffness for the walls of the buildings were based on the results of the shaking table tests noted above. The buildings were modelled using the finite element method. Double leaf walls were modelled using an equivalent single leaf plate element. Equivalent stiffness properties (Young's Modulus, Poisson's Ratio, and wall thickness) were calculated for the single element to model the properties of a double leaf wall, namely the cross sectional area, and the bending and shear stiffness. It was found that, without modification, the bending stiffness was overestimated by a factor of two.

The building models were subjected to a response spectrum analyses using the design response spectrum from The Australian Standard "Minimum design loads on structures - Part 4 : Earthquake Loads" AS1170.4-1993. The base shears, storey shears, bending stresses, connection forces, and drifts of each building were then examined. It was found that, in general, the required connection strength between the floor slab and the walls of each building could be provided, in practice. The calculated shear stresses were also found to be within the generally accepted capacities for unreinforced masonry walls. However, the maximum wall bending stress results suggested that some out-of-plane failures could be expected in the upper walls of some buildings. This was consistent with the observations of earthquake damage to many of the damaged unreinforced masonry buildings in past earthquakes.

The results of the response spectrum analyses were then compared to the results of equivalent static force analyses undertaken using the static force analysis procedures given in AS1170.4. It was found that the AS1170.4 procedures were generally conservative with regard to the results of the response spectrum analyses. The AS1170.4 estimates of the building periods placed all buildings, except the six storey building, in the constant acceleration region (for S = 1) of the design response spectrum as did the measured periods. It was therefore concluded that for seismic design based upon the design response spectrum in AS1170.4, the natural period calculation for an unreinforced building is not necessary. It was also noted that soft soil effects are implicitly deemed not to be important in the constant acceleration region of the design response spectrum since the design base shear calculations are independent of S in this region.

Evidence from recent earthquakes, including the 1989 Newcastle Earthquake (Newcastle Earthquake Study(1990)) suggested that the soil type does play a significant part in determining the level of force to which a structure in an earthquake is subjected. The exclusion of soil effects from the determination of the base shear may be acceptable for ductile structures. As a ductile structure is loaded, cracking occurs, resulting in a decrease in structural stiffness, an increase in building period, and therefore, a reduction in the induced design load as the change in period decreases the applied acceleration as it moves to the right on the design response spectrum and off the constant acceleration region. For a brittle structure, such as am unreinforced masonry building, cracking denotes a failure of the structure and the period shift cannot occur. This point may need to be investigated further.

While the AS1170.4 procedure was found to give consistently larger estimates for base shear, storey shear, and bending stress values obtained from the response spectrum analyses, the code based analysis was not always conservative with respect to the response spectrum analyses in accounting for torsional effects. Even taking into account the larger base shear values which were obtained from the code analysis, the maximum connection forces in some buildings were greater for the response spectrum analysis than for the code based analysis.

In light of the above results, refinements to the AS1170.4 equivalent static force analysis procedure were considered. It was based on the following assumptions:

(1) The response spectrum from the code was appropriate for use in Australia;

(2) The buildings were founded on firm soil sites such that the site factor was at least 1.0 (the refined procedure could be used for a site factor that is less than 1.0 as the procedure then becomes conservative); and

(3) The appropriate response modification factor for unreinforced masonry, $R_f$, was 1.5.

The amended design base shear value was then given by Equation 6.5.1 and is reproduced below:

$$V = 1.667 I a G_g \qquad (6.5.1)$$

where I, a, and $G_g$ are as defined in AS1170.4. The base shear can be distributed up the building according to the formula given in AS1170.4 using k = 1.0 (Equation 6.5.2). The torsional component of the response can be catered for by increasing the maximum calculated connection force by 30 percent.

The out-of-plane connection force was found to be accounted for using a modified connection force requirement from AS1170.4:

$$\text{force} = 10a \text{ kN per metre of wall} \qquad (6.5.3)$$

The out-of-plane bending stresses were also calculated based on the formula given in AS1170.4. The formula was simplified to Equation 6.5.4 shown below:

$$F_p = 1.8a\left(1+\frac{h_x}{h_n}\right)G_c \qquad (6.5.4)$$

This procedure should ensure an improved level of performance for the majority of unreinforced masonry buildings in Australia.

# 7.2 CONCLUSIONS

The results of this study suggest that it is possible to design and detail unreinforced masonry buildings to perform to an acceptable level during the moderate levels of earthquake excitation expected in Australia. However, attention to detail and supervision of the workmanship during construction are clearly important to ensure that a masonry building will perform as intended during earthquake excitation.

Some of the major findings of this study are:

(1) The natural period of most unreinforced masonry buildings is such that it falls in the constant acceleration region of the design response spectrum;

(2) The dynamic stiffness of an unreinforced masonry brickwork wall is an order of magnitude less than the accepted value used in design for static forces. Experimental results indicate values of Young's Modulus, E, of approximately 1000 MPa would be appropriate;

(3) A finite element model using a single "equivalent" element can be used to model double leaf brick masonry walls;

(4) The design procedure included in The Australian Standard "Minimum design loads on structures - Part 4 : Earthquake Loads" AS1170.4-1993 can be used for the design of unreinforced masonry buildings for earthquake induced forces. The torsional requirements of the code may need to be increased by about 30 percent to account for increased wall stresses due to the torsional response of the building; and

(5) The design procedures in AS1170.4 can easily be simplified to reflect the particular properties of unreinforced masonry and unreinforced masonry buildings.

# 7.3 FUTURE WORK

The results of this study can be applied to the design of unreinforced masonry buildings to improve its performance when subjected to earthquake excitation. However, further research is needed in some areas to further improve the understanding of the performance of unreinforced masonry buildings in earthquakes and to allow more accurate models of the behaviour to be developed.

In terms of masonry, further work is required to verify the design strength for use in seismic design. The dynamic stiffness of a wall panel has been found in this study to be less than the static stiffness. Whether similar effects are evident for the strength of masonry walls under dynamic and static loading requires further investigation. Experimental investigations to determine the expected strength of typical floor-to-wall connections under in-plane and out-of-plane loading is also required.

For the earthquake part of study, much work is needed to develop a design response spectrum for Australia based on Australian intra-plate earthquake data. Until a statistically significant set of actual intraplate earthquake ground motions are obtained. however, this can not be done. In the meantime, the whole area of Australian earthquake research and design is heavily dependant on the assumption of the type of ground motion that can be expected.

The use of the site factor, S, in the AS1170.4 needs examination. For example, an unreinforced masonry building on soft soil, according to the current code, must be designed for the same base shear, and hence connection forces, out-of-plane forces, and shear stresses as the same building constructed on a stiff clay. This does not seem to be consistent with observations of earthquake damage around the world.

# APPENDIX A - SAMPLING THEOREM

The sampling Theorem can be stated as:

*"It is necessary to take more than two points per cycle of the highest significant frequency component in a signal in order to recover that signal"*

This means that if a signal f(t) is sampled at times t = -2T, -T, 0, T, 2T, and so on, at a rate of $1/T = f_s$ samples per second, the frequency components of the signal greater than $f_s/2 = 1/2T$ cycles per second cannot be distinguished from the frequencies in the range of 0 to $f_s/2$ cycles per second.

# APPENDIX B - BUILDING DETAILS

In this appendix the details of the buildings studied in Chapter 3 and subsequently modelled in Chapters 5 and 6 are presented. The plans of the buildings are shown in Figures B.1 to B.9. The dimensions given in the plans are in millimetres. The plans are not necessarily to scale. The information on the buildings was gained from site visits and from the archives of the City of Adelaide where the building plans and building submissions are stored.

# B.1 EAST END MARKET BUILDINGS (EE2, EE3, AND EE4)

The three buildings from the East End market complex are shown in Figure B.1.

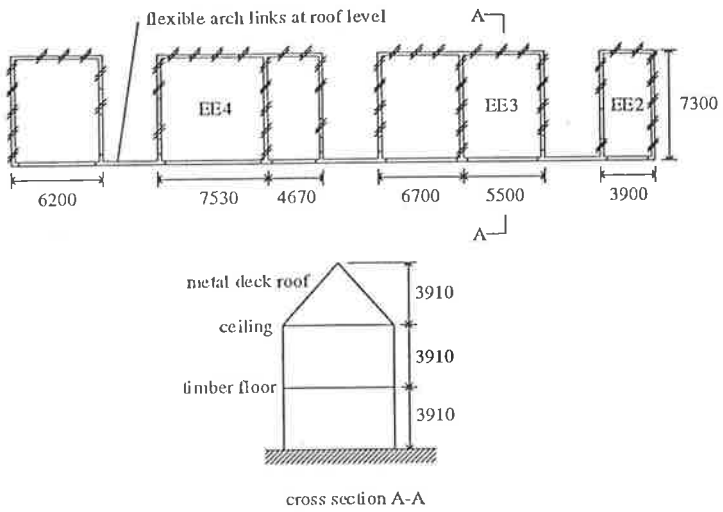


Figure B.1 Plans of buildings EE2, EE3, and EE4.

The East End Market buildings were constructed in the early 1900's from clay brick with a stone work facade. The three buildings were linked by a flexible masonry arch link at the roof level. It was considered that the links would not be stiff enough to provide a significant restraint to the walls of the buildings. All three buildings were of similar construction, the details of which are given in Table B.1.

Table B.1 Details of EE2, EE3, and EE4 construction.

| Number of Storeys | 2 |
|---|---|
| Construction of Suspended Floors | Timber joist with 140 mm thick timber floor boards |
| Construction of Roof | Timber frame with metal decking |
| Construction of External Walls | Double leaf brickwork without articulation |
| Construction of Internal Walls | Single leaf brickwork without articulation |
| Footing Type | Concrete strip footings |
| Soil Type | Clay |
| Stair and Lift Details | Timber stairs in EE2 and EE3, metal stairs in EE4 |

# B.2 WARD RESIDENCE (WARD)

The plan of the Ward Residence is shown in Figure B.2.

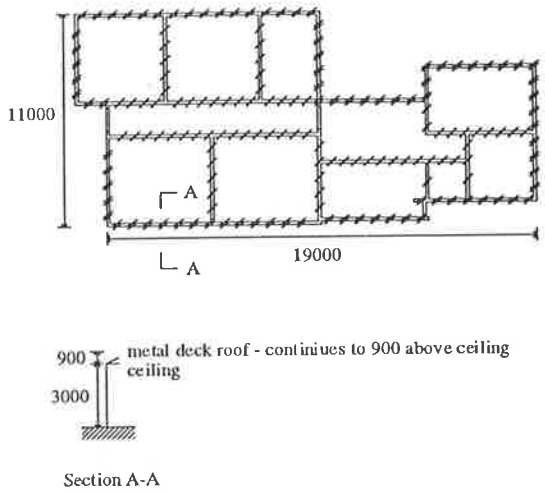


Figure B.2 Plan of building WARD

The Ward Residence was constructed in 1881. An addition was added to the rear of the house at a later date. The details of the construction are given in Table B.2.

Table B.2 Details of WARD construction.

| | |
|---|---|
| Number of Storeys | 1 |
| Construction of Suspended Floors | none |
| Construction of Roof | Timber frame with metal decking |
| Construction of External Walls | 13 inch bluestone for original building and double leaf brickwork without articulation for extension |
| Construction of Internal Walls | Single leaf brickwork without articulation |
| Footing Type | None on the original building, raft footing on the extension. |
| Soil Type | Clay |
| Stair and Lift Details | none |

# B.3 CHRISTIAN BROTHERS COLLEGE BUILDING (CBC)

The plan of the classroom block CBC is shown in Figure B.3

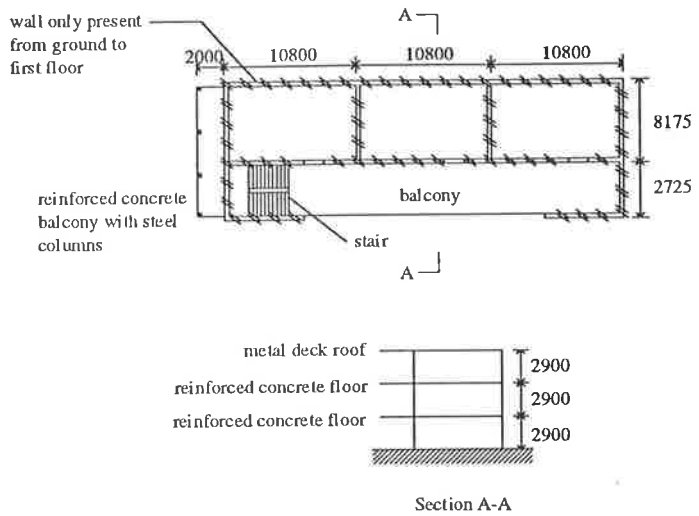


Figure B.3 Plan of building CBC

The Christian Brothers College classroom is a typical 1960's Adelaide building. It consists of a flat concrete slabs supported by masonry walls. One of the main walls of the building is present from the ground floor to the first floor only. Above this, the wall is replaced by windows. The details of the building are given in Table B.3.

Table B.3 Details of CBC construction.

| Number of Storeys | 3 |
|---|---|
| Construction of Suspended Floors | Flat 150 mm thick reinforced concrete slabs. |
| Construction of Roof | Metal deck with steel framing. |
| Construction of External Walls | Double leaf brickwork without articulation. |
| Construction of Internal Walls | Single leaf brickwork without articulation |
| Footing Type | Raft footing. |
| Soil Type | Clay |
| Stair and Lift Details | Reinforced concrete. |

# B.4 IRISH AUSTRALIA CLUB BUILDING (IAC)

The plan of the Irish Australia Club building is shown in Figure B.4.

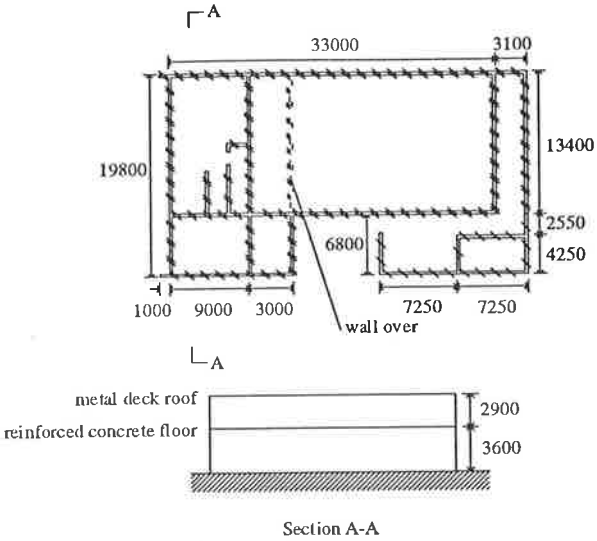


Figure B.4 Plan of building IAC.

The Irish Australia Club building consists of two parts. The front part of the building is a 2 storey building, and the rear part is a single storey meeting hall. The details of the building are given in Table B.4.

Table B.4 Details of IAC construction.

| | |
|---|---|
| Number of Storeys | 2 |
| Construction of Suspended Floors | Flat 160 thick reinforced concrete slab. |
| Construction of Roof | Metal deck with steel framing. |
| Construction of External Walls | Double leaf brickwork without articulation. |
| Construction of Internal Walls | Single and double leaf brickwork without articulation |
| Footing Type | Raft footing. |
| Soil Type | Clay |
| Stair and Lift Details | Reinforced concrete. |

# B.5 LEIGH TRUST INCORPORATED BUILDING (LTI)

The plan of the Leigh Trust Incorporated building is shown in Figure B.5.

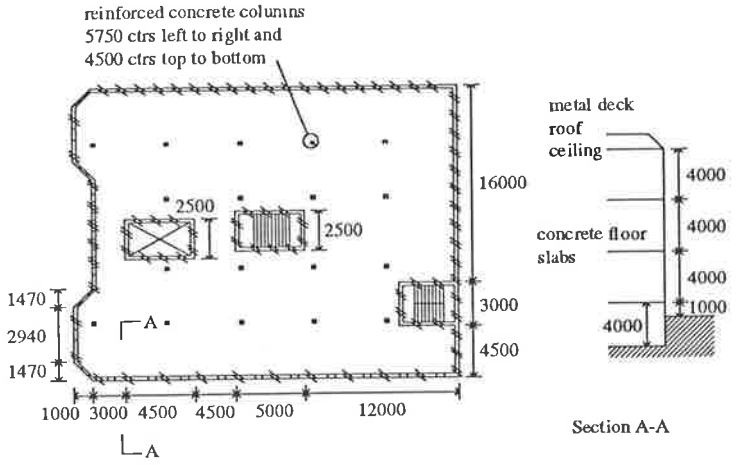


Building B.5 Plan of building LTI

The Leigh Trust Incorporated building consists of a box structure with internal reinforced concrete columns supporting a flat concrete slab. The interior also has two stair wells and a lift shaft. As part of a refurbishment in 1986 the building was checked for earthquake performance using the then current Australian Standard "SAA Earthquake Code" AS2121-1979. The details of the construction are given in Table B.5.

Table B.5 Details of LTI construction.

| | |
|---|---|
| Number of Storeys | 3 plus basement |
| Construction of Suspended Floors | Flat 100 thick reinforced concrete slab. |
| Construction of Roof | Metal deck with steel framing. |
| Construction of External Walls | Double leaf brickwork without articulation. |
| Construction of Internal Walls | none |
| Footing Type | Strip |
| Soil Type | Clay |
| Stair and Lift Details | Solid 125 mm walls on the lift shaft and stair wells with reinforced concrete stairs. |

# B.6 NOLAN SHANNON COMPANY BUILDING (NSC)

The plan of the Nolan Shannon Company building is shown in Figure B.6.

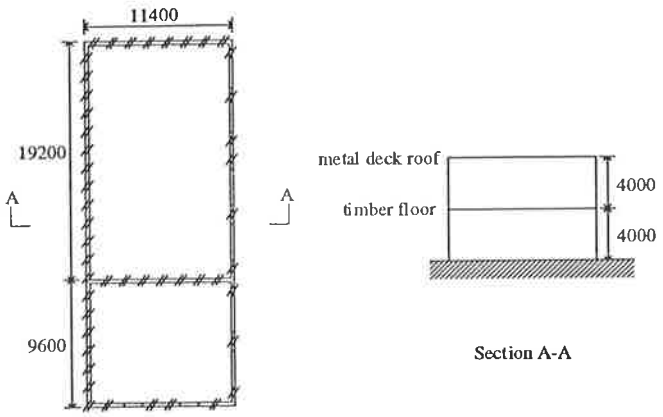


Figure B.6 Plan of building NSC

The Nolan Shannon Company building is a 1950's or 1960's warehouse type structure. A fire in the 1980's resulted in the rebuilding of part of the upper floor in concrete. The details of the building are given in Table B.6.

Table B.6 Details of NSC construction.

| | |
|---|---|
| Number of Storeys | 2 |
| Construction of Suspended Floors | Flat 110 thick reinforced concrete slab and traditional timber floor and joist. |
| Construction of Roof | Metal deck with timber framing. |
| Construction of External Walls | Double leaf brickwork without articulation. |
| Construction of Internal Walls | Single leaf brickwork without articulation. |
| Footing Type | Strip |
| Soil Type | Clay |
| Stair and Lift Details | Timber stairs. |

# B.7 SAINT PAULS BOOKSHOP (STP)

The plan of the Saint Pauls Bookshop is shown in Figure B.7.

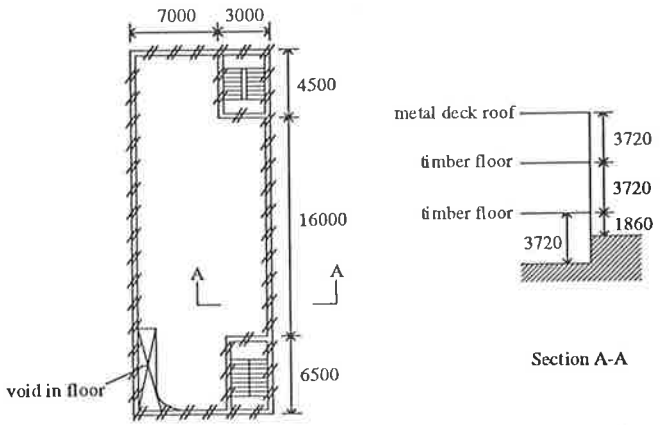


Figure B.7 Plan of building STP

The Saint Pauls Bookshop consists of timber suspended floors that have voids at one corner that result in the wall not having lateral support at these locations. The building also has a basement that is only partly underground. The details of the building are given in Table B.7.

Table B.7 Details of STP construction.

| | |
|---|---|
| Number of Storeys | 2 plus basement |
| Construction of Suspended Floors | Timber joist and floor board. |
| Construction of Roof | Metal deck with timber framing. |
| Construction of External Walls | Double leaf brickwork without articulation. |
| Construction of Internal Walls | none |
| Footing Type | Strip |
| Soil Type | Clay |
| Stair and Lift Details | Timber stairs. |

# B.8 OLIPHANT WING BUILDING (OLW)

The plans of the Oliphant Wing building is shown in Figure B.8.

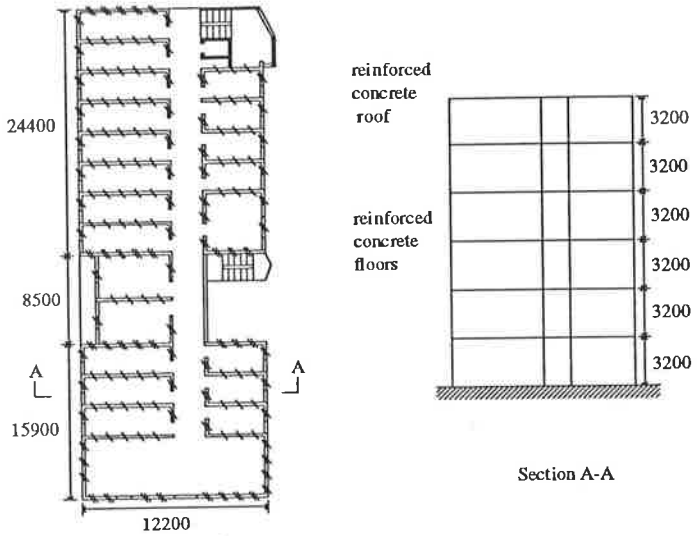


Figure B.8 Plan of building OLW

The Oliphant Wing building is a reinforced concrete flat slab on unreinforced masonry wall building designed in 1967. The building has an external staircase midway along its length and a reinforced concrete lift shaft at one end. The roof is also reinforced concrete. The details of the construction are given in Table B.8.

Table B.8 Details of OLW construction.

| Number of Storeys | 6 |
|---|---|
| Construction of Suspended Floors | 180 mm thick reinforced concrete flat slab. |
| Construction of Roof | 180 mm thick reinforced concrete flat slab. |
| Construction of External Walls | Double leaf brickwork without articulation. |
| Construction of Internal Walls | Single leaf brickwork without articulation. |
| Footing Type | Strip |
| Soil Type | Clay |
| Stair and Lift Details | Reinforced concrete stairs and reinforced concrete lift shaft. |

# B.9 KIDD UNITS (KIDA AND KIDB)

The plan of the Kidd Units is shown in Figure B.9.

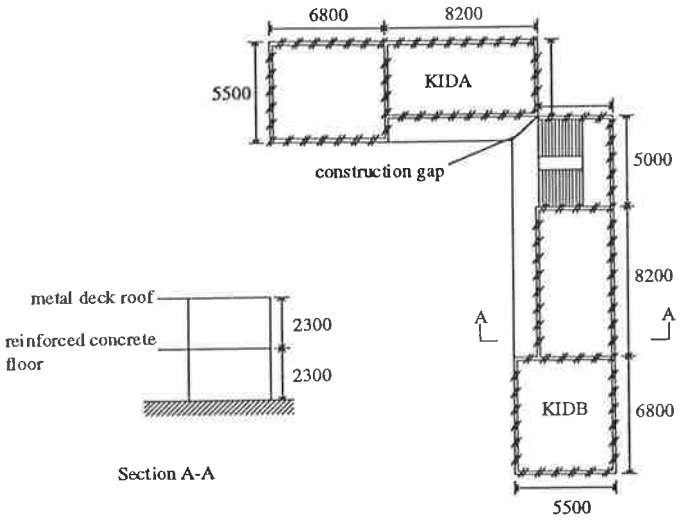


Figure B.9 Plan of KIDA and KIDB

The Kidd Units are two separate structures. The balconies meet but are separated by a construction joint. The two structures are of identical construction. The type of construction is typical of a number of units and apartment buildings in Adelaide. The details of the construction are given in Table B.9.

Table B.9 Details of KIDA and KIDB construction.

| Number of Storeys | 2 |
|---|---|
| Construction of Suspended Floors | 110 mm thick reinforced concrete flat slab. |
| Construction of Roof | Metal deck with timber framing. |
| Construction of External Walls | Double leaf brickwork without articulation. |
| Construction of Internal Walls | Double leaf brickwork without articulation. |
| Footing Type | Raft |
| Soil Type | Clay |
| Stair and Lift Details | Reinforced concrete stairs. |

# APPENDIX C - REGRESSION ANALYSIS

A regression analysis was performed on a set of data by minimising the square of the vertical distance between the data points and the regression line. The data was assumed to have non-constant variance. The weighting and regression analysis was based upon that contained in Ang and Tang (1975).

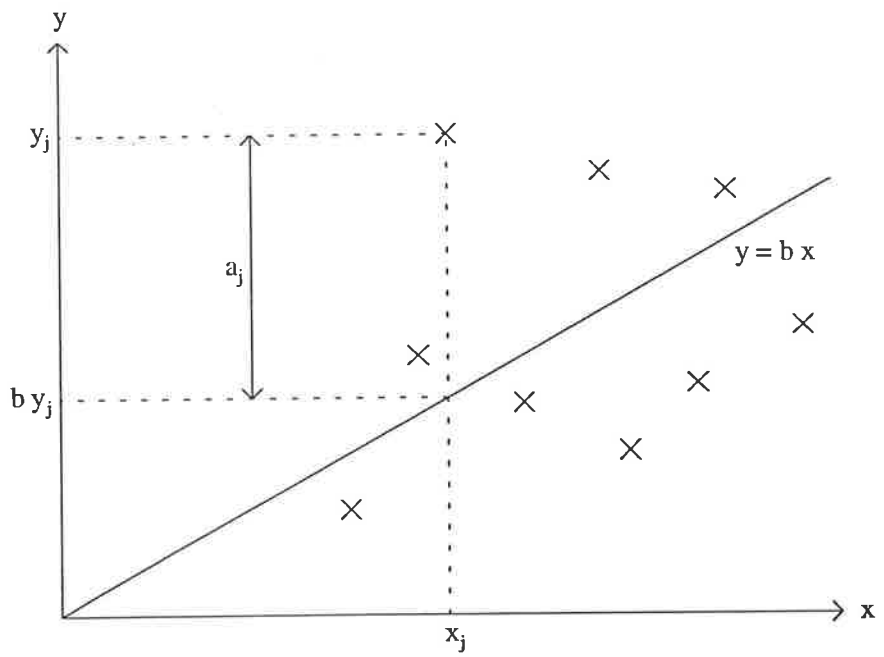


Figure C.1 Plot of data and regression line

Figure C.1 shows the linear regression line passing through the origin, y=bx, plotted along with a set of data. The vertical distance between the jth point of the data and the regression line is denoted as $a_j$ . The conditional variance about the regression line may be a function of the independent variable (x coordinate). The normal approach to the regression analysis is modified to take account of the variation in the conditional variance. The variation may be expressed as:

$$\mathrm{Var}(Y/x) = \sigma^2 g^2(x) \tag{C.1}$$

where g(x) is predetermined constant, and $\sigma$ is an unknown constant. In the case of this study it was assumed that the conditional standard deviation of the period (y axis) was assumed to increase linearly with the x value:

$$\mathrm{Var}(Y/x) = \sigma^2 x^2 \tag{C.2}$$

Thus:

$$w_i = \frac{1}{x_i^2} \tag{C.3}$$

To minimise the square of the vertical distance between the data point and the curve results in minimising:

$$q = \sum_{i=1}^{n} w_j a_j \tag{C.4}$$

substituting:

$$q = \sum_{j=1}^{n} \frac{1}{x_j^2}(y_j - bx_j)^2 \tag{C.5}$$

The minimum of q occurs when:

$$\frac{dq}{db} = 0 \tag{C.6}$$

and hence:

$$\frac{dq}{db} = -2\sum_{j=1}^{n} \frac{1}{x_j^2} x_j (y_j - bx_j) = 0 \tag{C.7}$$

$$\sum_{j=1}^{n} \frac{1}{x_j}(y_j - bx_j) = 0 \qquad (C.8)$$

$$\sum_{j=1}^{n} \frac{y_j}{x_j} - nb = 0 \qquad (C.9)$$

Therefore:

$$b = \frac{\sum_{j=1}^{n} \frac{y_j}{x_j}}{n} \qquad (C.10)$$

An unbiased estimate of the unknown $\sigma^2$ is:

$$s^2 = \frac{\sum w_j (y_j - bx_j)^2}{n-2} \qquad (C.11)$$

Hence, an estimate of the conditional variance is:

$$s_{Y/x}^2 = s^2 g^2(x) \qquad (C.12)$$

and:

$$s_{Y/x} = sg(x) \qquad (C.13)$$

With the conditional standard deviation used in this case:

$$s_{Y/x} = sx \qquad (C.14)$$

To calculate the confidence intervals, the students 't' distribution was used (Kreyzig (1983) and Ang and Tang (1975)). A one sided confidence interval was chosen, as explained in the text. The equation for the confidence interval line was then:

$$y = bx - t_{\alpha,n-2} s_{Y/x} \qquad (C.15)$$

To measure the fit of a regressed line to the data the reductions in the original variance of T, $R^2$, was calculated:

$$R^2 = (1 - \frac{S^2_{Y/x}}{S^2_Y}) \tag{C.16}$$

where:

$$S^2_Y = \frac{1}{n-1} \sum (y_j - \bar{y})^2 \tag{C.17}$$

Because of the dependence of the conditional variance of T on the value of the x coordinate it was decided to calculate $R^2$ at the mean value of the period so as to compare different regressed lines.

# APPENDIX D - TYPICAL ROOF LOAD CALCULATIONS

A typical roof would result in loads of the order of:

| | | |
|---|---|---|
| ceiling | 0.22 | (Gyprock) |
| tiles | 0.57 | (Terracotta - including framing) |
| | 0.97 kPa | (D.1) |

being applied to the walls that support it. A typical roof would span six metres between supports giving a load per unit length of wall of:

$$3 \text{ m} \times 0.79 \text{ kPa} = 2.4 \text{ kN/m} \quad \text{(D.2)}$$

The laboratory wall panels are 1.2 metres long:

$$2.4 \text{ kN/m} \times 1.2 \text{ m} = 2.9 \text{ kN} \quad \text{(D.3)}$$

As there are two wall panels being tested:

$$2.9 \text{ kN} \times 2 = 5.8 \text{ kN roof load} \quad \text{(D.4)}$$

The wall panels should therefore have a superimposed load representing the roof load of 5.8 kN. The result if the roof was spanning eight metres and each wall therefore supported four metres of roof would be:

$$4 \text{ m} \times 0.79 \text{ kPa} = 3.2 \text{ kN/m} \quad \text{(D.5)}$$

$$3.2 \text{ kN/m} \times 1.2 \text{ m} = 3.8 \text{ kN} \quad \text{(D.6)}$$

$$3.8 \text{ kN} \times 2 = 7.6 \text{ kN} \quad \text{(D.7)}$$

so that the superimposed roof load increases to 7.6 kN.

If the wall panels represented the lower half a wall there would be superimposed load from the upper part of the wall applied. If a double leaf wall was 2.4 metres high then the superimposed load would be:

$$1.2 \text{ m (high)} \times 19 \text{ kN/m}^3 \times 0.22 \text{ m (thick)} = 5.0 \text{ kN/m} \quad \text{(D.8)}$$

For two walls, 1.2 m long:

$$5.0 \text{ kN/m} \times 1.2 \text{ m} \times 2 = 12 \text{ kN superimposed load} \quad \text{(D.9)}$$

These calculations were used to determine reasonable levels of superimposed load to apply to the wall panel specimens for the shaking table tests.

# APPENDIX E - COMPARISON OF ADELAIDE RESULTS TO CALIFORNIAN RESULTS.

As was noted in Chapter 4, the test set-up used for the laboratory tests in this research was similar to the test set-up as used by Mengi and McNiven (1989) at the University of California at Berkeley for tests on unreinforced clay brick masonry. It was therefore possible to use the results from the Berkeley tests to predict the order of magnitude of the expected results from the tests conducted in Adelaide.

It is firstly assumed that the behaviour of the wall as a result of the induced horizontal shear force was that of a cantilever shear beam. This was based on the calculations in Appendix G that show that the majority of the deflection of the wall panels was made up of the shear deflection component than the bending deflection component (two thirds of the total was shear deflection). A typical cantilever shear beam is shown in Figure E.1.

The displacement of the shear beam is of the form:

$$\Delta = k\frac{PL}{AG} \qquad (E.1)$$

where P, L and A are as defined in Figure E.1, G is the shear modulus, $k$ is a constant, and $\Delta$ the deflection of the beam. As the test set-up used in both the Adelaide and Berkeley tests was the same it was assumed that $k$ was constant for both tests. Similarly, as both tests were carried out on clay brick masonry it was assumed that the shear modulus for both tests were equal. The panels used in the Berkeley tests were two single leaf 190 mm thick, 2440 mm long and 1830 mm high

clay masonry walls. This compares to the four 110 mm thick, 1175 mm long by 760 mm high clay masonry panels used in the Adelaide double leaf tests.

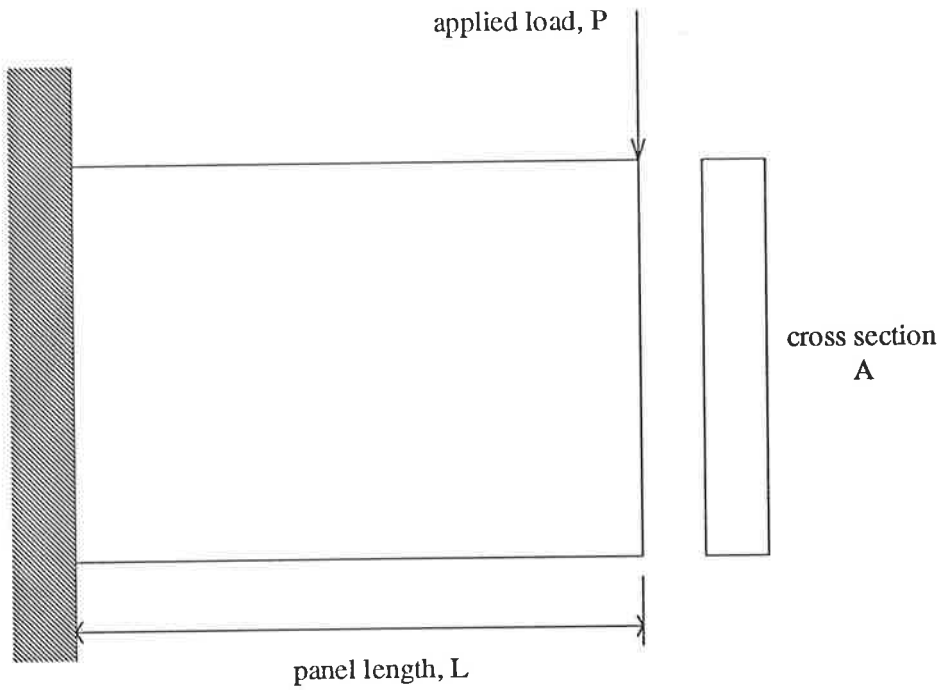


Figure E.1 Typical cantilever shear beam

The applied load was also different for the two tests. For earthquake simulator tests the applied load was an inertial load which was a linear function of the base acceleration and the vertical mass. Without information regarding the distribution of horizontal acceleration along the height of the wall it was assumed that it was constant for both tests even though, as will be seen later, the Berkeley tests had a significantly greater proportion of the total vertical mass at the roof level. The total mass for the Berkeley tests consisted of 12,729 kg of roof superimposed mass and 3,292 kg of mass due to the wall panels. The Adelaide tests, specifically the tests with typical roof load applied, 12 x 400 N, had 510.8 kg of roof superimposed mass and 650.8 kg of wall mass.

For a similar level of base acceleration, then the ratio of the displacement of the Adelaide test to the Berkeley test became:

$$\frac{\Delta_{Adelaide}}{\Delta_{Berkeley}} = \frac{\left(\frac{PL}{A}\right)_{Adelaide}}{\left(\frac{PL}{A}\right)_{Berkeley}} \qquad (E.2)$$

substituting in from previously:

$$\frac{\Delta_{Adelaide}}{\Delta_{Berkeley}} = \frac{\frac{1161.8 \times 0.76}{0.517}}{\frac{16021 \times 1.83}{0.9296}} \qquad (E.3)$$

and evaluating:

$$\frac{\Delta_{Adelaide}}{\Delta_{Berkeley}} = 0.054 \qquad (E.4)$$

It was expected that the maximum acceleration applied to the model specimens would be 0.5 g as this would be a conservative upper limit for any design earthquake in an area of low seismicity such as Australia. At a maximum acceleration of 0.472 g for the Berkeley tests, which was for the El Centro, 1940, earthquake record, the top displacement was 2.118 mm. Applying Equation E.4 to this result yields an expected displacement for the top of the panels in the Adelaide tests of 0.12 mm.

For the Adelaide single leaf specimens with the same axial stress as the double leaf specimens it was found that the load, P, was halved as was the cross sectional area. These two factors cancel when substituted in Equation E.2 and led to the same ratio as Equation E.4.

After the tests were completed it was possible to compare the results of the Adelaide tests to the Berkeley tests. None of the Adelaide tests had a peak acceleration that matched any of the reported Berkeley results. Subsequently, the expected ratios of deflections need to be corrected for the differing peak acceleration. As the applied load P is proportional to the base acceleration, the peak acceleration appears on the top line of Equation E.1. Further, the Berkeley tests were expected to have a centre of mass relatively higher than the Adelaide tests due to the larger proportion of mass at roof level for the Berkeley tests. The induced shear force for the walls was applied

through the centre of mass so the L term in Equation E.1 was affected by the difference in the centre of mass. The centre of mass for the Berkeley tests was found to be 1,640 mm from the base. This was 89 percent of the panel height. The centre of mass for the Adelaide tests was 547 mm from the base, 72 percent of the height. Modifying Equation E.4 with the ratios of the centre of mass yields:

$$\frac{\Delta_{Adelaide}}{\Delta_{Berkeley}} = 0.054 \times \frac{0.72}{0.89} \tag{E.5}$$

evaluating:

$$\frac{\Delta_{Adelaide}}{\Delta_{Berkeley}} = 0.043 \tag{E.6}$$

Comparing the actual results from Berkeley to Adelaide, the expected ratios are:

$$\left(\frac{\Delta_{Adelaide}}{\Delta_{Berkeley}}\right)_{expected} = 0.043 \frac{a_{Adelaide}}{a_{Berkeley}} \tag{E.7}$$

and the comparison is given in Table E.1

Table E.1 Comparison of Adelaide to Berkeley Results

| $a_{Adelaide}$ (g) | $\Delta_{Adelaide}$ (mm) | $a_{Berkeley}$ (g) | $\Delta_{Berkeley}$ (mm) | actual $\frac{\Delta_{Adelaide}}{\Delta_{Berkeley}}$ | expected $\frac{\Delta_{Adelaide}}{\Delta_{Berkeley}}$ |
|---|---|---|---|---|---|
| 0.184 | 0.026 | 0.149 | 0.629 | 0.041 | 0.053 |
| 0.264 | 0.033 | 0.285 | 0.966 | 0.034 | 0.039 |

The results show that the order of magnitude of the displacements measured in the Adelaide tests are consistent with those of the Berkeley tests. The difference in the expected results compared to the actual results can be attributed to factors such as workmanship, actual distribution in the acceleration, and the material properties (mortar composition, thickness etc).

# APPENDIX F - OVERTURNING AND UPLIFT CALCULATIONS

Overturning and uplift were checked for a typical 13 course wall panel from the shaking table test program. The typical wall panel is shown in Figure F.1.

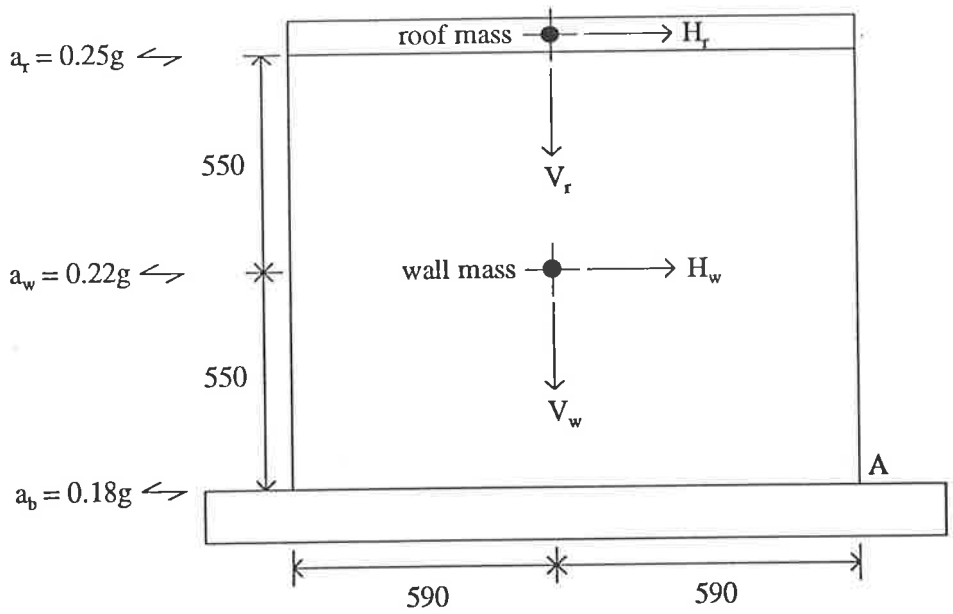


Figure F.1 Typical shaking table test specimen.

The mass of the masonry component of the wall test specimen (single leaf) was given by:

$$V_w = 0.11m \times 1.1m \times 1.18m \times 19\ kN/m^3 = 2.7\ kN \qquad (F.1)$$

and the mass of the roof (per leaf of brickwork) was given by:

$$V_r = 127.5 \text{ kg} \times 9.81 \text{ m/s}^2 \times 10^{-3} = 1.3 \text{ kN} \quad \text{(F.2)}$$

Calculation of the earthquake induced horizontal loads using the accelerations shown in Figure F.1 gave:

$$H_w = 2.7 \text{ kN} \times 0.22g = 0.6 \text{ kN} \quad \text{(F.3)}$$

and:

$$H_r = 1.3 \text{ kN} \times 0.25g = 0.3 \text{ kN} \quad \text{(F.4)}$$

For overturning, taking moments about point A shown in Figure F.1, firstly calculating the moment that causes overturning:

$$\Sigma H_i y_i = 0.6 \text{ kN} \times 0.55\text{m} + 0.3 \text{ kN} \times 1.1\text{m} = 0.7 \text{ kNm} \quad \text{(F.5)}$$

and calculating the moment that resists overturning:

$$\Sigma V_i z_i = 2.7 \text{ kN} \times 0.59\text{m} + 1.3 \text{ kN} \times 0.59\text{m} = 2.4 \text{ kNm} \quad \text{(F.6)}$$

Therefore the factor of safety against overturning was:

$$\frac{2.4 \text{ kNm}}{0.7 \text{ kNm}} = 3.4 \quad \text{(F.7)}$$

Overturning was therefore not a problem. Calculating the potential for uplift (tensile failure in the bottom mortar layer). The overturning moment, Equation F.5, was divided by the bending modulus, z, to determine the tensile stress at opposite corner to point A in Figure F.1. The bending modulus was given by:

$$z = \frac{110 \times 1180^2}{6} = 25.5 \times 10^6 \quad \text{(F.8)}$$

the tensile stress then becomes:

$$\sigma_t = \frac{0.7 \times 10^6}{25.5 \times 10^6} = 0.03 \text{ MPa} \quad \text{(F.9)}$$

The resisting stress due to the self weight of the wall and the roof on top was given by:

$$\sigma_c = \frac{2700 + 1300}{110 \times 1180} = 0.03 \text{ MPa} \qquad \text{(F.10)}$$

The tensile stress due to overturning was the same as the compressive stress due to the self weight of the panels and the roof. The factor of safety against uplift was the tensile strength of the brickwork.

# APPENDIX G - CALCULATION OF SHEAR AND BENDING COMPONENTS IN LABORATORY WALL SPECIMENS

In order to determine the component of shear deflection in the total deflection of the laboratory wall specimens calculation of the expected static bending and shear components of the total deflection of the laboratory wall specimens was undertaken. It was assumed that the four leaf wall was a simple cantilever beam of thickness equal to four times the thickness of one wall panels.

Considering the laboratory test specimen number 4. A cantilever beam consisting of a point load at the free end, a uniformly distributed load along the length of the beam, and a triangularly distributed load varying from zero at the support to maximum at the free end. The applied acceleration ranged from 0.184g at the base, linearly increasing to 0.247g at the free (top) end. The test set up is shown in Figure G.1.

The properties used to determine the components of the deflection were:

| | | |
|---|---|---|
| length | = | 1175 mm |
| height | = | 760 mm |
| width | = | 4 x 110 mm = 440 mm |
| density | = | 19 kN/m$^3$ |

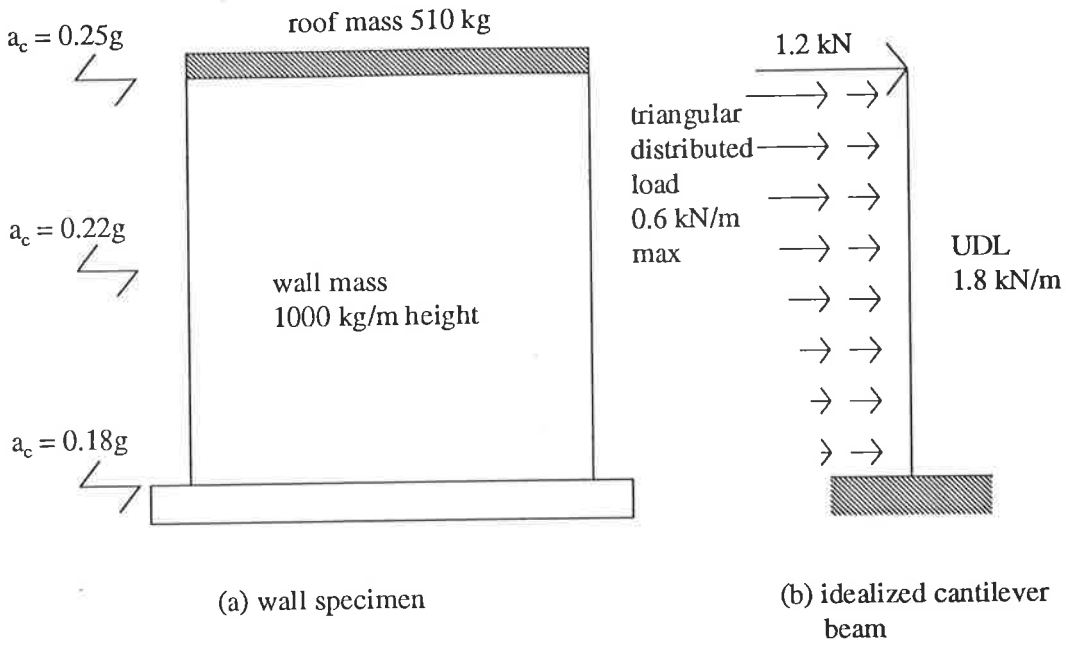


Figure G.1 Laboratory Wall Specimen Number 4

# G.1 BENDING COMPONENT

The bending component of the deflection was made up of three parts superimposed. The equations used for each part of the deflection were taken from Gere and Timoshenko (1987).

The deflection at the end of the cantilever due to the point load at the end of the cantilever was given by:

$$\delta = \frac{PL^3}{3EI} \qquad (G.1)$$

where P is the point load, L is the cantilever length, E is the Young's Modulus, and I is the second moment of area of the cross section. The deflection to the end of the cantilever due to the uniformly distributed load along the cantilever length was given by:

$$\delta = \frac{wL^4}{8EI} \qquad (G.2)$$

where w is the distributed load per unit length, and L, E, and I are as previously defined. The third part of the bending deflection, that due to the triangularly distributed load was given by:

$$\delta = \frac{11qL^4}{120EI} \qquad (G.3)$$

where q is the maximum value of the triangular load per unit length, and L, E, and I are as previously defined.

Substituting the values for the laboratory wall specimen number 4 yields an end bending deflection of:

$$\delta = \frac{4.6}{E} \qquad (G.4)$$

where E is in MPa and the deflection is in millimetres.

## G.2 SHEAR COMPONENT

As with the bending component, the shear component of the total deflection is made up of three parts superimposed. The deflections due to the point load and the uniformly distributed load are given in Roark and Young (1989). For the point load at the free end of the cantilever beam the deflection at the free end of the cantilever was given by:

$$\delta = F\frac{PL}{AG} \qquad (G.5)$$

where P is the point load at the end of the beam, L is the length of the beam, A is the cross sectional area, G is the shear modulus, and F is a factor depending on the form of the cross section, for rectangular cross sections F = 6/5. The deflection at the free end of the cantilever was given by:

$$\delta = \frac{1}{2} F \frac{wL^2}{AG} \qquad \text{(G.6)}$$

where F, A, G, and L are as previously defined and w is the uniformly distributed load per unit length. For the triangularly distributed load no shear deflection formula was found so the unit-load method as described in Gere and Timoshenko was used to determine the deflection. The resulting equation for the deflection for a triangularly varying distributed load on a cantilever with the maximum at the free end was:

$$\delta = \frac{1}{3} F \frac{qL^2}{AG} \qquad \text{(G.7)}$$

where F, L, A, and G are as previously defined and q is the maximum value of the triangularly distributed load per unit length.

Evaluating Equations G.5 to G.7 for the laboratory wall specimen number 4 yields a total shear deflection in millimetres of:

$$\delta = \frac{3.66}{G} \qquad \text{(G.8)}$$

where G is the shear modulus in MPa. The Young's Modulus and the shear modulus of a material are related by the formula:

$$G = \frac{E}{2(1+\nu)} \qquad \text{(G.9)}$$

E and G are as previously defined and ν is the Poisson's Ratio. Using a Poisson's ratio of 0.17 (the average of the Poisson's Ratio for the brick and mortar phase as reported in Section 2.5) the shear component of the deflection can be expressed in terms of the Young's Modulus. The shear deflection then became:

$$\delta = \frac{8.56}{E} \qquad \text{(G.10)}$$

# G.3 COMPARISON OF DEFLECTIONS

From Equations G.4 and G.10 it can be seen the bending deflection does not play a significant part in the overall deflection of the laboratory wall specimens. Just over one third of the total deflection was due to bending. In a wall in a real building, however, it would be expected that the length is very much greater than the height and the shear component of the deflection would dominate to an even greater degree.

# REFERENCES


ABRAMS, D.P. "Strength and behavior of unreinforced masonry elements" *Proceedings of the Tenth World Conference on Earthquake Engineering,* Madrid, Spain, 19-24 July, 1992.

ABRAMS, D.P. "A lesson learned from Loma Prieta on vulnerability of URM construction east of the Rockies" *Proceedings of the 1993 National Earthquake Conference,* Memphis, Tennessee, U.S.A., 2-5 May, 1993.

ADHAM, S.A. and EWING, R.D. "Interaction between unreinforced masonry walls and their roof diaphragms during earthquakes" *Proceedings of the North American Masonry Conference,* Boulder, Colorado, U.S.A., 14-16 August, 1978.

ADHAM, S.A. "Out-of-plane response of masonry walls" *Proceedings of the Third North American Masonry Conference,* Arlington, Texas, U.S.A., June, 1985.

ANAND, S.C. and YALAMANCHILI, K.K. "3-D Analysis of composite masonry walls subjected to earthquake loads" *Proceedings of the Ninth World Conference on Earthquake Engineering*, Tokyo, Japan, August 2-9, 1988.

ANG, H.S. and TANG, W.H. *Probability Concepts in Engineering Planning and Design Volume 1 - Basic Principals*, John Wiley and Sons, New York, 409 pages, 1975.

AOYAMA, H. "Outline of the earthquake provisions in the recently revised Japanese building code" *Bulletin of the New Zealand National Society for Earthquake Engineering*, Vol. 14, No. 2, June, pp 63-80, 1981.

ARMYTAGE, W.H.G. *A Social History of Engineering*, Faber and Faber, London, U.K., 379 pages, 1961.

ARYA, A.S. "Model studies of masonry buildings as related to earthquake resistant design requirements" *Proceedings of The International Research Conference on Earthquake Engineering,* Skopje, Yugoslavia, 30 June - 3 July, 1980.

ATC *"Applied Technology Council - Tentative provisions for the development of seismic regulations for buildings"*, Prepared by The Applied Technology Council, National Bureau of Standards, Palo Alto, California, 1984.

*"Australian Standard 1170.1 SAA Loading Code Part 1 : Dead and live loads and load combinations"*, Standards Australia, Sydney, Australia, 1989.

*"Australian Standard 1170.4 Minimum design loads on structures Part 4 : Earthquake Loads"*, Standards Australia, Sydney, Australia, 1993.

*"Australian Standard 2121 SAA Earthquake Code"*, Standards Australia, Sydney, Australia, 1979.

*"Australian Standard 3700 SAA Masonry Code"*, Standards Australia, Sydney, Australia, 1988.

BARIOLA, J.; GINOCCHIO, J.F. and QUIUN, D. "Out-of-plane seismic response of brick walls" *Proceedings of Fifth North American Masonry Conference*, University of Illinois at Urbana-Champaign, U.S.A., 3-6 June, 1990.

BASE, G.D. and BAKER, L.R. "Fundamental properties of structural brickwork" *Journal of the Australian Ceramic Society,* Vol. 9, No. 1, May, pp 1-6, 1973.

BENEDETTI, D. and BENZONI, G.M. "A numerical model for the seismic analysis of masonry buildings : Experimental correlations" *Journal of Earthquake Engineering and Structural Dynamics*, Vol. 12, No. 6, November, pp 817-831, 1984.

BERESFORD, F.D. "The Effect on Buildings of the Meckering Earthquake of October, 1968" *Earthquake Engineering Symposium,* The Institution of Engineers, Australia, Melbourne, Australia, 16-18 October, 1969.

BOUSSABAH, L. and BRUNEAU, M. "Review of the seismic performance of unreinforced masonry walls" *Proceedings of the Tenth World Conference on Earthquake Engineering,* Madrid, Spain, 19-24 July, 1992.

BOUWKAMP, J.C. and STEPHEN, R.M. "Ambient and forced vibration studies of a multi-storey pyramid shaped building" *Proceedings of the Fifth World Conference on Earthquake Engineering*, Rome, Italy, 25-29 June, 1973.

BRICENO, E.F.; ESPINOSA, A.F. and ARCIA, R. "Dynamic response study of the Palace Corvin Building in Caracas, Venezuela" *Proceedings of the Fifth World Conference on Earthquake Engineering*, Rome, Italy, 25-29 June, 1973.

BROOKS, D.S.; SVED, G. and PAYNE, D.C. "The stiffness of partially cracked brick walls" *Report Number R20,* The Department of Civil Engineering, The University of Adelaide, Adelaide, Australia, 23 pages, 1979.

BROOKS, D.S. "Strength and stability of brick masonry walls" *Report Number R30,* The Department of Civil Engineering, The University of Adelaide, Adelaide, Australia, 19 pages, 1980.

BROOKS, D.S. and PAYNE, D.C. "The effects of slenderness and load eccentricity on the design of load bearing masonry walls" *Proceedings of The Institution of Engineers, Australia Structural Engineering Conference*, Adelaide, South Australia, 3-5 October, 1990.

BROWNJOHN, J.M.W.; DUMANOGLU, A.A.; STEVERN, R.T. and TAYLOR, C.A. "Ambient vibration measurements of the Humber Suspension Bridge and comparison with calculated characteristics" *Proceedings of the Institution of Civil Engineers*, Part 2, Vol. 83, No. 9, September, pp 561-600, 1987.

BRUNEAU, M. "State-of-the-art report on seismic performance of unreinforced masonry buildings" *American Society of Civil Engineers Journal of Structural Engineering*, Vol. 120, No. 1, January, pp 230-251, 1994.

CALVI, G.M.; MAGENES, G.; PAVESE, A. and ABRAMS, D.P. "Large scale seismic testing of an unreinforced brick masonry building" *Proceedings of the Fifth United States National Conference on Earthquake Engineering*, Chicago, 10-14 July, 1994.

CHANDLER, A.M. "Combined seismic base shear and torsional loading provisions in the 1990 edition of the National Building Code of Canada" *Canadian Journal of Civil Engineering,* Vol. 18, No. 6, December, pp 945-953, 1991.

CHEN, C.K.; CZARNECKI, R.M. and SCHOLL, R.E. "Vibration tests of a 4-storey concrete structure" *Proceedings of the Sixth World Conference on Earthquake Engineering*, New Delhi, India, 10-14 January, 1977.

CHEN, S-W.J.; HIDALGO, P.A.; MAYES, R.L.; CLOUGH, R.W. and McNIVEN, H.D. "Cyclic loading tests of masonry single piers volume 2 - Height to width ratio of 1" *Earthquake Engineering Research Center Report*, No. 78/28, University of California, Berkeley, U.S.A., 179 pages, 1978.

CHEUNG, Y.K. and KASEMSET, C. "Approximate frequency analysis of shear wall framed structures" *Journal of Earthquake Engineering and Structural Dynamics*, Vol. 6, No. 2, March, pp 221-229, 1978.

CLOUGH, R.W., MAYES, R.L. and GULKAN, P. "Shaking table study of single-storey masonry houses volume 3 - Summary, conclusions, and recommendations" *Earthquake Engineering Research Center Report*, No. 79/25, University of California, Berkeley, U.S.A., 96 pages, 1979.

CLOUGH, R.W., GULKAN, P., MANOS, G.C. and MAYES, R.L. "Seismic testing of single storey masonry houses : Part 2" *American Society of Civil Engineers Journal of Structural Engineering*, Vol. 116, No. 1, January, pp 257-274, 1990.

CLOUGH. R.W. and PENZIEN, J. *Structural Dynamics*, 2nd Edition, McGraw-Hill Inc., New York, 738 pages, 1993.

COMERIO, M.C. "Impacts of the Los Angeles retrofit ordinance on residential buildings" *Earthquake Spectra,* Vol. 8, No. 1, February, pp 79-94, 1992.

COULL, A. and MUKHERJEE, P.R. "Natural vibrations of shear wall buildings on flexible supports" *Journal of Earthquake Engineering and Structural Dynamics*, Vol. 6, No. 3, May, pp 295-315, 1978.

DAVIDSON, E.B. and WANG, L.R.L. "A Study of the cyclic lateral resistance of low rise masonry wall panels" *Proceedings of the Third North American Masonry Conference,* Arlington, Texas, U.S.A., **[DAY]** June, 1985.

DEPPE, K. "The Whittier Narrows, California Earthquake of October 1, 1987 - Evaluation of strengthened and unstrengthened unreinforced masonry in the Los Angeles City" *Earthquake Spectra,* Vol. 4, No. 1, February, pp 157-180, 1988.

DHANASEKAR, M.; KLEEMAN, P.W. and PAGE, A.W. "Biaxial stress-strain relationships for brick masonry" *American Society of Civil Engineers Journal of Structural Engineering*, Vol. 111, No. 5, May, pp 1085-1100, 1985 (a).

DHANASEKAR, M.; PAGE, A.W. and KLEEMAN, P.W. "The failure of brick masonry under biaxial stress", *Proceedings of the Institution of Civil Engineers*, Part 2, Vol. 79, June, pp 295-313, 1985 (b).

DIEHL, J.G. "Roof-top ambient vibration measurements" *Proceedings of the Third United States National Conference on Earthquake Engineering,* Charleston, North Carolina, U.S.A., 24-28 August, 1986.

DUARTE, R.B. and SINHA, B.P. "Lateral strength of brickwork panels with openings" *Proceedings of the Institution of Civil Engineers*, Part 2, Vol. 94, No. 11, November, pp 397-402, 1992.

FOUTCH, D.A. and HOUSNER, G.W. "Observed changes in the natural periods of vibration of a nine storey steel frame building" *Proceedings of the Sixth World Conference on Earthquake Engineering*, New Delhi, India, 10-14 January,1977.

FOUTCH, D.A. and JENNINGS, P.C. "Dynamic tests on full-scale structures" *Proceedings of the Sixth World Conference on Earthquake Engineering*, New Delhi, India, 10-14 January,1977.

FUKUTA, T. "Seismic design in Mexico City" Research Paper No. 136, Building Research Institute, Ministry of Construction, Japan, December, 61 pages, 1991.

GATES, J.H., and SMITH, M.J. "Results of ambient vibration testing of bridges" *Proceedings of the Eighth World Conference on Earthquake Engineering*, San Francisco, U.S.A., 21-28 July, 1984.

GERE, J.H. and TIMOSHENKO, S.P. *Mechanics of Materials*, PWS-Kent Publishing Co., Boston, 807 pages, 1990.

GERSCH, W. and MARTINELLI, F. "Estimation of structural system parameters from stationary and non stationary ambient vibrations : An exploratory-confirmatory analysis" *Journal of Sound and Vibration* , Vol. 65, No. 3, August, pp303-318, 1979.

GERSCH, W. and BROTHERTON, T. "Estimation of stationary structural system parameters from non-stationary random vibration data : A locally stationary model method" *Journal of Sound and Vibration* , Vol. 81, No. 2, March, pp 215-227, 1982.

GHAZALI, M.Z. and RIDDINGTON, J.R. "Simple test method for masonry shear strength" *Technical Note No. 505 Proceedings of the Institution of Civil Engineers* Part 2, Vol. 85, September, pp 567-574, 1988.

GOEL, R.K. and CHOPRA, A.K. "Inelastic seismic response of one-storey, asymmetric-plan systems : effects of stiffness and strength distribution" *Journal of Earthquake Engineering and Structural Dynamics*, Vol. 19, No. 7, October, pp 949-970, 1990.

GRIMM, C.T. "Strength and related properties of brick masonry" *American Society of Civil Engineers Journal of Structural Engineering*, Vol. 101, No. ST1, January, pp 217-232, 1975.

GULKAN, P.; MAYES, R.L. and CLOUGH, R.W. "Shaking table study of single-storey masonry houses volume 1: Test structures 1 and 2" *Earthquake Engineering Research Center Report* No. 79/23, University of California, Berkeley, U.S.A., 260 pages, 1979.

GULKAN, P.; CLOUGH, R.W.; MAYES, R.L. and MANOS, G.C. "Seismic testing of single storey masonry houses : Part 1" *American Society of Civil Engineers Journal of Structural Engineering*, Vol. 116, No. 1, January, pp 235-256, 1990.

HENDRY, A.W. "The lateral strength of unreinforced brickwork" *The Structural Engineer*, Vol. 51, No. 2, February, pp 43-50, 1973.

HIDALGO, P.A.; MAYES, R.L.; McNIVEN, H.D. and CLOUGH, R.W. "Cyclic loading tests of masonry single piers volume 1 - Height to width ratio of 2" *Earthquake Engineering Research Center Report* No. 78/27, University of California, Berkeley, U.S.A., 131 pages, 1978.

HIDALGO, P.A.; MAYES, R.L.; McNIVEN, H.D. and CLOUGH, R.W. "Cyclic loading tests of masonry single piers volume 3 - Height to width ratio of 0.5" *Earthquake Engineering Research Center Report* No. 79/12, University of California, Berkeley, U.S.A., 144 pages, 1979.

HILL, D. *A History of Engineering in Classical and Medieval Times* Croom Held Ltd., Beckenham, Kent, U.K., 263 pages, 1984.

HOERNER, J.B. and JENNINGS, P.C. "Modal interference in vibration tests" *American Society of Civil Engineers Journal of the Engineering Mechanics Division*, Vol. 95, No. EM4, August, pp 827-839, 1969.

HOUSNER, G.W. and BRADY, A.G. "Natural periods of vibration of buildings" *American Society of Civil Engineers Journal of the Engineering Mechanics Division*, Vol. 89, No. EM4, August, pp 31-65, 1963.

HUTCHINSON, G.L.; MENDIS, P. and WILSON, J.L. "A review of the new Australian Earthquake Loading Standard AS 1170.4" *Australian Civil Engineering Transactions, Institution of Engineers, Australia*, Vol. CE36, No. 3, August, pp 235-244, 1994.

IBANEZ, P. and SHANMAN, R.D. "Identification of dynamic structural parameters from experimental data" *Proceedings of the Fifth World Conference on Earthquake Engineering*, Rome, Italy, 25-29 June, 1973.

JANKULOVSKI, E.; PARSANEJAD, S.; and SAMALI, B. "Earthquake resistance assessment of masonry buildings" *Proceedings of the Third National Masonry Seminar,* Brisbane, Australia, 14-15 July, 1994.

JANKULOVSKI, E. and PARSANEJAD, S. "Hysteresis behaviour of plain masonry walls : An experimental investigation" *Australasian Structural Engineering Conference*, Sydney, New South Wales, 21-23 September, 1994.

JURUKOVSKI, D.; KRSTEVSKA, L.; ALESSI, R.; DIOTALLEVI, P.P.; MERLI, M. and ZARRI, F. "Shaking table tests of three four-storey brick masonry models : Original and strengthened by RC core and by RC jackets" *Proceedings of the Tenth World Conference on Earthquake Engineering,* Madrid, Spain, 19-24 July, 1992.

KONIG, G.; MANN, W. and OTES, A. "Experimental investigations of the behaviour of unreinforced masonry walls under seismically induced loads and lessons derived" *Proceedings of the Ninth World Conference on Earthquake Engineering*, Tokyo, Japan, 2-9 August, 1988.

KARIOTIS, J.C.; EWING, R.D. and JOHNSON, A.W. "Predictions of stability of unreinforced masonry shaken by earthquakes" *Proceedings of the Third North American Masonry Conference,* Arlington, Texas, U.S.A., **[DAY]** June, 1985.

KREYSIG, E. *Advanced Engineering Mathematics* 5th edition, John Wiley, New York, 988 pages, 1983.

KWOK, Y-H, and ANG, A.H-S "Seismic damage analysis and design of unreinforced masonry" *SRS 536* The University of Illinois at Urbana-Champaign, U.S.A., 104 pages, 1987.

KWOK, K.C.S.; APPERLEY, L.W.; MATESIC, I.J. and MANGION, C.B. "Measurement of natural frequencies of vibration and damping ratios of tall buildings and structures" *Proceedings of The Institution of Engineers, Australia Structural Engineering Conference*, Adelaide, South Australia, 3-5 October, 1990.

MAGENES, G. and CALVI, G.M. "Cyclic behaviour of brick masonry walls" *Proceedings of the Tenth World Conference on Earthquake Engineering,* Madrid, Spain, 19-24 July, 1992.

MAGUIRE, J.R.; SEVERN, R.T., and TREVELYAN, J. "Assessing the dynamic properties and integrity of structures by the use of transient data" *Proceedings of the Eighth World Conference on Earthquake Engineering*, San Francisco, U.S.A., 21-28 July, 1984.

MANOS, G.C.; CLOUGH, R.W. and MAYES, R.L. "Shaking table study of single-storey masonry houses - Dynamic performance under three component seismic input and recommendations" *Earthquake Engineering Research Center Report* No. 83/11, University of California, Berkeley, U.S.A., 156 pages, 1983.

MAYES, R.L and CLOUGH, R.W. "A literature survey - Compressive, tensile, bond and shear strength of masonry" *Earthquake Engineering Research Center Report* No. 75/15, University of California, Berkeley, U.S.A., 190 pages, 1975a.

MAYES, R.L. and CLOUGH, R.W. "State of the art in seismic shear strength of masonry - An evaluation and review" *Earthquake Engineering Research Center Report* No. 75/21, University of California, Berkeley, U.S.A., 137 pages, 1975b.

MAYES, R.L.; OMOTE, Y. and CLOUGH, R.L. "Cyclic shear tests of masonry piers volume 1 - Test results" *Earthquake Engineering Research Center Report* No. 76/8, University of California, Berkeley, U.S.A., 93 pages, 1976a.

MAYES, R.L., OMOTE, Y. and CLOUGH, R.L. "Cyclic shear tests of masonry piers volume 2 - Analysis of test results" *Earthquake Engineering Research Center Report* No. 76/16, University of California, Berkeley, U.S.A., 70 pages, 1976b.

McNIVEN, H. and MENGI, Y. "A mathematical model for the inplane non-linear earthquake behaviour of brick masonry walls : Part 2 - Completion of the model" *Journal of Earthquake Engineering and Structural Dynamics*, Vol. 18, No. 2, February, pp 249-261,1989.

MENDOZA, L.; REYES, A. and LUCO, J.E. "Ambient vibration tests of the Mexicali General Hospital" *Earthquake Spectra*, Vol. 7, No. 2, February, pp 281-300, 1991.

MENGI, Y.; SUCUOGLU, H. and McNIVEN, H. "A linear mathematical model for the seismic inplane behaviour of brick masonry walls : Part 1 - Theoretical considerations" *Journal of Earthquake Engineering and Structural Dynamics*, Vol. 12, No. 3, May, pp 313-326, 1984.

MENGI, Y. and McNIVEN, H. "A mathematical model for the inplane non-linear earthquake behaviour of brick masonry walls : Part 1 - Experiments and proposed model" *Journal of Earthquake Engineering and Structural Dynamics*, Vol. 18, No. 2, February, pp 233-247, 1989.

MEYYAPPA, M. and CRAIG, J.I. "Highrise building identification using transient testing" *Proceedings of the Eighth World Conference on Earthquake Engineering,* San Francisco, U.S.A., 21-28 July, 1984.

MONGE, J. "An accurate estimation of the fundamental period of rectangular tall buildings" *Proceedings of the Eighth World Conference on Earthquake Engineering* , San Francisco, U.S.A., 21-28 July, 1984.

MOON, S.-K. and LEE, D.-G. "Effects of inplane floor slab flexibility on the seismic behaviour of building structures" *Engineering Structures,* Vol. 16, No. 2, February, pp 129-144, 1994.

MORONI, M.O.; ASTROZA, M. and GOMEZ, J. "Seismic force reduction factor for masonry building" *Proceedings of the Tenth World Conference on Earthquake Engineering,* Madrid, Spain, 19-24 July, 1992.

MUKHERJEE, P.R. and COULL, A. "Free vibrations of coupled shear walls on flexible bases" *Proceedings of the Institution of Civil Engineers* Part 2, Vol. 57, September, pp 493-511, 1974.

MURIA-VILA, D. "Dynamic properties of masonry buildings in Mexico City" *Proceedings of Fifth North American Masonry Conference*, University of Illinois at Urbana-Champaign, U.S.A., 3-6 June, 1990.

MUTO, K.; NAGATA, M.; UCHIYAMA, S.; UENO, H.; FUKUZAWA, E., and HANAJIMA, M. "Vibration test and simulation analysis of highrise building with V-shaped framing plan" *Proceedings of the Eighth World Conference on Earthquake Engineering*, San Francisco, U.S.A., 21-28 July, 1984.

NARAINE, K. and SINHA, S. "Cyclic behaviour of brick masonry under biaxial compression" *American Society of Civil Engineers Journal of Structural Engineering*, Vol. 117, No. 5, May, pp 1336-1355, 1991.

NARAINE, K. and SINHA, S. "Stress-strain curves for brick masonry in biaxial compression" *American Society of Civil Engineers Journal of Structural Engineering*, Vol. 118, No. 6, June, pp 1451-1461, 1992.

NEHRP *"Recommended Provisions for the Development of Seismic Regulations for New Buildings - Part 1 Provisions"*, National Earthquake Hazards Reduction Program, Federal Emergency Management Agency, Washington, DC, 1991.

NEHRP *"Recommended Provisions for the Development of Seismic Regulations for New Buildings - Part 2 Commentary"*, National Earthquake Hazards Reduction Program, Federal Emergency Management Agency, Washington, DC, 1991.

*"Newcastle Earthquake Study"* The Institution of Engineers, Australia (Melchers, R.E. ed.), Canberra, Australia, 1990.

NIELSEN, N.N. "Vibration tests of a nine storey steel frame building" *American Society of Civil Engineers Journal of the Engineering Mechanics Division*, Vol. 92, No. EM1, February, pp 81-110, 1966.

NIGBOR, R.L. "Full-scale ambient vibration measurements of the Golden Gate suspension bridge - Instrumentation and data acquisition" *Proceedings of the Eighth World Conference on Earthquake Engineering*, San Francisco, U.S.A., 21-28 July, 1984.

OHTA, T.; ADACHI, N.; UCHIYAMA, S.; NIWA, M. and TAKAHASHI, K. "Results of vibration tests on tall buildings and their earthquake response" *Proceedings of the Sixth World Conference on Earthquake Engineering*, New Delhi, India, 10-14 January, 1977.

PAGE, A.W. "Finite element model for masonry" *American Society of Civil Engineers Journal of Structural Engineering*, Vol. 104, No. ST8, August, pp 1267-1285, 1978.

PAGE, A.W. "The biaxial compressive strength of brick masonry" *Proceedings of The Institution of Civil Engineers* Part 2, Vol. 71, pp 353-365, 1981.

PAGE, A.W.; KLEEMAN, P.W. and DHANASEKAR, M. "An in-plane finite element model for brick masonry" *Proceedings of a Session held with Structures Congress '85,* The American Society of Civil Engineers, 18 September, 1985.

PAGE, A.W.; KLEEMAN, P.W.; STEWART, M.G., and MELCHERS, R.E. "Structural aspects of the Newcastle Earthquake" *Proceedings of The Institution of Engineers, Australia Structural Engineering Conference*, Adelaide, South Australia, 3-5 October, 1990.

PAGE, A.W. "A note on the shear capacity of membrane type dampproof courses" *Research Report 097.05.1994,* Department of Civil Engineering and Surveying, The University of Newcastle, Newcastle, Australia, 28 pages, 1994.

PANDE, G.N.; KRALJ, B. and MIDDLETON, J. "Analysis of the compressive strength of masonry given by the equation $f_k=k(f'_b)(f_m)$" *The Structural Engineer,* Vol. 72, No. 1, January, 1994.

PAYNE, D.C.; BROOKS, D.S., and SVED, G. "The analysis and design of slender brick walls" *Masonry International*, Vol. 4, No. 2, pp 55-65, 1990.

PETROVSKI, J.; JURUKOVSKI, D. and PASKALOV, T. "Dynamic properties of fourteen storey R.C. frame building from full scale forced vibration study and formulation of mathematical model" *Proceedings of the Fifth World Conference on Earthquake Engineering*, Rome, Italy, 25-29 June, 1973.

POMONIS, A.; SPENCE, R.J.S. and COBURN, A.W. "Shaking table tests on strong motion damagingness upon unreinforced masonry" *Proceedings of the Tenth World Conference on Earthquake Engineering,* Madrid, Spain, 19-24 July, 1992.

PRIESTLEY, M.J.N. and BRIDGEMAN, D.O. "Seismic resistance of brick masonry walls" *Bulletin of the New Zealand National Society for Earthquake Engineering*, Vol. 7, No. 4, December, pp 167-187, 1974.

PRIESTLEY, M.J.N.; THORBY, P.N.; McLARIN, M.W. and BRIDGEMAN, D.O. "Dynamic performance of brick masonry veneer panels" *Bulletin of the New Zealand National Society for Earthquake Engineering*, Vol. 12, No. 4, December, pp 314-323, 1979.

PRIESTLEY, M.J.N. "Seismic behaviour of unreinforced masonry walls" *Bulletin of the New Zealand National Society for Earthquake Engineering*, Vol. 18, No. 2, June, pp 191-205, 1985.

QAMARUDDIN, M.; CHANDRA, B. and ARYA, A.S. "Dynamic testing of brick building models" *Proceedings of The Institution of Civil Engineers* Part 2, Vol. 77, September, pp 353-365, 1984.

QAMARUDDIN, M.; ARYA, A.S. and CHANDRA, B. "Dynamic response of multi-storeyed brick buildings" *Journal of Earthquake Engineering and Structural Dynamics*, Vol. 13, No. 2, March, pp 135-150, 1985.

RAINER, J.H. "Force reduction factors for the seismic provisions of the National Building Code of Canada" *Canadian Journal of Civil Engineering*, Vol. 14, No. 4, August, pp 447-454, 1987.

REAY, A.M. and SHEPARD, R. "Dynamic characteristics of three adjacent reinforced concrete buildings" *Proceedings of The Institution of Civil Engineers* Part 2, Vol. 50, September, pp 25-47, 1971.

RIDDELL, R.; HIDALGO, P. and CRUZ, E. "Response modification factors for earthquake resistant design of short period buildings" *Earthquake Spectra,* Vol. 5, No. 3, August, pp 571-590, 1989.

RIDDINGTON, J.R. and GHAZALI, M.Z. "Hypothesis for shear failure in masonry joints" *Proceedings of The Institution of Civil Engineers* Part 2, Vol. 89, March, pp 89-102, 1990.

ROARK, R.J. and YOUNG, W.C. *Roark's Formulas for Stress and Strain,* 6th edition, McGraw-Hill, New York, 763 pages, 1989.

ROBINSON, L.M. "Discussion of : Seismic behaviour of unreinforced masonry walls by M.J.N. Priestley" *Bulletin of the New Zealand National Society for Earthquake Engineering*, Vol. 19, No. 1, March, pp 65-75, 1986.

SAN BARTOLOME, A.; QUIUN, D. and TORREALVA, D. "Seismic behaviour of a three-story half scale confined masonry structure" *Proceedings of the Tenth World Conference on Earthquake Engineering,* Madrid, Spain, 19-24 July, 1992.

SEAOC *"Recommended Lateral Force Requirements and Tentative Commentary"*, Seismology Committee, Structural Engineers Association of California, San Francisco, 1988.

SHING, P.B.; LOTFI, H.R.; BARZEGARMEHRABI, A. and BRUNNER, J. "Finite element analysis of shear resistance of masonry wall panels with and without confining frames" *Proceedings of the Tenth World Conference on Earthquake Engineering,* Madrid, Spain, 19-24 July, 1992.

SOROUSHIAN, P.; OBASEKI, K., and CHOI, K-B. "Nonlinear modelling and seismic analysis of masonry shear walls" *American Society of Civil Engineers Journal of Structural Engineering*, Vol. 114, No. 5, May, pp 1106-1119, 1988.

SOUCY, Y. and DEERING, D.W. "Effects of data acquisition conditions on modal testing of a simple structure" *Experimental Techniques*, Vol. 13, No. 10, October, pp 35-39, 1989.

STAFFORD-SMITH, B. and CROWE, E. "Estimating periods of vibration of tall buildings" *American Society of Civil Engineers Journal of Structural Engineering*, Vol. 112, No. 5, May, pp 1005-1019, 1986.

STEPHEN, R.M. and BOUWKAMP, J.G. "Dynamic behavior of an eleven storey masonry building" *Proceedings of the Sixth World Conference on Earthquake Engineering*, New Delhi, India, 10-14 January, 1977.

STUBBS, I.R. and McLAMORE, V.R. "The ambient vibration survey" *Proceedings of the Fifth World Conference on Earthquake Engineering*, Rome, Italy, 25-29 June, 1973.

SUCUOGLU, H.; MENGI, Y. and McNIVEN, H. "A linear mathematical model for the seismic inplane behaviour of brick masonry walls : Part 2 - Determination of the model parameters through optimisation using experimental data" *Journal of Earthquake Engineering and Structural Dynamics*, Vol. 12, No. 3, May, pp 327-346, 1984.

SVED, G.; PAYNE, D.C. and BROOKS, D.S. "Finite element - Finite difference analysis of cracked brick walls" *Report Number R52,* The Department of Civil Engineering, The University of Adelaide, Adelaide, Australia, 10 pages, 1982.

TAOKA, G.T.; FURUMOTO, A.S. and CHIU, A.N.L. "Natural periods of a tall shear wall building" *Proceedings of the Fifth World Conference on Earthquake Engineering*, Rome, Italy, 25-29 June, 1973.

TENA-COLUNGA, A. and ABRAMS, D.P. "Response of an unreinforced masonry building during the Loma Prieta Earthquake" *Proceedings of the Tenth World Conference on Earthquake Engineering,* Madrid, Spain, 19-24 July, 1992.

TOMAZEVIC, M., and ZARNIC, R. "Shaking-table study of a four-storeyed masonry building model" *Proceedings of the Eighth World Conference on Earthquake Engineering*, San Francisco, U.S.A., 21-28 July, 1984.

TOMAZEVIC, M. "Dynamic modelling of masonry buildings : storey mechanism model as a simple alternative" *Journal of Earthquake Engineering and Structural Dynamics*, Vol. 15, No. 6, August, pp 731-749, 1987.

TOMAZEVIC, M. and SHEPPARD, P. "Mathematical modelling of masonry buildings for earthquake resistance analysis" *Engineering Aspects of the Earthquake Phenomena* (Koridze, A. editor), Omega Scientific, Wallingford, Oxon, U.K., pp 121-135, 1987.

TOMAZEVIC, M. and VELECHOVSKY, T. "Some aspects of testing small-scale masonry building models on simple earthquake simulators" *Journal of Earthquake Engineering and Structural Dynamics*, Vol. 21, No. 11, November, pp 945-963, 1992.

TOMAZEVIC, M. and WEISS, P. "Seismic behaviour of plain and reinforced masonry buildings" *American Society of Civil Engineers Journal of Structural Engineering*, Vol. 120, No. 2, February, pp 323-338, 1994.

TORKAMANI, M.A.M. and AHMADI, A.K. "Stiffness identification of a tall building during construction period using ambient vibration tests" *Journal of Earthquake Engineering and Structural Dynamics*, Vol. 16, No. 8, November, pp 1177-1188, 1988.

TSO, W.K. and NAUMOSKI, N. "Period-dependant seismic force reduction factors for short period structures" *Canadian Journal of Civil Engineering* Vol. 18, No. 4, August, pp 568-574, 1991.

UANG, C-M. "Comparison of seismic force reduction factors used in U.S.A. and Japan" *Journal of Earthquake Engineering and Structural Dynamics*, Vol. 20, No. 4, April, pp 389-397, 1991.

UBC *"Uniform Building Code"* International Conference of Building Officials, Whittier, California, 1991.

WARD, H.S. "Experimental techniques and results for dynamic tests on structures and soils" *Proceedings of the Sixth World Conference on Earthquake Engineering*, New Delhi, India, 10-14 January, 1977.

WESLEY, D.A.; KENNEDY, R.P. and RICHTER, P.J. "Analysis of the seismic collapse capacity of unreinforced masonry wall structures" *Proceedings of the Seventh World Conference on Earthquake Engineering*, Istanbul, Turkey, 8-13 September, 1980.

WEST, H.W.H.; HODGKINSON, H.R. and HASELTINE, B.A. "The resistance of brickwork to lateral loading : Part 1 - Experimental methods and results of tests on small specimens and full sized walls" *The Structural Engineer,* Vol. 55, No. 10, October, pp 411-421, 1977.

WILLIAMS, C. "Vibration monitoring of large structures" *Experimental Techniques,* Vol. 8, No. 12, December, pp 29-32, 1984.

WILSON, E.L.; DER KIUREGHIAN, A. and BAYO, E.P. "A replacement for the SRSS method in seismic analysis" *Journal of Earthquake Engineering and Structural Dynamics*,Vol. 9, No. 2, March, pp 187-194, 1981.

YOKEL, F. and FATTAL, S.G. "Failure hypothesis for masonry shear walls" *American Society of Civil Engineers Journal of Structural Engineering*, Vol. 102, No. ST3, March, pp 515-532, 1976.

ZHU, T.J.; TSO, W.K. and HEIDEBRECHT, A.C. "Evaluation of base shear provisions in the 1985 edition of the National Building Code of Canada" *Canadian Journal of Civil Engineering*, Vol. 16, No. 1, February, pp 22-35, 1989.

ZHUGE, Y.; YANG, Y.; THAMBIRATNAM, D. and CORDEROY, H.J.B. "On the lateral behaviour of brick masonry structures under lateral loads" *13th Australasian Conference on the Mechanics of Structures and Materials*, The University of Wollongong, 5-7 July, 1993.

# ADDENDUM

This addendum contains further information and clarification as suggested by the assessors.

The shaking table tests were conducted using the most common brick type manufactured in Adelaide which were a nominal 230 mm x 70 mm x 90 mm. The size given on page 98 is incorrect. The actual sizes varied from 230 to 236 mm long by 109 to 113 mm wide. The height was generally a uniform 70 mm. Table AD.1 gives further information regarding the size of the wall test panels described in Chapter 4 and expands upon the information in Table 4.3.1.

The "Masonry Wall Panel Width" was the total width of masonry making up one of the two walls of the test panel pair. For the double leaf specimens it was the width of two brick leafs but not the cavity, and for the single leaf wall pairs was the width of one leaf of brickwork. The length of the wall panels were 1125 mm for all tests.

The shear forces calculated for the test wall panels and described on page 104 were determined using the approach outlined in Appendix F (Equations F.1, F.2, F.3, and F.4). The associated masses are given in Appendix F as $V_w$ and $V_r$ .

The cracking patterns observed in the masonry wall panels are as described in Figure 4.4.1. Stiffness calculations were based on measurements made prior to the onset of rocking.

The effects of stocky piers and openings in wall panels was not examined as part of this research project.

Table AD.1 Shaking Table Test Panel Details.

| Wall Test Pair Number | Number of Courses | Height of Panel (mm) | Double or Single Leaf (D/S) | Masonry Wall Panel Width[1] (mm) |
|---|---|---|---|---|
| 1 | 13 | 1135 | D | 180 |
| 2 | 13 | 1135 | D | 180 |
| 3 | 13 | 1135 | D | 180 |
| 4 | 9 | 795 | D | 180 |
| 5 | 9 | 795 | D | 180 |
| 6 | 9 | 795 | D | 180 |
| 7 | 9 | 795 | D | 180 |
| 8 | 9 | 825 | D | 180 |
| 9 | 9 | 795 | S | 90 |
| 10 | 9 | 795 | S | 90 |
| 11 | 9 | 795 | S | 90 |
| 12 | 9 | 795 | S | 90 |
| 13 | 9 | 795 | S | 90 |
| 14 | 9 | 795 | D | 180 |
| 15 | 9 | 795 | D | 180 |

The bending stresses given in Tables 5.61 to 5.6.11 are the earthquake induced bending stresses and do not include any dead load.

Equations 6.2.4 and 6.2.5 are intended for use with rigid diaphragm systems.